

KIT SCIENTIFIC REPORTS 7639

# **1<sup>st</sup> Annual Workshop Proceedings of the Collaborative Project "Fast / Instant Release of Safety Relevant Radionuclides from Spent Nuclear Fuel" (7<sup>th</sup> EC FP CP FIRST-Nuclides)**

Budapest 09 – 11 October 2012

Bernhard Kienzler, Volker Metz, Lara Duro, Alba Valls  
(eds.)



Bernhard Kienzler, Volker Metz, Lara Duro, Alba Valls (eds.)

**1st Annual Workshop Proceedings of the Collaborative Project  
“Fast / Instant Release of Safety Relevant Radionuclides from  
Spent Nuclear Fuel” (7th EC FP CP FIRST-Nuclides)**

Budapest 09 - 11 October 2012

**Karlsruhe Institute of Technology**  
**KIT SCIENTIFIC REPORTS 7639**

# **1<sup>st</sup> Annual Workshop Proceedings of the Collaborative Project “Fast / Instant Release of Safety Relevant Radionuclides from Spent Nuclear Fuel” (7<sup>th</sup> EC FP CP FIRST-Nuclides)**

Budapest 09 - 11 October 2012

Bernhard Kienzler  
Volker Metz  
Lara Duro  
Alba Valls  
(eds.)

Report-Nr. KIT-SR 7639

This report is printed in black and white. The report showing the original colours in several photos, tables, figures and logos can be downloaded from the homepage of KIT Scientific Publishing.

Karlsruher Institut für Technologie (KIT)  
Institut für Nucleare Entsorgung

Amphos 21 Consulting S. L.  
Passeig de Garcia i Faria, 49–51, 1<sup>o</sup>–1<sup>a</sup>

## Impressum

Karlsruher Institut für Technologie (KIT)  
KIT Scientific Publishing  
Straße am Forum 2  
D-76131 Karlsruhe  
www.ksp.kit.edu

KIT – Universität des Landes Baden-Württemberg und  
nationales Forschungszentrum in der Helmholtz-Gemeinschaft



Diese Veröffentlichung ist im Internet unter folgender Creative Commons-Lizenz  
publiziert: <http://creativecommons.org/licenses/by-nc-nd/3.0/de/>

KIT Scientific Publishing 2013  
Print on Demand

ISBN 978-3-86644-980-0

## FOREWORD

The present document is the proceedings of the 1<sup>st</sup> Annual Workshop (AW) of the EURATOM FP7 Collaborative Project FIRST-Nuclides (Fast / Instant Release of Safety Relevant Radionuclides from Spent Nuclear Fuel). The electronic version of these proceedings is also available in the webpage of the project (<http://www.firstnuclides.eu/>). The workshop was hosted by MTA-EK and held in Budapest (Hungary) 9<sup>th</sup> – 11<sup>th</sup> October 2012. The project started in January 2012 and has three years duration. It has 10 beneficiaries and 11 associated groups. All of them have participated in the 1<sup>st</sup> AW as well as external interested groups.

The proceedings serve several purposes. The key purpose is to document and make available to a broad scientific community the outcome of the FIRST-Nuclides project. For this reason, a considerable part of the project activity reporting is done through the proceedings, together with the outcome of scientific-technical contributions and Topical Sessions on different topics of interest for the development of the project. In the 1<sup>st</sup> AW of FIRST-Nuclides, the topical session focused on the characteristics and modelling of spent nuclear fuel. Additional purposes of the proceedings are to ensure on-going documentation of the project outcome, promote systematic scientific-technical development throughout the project and to allow thorough review of the project progress.

All Scientific and Technical papers submitted for the proceedings have been reviewed by the EUG (End-User-Group). The EUG is a group specifically set up within the project in order to represent the interest of the end users to the project and their needs. To this aim, the composition of the EUG includes organisations representing national waste management or national regulatory interests and competence.

The proceedings give only very brief information about the project structure and the different activities around the project. More information about the project can be found in detail under <http://www.firstnuclides.eu/>.

Thanks are due to all those who submitted Scientific and Technical contributions for review and, especially, the workpackage leaders who provided the summary of the different workpackages for publication in these proceedings. We also want to give a special thanks to the reviewers, members of the EUG, whose effort and hard work reflect their commitment and dedication to the project and ensure a proper direction of the research within the project programme.





## Table of Contents

<b>THE PROJECT</b> .....	<b>1</b>
<b>1<sup>ST</sup> ANNUAL WORKSHOP</b> .....	<b>5</b>
Objectives .....	5
RTD sessions .....	5
Poster presentations .....	8
Topical session .....	8
Additional presentations .....	8
Structure of the proceedings .....	9
<b>WP OVERVIEW</b> .....	<b>11</b>
<b>S + T CONTRIBUTIONS</b> .....	<b>27</b>
<b>POSTERS</b> .....	<b>207</b>
<b>TOPICAL SESSIONS</b> .....	<b>211</b>
<b>PRESENTATIONS BY ASSOCIATED GROUPS</b> .....	<b>223</b>



## THE PROJECT

The EURATOM FP7 Collaborative Project “Fast / Instant Release of Safety Relevant Radionuclides from Spent Nuclear Fuel (CP FIRST-Nuclides)” started in January 1, 2012 and extends over 3 years. The European nuclear waste management organisations contributing to the Technology Platform “Implementing Geological Disposal (IGD-TP)” considered the fast / instant release of safety relevant radionuclides from high burn-up spent nuclear fuel as one of the key topics in the deployment plan. For this reason, the CP FIRST-Nuclides deals with understanding the behaviour of high burn-up uranium oxide (UO<sub>2</sub>) spent nuclear fuels in deep geological repositories.

The fast / instant release of radionuclides from spent nuclear fuel was investigated in a series of previous European projects (such as SFS (Poinsot et al., 2005; Johnson et al., 2004) NF-PRO (Sneyers, 2008) and MICADO (Grambow et al., 2010)). In addition, there were several studies mainly of the French research programs that investigated and quantified the rapid release (Ferry et al., 2008; Lovera et al., 2003; Johnson et al., 2004, 2005). However, several important issues are still open and consequently, the CP FIRST-Nuclides aims on covering this deficiency of knowledge, determining, for example, the “instant release fraction (IRF)” values of iodine, chlorine, carbon and selenium that are still largely unknown.

Fuel elements from different Light Water Reactors (LWRs), with different enrichments, burn-up and average power rates need to be disposed of in Europe. This waste type represents one of the sources for the release of radionuclides after loss of integrity of a disposed canister. The quantification of time-dependent release of radionuclides from spent high burn-up UO<sub>2</sub> fuel is required for safety analyses. The first release fraction consists of radionuclides in gaseous form, and those showing a high solubility in groundwater.

LWRs use conventional oxide fuels with initial enrichments of up to 5 wt.% <sup>235</sup>U for reaching average burn-up of  $\leq 60$  GWd/t<sub>HM</sub>. During the use of UO<sub>2</sub> in a reactor, a significantly higher burn-up takes place at the rim of the fuel pellets. The physico-chemical properties of the fuel are further complicated by additions of gadolinium oxide and/or chromium oxide, which is used for criticality control or to adjust the UO<sub>2</sub> grain sizes for minimizing fission gas release (FGR). Moreover, the fission products of uranium cause expansion in the UO<sub>2</sub> crystal structure leading to disturbances of the fuel matrix. The chemical stability of the fission products oxides in the UO<sub>2</sub> matrix, can be classified into different groups: (i) the rare earth elements and Y, Zr, Ba and Sr, whose oxides form either solid solutions with UO<sub>2</sub> or single phase precipitates; (ii) Mo, Cs and Rb, which are either oxidized or not, depending on

the O/U ratio; and (iii) elements like Ru, with unstable oxides which form metallic precipitates within the UO<sub>2</sub>.

The CP is organized in six workpackages (WP): WP1, “Samples and tools” deals with the selection, characterization and preparation of the materials to be studied and the set-up of experimental and organisational tools. In this sense, one of the essential requirements of the project is that typical and sufficiently well characterized spent nuclear fuel is being used for the experiments and modelling studies. WP2 covers the “Gas release and rim and grain boundary diffusion experiments” and WP3 addresses “Dissolution based release studies”. This includes determining the chemical form of released radionuclides, fission gases, <sup>135</sup>Cs, <sup>129</sup>I, <sup>14</sup>C, <sup>79</sup>Se, <sup>99</sup>Tc and <sup>126</sup>Sn. WP4 “Modelling” deals with modelling of release/retention processes of fission products in the spent fuel structure. Special attention is attributed to fission product migration along the grain boundaries, the effects of fractures in the pellets and of holes/fractures in the cladding. The modelling work within FIRST-Nuclides will help to clarify which geometric scales dominate the fast/instant release.

WP5 “Knowledge, reporting and training” is responsible for the knowledge management generated within the project, the state-of-the-art report, the general reporting, keeping the documentation up-to-date and organizing training measures. The management of the Collaborative Project is included in WP6.

The project is implemented by a Consortium with ten beneficiaries (Karlsruher Institut fuer Technologie (KIT) Germany, Amphos 21 Consulting S.L. (AMPHOS21) Spain, Joint Research Centre – Institute for Transuranium Elements (JRC-ITU) European Commission, Forschungszentrum Juelich GmbH (JÜLICH) Germany, Paul Scherer Institut (PSI) Switzerland, Studiecentrum voor Kernenergie (SCK•CEN) Belgium, Centre National de la recherche scientifique (CNRS) France, Fundacio Centre Technologic (CTM) Spain, Magyar Tudományos Akadémia Energiatudományi Kutatóközpont (MTA-EK) Hungary, and Studsvik Nuclear AB (STUDSVIK) Sweden). *The Coordination Team* consists of KIT (Coordinator) and AMPHOS21 (Coordination Secretariat) which are responsible for project management, knowledge management, documentation, dissemination and training. Their responsibilities include further the coordination of the project work and activities, communication between the Project Consortium and the European Commission, monitoring the use of resources and transferring financial resources, communication between different project beneficiaries and bodies, documentation of the project outcome and its dissemination and communication to interested parties.

Several organisations from France (Commissariat à l'énergie atomique et aux énergies alternatives, CEA), USA (Los Alamos National Laboratory, SANDIA National Laboratories), UK (Nuclear

Decommissioning Authority (NDA, Center for Nuclear Engineering of the Imperial College London), National Nuclear Laboratory (NNL) and a consortium coordinated by the University Cambridge), Finland (Posiva Oy, Teollisuuden Voima (TVO)), Spain (CIEMAT) and Germany (Gesellschaft für Anlagen- und Reaktorsicherheit (GRS) mbH) contribute to the project without any funding as *Associated Groups (AG)*. These groups have particular interest in the exchange of information. Finally, a group of six implementation and regulatory oriented organizations (SKB (Sweden), NAGRA (Switzerland), ONDRAF/NIRAS (Belgium), ANDRA (France), BfS (Germany), ENRESA (Spain) participate as an “*End-User Group (EUG)*”. This group ensures that end-user interests (waste management organisations and one regulator) are reflected in the project work reviewing the project work and the scientific-technical outcome.

## References

- Ferry C., Piron J.P., Poulesquen A., Poinssot C. (2008) Radionuclides release from the spent fuel under disposal conditions: Re-Evaluation of the Instant Release Fraction. MRS Proceedings, 1107, 447.
- Grambow, B., Bruno, J., Duro, L., Merino, J., Tamayo, A., Martin, C., Pepin, G., Schumacher, S., Smidt, O., Ferry, C., Jegou, C., Quiñones, J., Iglesias, E., Villagra, N.R., Nieto, J.M., Martínez-Esparza, A., Loida, A., Metz, V., Kienzler, B., Bracke, G., Pellegrini, D., Mathieu, G., Wasselin-Trupin, V., Serres, C., Wegen, D., Jonsson, M., Johnson, L., Lemmens, K., Liu, J., Spahiu, K., Ekeroth, E., Casas, I., de Pablo, J., Watson, C., Robinson, P., Hodgkinson, D. (2010) Final Report of the Project MICADO: Model uncertainty for the mechanism of dissolution of spent fuel in nuclear waste repository.
- Johnson L., Ferry C., Poinssot C., Lovera P. (2005) Spent fuel radionuclide source-term model for assessing spent fuel performance in geological disposal. Part I: Assessment of the instant release fraction. Journal of Nuclear Materials, 346, 56-65.
- Johnson, L., Poinssot, C., Ferry, C., Lovera, P. (2004) Estimates of the instant release fraction for UO<sub>2</sub> and MOX fuel at t=0. Report of the SFS Project of the 5<sup>th</sup> Euratom Framework Program.
- Lovera P., Férry C., Poinssot C., Johnson L. (2003) Synthesis report on the relevant diffusion coefficients of fission products and helium in spent nuclear fuel CEA Report, CEA-R-6039.

Poinsot, C., Ferry, C., Kelm, M., Granbow, B., Martínez, A., Johnson, L., Andriambolona, Z., Bruno, J., Cachoir, C., Cavendon, J.M., Christensen, H., Corbel, C., Jégou, C., Lemmens, K., Loida, A., Lovera, P., Miserque, F., de Pablo, J., Poulesquen, A., Quiñones, J., Rondinella, V., Spahiu, K., Wegen, D.H. (2005) Spent fuel stability under repository conditions – Final report of the European SFS Project.

Sneyers, A. (2008) Understanding and Physical and Numerical Modelling of the Key Processes in the Near Field and their Coupling for Different Host Rocks and Repository Strategies NF-PRO Project.

## 1<sup>st</sup> ANNUAL WORKSHOP

The 1<sup>st</sup> Annual Project Workshop of the FIRST-Nuclides project was held in Budapest (Hungary) 9<sup>th</sup> – 11<sup>th</sup> October 2012. The workshop was hosted by MTA-EK. There were 44 attendees at the workshop, representing beneficiaries, associated groups, the End-User Group and project external organizations. The workshop was organized in three days of oral presentations of results obtained within the project and a topical session on characteristics and modelling of spent nuclear fuel.

### Objectives

The Workshop combines different activities and meetings with the following objectives:

- Informing about the scientific progress. Plenary sessions are used for giving overviews by the workpackage leaders and communicating detailed results and planned activities by the beneficiaries.
- Informing about the administrative status.
- Informing/agreeing upon forthcoming reporting.
- Discussing various topics of interest for the consortium.
- Agreeing upon the forthcoming work program.

Emphasis was on scientific-technical topics with administrative issues kept to the minimum necessary.

### RTD sessions

The workshop included plenary sessions where the results from the different workpackages were presented. Next to an overview of the achievements within the respective WP, scientific highlights were presented. The following presentations were given within the project.

#### WP1 session

- V. Metz. Overview of Activities within WP1 “Samples and Tools”
- V. Metz, A. Loida, E. González-Robles, E. Bohnert, B. Kienzler. Characterization of irradiated PWR UOX fuel (50.4 GWd/t<sub>HM</sub> burn-up) used for leaching experiments. Contribution of KIT-INE to WP1 “Samples and Tools”
- D.H. Wegen, D. Papaioannou, R. Nasyrow, R. Gretter. Non-destructive analysis of a PWR fuel segment with a burn-up of 50.4 GWd/t<sub>HM</sub>

- H. Curtius. HTR spent fuel - selected material for FIRST-Nuclides-
- A. Froideval Zumbiehl, E. Curti, I. Günther-Leopold. WP1: Selection and description of spent fuel samples selected for PSI studies in frame of the FIRST Nuclides project
- K. Govers, M. Verwerft, W. Van Renterghem, K. Lemmens, T. Mennecart, C. Cachoir, L. Adriaensen, A. Dobney, M. Gysemans. Characterisation of SCK·CEN fuel samples used for leach tests in FIRST-Nuclides
- J. Vandenborre. Radiolytic corrosion of grain boundaries onto the UO<sub>2</sub> TRISO particle surface: WP1 - Solid characterization and irradiation cell development
- R. Sureda, J. de Pablo, I. Casas, F. Clarens, D. Serrano-Purroy, P. Carbol, J.P. Glatz, D. Papaioannou, V. Rondinella. SNF selected for the FIRST Nuclides WP1
- Z. Hózer, E. Slonszki. Characterisation of spent VVER-440 fuel (WP1)
- O. Roth. Sample Selection and Characterization at Studsvik

### WP2 session

- D.H. Wegen. WP2: Fission Gas Release and Rim and Grain Boundary Diffusion
- D.H. Wegen, D. Papaioannou, W. de Weerd. Sampling and Measurement of Fission Gas from Spent Nuclear Fuel
- E. Bohnert, E. González-Robles, M. Herm, B. Kienzler, M. Lagos, V. Metz. Determination of Gaseous Fission and Activation Products Released from 50.4 GWd/t PWR Fuel – Contribution of KIT-INE to WP2
- O. Roth. Preparations and experimental start-up at Studsvik WP2
- P. Carbol, I. Marchetti. Oxygen and Water Diffusion into 42 GWd/t<sub>HM</sub> UO<sub>2</sub> Fuel under Reducing Conditions
- H. Curtius. HTR Spent Fuel -Microstructure and Radionuclide Inventory-
- J. Vandenborre, A. Traboulsi, G. Blain, J. Barbet, M. Fattahi. Radiolytic Corrosion of Grain Boundaries onto the UO<sub>2</sub> TRISO Particle Surface: WP2 – First in situ RAMAN tests under He<sup>2+</sup> irradiation

### WP3 session

- K. Lemmens. Introduction : overview of activities within WP3
- Z. Hózer, E. Slonszki. Evaluation of activity concentration data measured at Paks NPP



- D. Serrano-Purroy, L. Aldave de las Heras, J. P. Glatz, R. Sureda, F. Clarens, J. de Pablo, I. Casas. Overview of activities. Experimental set-up
- O. Roth, J. Low, A. Puranen, D. Cui, C. Askeljung. Preparations and experimental start-up at Studsvik WP3
- E. González-Robles, E. Bohnert, A. Loida, N. Müller, V. Metz and B. Kienzler. Characterization of 50.4 GWd/t PWR fuel and set-up of dissolution experiments
- Th. Mennecart, K. Lemmens, K. Govers, L. Adriaensen, C. Cachoir, A. Dobney, M. Gysemans, W. Van Renterghem, M. Verwerft. Concept of leach tests for the experimental determination of IRF radionuclides from Belgian high-burnup spent nuclear fuel in “FIRST-Nuclides”
- I. Günther-Leopold, E. Curti, A. Froideval Zumbiehl. XRF/XAS feasibility study for radionuclides determination in spent fuel samples

#### WP4 session

- J. de Pablo. WP4 – Overview of activities
- M. Pečala, A. Idiart, L. Duro, O. Riba. Modelling of SF Saturation with Water (Approach, Preliminary Results and Potential Implications)
- B. Kienzler, C. Bube, V. Metz, E. González-Robles Corrales. Modelling of boundary and initial conditions for upscaling migration / retention processes of fission products in the spent nuclear fuel structure
- I. Casas, A. Espriu, D. Serrano-Purroy, A. Martínez-Esparza, J. de Pablo. IRF modelling from high burn-up spent fuel leaching batch and dynamic leaching experiments

#### WP5 session

- A. Valls. Status and overview of WP5
- E. González-Robles, V. Metz, B. Kienzler, O. Riba, A. Valls, L. Duro. State of the art (WP5: Deliverable 5.1)

## Poster presentations

The following posters were presented during the 1<sup>st</sup> Annual Workshop:

- B. Kienzler, V. Metz, L. Duro, A. Valls, V. Montoya. Generic Poster of FIRST-Nuclides project
- E. González-Robles, B. Kienzler, V. Metz, A. Valls, O. Riba, L. Duro. State of the art of the Fast/Instant Release Fraction

## Topical session

The Topical Sessions aim at covering the key areas along with the project. In these proceedings, topical sessions held in the kick-off meeting are also included. Those topical sessions focused on characterization and modelling of the spent nuclear fuel behaviour under repository conditions.

Presentations within this topic were the following:

- O. Beneš. Thermodynamics of Fission Products in spent nuclear fuel
- C. Gebhardt, W. Goll. Characteristics of Spent Nuclear Fuel
- D. Serrano-Purroy, J. P. Glatz. Impact of the irradiation history of nuclear fuels on the corrosion behaviour in a disposal environment
- P. Van Uffelen. The potential of TRANSURANUS for source term calculations of spent fuel

## Additional presentations

Additional presentations were given on a topic of general interest, especially the context of the present project within the EURATOM FP7 program on geologic disposal. These presentations were given by the associated group. Additional presentations given during the kick-off meeting are also included.

- D. Hambley. Long term behaviour of spent AGR fuel in repository
- A. Meleshyn, J. Wolf, U. Noseck, G. Bracke. Source term modelling for spent fuel elements in performance assessment
- D. Reed. Applicability of Past Spent Fuel Research in the US to a Salt-Based HLW Repository

- D. C. Sassani. Brief Overview of Used Fuel Degradation & Radionuclide Mobilization Activities within the Used Fuel Disposition Campaign

### **Structure of the proceedings**

The proceedings are divided into the following sections:

- WP activity overviews
- Individual Scientific and Technical Contributions, containing reviewed scientific and technical manuscripts
- Posters presented in the 1<sup>st</sup> Annual Workshop
- Contribution of external experts presenting issues of interest for the project within the Topical Sessions
- Additional presentations given by members of the associated group

All the scientific-technical contributions submitted were reviewed by the EUG members (End-User-Group).



# **WP OVERVIEW**



# OVERVIEW WP1: SAMPLES AND TOOLS

Volker Metz

Karlsruher Institut fuer Technologie (KIT), DE

## Introduction

The first workpackage deals with selection, characterization and preparation of appropriate spent nuclear fuels samples and set-up of tools for handling and transportation of the highly radioactive material. The overall objectives of WP1 are:

- Provision documentation of available experimental and theoretical data on high burn-up spent nuclear fuel (HBU-SNF) material;
- selection of those HBU-SNF samples for subsequent experimental investigations, where key parameters regarding fuel history and irradiation characteristics are sufficiently known and publication of these parameters is permitted;
- preparation of selected HBU-SNF samples for subsequent structural and chemical characterisation as well as experimental investigations within WP2 and WP3.

Six months after the start of the project, available experimental and theoretical data were documented in Deliverable 1.1 (Metz et al., 2012a). In these Proceedings of the 1<sup>st</sup> Annual Workshop, new results of the characterisation of selected samples and activities related to the sample preparations are reported.

Since the activities within WP1 are a prerequisite for further experimental investigations within CP FIRST-Nuclides, all experimentally working Beneficiaries contribute to this workpackage.

## Achievements

KIT provided a spent nuclear fuel rod segment with an average discharge burnup of 50.4 GWd/t<sub>HM</sub>, which was transported to JRC-ITU for characterisation, gas sampling, cutting and sampling of fuel pellets. Characteristics of the fuel rod segment are described in Metz et al. (2012b). They compared values of the average burnup and the initial <sup>235</sup>U enrichment of the HBU-SNF samples selected by KIT and the other Beneficiaries and to respective values of fuel assemblies irradiated BWR and PWR fuels reported by the NEA Nuclear Science Committee (2006). The 50.4 GWd/t<sub>HM</sub> fuel rod segment was inspected visually for defects and a  $\gamma$ -scan of the segment was recorded by JRC-ITU (Wegen et al.,

2012a). Furthermore, the JRC-ITU team determined the oxide thickness along the segment's cladding, punctured the segment for gas sampling and prepared pellet-sized samples by dry cutting (Wegen et al., 2012b; Wegen et al., 2012c). The oxide thickness data are in good agreement with results of the  $\gamma$ -scanning (Wegen et al., 2012b). Gas analyses were conducted within workpackage 2 of FIRST-Nuclides, and results are given by González-Robles et al. (2012). Some of the pellet-sized samples are provided by JRC-ITU to KIT for dissolution-based experiments, other pellet-sized samples of the fuel rod segment are used for further post irradiation examinations by JRC-ITU (Wegen et al., 2012b). Curtius and Bosbach (2012) report manufacturing data and irradiation characteristics as well as radionuclide inventories of five  $\text{UO}_2$  TRISO fuel pebbles irradiated in the Petten High Flux Reactor. A burnup of about  $107 \text{ GWd/t}_{\text{HM}}$  was calculated for the end of the irradiation. Coated particles were isolated from the pebbles and transported to JÜLICH for scanning electron microscope examinations and dissolution-based experiments. For dissolution-based experiments and spectroscopic studies, PSI selected two HBU  $\text{UO}_2$  fuel rods and one HBU mixed oxide fuel rod having burn-ups in the range of 57.5 to  $63 \text{ GWd/t}_{\text{HM}}$ . For each of the selected fuel rods one suitable fuel segment was selected and a segment cutting plan was compiled. Manufacturing and operational data of the fuel rods, cutting plans, and the set-up of their leach experiments are described by Günther-Leopold et al. (2012). SCK•CEN studies a fuel rod with an average discharge burnup of  $51 \text{ GWd/t}_{\text{HM}}$ . Govers et al. (2012) presents the characteristics of the fuel rod that will be used for dissolution-based experiments. Details on the fuel manufacturing, irradiation history, calculated isotopic inventory and the temporal inventory evolution are given. Based on the  $\gamma$ -scanning of the fuel rod, a segment cutting plan was developed (Govers et al., 2012). CNRS selected non-irradiated  $\text{UO}_2$  TRISO particles for studies on the corrosion at  $\text{UO}_2$  grain boundaries under cyclotron radiation. Vandenborre et al. (2012) reports on scanning electron microscope examinations and geometric properties of the studied TRISO particles. Set-up of analytical tools and first in situ tests were performed within workpackage 2 of FIRST-Nuclides, and details are given by Vandenborre et al. (2012). MTA-EK compiles characteristic data on damaged VVER-440 fuel stored in the spent fuel storage pool of the Paks-2 power plant since an incident in April 2003. Hózer and Slonszki (2012) present design and operational characteristics data of these spent VVER-440 fuel rods. Details are given about the post-incident history, calculations of power history and burnup dependent parameters (e.g., linear power, fuel temperature, gap width). A summary on the radionuclide inventories of 30 damaged fuel assemblies and the radionuclide inventory of a leaking fuel assembly is given by Hózer and Slonszki (2012). STUDSVIK selected six HBU  $\text{UO}_2$  fuel rods having burn-ups in the range of 50.2 to  $70.2 \text{ GWd/t}_{\text{HM}}$  for dissolution-based experiments. Roth and Puranen (2012) summarize the process of selecting the HBU-SNF samples and preparations made for



the start of the experiments. Characteristics of the fuel rods are reported in Metz et al. (2012a). Based on  $\gamma$ -scanning of the fuel rods, segment cutting plans were developed; an exemplary  $\gamma$ -scan and cutting plan is shown by Roth and Puranen (2012).

## References

- Curtius, H. and Bosbach, D. (2012) HTR spent fuel - selected material for FIRST.Nuclides. 7<sup>th</sup> EC FP – FIRST-Nuclides 1<sup>st</sup> Annual Workshop Proceedings (Budapest, Hungary).
- González-Robles, E., Bohnert, E., Loida, A., Müller, N., Lagos, M., Metz, V., Kienzler, B. (2012) Fission gas measurements and description of leaching experiments with of KIT's irradiated PWR fuel rod segment (50.4 GWd/t<sub>HM</sub>). 7<sup>th</sup> EC FP – FIRST-Nuclides 1<sup>st</sup> Annual Workshop Proceedings (Budapest, Hungary).
- Govers, K., Verwerft, M., Van Renterghem, W., Lemmens, K., Mennecart, T., Cachoir, C., Adriaensen, L., Dobney, A., Gysemans, M. (2012) Characterization of SCK•CEN fuel samples used for leach tests in FIRST-Nuclides. 7<sup>th</sup> EC FP – FIRST-Nuclides 1<sup>st</sup> Annual Workshop Proceedings (Budapest, Hungary).
- Günther-Leopold, I., Linder, H., Froideval Zumbiehl, A., Curti, E. (2012) Selection of high burn-up fuel samples for leach experiments and spectroscopical studies at PSI. 7<sup>th</sup> EC FP – FIRST-Nuclides 1<sup>st</sup> Annual Workshop Proceedings (Budapest, Hungary).
- Hózer, Z. and Slonszki, E. (2012) Characterisation of spent VVER-440 fuel to be used in the FIRST-Nuclides project. 7<sup>th</sup> EC FP – FIRST-Nuclides 1<sup>st</sup> Annual Workshop Proceedings (Budapest, Hungary).
- Metz, V., Bohnert, E., Bube, C., González-Robles, E., Kienzler, B., Loida, A., Müller, N., Carbol, P., Glatz, J. P., Nasyrow, R., Papaioannou, D., Rondinella, V. V., Serrano Purroy, D., Wegen, D., Curtius, H., Klinkenberg, H., Günther-Leopold, I., Cachoir, C., Lemmens, K., Mennecart, T., Vandenborre, J., Casas, I., Clarens, F., de Pablo, J., Sureda Pastor, R., Hózer, Z., Slonszki, E., Ekeroth, E., Roth, O. (2012a) Fast / Instant Release of Safety Relevant Radionuclides from Spent Nuclear Fuel (FIRST-Nuclides): Characterisation of spent nuclear fuel samples to be used in FIRST-Nuclides – relevance of samples for the Safety Case. FIRST-Nuclides Deliverable D1.1.

Metz, V., Loida, A., González-Robles, E., Bohnert, E., Kienzler, B. (2012b) Characterization of irradiated PWR UOX fuel (50.4 GWd/t<sub>HM</sub>) used for leaching experiments. 7<sup>th</sup> EC FP – FIRST-Nuclides 1<sup>st</sup> Annual Workshop Proceedings (Budapest, Hungary).

NEA (2006) Very High Burn-ups in Light Water Reactors. OECD Nuclear Energy Agency, NEA publication 6224, ISBN 92-64-02303-8.

Roth, O. and Puranen, A. (2012) Selection of materials, preparations and experimental set-up. 7<sup>th</sup> EC FP – FIRST-Nuclides 1<sup>st</sup> Annual Workshop Proceedings (Budapest, Hungary).

Vandenborre, J., Traboulsi, A., Blain, G., Fattahi, M. (2012) Radiolytic corrosion of grain boundaries onto the UO<sub>2</sub> TRiso particle surface. 7<sup>th</sup> EC FP – FIRST-Nuclides 1<sup>st</sup> Annual Workshop Proceedings (Budapest, Hungary).

Wegen, D.H., Papaioannou, D., Nasyrow, R., Rondinella, V.V., Glatz, J.P. (2012a) Non-destructive analysis of a PWR fuel segment with a burn-up of 50.4 GWd/t<sub>HM</sub> – Part I: Visual examination and  $\gamma$ -scanning. 7<sup>th</sup> EC FP – FIRST-Nuclides 1<sup>st</sup> Annual Workshop Proceedings (Budapest, Hungary).

Wegen, D.H., Papaioannou, D., Nasyrow, R., Rondinella, V.V., Glatz, J.P. (2012b) Non-destructive analysis of a PWR fuel segment with a burn-up of 50.4 GWd/t<sub>HM</sub> – Part II: Defect determination. 7<sup>th</sup> EC FP – FIRST-Nuclides 1<sup>st</sup> Annual Workshop Proceedings (Budapest, Hungary).

Wegen, D.H., Papaioannou, D., Gretter, R., Nasyrow, R., Rondinella, V.V., Glatz, J.P. (2012c) Preparation of samples for IRF investigations and post Irradiation examinations from 50.4 GWd/t<sub>HM</sub> PWR fuel. 7<sup>th</sup> EC FP – FIRST-Nuclides 1<sup>st</sup> Annual Workshop Proceedings (Budapest, Hungary).

# OVERVIEW WP2: GAS RELEASE + RIM AND GRAIN BOUNDARY DIFFUSION

Detlef Wegen

Joint Research Centre – Institute for Transuranium Elements (JRC-ITU), European Commission

## Introduction

Workpackage 2 (WP2) consists of two main components. In the first component “Experimental determination of fission gas release” the focus is on the quantification of fission gases and fission gas release in high burn-up (HBU) UO<sub>2</sub> spent nuclear fuels (SNF). Fission gas sampled in the plenum of a fuel rod will be analysed as well as the grain boundary inventory and the cross sectional distribution of fission gases and volatile fission products.

The second component “Rim and grain boundary diffusion” deals with investigations on oxygen diffusion in spent UO<sub>2</sub>-fuel. The examination diffusion effects will result in the quantification of water penetration into the grain structures and subsequent corrosion/diffusion phenomena. Furthermore, investigations on irradiated and unirradiated fuel kernels separated from high temperature reactor (HTR) fuel are planned which are complementary to those on light water reactor (LWR) fuel.

The following five institutions are collaborating in WP2.

The *Joint Research Centre – Institute for Transuranium Elements (JRC-ITU)* is the leading organization for WP2. In the first project year the fission gas release from a spent fuel rod owned by KIT will be measured. The determination of the inventory of fission gas and fission products in grain boundaries are foreseen for the second and third project year.

The investigation of diffusion effects will start in the first project year with the characterisation and preparation of spent fuel samples, which will be used for corrosion experiments in H<sub>2</sub><sup>18</sup>O water at room temperature during the second project year. In the last year the <sup>18</sup>O/<sup>16</sup>O depth profiles will be determined to quantify the oxygen diffusion in SNF.

The *Karlsruher Institut für Technologie (KIT)* will in the first project year analyse fission and activation products in the gas phase from a punctured fuel rod segment. The development, testing and implementation of analytical methods for fission and activation products will be carried out in project year one and two. Leaching experiments in which gas and solution analyses are foreseen will be started in the first year and last until project month 33.

*Studsvik Nuclear AB (STUDSVIK)* will in the frame of WP2, investigate the radial fission gas and volatile fission product distribution (Xe, I, and Cs) by Laser-Ablation Mass Spectroscopy (LA-MS) on HBU PWR and BWR SNF.

*Forschungszentrum Jülich GmbH (JÜLICH)* is working on spent high temperature reactor fuel (HTR). The radionuclide inventory in the fuel kernel and in the coatings as well as the microstructure and the elemental distribution will be analysed before leaching in the first half of the project. Investigations of the microstructure and of the elemental distribution of the fuel kernel and of the coatings will be performed before (first half of the project) and after leaching (second half of the project). Within the first half of the project the radionuclide inventory in the fuel kernel and in the coatings will be determined and compared to calculated values as well. After cracking of the tight coatings the fission gas release fraction will be measured in the first 18 months. Then static leaching experiments with the separated fuel kernels and coatings will start in year two in order to determine the fast instant radionuclide release fraction.

Unirradiated tristructural-isotropic (TRISO) fuel particles are investigated by the Centre National de la Recherche Scientifique (CNRS) at the ARRONAX cyclotron under  $\text{He}^{2+}$ -beam irradiation in the dose rate range of 0 - 100 Gy/min. The corrosion of  $\text{UO}_2$  TRISO particles is investigated in view of grain boundary effects and secondary phase formation and the influence of hydrogen. The experiments will be started in the beginning of the second project year with studies on the role of grain boundaries followed by investigations under hydrogen and under varying dose rates.

## **Achievements**

After six month experimental work programme the outcome is coined by preparatory work, testing of new experimental set-ups and characterisation of materials and samples.

JRC-ITU has done fission gas sampling and analysis from a PWR fuel rod owned by KIT (Wegen et al., 2012). The total amount of gas, the gas pressure in the rod and the free volume was determined. The gas samples were shared with KIT for further analyses.

The gas composition was determined by KIT using a quadrupole mass spectrometer with batch inlet system (Bonhert et al., 2012). A method to determine  $^{14}\text{C}$  in gas and aqueous solutions by liquid scintillation counting is under development.

STUDSVIK has planned laser ablation studies on a BWR and on a PWR UOX fuel (Roth, 2012).

JRC-ITU has started the preparation of the oxygen/water diffusion study (Carbol and Marchetti, 2012). The spent fuel was selected and the transfer of ownership is on-going. ITU's shielded SIMS has been prepared for measurements on spent fuel fragments (holder, procedures etc.).  $^{18}\text{O}$ -labelled water (>98 at.%  $\text{H}_2^{18}\text{O}$ ) was purchased. This was difficult because the amount is limited and most of the produced  $^{18}\text{O}$  is needed for the production of  $^{18}\text{F}$ , which is widely used in PET (positron emission tomography).

JÜLICH has started to analyse the microstructure and elemental distribution before leaching as well as the radionuclide inventory in the fuel kernel and in the coatings (Curtius et al., 2012). The surface of the fuel kernel shows large grains and the metallic precipitates appear as hexagonal platelets. The elements Cs, O, U, Mo, Xe, Zr, and Tc were identified whereas higher amounts of the volatile elements Cs and Xe were detected in the surrounding buffer. Furthermore, the elements Am, Pu, Cm, U, Eu, Ce, Sr, Tc, and Pr were found quantitatively within the kernel while Cs behaved differently. About 95% of the activity was found in the coatings.

CNRS has in WP2 set-up the analytical tools. First in situ tests were carried out.  $\text{UO}_2$  solid was immersed in ultra pure water and irradiated at the ARRONAX facility with a  $\text{He}^{2+}$  beam. During irradiation first Raman spectra were measured in situ (Vandenborre et al., 2012).

## References

Bohnert, E., Gonzáles-Robles, E., Herm, M., Kienzler, B., Lagos, M., Metz, V. (2012) Determination of Gaseous Fission and Activation Products Released from 50.4 GWd/t PWR Fuel. Presentation. 7<sup>th</sup> EC FP – FIRST-Nuclides, 1<sup>st</sup> Annual Workshop (Budapest, Hungary).

Carbol, P. and Marchetti, I. (2012) Oxygen and Water Diffusion into 42 GWd/tHM  $\text{UO}_2$  Fuel Under Reducing Conditions. Presentation. 7<sup>th</sup> EC FP – FIRST-Nuclides, 1<sup>st</sup> Annual Workshop (Budapest, Hungary).

Curtius, H., Müller, E., Müskes, H. W., Klinkenberg, M., Bosbach, D. (2012) HTR Spent Fuel - Microstructure and Radionuclide Inventory-. 7<sup>th</sup> EC FP – FIRST-Nuclides, 1<sup>st</sup> Annual Workshop (Budapest, Hungary).

Roth O. (2012) Preparations and Experimental Start-up at Studsvik WP2. Presentation. 7<sup>th</sup> EC FP – FIRST-Nuclides, 1<sup>st</sup> Annual Workshop (Budapest, Hungary).

Vandenborre, J., Traboulsi, A., Blain, G., Barbet, J., Fattahi, M. (2012) Radiolytic Corrosion of Grain Boundaries onto the UO<sub>2</sub> TRISO Particle Surface. 7<sup>th</sup> EC FP – FIRST-Nuclides, 1<sup>st</sup> Annual Workshop (Budapest, Hungary).

Wegen, D.H., Papaioannou, D., De Weerd, W., Rondinella, V.V., Glatz, J.P. (2012) Fission Gas Release Measurement on 50.4 GWd/t<sub>HM</sub> PWR Fuel. 7<sup>th</sup> EC FP – FIRST-Nuclides, 1<sup>st</sup> Annual Workshop (Budapest, Hungary).

## OVERVIEW WP3: DISSOLUTION BASED RELEASE

Karel Lemmens

Studiecentrum voor Kernenergie (SCK-CEN), BE

The overall objective of WP3 is the quantification of the fast release of radionuclides by means of leach tests with spent nuclear fuel, and – to the extent possible – the determination of their chemical speciation. Such leach tests are performed by INE, PSI, Studsvik, SCK•CEN, ITU and CTM. The experiments are done with PWR fuels having a burnup in the range of 45 to 70 MWd/kg<sub>HM</sub>, with BWR fuels of 50-60 MWd/kg<sub>HM</sub>, and a MOX fuel of 63 MWd/kg<sub>HM</sub> (average burnups).

The radionuclides that are susceptible to fast release are situated in various compartments of the fuels, i.e. in the gap between the fuel and the cladding, in the large fissures, in the grain boundaries, and in the cladding. Hence, the release to be expected in the leach tests depends on the physical preparation of the fuel samples from the fuel rods. The most complete information can be obtained by exposing different fuel compartments to the leachant. The programme therefore foresees tests with cladded fuel segments (segments cut from the fuel rods, a few mm to 2.5 cm long, exposed to the leachant on the top and bottom surface, but radially covered by the cladding), with fuel fragments (not covered by the cladding), and with fuel powder (maximum grain boundary exposure). For some fuels, fragments and powder from the centre and the periphery of the fuel are tested separately. In other leach tests, the cladding is separated from the fuel fragments, and the cladding with the adhering fuel residues is leached together with the fragments. In still other experiments, the cladding with the adhering fuel residues is leached separately (without the fuel fragments). Lastly, the cladding can be leached after removal of the fuel residues, to determine the specific release from the cladding.

The radionuclide release measured in the leach tests depends to some extent on the leach test conditions, i.e. the composition of the leachant and the atmosphere. To reduce the related effects and to ease the intercomparison of the results, most tests are done in a harmonized solution of 19 mM NaCl + 1 mM NaHCO<sub>3</sub>. The atmosphere under which the tests are performed is mostly oxidizing, but the oxidation is limited by closure of the leach vessels. One laboratory uses a reducing atmosphere (argon with hydrogen gas). During the leach test, the composition of the leachant is verified at different time intervals. The last sampling is foreseen 12 months after the start of the experiments, but in some cases (particularly with fuel powder) the sampling will be stopped after 40-60 days.

The exact experimental setup of the leach tests is different for the various laboratories. Some laboratories replace the solution completely at the sampling intervals, other laboratories take only small samples. The equipment and procedures are not standardized.

The radiochemical analyses always include the Cs and I isotopes, which are well known for their fast release and which show a similar behaviour as the fission gasses. Much attention is given also to  $^{79}\text{Se}$  and  $^{14}\text{C}$ , i.e. isotopes for which the release and speciation is poorly understood. Special efforts are done to lower the detection limit for  $^{79}\text{Se}$ . One laboratory plans specific surface analyses to determine the Se distribution on a  $\mu\text{m}$ -scale and to determine the oxidation state of the Se in the fuel. Another laboratory foresees specific analytical treatments to distinguish organic from inorganic  $^{14}\text{C}$ . Other isotopes are measured as well, e.g.  $^{90}\text{Sr}$  and U isotopes, which allow to estimate the fuel oxidation before and during the leach tests. One laboratory also intends to measure the released gasses (Kr, Xe,  $\text{H}_2$ ,  $\text{O}_2$ ).

As a complement to the leach tests performed on fuel samples under controlled laboratory conditions, the leaching behaviour of damaged and leaking VVER fuels is studied. These fuel rods have been stored since 2003 (damaged fuel) and 2009 (leaking fuel) in pools with a pH 4 and 7, containing 15-21 g/kg boric acid.

The leach tests are currently in the preparation phase. Radionuclide release measurements are therefore not yet available. The papers hereafter describe the experimental setup and analyses planned by the various laboratories contributing to WP3.



# OVERVIEW WP4: MODELLING

Joan de Pablo

Fundació Centre Technologic (CTM), ES

## Objectives

The objectives of WP4 cover initial speciation of fission products in LWR fuel, and multi-scale modelling of the migration / retention processes of fission products in the HBU spent fuel, in the cladding, and the estimation of the fission product total release through the spent fuel rod.

On the other hand, a semi-empirical model will be developed to predict fission product release to water from gap, grain boundaries and grains.

## Introduction

In this project, the following parts of the fuel will be taken into account (see **Table 1**)

*Table 1: Radionuclides and Part of the Fuel considered in FIRST-Nuclides*

GAP	Fission gases, volatiles ( $^{129}\text{I}$ , $^{137}\text{Cs}$ , $^{135}\text{Cs}$ , $^{36}\text{Cl}$ , $^{79}\text{Se}$ , $^{126}\text{Sn}^*$ ). Also $^{14}\text{C}$ (non-volatile but partially segregated)
GRAIN BOUNDARY	Fission gases, volatiles ( $^{129}\text{I}$ , $^{137}\text{Cs}$ , $^{135}\text{Cs}$ , $^{36}\text{Cl}$ , $^{79}\text{Se}$ , $^{126}\text{Sn}^*$ ), segregated metals ( $^{99}\text{Tc}$ , $^{107}\text{Pd}$ )
RIM	Fission gases, volatiles ( $^{129}\text{I}$ , $^{137}\text{Cs}$ , $^{135}\text{Cs}$ , $^{36}\text{Cl}$ , $^{79}\text{Se}$ , $^{126}\text{Sn}^*$ ), Sr

\* more relevant for MOX

Besides, the dissolution of the matrix will also be considered to differentiate radionuclide release from the grains.

In two recent papers, Serrano-Purroy et al. (2012) and Roudil et al. (2007), IRF were determined at two different times, 10 and 60 days respectively. In both cases, the release of selected radionuclides followed after more than one year but a lower rate. Therefore, IRF should be probably correlated to the instant that water contacts the gap and grain boundaries and not with time, thus the time needed for pellet saturation is one of the important parameters. In this context, it is important to assess the water saturation time.

## Modeling

### 1) *Radionuclide Characteristics in the Fuel*

KIT performed for a rod segment the calculation of the burn-up and decay history by using web-KORIGEN.

Temperature history and the calculation of the rim zone burn-up and thickness as well as the rim porosity.

### 2) *Water saturation of the fuel*

AMPHOS 21 assessed the saturation time of SNF under conditions representative of a deep underground repository and laboratory.

### 3) *Modeling of radionuclide release to water*

UPC-CTM is developing a semi-empirical model is based on the experimental fitting by using three different first-order kinetic equations corresponding to different parts of the fuel: gap, cracks, external or internal grain boundaries, rim structure, and finally grains (matrix).

## References

Roudil, D., Jégou, C., Broudic, V., Muzeau, B., Peugeot, S., Deschanel, X. (2007) Gap and grain boundaries inventories from pressurized water reactor spent fuels. *Journal of Nuclear Materials*, 362, 411-415.

Serrano-Purroy, D., Clarens, F., González-Robles, E., Glatz, J.P., Wegen, D.H., de Pablo, J., Casas, I., Giménez, J., Martínez-Esparza, A. (2012) Instant release fraction and matrix release of high burn-up UO<sub>2</sub> spent nuclear fuel: Effect of high burn-up structure and leaching solution composition. *Journal of Nuclear Materials*, 247, 249-258.

# OVERVIEW WP5: KNOWLEDGE, REPORTING AND TRAINING

Alba Valls

Amphos 21 Consulting S.L. (AMPHOS21), ES

Work package 5 (WP5) of the FIRST-Nuclides project is focused on knowledge management and knowledge dissemination, reporting and training. The objectives of this WP are (i) to provide access to all scientific-technical results for all interested parties, (ii) to elaborate a state of the art report and (iii) to organize, within the project, training and education for the next generation of spent nuclear fuel specialists.

Several dissemination activities are foreseen along the project. They are mainly centered on making accessible all the information related with the project to the interest parties such as the beneficiaries of the project itself or the scientific community. The dissemination is done via various channels: newsletters, presentations, posters, project webpage, annual workshops, proceedings, etc. The webpage of the project consists on a public site where all the information of the organization and objectives of the project are available as well as the public deliverables produced along the project life. The information/reports are periodically updated and all the uploaded material will be available for 5 years after the end of the project. In addition, an intranet is created for the members of the FIRST-Nuclides with the aim of facilitating the communication between the members of the project consortium.

The first version of the State of the art report is already published (Kienzler et al., 2012) and it is available at the project website (<http://www.firstnuclides.eu/>). This report is divided in two parts, the first one presents basic information of spent fuel, such as the characterization of nuclear fuel, irradiation and temperature induced processes in UO<sub>2</sub> during its use in reactors, and disposal concepts for spent nuclear fuel in different countries. In the second part of the report, the state of the art on fast release fraction is documented by a summary of results obtained from more than 100 published experiments using different samples, experimental techniques, and duration of the experiments. The State of the Art report will be regularly updated with respect to the advances achieved within the project.

Three different training measures are planned during the FIRST-Nuclides project:

- (i) organizing invited lectures within the annual workshops, given by external experts regarding issues of interest in the frame of FIRST-Nuclides. In the 1<sup>st</sup> Annual Workshop,

staff from AREVA was invited to give a presentation on ‘Characteristics of Spent Nuclear Fuel’;

- (ii) organizing training on the job through mobility measures between partners. Training mobility measures are offered to the project beneficiaries and to organizations from the EU and Switzerland. These measures are not open to third countries even in the Associated Group.
- (iii) organizing training courses. KIT-INE will provide for a training course in summer 2013, on hot cells work to improve the handling and waste management techniques and to boost the safety awareness of scientific. Attendants will receive practical training as well as script of the course.

During the second year of the project, it is foreseen to edit the second newsletter and to organize the second annual workshop. An update of the State of the Art report will be delivered.

## References

Kienzler, B., Metz, V., González-Robles, E., Montoya, V., Valls, A., Duro, L. (2012) State-of-the-Art and Rationale for Experimental Investigation. Deliverable 5.1. FIRST-Nuclides project.

## **S + T CONTRIBUTIONS**



<b>IRF MODELLING FROM HIGH BURN-UP SPENT FUEL LEACHING EXPERIMENTS</b>	
IGNASI CASAS, ALEXANDRA ESPRIU, DANIEL SERRANO-PURROY, AURORA MARTÍNEZ-ESPARZA, JOAN DE PABLO.....	31
<b>SELECTION AND CHARACTERISATION OF HTR FUEL</b>	
HILDE CURTIUS, EMIL MÜLLER , HANS WALTER MÜSKES, MARTINA KLINKENBERG, DIRK BOSBACH ..	41
<b>A COMBINED XRF / XAS STUDY OF SOME INSTANT RELEASE FRACTION RADIONUCLIDES IN HIGH BURN-UP UO<sub>2</sub> SPENT NUCLEAR FUEL</b>	
A. FROIDEVAL ZUMBIEHL, E. CURTI, I. GÜNTHER-LEOPOLD .....	53
<b>FISSION GAS MEASUREMENTS AND DESCRIPTION OF LEACHING EXPERIMENTS WITH OF KIT'S IRRADIATED PWR FUEL ROD SEGMENT (50.4 GWD/THM)</b>	
ERNESTO GONZÁLEZ-ROBLES, ELKE BOHNERT, ANDREAS LOIDA, NIKOLAUS MÜLLER, VOLKER METZ, BERNHARD KIENZLER.....	61
<b>CHARACTERIZATION OF SCK•CEN FUEL SAMPLES USED FOR LEACH TESTS IN FIRST- NUCLIDES</b>	
KEVIN GOVERS, MARC VERWERFT, WOUTER VAN RENTERGHEM, KAREL LEMMENS, THIERRY MENNECART, CHRISTELLE CACHOIR, LESLEY ADRIAENSEN, ANDREW DOBNEY, MIREILLE GYSEMANS .....	71
<b>SELECTION OF HIGH BURN-UP FUEL SAMPLES FOR LEACH EXPERIMENTS AND SPECTROSCOPICAL STUDIES AT PSI</b>	
INES GÜNTHER-LEOPOLD, HANS-PETER LINDER, ANNICK FROIDEVAL ZUMBIEHL, ENZO CURTI.....	79
<b>CHARACTERISATION OF SPENT VVER-440 FUEL TO BE USED IN THE FIRST-NUCLIDES PROJECT</b>	
ZOLTÁN HÓZER, EMESE SLONSKI .....	87
<b>MODELLING OF BOUNDARY AND INITIAL CONDITIONS FOR UPSCALING MIGRATION / RETENTION PROCESSES OF FISSION PRODUCTS IN THE SPENT NUCLEAR FUEL STRUCTURE</b>	
BERNHARD KIENZLER, CHRISTIANE BUBE, ERNESTO GONZÁLEZ-ROBLES CORRALES, VOLKER METZ.....	103
<b>CONCEPT OF LEACH TESTS FOR THE EXPERIMENTAL DETERMINATION OF IRF RADIONUCLIDES FROM BELGIAN HIGH-BURNUP SPENT NUCLEAR FUEL IN FIRST- NUCLIDES</b>	
THIERRY MENNECART, KAREL LEMMENS, KEVIN GOVERS, ADRIAENSEN LESLEY, CHRISTELLE CACHOIR DOBNEY ANDREW, GYSEMANS MIREILLE, VAN RENTERGHEM WOUTER, VERWERFT MARC.....	111
<b>CHARACTERIZATION OF IRRADIATED PWR UOX FUEL (50.4 GWD/THM) USED FOR LEACHING EXPERIMENTS</b>	
VOLKER METZ, ANDREAS LOIDA, ERNESTO GONZÁLEZ-ROBLES, ELKE BOHNERT, BERNHARD KIENZLER.....	117

<b>MODELLING OF SPENT FUEL SATURATION WITH WATER – APPROACH, PRELIMINARY RESULTS AND POTENTIAL IMPLICATIONS</b>	
MAREK PEKALA, ANDRÉS IDIART , LARA DURO, OLGA RIBA .....	125
<b>MODELLING OF SPENT FUEL SATURATION WITH WATER –SELECTION OF MATERIALS, PREPARATIONS AND EXPERIMENTAL SET-UP</b>	
OLIVIA ROTH AND ANDERS PURANEN .....	137
<b>WP3. DISSOLUTION BASED RELEASE JOINT CONTRIBUTION ITU-CTM</b>	
DANIEL SERRANO-PURROY, LAURA ALDAVE DE LAS HERAS, JEAN PAUL GLATZ, VINCENZO V. RONDINELLA, FREDERIC CLARENS, JOAN DE PABLO, IGNASI CASAS, ROSA SUREDA.....	145
<b>PREVIOUS INVESTIGATIONS ON THE INSTANT RELEASE FRACTION AND GENERAL DESCRIPTION OF THE PROJECT</b>	
ALBA VALLS, OLGA RIBA, LARA DURO, ERNESTO GONZÁLEZ-ROBLES CORRALES, BERNHARD KIENZLER, VOLKER METZ .....	153
<b>RADIOLYTIC CORROSION OF GRAIN BOUNDARIES ONTO THE UO<sub>2</sub> TRISO PARTICLE SURFACE</b>	
JOHAN VANDENBORRE, ALI TRABOULSI, GUILLAUME BLAIN, JACQUES BARBET, MASSOUD FATTAHI .....	161
<b>NON-DESTRUCTIVE ANALYSIS OF A PWR FUEL SEGMENT WITH A BURN-UP OF 50.4 GWD/THM – PART I: VISUAL EXAMINATION AND <math>\gamma</math>-SCANNING</b>	
DETLEF H. WEGEN, DIMITRIOS PAPAIOANNOU, RAMIL NASYROW, VINCENZO V. RONDINELLA, JEAN-PAUL GLATZ .....	173
<b>NON-DESTRUCTIVE ANALYSIS OF A PWR FUEL SEGMENT WITH A BURN-UP OF 50.4 GWD/THM – PART II: DEFECT DETERMINATION</b>	
DETLEF H. WEGEN, DIMITRIOS PAPAIOANNOU, RAMIL NASYROW, VINCENZO V. RONDINELLA, JEAN-PAUL GLATZ .....	183
<b>PREPARATION OF SAMPLES FOR IRF INVESTIGATIONS AND POST IRRADIATION EXAMINATIONS FROM 50.4 GWD/THM PWR FUEL</b>	
DETLEF H. WEGEN, DIMITRIOS PAPAIOANNOU, RALF GREYTER, RAMIL NASYROW, VINCENZO V. RONDINELLA, JEAN-PAUL GLATZ .....	193
<b>FISSION GAS RELEASE MEASUREMENT ON ONE 50.4 GWD/THM PWR FUEL SEGMENT</b>	
DETLEF H. WEGEN, DIMITRIOS PAPAIOANNOU, WIM DE WEERD, VINCENZO V. RONDINELLA, JEAN-PAUL GLATZ .....	201



# IRF MODELLING FROM HIGH BURN-UP SPENT FUEL LEACHING EXPERIMENTS

Ignasi Casas<sup>1\*</sup>, Alexandra Espriu<sup>1</sup>, Daniel Serrano-Purroy<sup>3</sup>, Aurora Martínez-Esparza<sup>4</sup>,  
Joan de Pablo<sup>1,2</sup>

<sup>1</sup> Universitat Politècnica de Catalunya Barcelona Tech (UPC)

<sup>2</sup> Fundació Centre Tecnològic (CTM), ES

<sup>3</sup> Joint Research Centre – Institute for Transuranium Elements (JRC-ITU), European Commission

<sup>4</sup> ENRESA, ES

\* Corresponding author: ignasi.casas@upc.edu

## Abstract

This work focuses on the Instant Release Fraction modeling of several leaching experiments performed with a High Burn-up Spent Fuel of 60 MWd/kg<sub>U</sub>. Experimental results from powder samples from different parts of the fuel and clad fuel (CS) segment samples were evaluated. Data were obtained by using different experimental devices, both batch (static) and continuous flow system (dynamic).

Uranium, technetium and cesium release have been studied by using a kinetic model which consists of three functions for first order kinetics representing different parts of the fuel. A good fit has been obtained in all the cases.

## Introduction

Instant Release Fraction (IRF) refers to the fraction of the inventory of relevant radionuclides (RN) that may be rapidly released from the fuel after a failure of canister. From a theoretical point of view, soluble radionuclides outside of the UO<sub>2</sub>-matrix will be released immediately resp. intaneously when water is in contact with the failed canister. Different assessments of the RN percentage corresponding to this IRF have been proposed from different authors. A good discussion of this can be found in Johnson et al. (2004) where for high burn-up (HBU) fuels the estimation of best and pessimistic values differed by more than 50%. It is pointed out in the same report that the contribution from gap and grain boundary to the IRF is also unclear.

These inconsistencies promoted important experimental programs on IRF from High Burn-up Fuel. It started with the NF-PRO project (Clarens et al., 2007) and is followed with the present FIRST-Nuclides project.

To obtain information about the location of the different RN's, powders from the center and the periphery of the fuel and clad segments were leached in different media (González-Robles, 2011).

A recent paper (Serrano-Purroy et al., 2012) discussed the contribution from external and internal grain boundaries to identify the RN release, taking into account leaching experiments. In the same sense, Roudil et al. (2007) discussed the contribution of the gap and grain boundaries to the IRF.

In these experiments, it is necessary to define the duration of the leaching to determine the IRF. Nowadays this time is selected somewhat arbitrarily, in the works commented above, Serrano-Purroy et al. used 10 days to determine the IRF while Roudil et al. established 60 days. In both works, the total release of selected radionuclides after more than one year of leaching time showed a lower rate. It is questioned if this lower release rate is related to the possibility of the water to contact grain boundaries or to ability of water to dissolve the matrix.

In this work, data of the leaching experiments performed with a HBU fuel (González-Robles, 2011; Serrano-Purroy et al., 2012) will be used for applying a semi-empirical model to determine the contribution of the different parts of the fuel to the IRF.

## 1. Conceptual model

The conceptual model for SNF dissolution is developing as a sum of different fuel parts. The dissolution of each different phase is considered as first order kinetics.

$$m_{RN}(t) = \sum_{i=1}^N m_{RN,i\infty} \cdot (1 - e^{-k_i \cdot t}) \quad \text{eq. 1}$$

The main parameters are  $m_{RN}(t)$  which means the total measured cumulative moles dissolved of the correspondent fission product at a time  $t$ ,  $m_{RN,i\infty}$  which means the total moles present for the specified dissolving phase of the fission product and  $k_i$  is the kinetic constant for the dissolution of that phase.

The model has a number of implicit assumptions and limitations. We assume the homogeneity of the different samples; in the case of powders this means that every single particle has the same size,

composition and radionuclide distribution. In the case of cladded fuel samples, it is assumed that the fuel surface is regular.

The model considers also matrix dissolution, since its dissolution rate will be the rate as the different radionuclides located inside the matrix will release.

## 2. Samples

The characteristics and preparation of the spent fuel samples that we have used in the model exercise are given in detail elsewhere (González-Robles, 2011). A summary of these characteristics is given in **Tables 1** and **2**. Two different powders were used, one from the periphery (called “out”) and another from the center of the pellet (called “core”). CS refers to cladded segment.

*Table 1: Characteristics of the Spent Fuel*

<b>Fuel</b>	<b>60BU</b>
Reactor type	PWR
BU (MWd/kgU)	60
Length cycle (days)	352
<sup>235</sup> U enrichment (weight %)	3.95
Number of irradiation cycles	5
End of irradiation	March 2001
Fission Gas Release (%)	15

*Table 2: Physical characterization of powder and segmented samples*

<b>Sample denomination</b>	<b>Size</b>
60BU-CORE	68 ± 15 µm
60BU-OUT	82 ± 8 µm
60BU-CS	Length: 12.7mm Diameter: 10.7mm Weight: 8.9647 g

**Table 3** shows the leaching experiments that have been modeled in the present work.

**Table 3:** Powder and segmented samples used in the modeling exercise. In all cases the modeled radionuclides are the same: U, Cs and Tc

SAMPLE	EXPERIMENT
Powder (OUT)	Static
	Dynamic
Powder (CORE)	Static
	Dynamic
Pellet	Static

### 3. Results and discussion

Two radionuclides, Cesium and Technetium (in addition to Uranium), have been chosen for this preliminary modeling. Cesium due to its known high release and Technetium because there are some doubts if this element has a significant contribution to IRF. Technetium is present in fuel as insoluble alloy (Johnson et al., 2004). Although its release is very small, it is segregated significantly to grain boundaries. Besides, Uranium is also modeled for determining the release associated to the matrix dissolution.

In **Figure 1**, cumulative moles of the three radionuclides for powder out-sample by using a dynamic system (see Serrano-Purroy et al., 2011) are shown as a function of time. At the beginning, the three elements show a rather similar behavior, with a fast initial release. After this initial period, the rate of release decreases for the three radionuclides, although Uranium and Technetium slow down more significantly than Cesium.

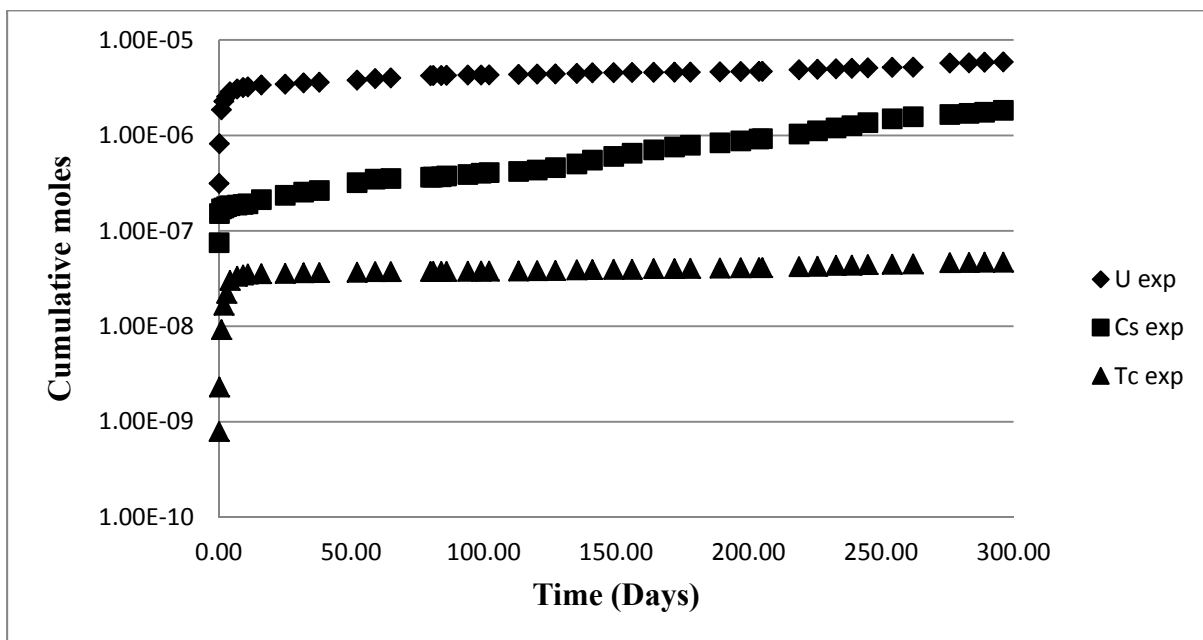


**Figure 1:** U, Cs and Tc cumulative moles vs. time for powder out-samples in a dynamic system

In all the experiments and for the three elements it was possible to fit the experimental data to an expression with three different kinetic constants corresponding to different parts of the fuel:

$$m_{RN}(t) = m_{RN,1\infty} \cdot (1 - e^{-k_1 \cdot t}) + m_{RN,2\infty} \cdot (1 - e^{-k_2 \cdot t}) + m_{RN,3\infty} \cdot (1 - e^{-k_3 \cdot t}) \quad \text{eq. 2}$$

The expression eq. 2 is the proposed model to predict the release of any radionuclide. It is necessary to determine the following six parameters:  $m_{RN,1\infty}$ ,  $m_{RN,2\infty}$ ,  $m_{RN,3\infty}$ ,  $k_1$ ,  $k_2$  and  $k_3$ . Though, since the total mass of a certain radionuclide is known from the inventory, then  $m_{RN,3\infty}$  is deduced from  $m_{RN,1\infty}$  and  $m_{RN,2\infty}$ .

First of all, the Uranium results were modeled in order to find  $k_3$ , since this constant should correspond to the matrix dissolution kinetic constant. Then, Cesium and Technetium were modeled taking the same value for  $k_3$ , assuming that it would correspond to the fraction of each radionuclide released from the matrix assuming congruent dissolution.

In **Figures 2, 3, and 4** experimental data obtained for the three radionuclides from static tests with powder OUT and CORE samples are presented together with the  $m_{RN}(t)$  values obtained from the fitting of equation eq. 2. As it is observed a fairly good fitting is always obtained.

**Figure 5** shows Cesium data obtained from the static experiment with the cladded segment. In this Figure the three contributions of equation eq. 2 are presented together with the total  $m_{RN}(t)$  values.

A summary of the fitting parameters obtained for the whole set of experiments studied is summarized in **Table 4**.

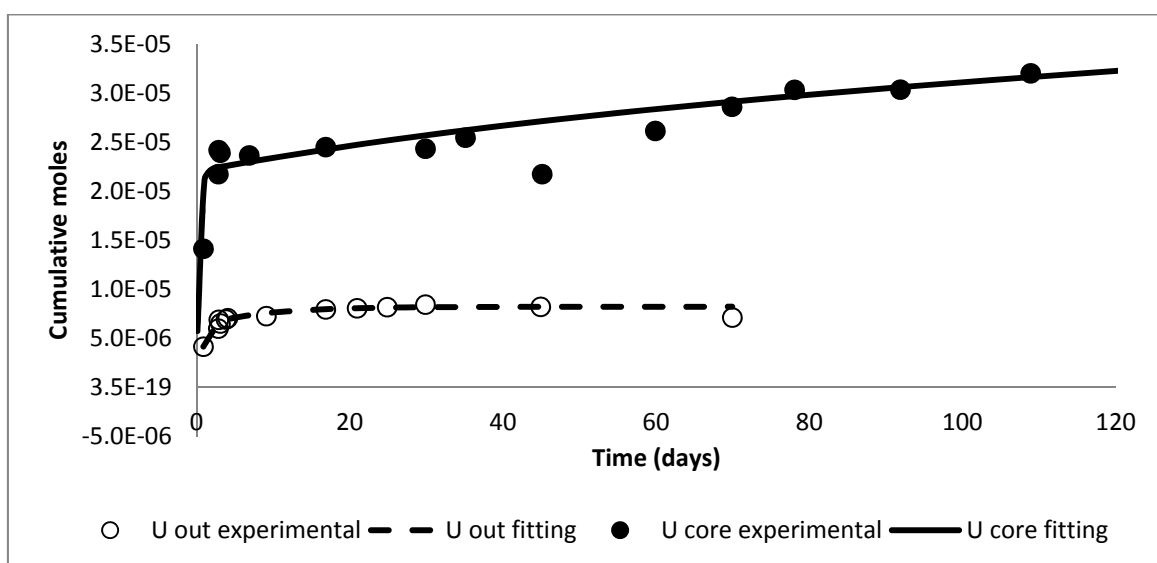


**Figure 2:** Uranium fitting from static experiments

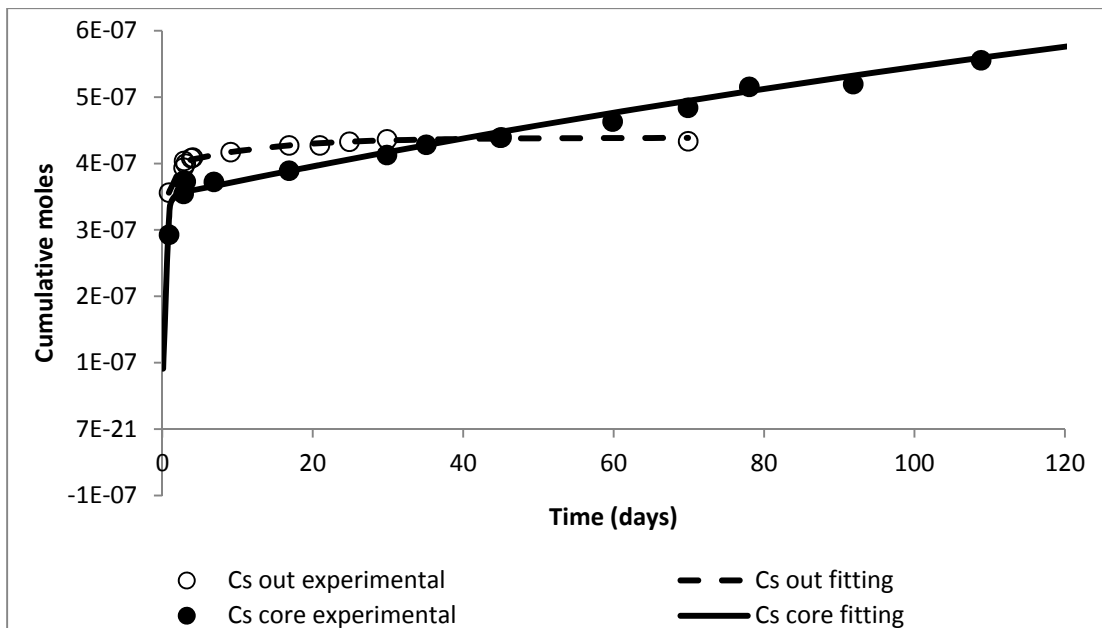


Figure 3: Cesium fitting from static experiments

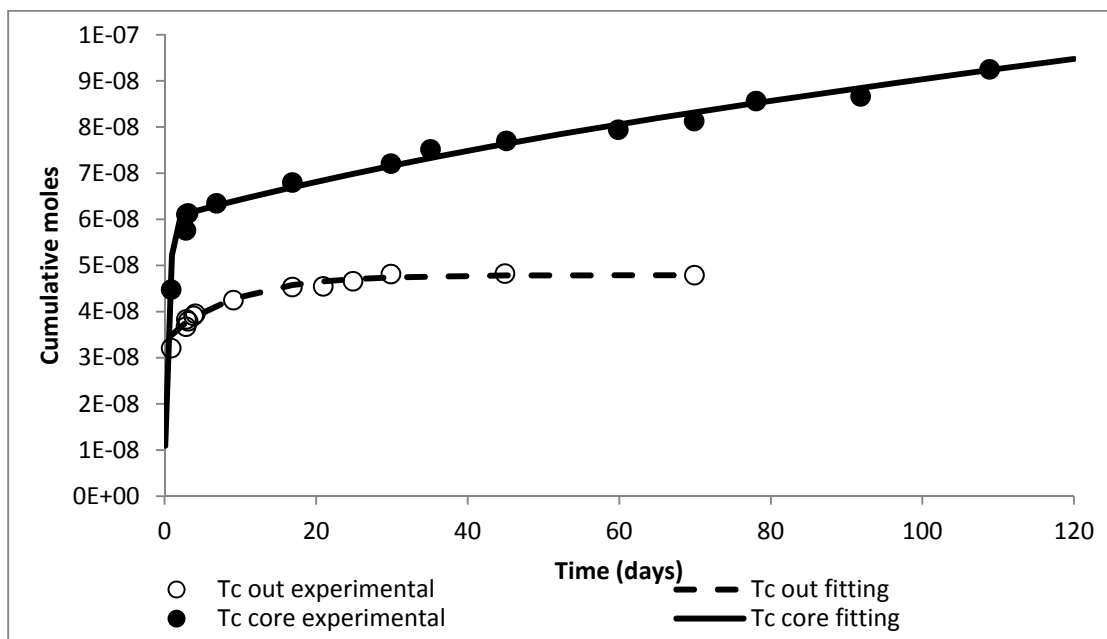
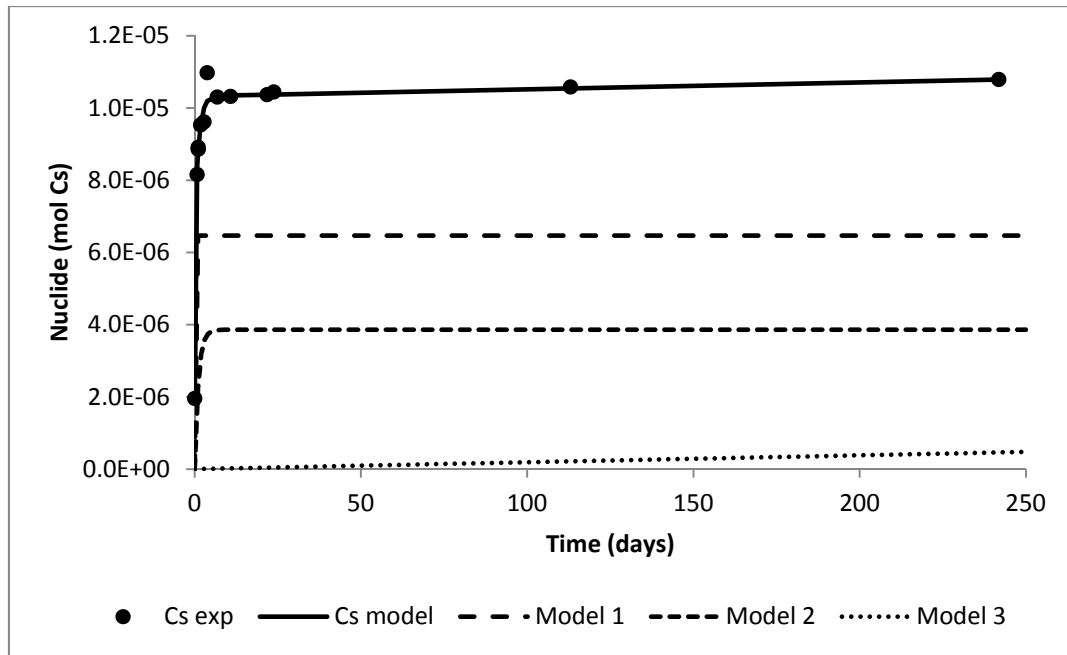


Figure 4: Technetium fitting from static experiments



**Figure 5:** Cesium fitting from static experiments using a cladded fuel segment

In the case of uranium, the initial release ( $m_1+m_2$ ) is attributed to the dissolution of either oxidized layers and/or fine particles resulting from the drilling process. This initial release is almost negligible in the cladded fuel segment sample.

In powder samples, Cesium initial release ( $m_1+m_2$ ) can be attributed to grain boundaries. Roughly, for the presented data, Cesium releases vary from 5 to 15%. The  $k_3$  values for Uranium and Cesium are similar indicating a congruent dissolution at the end of the experiments.

**Table 4:** Fitting parameters of expression eq. 2 for the experiments modeled in this work

Exp.	Sample	Nuclide	$m_1$ (%)	$m_2$ (%)	$m_3$ (%)	$k_1$ ( $d^{-1}$ )	$k_2$ ( $d^{-1}$ )	$k_3$ ( $d^{-1}$ )
Static	Powder- OUT	U	0.80	0.21	98.99	1.07	0.06	6.00E-07
		Cs	4.32	0.48	95.19	2.57	0.07	6.00E-07
		Tc	0.89	0.31	98.80	2.21	0.04	6.00E-07
	Powder- CORE	U	2.66	0.48	96.85	3.00	0.02	6.00E-05
		Cs	4.92	5.62	89.45	3.00	$5.00 \cdot 10^{-3}$	6.00E-05
		Tc	1.83	0.4	97.77	2.00	0.01	6.00E-05
Dynamic	Powder- OUT	U	0.10	0.03	99.9	1.00	$7.00 \cdot 10^{-2}$	2.30E-06
		Cs	0.50	12.4	87.1	6.00	$8.00 \cdot 10^{-4}$	2.50E-06
		Tc	0.02	0.19	97.79	3.50	0.30	2.10E-06
	Powder- CORE	U	0.19	0.05	99.76	2.00	0.04	6.50E-06
		Cs	0.50	15.6	83.9	4.00	$4.1 \cdot 10^{-3}$	6.50E-06
		Tc	0.08	0.12	99.8	3.00	0.03	6.50E-05

Exp.	Sample	Nuclide	m <sub>1</sub> (%)	m <sub>2</sub> (%)	m <sub>3</sub> (%)	k <sub>1</sub> (d <sup>-1</sup> )	k <sub>2</sub> (d <sup>-1</sup> )	k <sub>3</sub> (d <sup>-1</sup> )
Static	Pellet	U	0.007	0.005	99.99	0.63	1.45 · 10 <sup>-3</sup>	3.00E-09
		Cs	3.91	2.33	93.76	9.64	0.88	1.23E-05
		Tc	0.02	0.004	99.98	5.08	0.25	1.66E-06

As seen in **Table 4**, a different behavior is observed for the clad fuel segment sample: m<sub>1</sub> might be the contribution from the gap and cracks, while m<sub>2</sub> could be due to grain boundary dissolution. On the other hand, it is observed that k<sub>3</sub> is much higher for Cesium than for Uranium, indicating that in this experiment both elements are not congruently dissolved at the end of the experimental time.

Uranium and Technetium release are similar in all the samples, but k<sub>3</sub> values differ in several experiments. This fact would indicate that dissolution is not congruent and it could indicate the Technetium segregation to grain boundaries.

### Conclusions and Future work

This work is a preliminary attempt to model IRF experimental data taking into account radionuclide location: gap, grain boundary, internal grain boundary and matrix, as well as the high burn-up structure.

The model is conceptually based on the contribution of different phases dissolving simultaneously, and allows to present hypothesis of the source terms of each radionuclide.

Several sets of experiments have been successfully modeled, which is giving confidence that the overall release of the radionuclides can be fitted adequately.

This kind of modeling is planned to be applied in the future to the experimental data generated in the First-Nuclides project.

### Acknowledgement

*The research leading to these results has received funding from the European Union's European Atomic Energy Community's (Euratom) Seventh Framework Programme FP7/2007-2011 under grant agreement n° 295722 (FIRST-Nuclides project).*



## References

- Clarens, F., Serrano-Purroy, D., Martínez- Esparza, A., Glatz, J-P., de Pablo, J., Wegen, D., Christiansen, B., Casas, I., González-Robles, E., Gago, J.A. (2007) RN fractional release of spent fuel as a function of burn-up: Effect of RIM. 6<sup>th</sup> EC FP – NF-PRO, 4<sup>th</sup> Annual Workshop, (Brussels Belgium).
- González-Robles, E. (2011) Study of Radionuclide Release in commercial UO<sub>2</sub> Spent Nuclear Fuels. Effect of Burn-up and High Burn-up Structure. PhD Thesis, UPC-Barcelona Tech.
- Johnson, L., C. Ferry, C. Poinssot, P. Lovera (2004) Estimates of the Instant Release Fraction for UO<sub>2</sub> and MOX fuels at t=0. Nagra Technical Report 04-08.
- Roudil, D., Jégou, C., Broudic, V., Muzeau, B., Peugeot, S., Deschanel, X (2007) Gap and grain boundaries inventories from pressurized water reactors spent fuels. *Journal of Nuclear Materials*, 362, 411-415.
- Serrano-Purroy, D., Clarens, F., González-Robles, E., Glatz, J., Wegen, D., de Pablo, J., Casas, I., Giménez, J., Martínez-Esparza, A. (2012) Instant release fraction and matrix release of high burn-up UO<sub>2</sub> spent nuclear fuel: Effect of high burn-up structure and leaching solution composition. *Journal of Nuclear Materials*, 427, 249-258.



# SELECTION AND CHARACTERISATION OF HTR FUEL

Hilde Curtius<sup>\*</sup>, Emil Müller, Hans Walter Müskes, Martina Klinkenberg, Dirk Bosbach

Forschungszentrum Juelich GmbH (JÜLICH), DE

\* Corresponding author: h.curtius@fz-juelich.de

## Abstract

Spent UO<sub>2</sub> fuel samples produced for High Temperature Reactors (HTR) are used by Jülich within the project FIRST-Nuclides. After grinding and polishing of the miniature fuel element (the so-called coated particle) the obtained polished specimen was investigated with ESEM (Environmental scanning electron microscope) in order to gain information of the microstructure. Big pores and metallic islands are visible. An elemental mapping was performed and the elements Cs, Xe, Mo, Zr, U, O, Si and C were identified clearly. As expected the volatile elements Cs and Xe are mainly detected in the surrounding porous carbon layer, the so-called buffer.

ESEM investigation was performed with the fuel kernel itself. Big grains but small pores are visible at the periphery. The metallic islands form hexagonal platelets and contain the elements Zr, Tc, Mo.

The activities of nuclides of Cs, Eu, Ce, Ru, Sb, Rh, Pr and Am in a coated particle were determined by gamma spectrometric measurement. The measured values agree with the calculated values. A selective cracking process and a separation step were developed to distinguish clearly between the elemental distribution within the fuel kernel and the coatings. The fuel kernel and the coatings were leached respectively dissolved and the solutions obtained were analysed. The elements Am, Pu, Cm, U, Eu, Ce, Sr, Tc, and Pr are located quantitatively within the kernel. The activity distribution of the element Cs is extremely different. About 95% of the activity of Cs was detected in the coatings. Due to the low oxygen potential of the fuel-kernel and considering carbon oxidation during irradiation ternary Cs compounds are not stable and the only stable phase for Cs is gaseous. In this chemical form Cs was released from the fuel-kernel to the coatings.

## Introduction

Five fuel pebbles from the German production AVR GLE-4/2 were used at the High Flux Reactor in Petten and an experiment was performed which was called HFR-EU1bis. The irradiation started on

9 September 2004. After 249 full effective power days the experiment was terminated on 18 October 2005. For the pebble HFR-EU1bis/2 a burn-up of 10.2 % FIMA was determined. More experimental details are given in the following section “Selection of material”. Coated Particles drilled out from the pebble HFR-EU1bis/2 will be used in WP2.

WP2 focus on four topics:

1. The microstructure (grain boundaries, morphology, metallic islands, pore size and gas bubbles) before and after leaching.
2. Elemental mapping will go along with these investigations.
3. The determination of the radionuclide inventory by wet chemistry and other analytic tools. The experimental data obtained will be compared to the calculated radionuclide inventory.
4. The characterisation of the fission gas fraction and of the fast/instant release fraction of volatile radionuclides after contact with groundwater represents the main working goals.

Preliminary results of the four topics, microstructure, elemental mapping, radionuclide inventory and radionuclide distribution between coatings and fuel kernel are presented at the first annual workshop.

## 1. Selection of material

At the High Flux Reactor in Petten the experiment HFR-EU1bis was performed (Fütterer et al., 2006) using five fuel pebbles from the German production AVR GLE-4/2.

These fuel pebbles had a diameter of 60 mm and mainly consist of graphite. Each fuel pebble contained about 9560 so called TRISO coated particles with 502-micron diameter  $\text{UO}_2$  kernels, having 16.76  $^{235}\text{U}$  wt% enrichment; coating thickness were approximately 92, 40, 35 and 40 micron for porous carbon buffer, inner dense pyrocarbon layer (IPyC), silicon carbide (SiC) and outer dense pyrocarbon layer (oPyC). A fuel pebble represents a fuel element whereas a coated particle can be regarded as a “miniature fuel element” of about 1 mm in diameter. In **Figure 1** a fuel element (pebble) and a TRISO coated particle are illustrated.

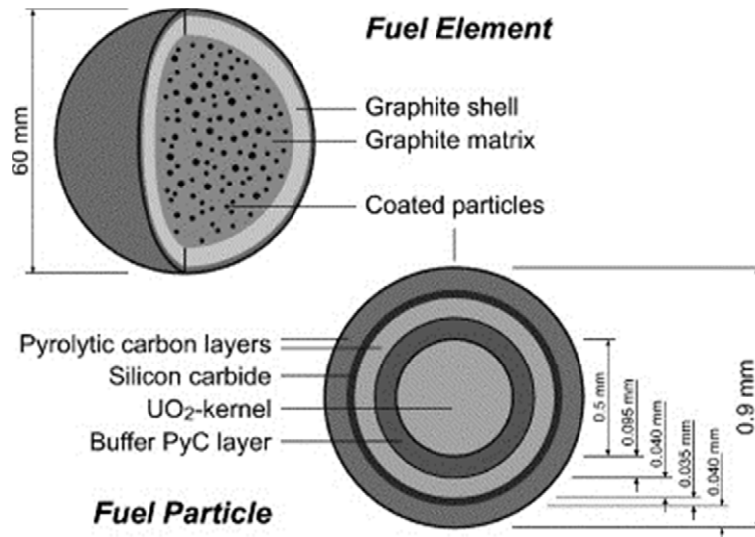


**Figure 1:** Design of a fuel element and a TRISO coated fuel particle

One pebble irradiated in Petten was called HFR-EU1bis/2 and a burn-up of 10.2% FIMA was determined. The main data are summarized in (Fütterer et al., 2008) and in **Table 1**.

**Table 1:** Main irradiation data for the pebble HFR-EU1bis/2

Nuclide	Bq/mgU
Enrichment	16.76 wt% $^{235}\text{U}$
Irradiation at:	High Flux Reactor Petten
Reactor cycles:	10
Irradiation:	249.55 (efpds)
Thermal fluences:	$2.23 \times 10^{25} \text{ m}^{-2}$
Fast fluences:	$3.98 \times 10^{25} \text{ m}^{-2}$
Central temperature of pebbles:	1250 °C
Power density:	30 W/cm <sup>3</sup>
FIMA:	10.2 %, (95.57 GWd/t)

From the fuel element named HFR-EU1bis/2 the TRISO coated particles were isolated by drilling and transported to the Forschungszentrum Jülich in December 2011.

With the OCTUPOS code the activities of the main radionuclides were calculated after a cool-down period of 1749 days (**Table 2**).

## 2. Microstructure investigations of the spent fuel sample and elemental mapping

A TRISO coated particle was embedded in a resin (Araldit DBF CH and Aradur HY 951) under vacuum. After 48 h a grinding and polishing process was performed. The wet grinding process was performed using sandpaper (SiC type, 35  $\mu\text{m}$  and 22  $\mu\text{m}$ ). As last step a wet polishing of the sample was performed with sandpaper (SiC-type, 5  $\mu\text{m}$ ). In **Figure 1** the polished specimen embedded in the resin is shown.

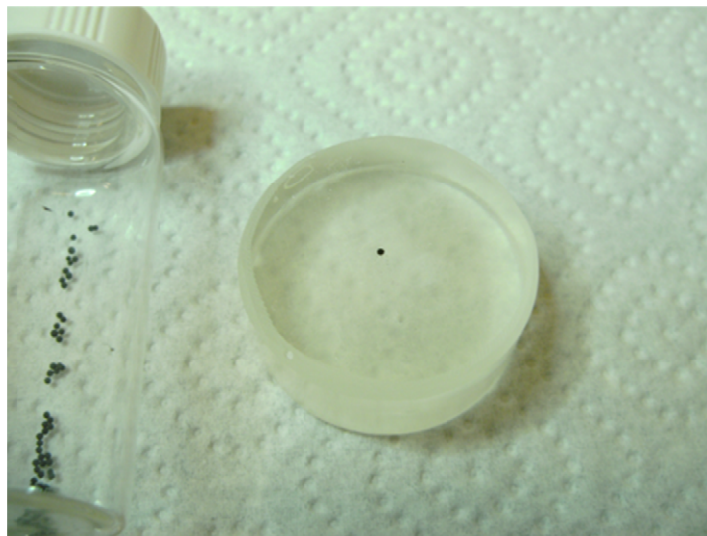


*Figure 1: TRISO coated fuel particle embedded in resin*

The prepared sample was then investigated with an environmental scanning electron microscope (ESEM).

A FEI Quanta 200 FEG instrument was used. The instrument is equipped with three detectors. The gaseous large field Secondary Electron-detector was used to characterize the morphology (grain boundaries, porosity). The back Scattered Electron-Detector was used to obtain chemical information due to the z-contrast (atomic number of the elements). With the Apollo X Drift detector the elemental mapping was performed (detection limit 0.1 wt%).

In **Figure 2** the SEM photo of the polished irradiated TRISO coated particle is shown. The polishing step was performed till the  $\text{UO}_2$  kernel was 350  $\mu\text{m}$  in diameter. Further grinding and polishing to the maximum diameter (500  $\mu\text{m}$ ) was not performed because it could be possible that the fuel kernel would get lost. Clearly the three tight coatings are visible. Due to the pressure build up during the irradiation period the porous carbon layer of the CP was pressed and a gap did formed.

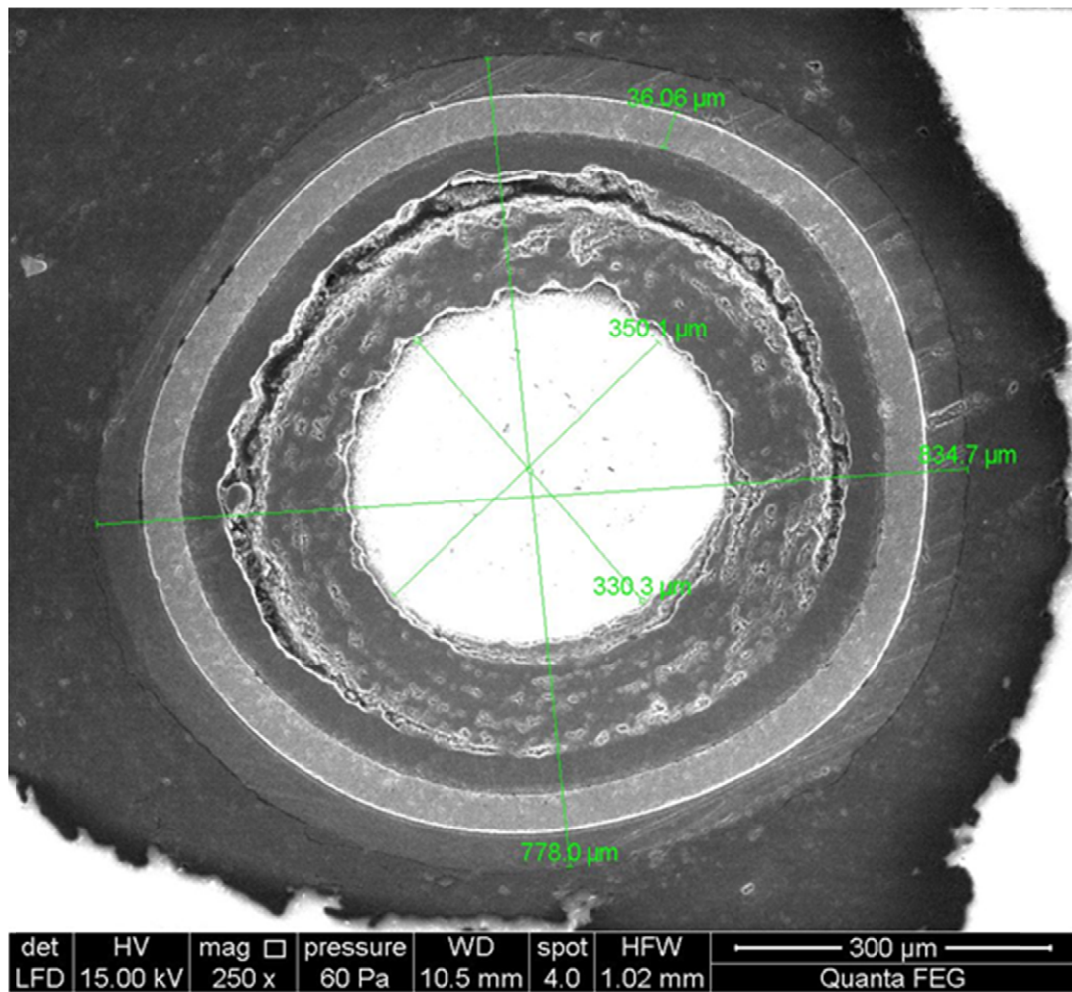


**Figure 2:** Polished TRISO coated fuel particle

The  $\text{UO}_2$  surface of the polished specimen itself is covered with big pores (up to 20  $\mu\text{m}$  in size) and many metallic inclusions (green circles) are visible (**Figure 3**).

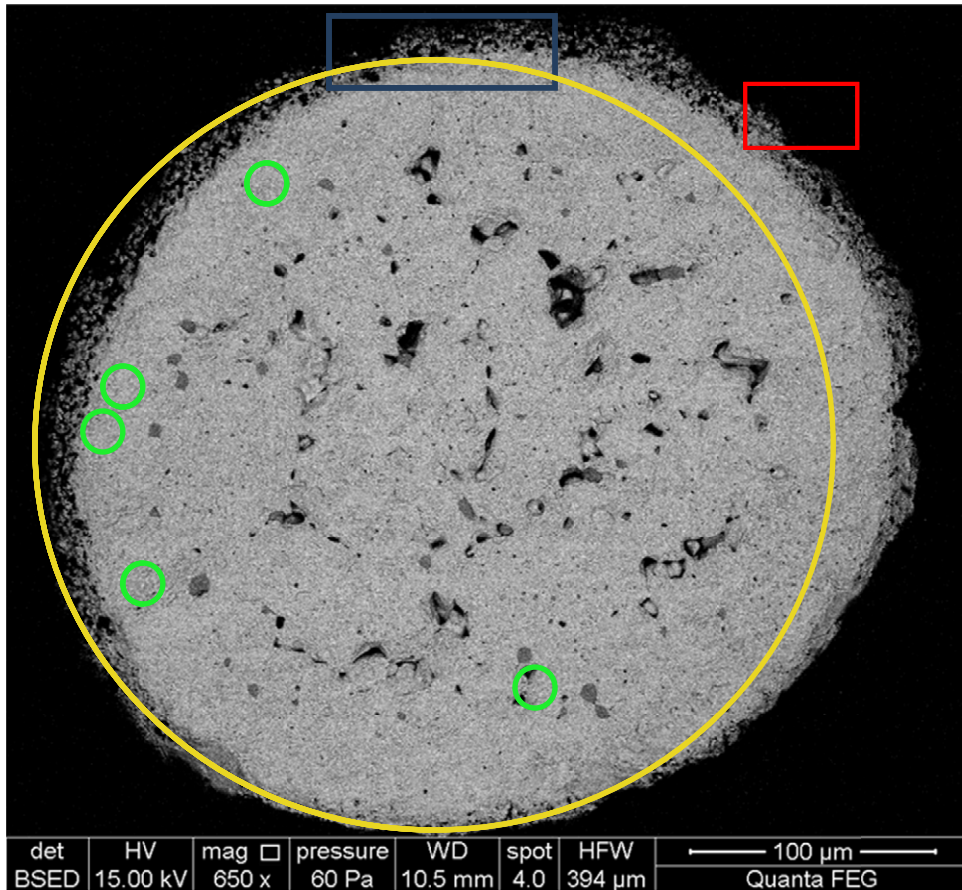


**Figure 3:** View of the  $UO_2$  surface covered with pores and metallic islands

Results from the elemental mapping did indicate the presence of Mo up to 8.4 wt% in these green spots. In the red and blue area (region of the buffer respectively region between kernel and buffer) a high accumulation of the fission gas Xe and the element Cs was determined indicating their high volatility. In the yellow area (whole surface of the kernel) the elements C, O, Si, U, Zr, Mo and Cs were identified clearly.

Besides the polished specimen investigations were focused on the microstructure of the periphery of the fuel kernel itself. A crack process was started using a modified micrometer screw and a self-constructed sample device. It was possible to separate the coatings from the fuel kernel selectively. The coatings were collected in a 20 ml polyethylene vial. The fuel kernel was stucked on a sample holder and analysed by SEM technique. Large grains (up to 112  $\mu m$ ) and grain boundaries are visible clearly (**Figure 4**). The elemental mapping revealed the presence of the following main elements: C 34.30 wt%, O 6.79 wt%, Zr 0.79wt%, Mo 4.82 wt%, Tc 2.02wt%, U 48.29 wt%, Cs 1.24 wt%. Nice metallic islands as hexagonal platlets (average size approximately 3  $\mu m$ ) are visible (**Figure 5**) and an elemental mapping reveal the presence of Mo 20.35 wt% , Zr 3.12 wt% and Tc 5.13 wt%.



At the periphery of the fuel kernel large grains and small pores exist. Many metallic islands as hexagonal platelets are detected as well.

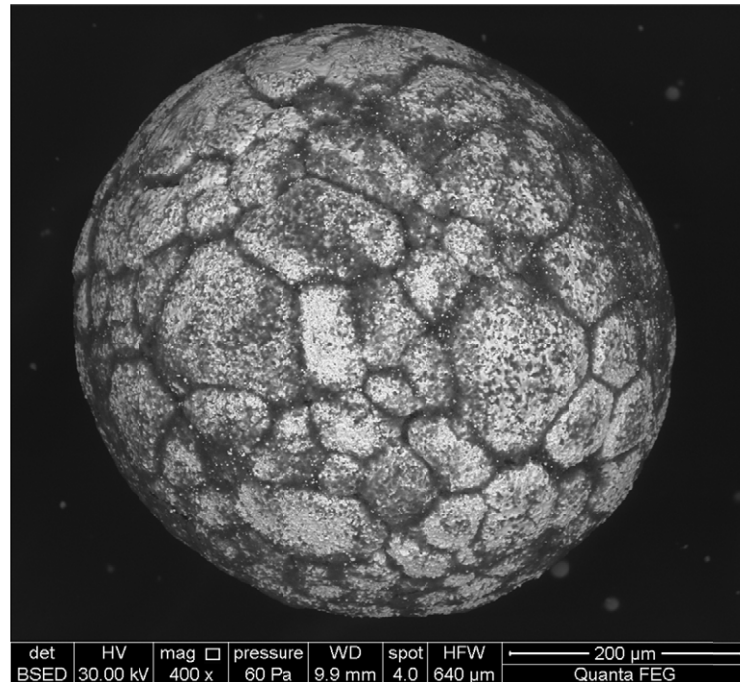


**Figure 4:** View of the UO<sub>2</sub> fuel kernel

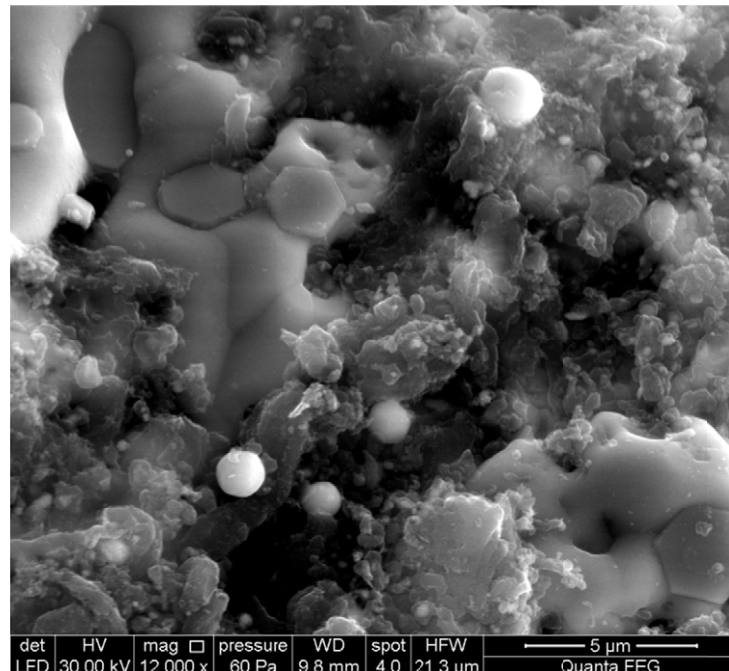


**Figure 5:** View of the UO<sub>2</sub> fuel kernel periphery with the metallic precipitates as hexagonal platelets

### 3. Radionuclide inventory

#### 3.2 *Gamma measurement of an irradiated coated particle*

The radionuclide inventory was calculated with the OCTOPUS code (Fütterer et al., 2008) after a cool-down period of 1749 days after end of irradiation on 18<sup>th</sup> October 2005. In **Table 1** the main radioisotopes and their activities for a coated particle (CP) are summarized. In order to compare these calculated values to measured values a gamma spectrometric measurement was performed. The irradiated TRISO coated particle was placed in a polyethylene tube, closed and the measurement was started. Two different detectors were attached to the gamma spectrometer; a HPGe detector type PGC 2018, Bias: 2500 V positive and a low energy germanium (LEGe) detector. The measure time was 86,400 sec. The sample has a distance to the HPGe detector of 60 cm and 50 cm to the LEGe detector. For determination of the radionuclide activities the software Gamma-W version 2.44 was used. The uncertainties of the values obtained are in the range between 10 to 13%.

The measured activities agree with the calculated values quite well (**Table 2**).

#### 3.3 *Determination of radionuclide activities by wet chemistry and different analytic tools*

After the gamma spectrometric measurement of the CP (coated particle) a crack process was started using a modified micrometer screw and a self-constructed sample device. It was possible to separate the coatings from the fuel kernel selectively. The coatings were placed in a 20 ml polyethylene vial. Then 10 ml Thorex reagent (mixture of 13 M HNO<sub>3</sub>, 0.05 M HF and 0.1 M Al(NO<sub>3</sub>)<sub>3</sub> x 9 H<sub>2</sub>O) was added and leaching was performed for 7 days. The isolated fuel kernel was placed in a 20 ml polyethylene vial and dissolved completely in 10 ml Thorex reagent.

Both sample solutions were used for further analytical steps in order to compare the calculated values to the measured activities and to gain information about the elemental distribution between coatings and fuel kernel.

First the activity of tritium in the chemical form as HTO was determined. From each sample solution 100 µl were diluted with 9.9 ml water and a subboil process (70°C) was performed. The condensate was collected and 1 ml was used for the β-measurement, performed with a Liquid Scintillation Counter (LSC, TRICARB 2200 A, Packard). Results are summarized in **Table 1** and indicate that only small activities (about 3.2%) of tritium as HTO are only present in the kernel. The main activity of tritium is expected in the gas fraction. Another β-measurement using 0.1 ml from each sample solution was

performed and the activity of  $^{241}\text{Pu}$  was determined.  $^{241}\text{Pu}$  is quantitatively present in the kernel (**Table 1**) and was not detected in the coatings (detection limit: 0.1 Bq/sample).

Then 1 ml from each sample solution was filled in a polyethylene vial and a  $\gamma$ -measurement was performed (HPGe detector type PGC 2018, Bias:2500 V positiv, counting time: 86,400 s, software: Gamma-W Version: 2.44: using  $^{152}\text{Eu}$  as standard solution with the same geometry, distance 15 cm). The uncertainties of the measured activities are in the range between 5% (high values) to 20% (low values). The radioisotopes  $^{144}\text{Pr}$ ,  $^{144}\text{Ce}$ ,  $^{154}\text{Eu}$  and  $^{155}\text{Eu}$  were identified and detected quantitatively in the kernel, but only about 5% of the activity of Cs was detected. Within the coatings the activity of Cs was determined to be about 95%. Under the conditions of irradiation a very low oxygen potential was present (taken carbon oxidation into account as well). Under this condition Cs does not form stable ternary compounds and the only stable phase is the gaseous one. A high release of Cs from the fuel kernel to the coatings took place (Barrachin et al., 2011).

Besides Cs the radioisotope  $^{90}\text{Sr}$  strongly contributes to the activity of the sample. The activity of  $^{90}\text{Sr}$  was determined after the following selective separation steps; 1 ml of each sample solution was diluted with 0.67 ml of a 1 M  $\text{HNO}_3$  solution. Then 1 ml of this solution was used to quantify the  $^{90}\text{Sr}$  activity. A colum (6 ml in volume) was filled with a suspension of 1 g resin (Sr-Resin, Eichrom-Company) in 5 ml of a 2 M  $\text{HNO}_3$  solution. The colum was washed two times with 5 ml of a 2 M  $\text{HNO}_3$  solution and then 5 ml of a 8 M  $\text{HNO}_3$  solution was added. Afterwards the sample solution was added to the column. The sample vial was rinsed with 1 ml of a 8 M  $\text{HNO}_3$  solution and this solution was added to the colum as well. Then a washing step with 10 ml of a 8 M  $\text{HNO}_3$  solution was performed. The washing solution was collected. After the washing steps  $^{90}\text{Sr}$  was eluated by using 10 ml of a 0.05 M  $\text{HNO}_3$  solution. Immediatly 1 ml of the eluat was used for the  $\beta$ -measurement. The main activity (  $95 \pm 2\%$ ) of Sr was detected in the kernel.

Then the activity of technetium was determined. First the washing solution of the Sr partition process was evaporated. The obtained residue was dissolved in a 2 M  $\text{HNO}_3$  solution (about 2 ml) and then used as sample soltuion for the Tc stripping. A colum (6 ml in volume) was filled with a suspension of 1 g Tc-Resin (TEVA-Resin, Eichrom-Company) in 5 ml of a 2 M  $\text{HNO}_3$  solution. The colum was washed two times with 5 ml of a 2 M  $\text{HNO}_3$  solution. Then the sample solution was added. Washing steps were performed with 10 ml of a 2 M  $\text{HNO}_3$  solution. After the washing process Tc was eluated with 10 ml of a 8 M  $\text{HNO}_3$  solution. The eluate was evaporated and the residue was dissolved in 1 ml of a 2 M  $\text{HNO}_3$  solution and the activity of Tc was determined by LSC. Tc is quantitatively present in the kernel.

An alpha-spectrometer (Octete, company Ortec, PIPS-detector (planar implanted passivated silicon)) was used to analyze the activities of the radionuclides U, Pu, Am, Np and Cm. 0.1 ml from both samples solutions were vaporized directly on metal disks and the measurement was performed for 250,000 sec. The results indicate that with these radionuclides are completely present in the kernel (**Table 2**). The activity for Np was below the detection limit.

**Table 2:** Radionuclide activities for a coated particle (CP) (uranium mass of 0.60476 mg) calculated with the OCTOPUS code (date: august 2010), measured activities \*\* for the coatings and for the fuel kernel from the sample solutions (date august 2012) and measured activities for the intact CP\* by  $\gamma$ -measurement (date august 2012).

Nuclide	Bq/CP	Bq/kernel **	Bq/coatings**	Bq/CP*
<sup>3</sup> H	2.37E+04	6.84E+02	n.d.	n.d.
<sup>90</sup> Sr	4.11E+06	3.18E+06	0.17E+06	
<sup>90</sup> Y	4.11E+06	3.18E+06	0.17E+06	
<sup>99</sup> Tc	9.86E+02	1.31E+03	0.97E+01	
<sup>106</sup> Ru	2.34E+06	1.33E+05	7.28E+04	3.10E+05
<sup>125</sup> Sb	3.95E+05	1.52E+04	3.54E+02	8.10E+04
<sup>134</sup> Cs	1.51E+06	2.58E+04	0.80E+06	0.84E+06
<sup>137</sup> Cs	6.47E+06	4.00E+05	6.36E+06	6.56E+06
<sup>144</sup> Pr	2.06E+06	0.35E+06	1.46E+03	0.37E+06
<sup>144</sup> Cer	2.05E+06	0.36E+06	1.18E+03	0.31E+06
<sup>154</sup> Eu	2.23E+05	1.14E+05	2.85E+02	1.20E+05
<sup>155</sup> Eu	1.22E+05	4.67E+04	1.52E+02	0.49E+05
<sup>234</sup> U	1.42E+02	1.82E+02	n.d.	
<sup>235</sup> U	2.95E+00	n.d.	n.d.	
<sup>236</sup> U	2.59E+01	3.33E+01	n.d.	
<sup>237</sup> Np	1.48E+01	n.d.	n.d.	
<sup>238</sup> Pu	5.75E+04	7.03E+04	2.45E+02	
<sup>239</sup> Pu	1.37E+04	1.09E+04	1.41E+01	
<sup>240</sup> Pu	1.69E+04	1.35E+04	1.55E+01	
<sup>241</sup> Pu	4.39E+06	2.47E+06	n.d.	
<sup>241</sup> Am	3.91E+04	3.11E+04	1.05E+02	2.15E+04
<sup>244</sup> Cm	1.20E+04	0.90E+04	1.33E+01	

n.d. : not detected

## **Conclusions and Future work**

Within the project First Nuclides UO<sub>2</sub>TRISO coated particles are used as spent fuel samples. ESEM investigations were performed to obtain information of the microstructure and of the elemental distribution. Big pores, large grains and metallic precipitates are visible in a polished specimen. The elements Cs, O, U, Mo, Xe, Zr and Si were identified whereas higher amounts of the volatile elements Cs and Xe were detected in the surrounding buffer. The periphery of an isolated fuel kernel revealed big grains and small pores. The metallic islands appear as hexagonal platelets and the elements Mo, Zr and Tc were identified clearly.

The activities of the elements Cs, Eu, Ce, Ru, Sb, Rh, Pr and Am of a coated particle were determined by  $\gamma$ -spectroscopy and agree with the calculated values.

A selective cracking, separation and dissolution/leaching step was performed to distinguish clearly between the elements in the fuel kernel and in the coatings. Then the radionuclides were identified by different analytical tools and their activities were determined.

The elements Am, Pu, Cm, U, Eu, Ce, Sr, Tc, and Pr are located quantitatively within the kernel according to the results. The element Cs is different. About 95% of the activity was found in the coatings. During irradiation a very low oxygen potential developed and under this condition Cs is only stable in atomic form in the gas phase. In this chemical form Cs the drastic release of Cs from the fuel kernel can be explained.

In future work the fission gas released during the crack process will be analysed. Further on in the beginning of 2013 isolated fuel kernels will be leached under oxic and anoxic/reducing conditions.

## **Acknowledgement**

Special thanks to Dr. Eric Mauerhofer and Norman Liek for the gamma- and alpha measurements.

*The research leading to these results has received funding from the European Union's European Atomic Energy Community's (Euratom) Seventh Framework Programme FP7/2007-2011 under grant agreement n° 295722 (FIRST-Nuclides project).*

## References

Barrachin, M., Dubourg, R., de Groot, S., Kissane, M. P., Bakker, K. (2011) Fission-product behaviour in irradiated TRISO-coated particles: Results of the HFR-EU-1bis experiment and their interpretation. *Journal of Nuclear Materials*, 415, 104-116.

Fütterer, M. A., Berg, G., Toscano, E., Bakker, K. (2006) Irradiation results of AVR fuel pebbles at increased temperature and burn-up in the HFR Petten. 3<sup>rd</sup> International Topical Meeting on High Temperature Reactor Technology, (Johannesburg, South Africa), B00000035.

Fütterer, M.A., Berg, G., Marmier, A., Toscano, E., Freis, D., Bakker, de Groot, S. (2008) Results of AVR fuel pebble irradiation at increased temperature and burn-up in the HFR Petten. *Nuclear Engineering and Design*, 238, 2877-2885.

# A COMBINED XRF / XAS STUDY OF SOME INSTANT RELEASE FRACTION RADIONUCLIDES IN HIGH BURN-UP UO<sub>2</sub> SPENT NUCLEAR FUEL

Annick Froideval Zumbiehl\*, Enzo Curti, Ines Günther-Leopold

Paul Scherrer Institut (PSI), CH

\* Corresponding author: annick.froideval@psi.ch

## Abstract

A combined X-ray fluorescence (XRF) and X-ray absorption spectroscopy (XAS) study of some relevant instant release fraction radionuclides - such as Se, Cs, and I - is proposed to be conducted on high burn-up UO<sub>2</sub> spent nuclear fuel in order to gain insight into the redox state and the microscopic distribution patterns of these radionuclides. This report mainly focuses on the description of the experimental methodology.

## Introduction

In the safety case for high-level radioactive waste repositories, aqueous corrosion of the waste plays a central role, since it determines the source term of radionuclide release to the environment. The direct disposal of irradiated nuclear fuel is an option adopted in many countries, implying that radionuclide release studies from spent UO<sub>2</sub> and MOX fuel are critical for the safety case. One of the major issues to be resolved is the reliable determination of the so-called “Instant Release Fraction” (IRF) i.e. the cumulative inventory fraction of segregated easily soluble nuclides (<sup>129</sup>I, <sup>135</sup>Cs, <sup>36</sup>Cl, <sup>79</sup>Se, <sup>14</sup>C, <sup>99</sup>Tc) which is released within weeks/months on contact with aqueous solutions. This initial phase is followed by slow radionuclide release following the dissolution of the UO<sub>2</sub>/PuO<sub>2</sub> lattice (“matrix dissolution”).

In the present study, we propose to gain insight into the chemical speciation and microscopic distribution patterns of some relevant IRF radionuclides such as Se, Cs and I, present in high burn-up UO<sub>2</sub> spent nuclear fuel. An analytical approach based on the combined use of synchrotron-based techniques such as X-ray absorption spectroscopy (XAS) and X-ray fluorescence (XRF) will thus be conducted on such radioactive nuclear material. The spectroscopic characterization (both on the microscopic and on the macroscopic scale) of selected IRF nuclides within the spent fuel matrix may

greatly help in understanding the mechanisms of fast initial release in aqueous solutions. We will particularly focus on Se, since this is the least known among the IRF nuclides. For instance, in recent experiments it was not possible to detect Se by ICP-MS in the leaching solution after interaction between spent nuclear fuel and aqueous solution, implying a leached inventory fraction of less than 0.22% (Johnson et al., 2012). Such results would be understandable if Se is present as (insoluble) reduced species ( $\text{Se}^0$  or  $\text{Se}^{-\text{II}}$ ) in the pristine spent fuel and would not undergo oxidation to soluble oxidized species ( $\text{Se}^{\text{IV}}$  or  $\text{Se}^{\text{VI}}$ ) during the leaching process. Therefore, one of the main goals of the proposed X-ray spectroscopic study will be the determination of the oxidation state of Se in the selected spent fuel samples before and after aqueous leaching.

## Materials

Two classes of materials are foreseen to be investigated in a first step of the experimental study:

(i) a high burn-up ( $\sim 75$  GWd/t, 9 cycles)  $\text{UO}_2$  spent nuclear fuel irradiated in the Leibstadt nuclear plant (KKL),

(ii) several non-irradiated  $\text{UO}_2$  reference materials containing simultaneously Se, Cs and I in amounts covering the concentration ranges expected in spent fuel.

The above mentioned fuel sample was selected for the feasibility study since the samples chosen for the FIRST-Nuclides leach experiments are not yet prepared in the hot cells of PSI (the work is scheduled for 2013) whereas a subsample of this rod is easily accessible due to earlier investigations in the frame of other post irradiation examination programs. Although the burn-up of this fuel is slightly higher than the samples envisaged for the leach experiments (57 – 64 GWd/t), a successful investigation of the 9 cycles- $\text{UO}_2$  fuel would give important insight into the Se redox state and would prove the depicted analytical concept.

It is foreseen to prepare the high burn-up  $\text{UO}_2$  spent nuclear fuel from KKL by using the peeling test method described in Degueldre et al. (2011). This method consists of polishing a section of the fuel segment by successively using silicon carbide and sand abrasive papers. The freed micro-particles of fuel are then removed from the surface of the fuel section and collected by pressing the fuel section on a piece of adhesive Kapton tape (see **Figure 1**). The peeling preparation method has the advantage to allow reducing the spent fuel sample to a size which limits the sample activity below  $100 \text{ LA}^1$  allowed at the microXAS beamline. A Kapton tape subsample with a total activity below the  $100 \text{ LA}$  limit will

---

<sup>1</sup> LA stands for the Swiss licensing limit, specified in Annex 3 Column 10 of the “Strahlenschutzgesetz, March, 22nd, 1991”



then be prepared for investigation at the microXAS beamline during an “active” measurement campaign.

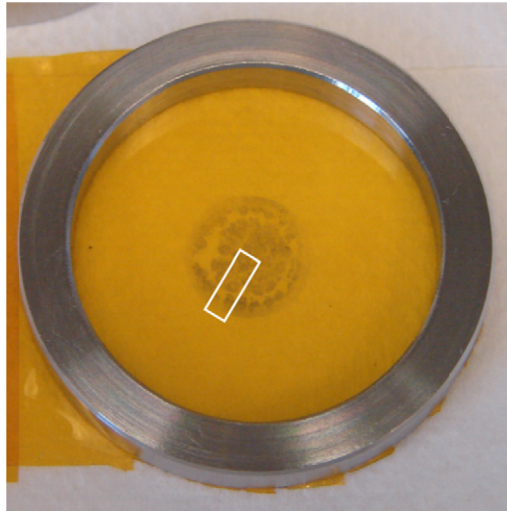


**Figure 1:** Picture of a MOX fuel segment cross section prepared by the peeling method (taken from Degueldre et al. 2011)

The  $\text{UO}_2$  reference materials (natural or depleted U) will be prepared with different concentrations of Se, Cs and I (approx. 10 ppm, 100 ppm, and 1000 ppm) in order to cover the range expected in low as well as in high burn-up spent fuel. **Figure 2** shows the estimated total Se concentrations in  $\text{UO}_2$  spent nuclear fuel from reactors operated with  $^{235}\text{U}$  and thermal neutrons.

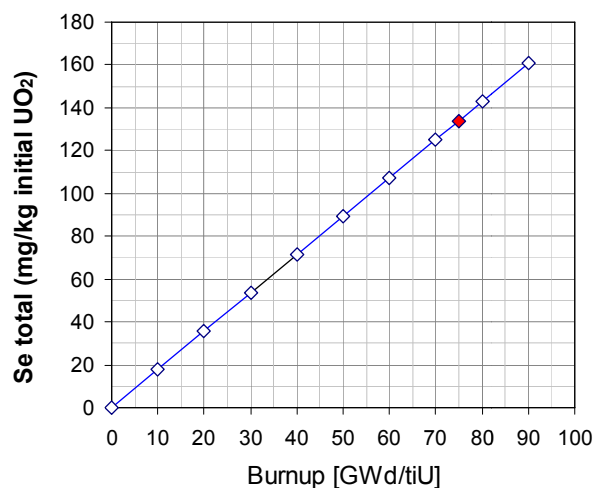


**Figure 2:** Total Se concentrations induced by fission of  $^{235}\text{U}$  by thermal neutrons as a function of burn-up, calculated using the fission yields of all relevant Se isotopes given in the IAEA interactive database (<http://www-nds.iaea.org/relnsd/vchart/>) assuming an energy of 200 MeV/fission. The red point corresponds to the KKL sample considered for the XAS/XRF feasibility study.

## Experimental approach

The spectroscopic characterization (both on the microscopic and on the macroscopic scale) of selected IRF nuclides within the spent fuel matrix is proposed to be investigated by using synchrotron-based techniques such as (micro-)X-ray fluorescence spectroscopy (micro-XRF) and micro-X-ray absorption spectroscopy (micro-XAS). Particular attention has been paid to choose suitable beamlines in terms of technical capabilities and allowance for active samples. The INE-beamline (ANKA synchrotron facility, KIT, Eggenstein-Leopoldshafen, Germany) and the microXAS beamline (SLS, Villigen PSI, Switzerland) were found to meet the necessary requirements for carrying out measurements on radioactive samples. However, they differ in the technical specifications:

(i) The range of photon energies delivered at the INE-beamline would allow collecting XANES spectra at the Se K-edge, as well as at the Cs L<sub>1</sub>-edge and the I L<sub>1</sub>- and I L<sub>2</sub>-edges; in contrast, the microXAS beamline has a more restricted energy range allowing measurements to be made only at the Se K-edge.

(ii) The micro-focusing capabilities of the microXAS beamline are excellent (with a size of the beam at the sample surface in the order of  $\sim 1 \times 1 \mu\text{m}^2$ ) making it the beamline of choice to collect spectroscopic information with a spatial resolution in the low micrometer level.

(iii) The primary photon intensity at the microXAS beamline is about a factor 100 larger than at the ANKA beamline.

(iv) ANKA has much higher activity limits, which would in principle allow the preparation of larger (and thus more representative) UO<sub>2</sub> spent fuel samples with a continuous surface.

Thanks to a past successful study performed at the microXAS beamline (SLS) on the characterization of plutonium-uranium mixed oxide by coupling micro-X-ray diffraction and absorption investigations (Degueldre et al., 2011), we believe that a similar synchrotron-based analytical approach could be conducted on a high burn-up spent UO<sub>2</sub> fuel sample (see **Table 1**). However, measuring IRF nuclides in a heavy spent fuel matrix is more challenging than only recording U and Pu absorption spectra. Specifically, the low concentrations in the 100 - 4000 ppm range and lower beam energies involved ( $E < 13 \text{ keV}$ ) will limit the number of excitable atoms.

These potential difficulties were the main reason for the decision taken to use non-irradiated UO<sub>2</sub> reference materials for a feasibility study. They will be used in preliminary measurements for verifying the detection limits for I, Cs and Se measurements in real spent fuel samples. Afterwards, micro- and bulk-XANES spectra are foreseen to be recorded at the Se K-edge on the high burn-up UO<sub>2</sub> fuel

sample. Such absorption spectra are expected to allow determining the redox state distribution of Se in the spent fuel sample with a spatial resolution close to few micrometers. This information is important to understand where, in the spent fuel texture, selenium is present as immobile Se(-II), Se(0) or mobile Se(IV), Se(VI) species contributing to the IRF. Knowledge of the redox state is expected to yield basic information on the mobility of these nuclides. For instance, selenium is known to be immobile in the reduced states Se(-II) and Se(0), whereas it becomes easily soluble upon oxidation to Se(IV), Se(VI) (Scheinost and Charlet, 2008). A proposal for beamtime request at the microXAS beamline will be submitted by Sept. 15, 2012.

Moreover, a beamtime proposal has been submitted to ANKA in the frame of the call n°20 (beamtime campaign: Oct. 2012 - March 2013) in order to obtain access to the INE beamline. The proposed experiment aims at investigating, on a microscopic (micrometer) scale, by means of XAS/XRF: (i) the distribution of IRF nuclides (Cs, I, Se) within the spent fuel texture, specifically whether I, Cs and Se are enriched in the porous rim of high burn-up spent fuel grains; (ii) the redox state and atomic coordination environment of Se through bulk via if possible) micro-EXAFS (if possible); (iii) the redox state of Se and I via micro-XANES measurements which will yield important information on the mobility of these nuclides. Unfortunately, beamtime could not be allocated in spite of the excellent scientific judgment of the proposal. Nevertheless, thanks to the common scientific interest, INE has agreed to provide – if possible within the very restricted beamtime currently available – “in-house” access to the INE beamline. This beamtime would be devoted to the aforementioned feasibility XAS/XRF study with UO<sub>2</sub> reference materials aiming at determining the detection limits of Se, Cs, I in UO<sub>2</sub>. Depending on the time schedule of the INE beamline, two options have been offered to us: (i) the allocation of two days of beamtime within the “in-house” beamtime pool or (ii) occasional test measurements depending on the time schedule of the beamline (see **Table 1**).

**Table 1:** Synchrotron-based methodology proposed to be conducted at the Swiss Light Source (SLS, Villigen PSI, Switzerland) and/or at the ANKA facility (Eggenstein-Leopoldshafen, Germany) in order to investigate relevant IRF nuclides in high burn-up  $UO_2$  spent fuel and in non-irradiated  $UO_2$  reference samples containing Se mixed with Cs and I

Techniques	Samples foreseen to be investigated:		
	high burn-up $UO_2$ spent fuel (from KKL nuclear plant)		$UO_2$ reference samples containing Se mixed with Cs and I <sup>a</sup>
	<b>Accessible elements and their corresponding emission lines:</b>		
(micro-)XRF	Se- $K\alpha_{1,2}$	Se- $K\alpha_{1,2}$	Se- $K\alpha_{1,2}$
	I- $L\alpha_{1,2}$		I- $L\alpha_{1,2}$
	Cs- $L\gamma_1$ , Cs- $L\beta_1$		Cs- $L\gamma_1$ , Cs- $L\beta_1$
	<b>Absorption edges:</b>		
(micro-)XANES	Se-K,	Se-K	Se-K
	Cs- $L_1$		Cs- $L_1$
	I- $L_1$ , I- $L_2$		I- $L_1$ , I- $L_2$
Beamline (facility)	INE (ANKA)	microXAS (SLS)	INE (ANKA)
Sample	$UO_2$ spent fuel	$UO_2$ spent fuel	$UO_2$ - reference samples ( <i>feasibility study</i> )
Status of the beamtime request	submitted, but not accepted (on waiting list)	to be submitted (by Sept. 15)	“in-house” INE beamtime, or, test measurements

Note: <sup>a</sup> The selenium, caesium and iodine concentrations will be approx. 10, 100, and 1000 ppm.

## Conclusions

An analytical approach based on the combined use of the (micro-)XRF and the (micro-)XAS synchrotron methods is proposed to be applied to a high burn-up  $UO_2$  spent fuel in order to gain insights into the redox state and the microscopic distribution patterns of some relevant IRF radionuclides such as Se, Cs and I, present in the nuclear material.

## Acknowledgements

Acknowledgments are due to J. Rothe, K. Dardenne (ANKA, KIT-INE) for their scientific interest in this project and for their technical and scientific advices in order to prepare a possible measurement campaign at the INE beamline (ANKA). D. Grolimund and C. Borca from the microXAS beamline (SLS, PSI) are also thanked for their scientific interest and their willingness to collaborate on this project. M. Martin and A. Bullemer (AHL/PSI) are thanked for the provision and for the preparation of the high burn-up  $UO_2$  spent nuclear fuel. The support of the group «Isotope and elemental analysis» (AHL/PSI) in preparation of the references samples is also thanked. Bernhard Kienzler (KIT-INE) is

greatly acknowledged for helpful discussions and his precious advice to carry out a preliminary feasibility study at ANKA with low-activity material.

*The research leading to these results has received funding from the European Union's European Atomic Energy Community's (Euratom) Seventh Framework Programme FP7/2007-2011 under grant agreement n° 295722 (FIRST-Nuclides project).*

## References

Deguelde, C., Martin, M., Kuri, G., Grolimund, D., Borca, C. (2011) Plutonium-uranium mixed oxide characterizations by coupling micro-X-ray diffraction and absorption investigations. *Journal of Nuclear Materials*, 416, 142-150.

Johnson, L., Günther-Leopold, I., Kobler Waldis, J., Linder, H. P., Low, J., Cui, D., Ekeroth, E., Spahiu, K., Evins, L. Z. (2012) Rapid aqueous release of fission products from LWR fuel: Experimental results and correlations with fission gas release. *Journal of Nuclear Materials*, 420, 54-62.

Scheinost, A. and Charlet, L. (2008) Selenite Reduction by Mackinawite, Magnetite and Siderite: XAS Characterization of Nanosized Redox Products. *Environmental Science and Technology*, 42, 1984-1989.



# FISSION GAS MEASUREMENTS AND DESCRIPTION OF LEACHING EXPERIMENTS WITH OF KIT'S IRRADIATED PWR FUEL ROD SEGMENT (50.4 GWD/THM)

Ernesto González-Robles\*, Elke Bohnert, Andreas Loida, Nikolaus Müller, Volker Metz, Bernhard Kienzler.

Karlsruher Institute fuer Technology (KIT), DE

\* Corresponding author: ernesto.gonzalez-robles@kit.edu

## Abstract

The study of the instant release fraction requires a better knowledge of the fission gas release and the radionuclide release during leaching experiments. In the present communication we explain the methodology to measure the fission gas release from a fuel rod puncturing test and, the instant release fraction from leaching experiments with samples from the same fuel rod segment. Additionally, a complete description of the materials, conditions and analytical methods that will be used during the leaching experiment is given. Results of the gas analyses from the puncturing test are presented.

## 1. Introduction

The disposal in deep bedrock repositories is considered as the preferred option for the management of spent nuclear fuel, SNF, in many countries (Johnson and Shoesmith, 1988; Shoesmith, 2000; Bruno and Ewing, 2007). The aim is to permanently and safely dispose of the radioactive material so that it is isolated from the biosphere for an appropriate length of time. A multi-barrier system is interposed between the SNF and the environment considering the SNF itself as the first technical barrier. In safety assessments for disposal of spent nuclear fuel (SNF) in deep underground repository, failure of canisters and loss of the integrity of fuel rods is considered in the long term. Some of the radionuclides within the SNF material will be directly exposed to water contact after the barrier failure. Assessing the performance of SNF in a potential future geological disposal system requires the understanding and quantification of the radionuclide release.

The release of the radionuclides into water will be constituted by two main processes (Johnsson et al., 2005; Poinssot et al., 2005): i) short term release of the so-called instant release fraction (IRF); ii) long term release dominated by the dissolution of the UO<sub>2</sub> grains, which is referred as matrix contribution.

The IRF is due to the segregation of a part of the radionuclide inventory to the gap interface between the cladding and the pellet, the fractures as well as to grain boundaries. The radionuclides that will be segregated are: fission gases (Kr and Xe), volatiles elements ( $^{129}\text{I}$ ,  $^{137}\text{Cs}$ ,  $^{135}\text{Cs}$ ,  $^{36}\text{Cl}$  and  $^{79}\text{Se}$ ) and segregated metals ( $^{99}\text{Tc}$  and  $^{126}\text{Sn}$ ) (Johnson et al., 2004). The degree of segregation of the various radionuclides is highly dependent on in-reactor fuel operating parameters such as linear power rating, fuel temperature, burn-up, ramping processes, and interim storage time. In the case of the fission gases, the gas release occurs by diffusion to grain boundaries, grain growth accompanied by grain boundary sweeping, gas bubble interlinkage and intersection of gas bubbles by cracks in the fuel (Johnson and Shoemith, 1988). The fission gas release is more correlated to the linear heat rating, which is also correlated to fuel temperature, than to the burn-up of the SNF (Kamikura, 1992, Johnson et al., 2004). The conditions during irradiation ensure that linear heat ratings are kept low and the fission gas release is minimised. The radionuclides located in the gap interface will be released after some weeks, whereas a complete release of the radionuclides segregated in the grain boundaries will take several months or even years.

During the last decade three European projects, SFS (Poinssot et al., 2005), NF-PRO (Grambow et al., 2008) and MICADO (Grambow et al., 2010) were carried out, in which, the IRF concept was revised and redefined as the radionuclide inventory located within microstructures with low confinement properties: fuel plenum, gap zone, fracture surfaces, the rim zone with high burn-ups structures and grain boundaries (Grambow et al., 2010).

The present work aims to analyse gases (in particular fission gases) released into the plenum of the fuel rod, and the development of an experimental procedure to measure the radionuclides that constitute the IRF during the performance of leaching experiments.

## **2. Materials, methods and results**

### *2.1 Investigated 50.4 GWd/t<sub>HM</sub> PWR fuel rod segment*

For the experimental studies, KIT-INE provided a HBU-SNF rod segment which had been irradiated during four cycles in the PWR Gösgen (KKG), Switzerland, and discharged in May 1989. During reactor operation an average burn-up of 50.4 GWd/t<sub>HM</sub> was achieved. Characteristic data of the studied segment N0204 of the KKG-BS fuel rod SBS1108 are given by Metz et al. (2012) and Wegen et al. (2012).



## 2.2 Gas analysis

Prior to the start of the leaching experiments, the fuel rod segment was carried to ITU for two purposes: i) characterization of the fuel rod segment (by means of non-destructive analyses in the first year of the FIRST-Nuclides project) and a puncturing to estimate the amount of fission gases present in the fuel rod segment; ii) the preparation of pellet-sized SNF samples.

### 2.2.1 *Experimental procedure*

Once the puncturing of the fuel rod segment was performed at ITU, the pressure was measured and gases were collected in stainless steel single-ended miniature sampling cylinders. The SS-4CS-TW-50 Swagelok gas sampling cylinders were characterised by a volume of 50 ml, a length of 159 mm, an outer diameter for tube fitting of 9.5 mm and an inner diameter for tube socket weld connection of 6.4 mm (**Figure 1**). The volume of the tubes is known and the total amount of gas could be calculated.

The cylinders were carried back to KIT-INE, where the gases were analysed by means of a quadrupole gas mass spectrometer (gas MS). The gas MS (GAM400, In Process Instruments, Bremen, Germany) was equipped with a Faraday and SEV detector and a batch inlet system (**Figure 1**). The batch-type gas inlet system was optimised for low gas sample consumption. Within the gas dosage and inlet system, the total gas pressure was controlled at four successive positions. It applied three different expansion-volumes to charge relatively low gas contents in the desired pressure range. Ten scans of each gas sample were measured, using the SEV-detector, and the mean value was taken. Calibration of the gas MS analysis was performed in the same pressure range as the respective range for analyses of the sample aliquots.

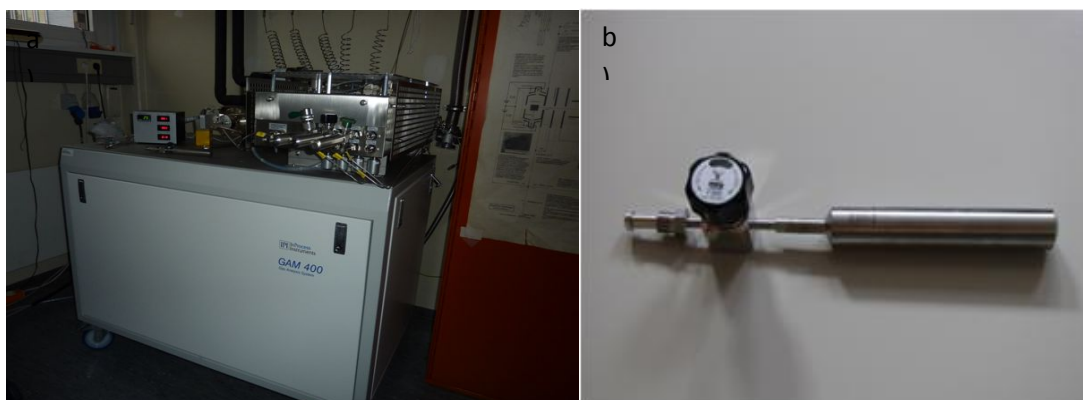


**Figure 1:** a) Image of GAM400 quadrupole gas mass spectrometer b) Image of a stainless steel single-ended miniature sampling cylinder used to collect gas samples

### 2.2.2 *Results*

**Table 1** presents the average values of gases measured in the samples taken from the puncturing test of the 50.4 GWd/t<sub>HM</sub> fuel rod segment. O<sub>2</sub> and N<sub>2</sub> contents in the gas composition (0.31 and 1.3 vol.%, respectively) are related to air contamination during the sampling of the cylinders. The gas released from the plenum of the punctured fuel rod segment contains a measurable content of CO<sub>2</sub>. In the past, similar CO<sub>2</sub> contents were observed in various fuel rod puncturing tests performed by some of the FIRST-Nuclides project partners, i.e. ITU, PSI, SCK-CEN and Studsvik. The measured contents of Kr and Xe will be compared to their calculated total inventory in the 50.4 GWd/t<sub>HM</sub> fuel rod segment, in order to determine the percentage of the fission gas released into the plenum.

**Table 1:** Concentration of gases and absolute gas volumes sampled during the puncturing test of the 50.4 GWd/t<sub>HM</sub> fuel rod segment

Gas	Concentration (vol.%)	Volume (cm <sup>3</sup> )
Ar	0.28	0.40
CO <sub>2</sub>	0.13	0.18
N <sub>2</sub>	1.3	1.87
O <sub>2</sub>	0.31	0.44
Kr	1.5	2.1
Xe	18	26
He	78	111

### 2.2.3 *Leaching experiments*

Three leaching experiments with samples of the 50.4 GWd/t<sub>HM</sub> fuel rod segment are foreseen to be conducted under anoxic conditions. The samples will be: one clad segment (as a pellet) and two declad SNF fragments. The experiments will be carried out in Ti-lined VA autoclaves (total volume 250 ml; **Figure 2**), with two valves in the lid to allow sampling of gases and of solutions during the experiment. A 10 mM NaCl + 1 mM NaHCO<sub>3</sub> solution is chosen as leachant, and the anoxic conditions will be achieved by application of a H<sub>2</sub> + Ar reducing atmosphere within the autoclaves ( 37 bar Ar +3 bar H<sub>2</sub>).

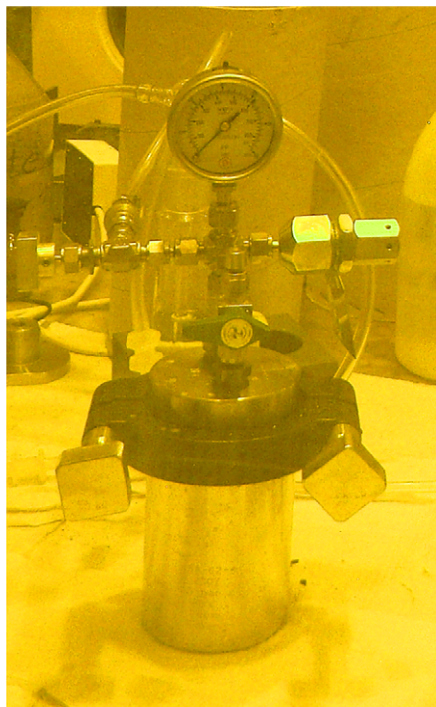


**Figure 2:** Image of a Ti-lined VA autoclave inside the shielded box-line of KIT-INE

At the beginning of the experiments two washing cycles will be performed with the same leachant as described before. At the end of each wash cycle, aliquots will be sampled for further analysis and the solution will be completely renewed. In the following static phase of the leaching experiments, small solution aliquots will be sampled at different time intervals to determine the kinetics of the IRF release. The leachant will not be replenished during this static phase.

#### 2.2.4 Gas sampling procedure

In parallel to the sampling of solution aliquots, the gas phase of the autoclaves will be frequently sampled. The main interest is in the release of the fission gases, Kr and Xe, as well as the radiolytic gases, H<sub>2</sub> and O<sub>2</sub>. **Figure 3** shows the system required to collect the gases from the autoclave positioned inside the shielded box-line of KIT-INE. Analyses of the gas samples will be performed using the quadropole gas MS system described above.

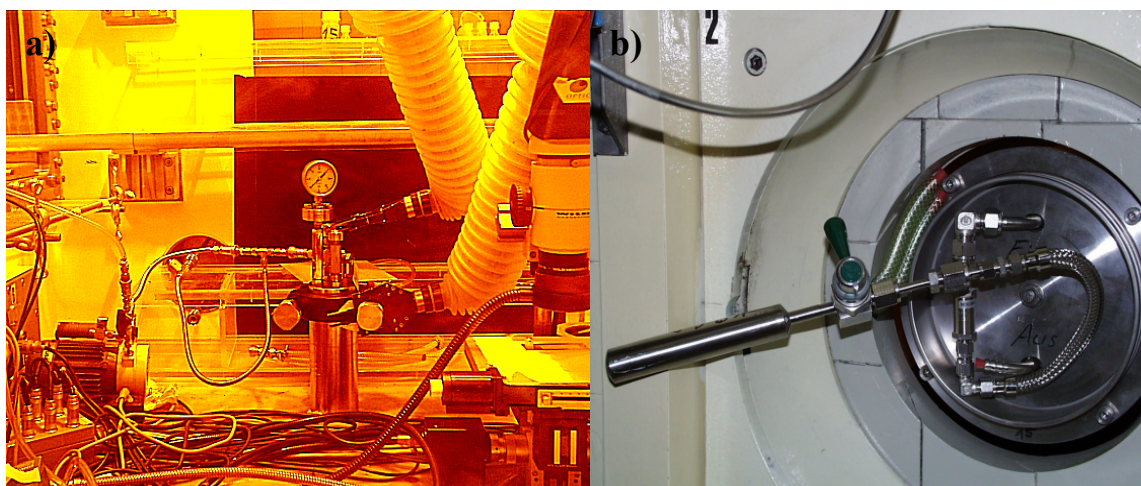


**Figure 3:** Images of the gas sampling system that will be using during the leaching experiments. a) Image of the interior of the shielded box-line of KIT-INE, showing the Titanium valves and stainless steel tubings, which connect the autoclave to the out of the hot cell. b) Image of out part of the hot cell, showing the connection between the autoclave (coming from the previous figure) and the sample cylinder used to collect the gases.

### 2.2.5 Aqueous sampling procedure

The aqueous solution will be analysed to determine the specific activity of  $^{134}\text{Cs}$ ,  $^{135}\text{Cs}$ ,  $^{137}\text{Cs}$ ,  $^{90}\text{Sr}$ ,  $^{241}\text{Pu}$ ,  $^{129}\text{I}$ ,  $^{79}\text{Se}$ ,  $^{14}\text{C}$ ,  $^{36}\text{Cl}$ ,  $^{238}\text{Pu}$ ,  $^{239}\text{Pu}$ ,  $^{240}\text{Pu}$ ,  $^{238}\text{U}$ ,  $^{99}\text{Tc}$ ,  $^{237}\text{Np}$ . Following analysis methods will be applied:

- $\gamma$ -spectrometry for concentration measurements of  $^{134}\text{Cs}$ ,  $^{137}\text{Cs}$ . The separation of these radionuclides from the original solution is described in Grambow et al. (1996). Afterwards the analysis is performed by means of Ge-detectors (EGC-15-185-R and GX3018, Canberra Industries Inc, Meriden, USA).
- Liquid scintillation counting (LSC) using a Packard Tri-Carb 3110TR Low activity scintillation analyser (Perkin Elmer INC, Waltham, USA) to quantify:  $^{90}\text{Sr}$ ,  $^{241}\text{Pu}$ ,  $^{14}\text{C}$ . Solution aliquots will be homogenised with a LSC-Cocktail (Ultima Gold XR, Packard) before measurement.
- $\alpha$ -spectrometry will be used to determine the amount of  $^{238}\text{Pu}$ ,  $^{239}\text{Pu}$ ,  $^{240}\text{Pu}$  using a analysis chamber with a S100 field channel analysator ( $^{238}\text{Pu}$ ,  $^{239/240}\text{Pu}$ ) and passivated implanted planar silicon (PIPS) detectors (Canberra 74/01, Canberra Industries Inc, Meriden, USA) which combine high resolution and low backgrounds in a rugged alpha detector with active areas up to  $1200\text{ mm}^2$ . It integrates into one package a stainless steel vacuum chamber for low backgrounds and ease of cleaning, a vacuum gauge, detector bias supply, preamp/amplifier, pulser, discriminator, counter, and digital display. A stainless steel shelf and sample holder are

included for reproducible detector/sample spacing, which is user selectable from 1 to 49 mm, in 4 mm increments

- Inductively coupled plasma mass spectrometer (ELAN 6100, Perkin Elmer Inc, Waltham, USA) to measure the concentrations of  $^{79}\text{Se}$ ,  $^{238}\text{U}$ ,  $^{99}\text{Tc}$ ,  $^{237}\text{Np}$ .

### 3. Summary and future work

KIT-INE provided a 50.4 GWd/t<sub>HM</sub> fuel rod segment in the ownership of KIT-INE, where all data and findings can be published without restrictions. This HBU-SNF was transported to ITU for characterisation, gas sampling, cutting and sampling of fuel pellets. Gas samples and fuel pellets were returned to KIT for further investigations. Results of the measured fission gas contents will be compared to their theoretical total inventory in order to estimate the percentage of fission gas that was released into the plenum of the fuel rod segment. The analytical method for the gas measurements will also be applied to fission gases obtained during dissolution based experiments.

KIT-INE will perform three static leaching experiments with a pellet-sized cladded segment and two decladded SNF fragments. These experiments will be conducted under reducing conditions in autoclaves performing regular sampling of gases and solutions. The methodology that will be followed during the performance of the leaching experiment is explained in the present communication. Within the following months the leaching experiments will be started.

### Acknowledgements

The authors would like to thank our colleagues at JRC-ITU, in particular to R. Gretter, Ramil Nasyrow, Dimitrios Papaioannou, Wim de Weerd and Detlef Wegen for performing the puncturing test of the 50.4 GWd/t<sub>HM</sub> PWR fuel segment, as well as for non-destructive analyses, cutting the segment and further activities related to the characterization of the samples.

*The research leading to these results has received funding from the European Union's European Atomic Energy Community's (Euratom) Seventh Framework Programme FP7/2007-2011 under grant agreement n° 295722 (FIRST-Nuclides project).*

## References

- Bruno, J. and Ewing, R.C. (2006) Spent nuclear fuel. *Elements*, 2, 343-349.
- Grambow, B., Loida, A., Dressler, P., Geckeis, H., Gago, J., Casas, I., de Pablo, J., Gimenez, J., Torrero M.E. (1996) Long-term safety of radioactive waste disposal: Chemical reaction of fabricates and high burn-up spent UO<sub>2</sub> fuel with saline brines. Final report FZKA 5702 Forschungszentrum, Karlsruhe, Germany.
- Grambow, B., Lemmens, K., Minet, Y., Poinssot, C., Spahiu, K., Bosbach, D., Cachoir, C., Casas, I., Clarens, F., Christiansen, B., de Pablo, J., Ferry, C., Giménez, J., Gin, S., Glatz, J.P., Gago, J. A., Gonzalez Robles, E., Hyatt, N. C., Iglesias, E., Kienzler, B., Luckscheiter, B., Martinez-Esparza, A., Metz, V., Ödegaard-Jensen, A., Ollila, K., Quiñones, J., Rey, A., Ribet, S., Rondinella, V. V., Skarnemark, G., Wegen, D. H., Serrano-Purroy, D., Wiss, T. (2008) Final Synthesis Report for NF-PRO: “Understanding and Physical and Numerical Modelling of the Key Processes in the Near-Field and their Coupling for Different Host Rocks and Repository Strategies”. RTD Component 1: Dissolution and release from the waste matrix. F16W-CT-2003-02389. European Commission, Brussels, Belgium.
- Grambow, B., Bruno, J., Duro, L., Merino, J., Tamayo, A., Martin, C., Pepin, G., Schumacher, S., Smidt, O., Ferry, C., Jegou, C., Quiñones, J., Iglesias, E., Rodríguez-Villagra, N., Nieto, J. M., Martinez-Esparza, A., Loida, A., Metz, V., Kienzler, B., Bracke, G., Pellegrini, G., Mathieu, G., Wasselin-Trupin, V., Serres, C., Wegen, D., Jonsson, M., Johnson, L., Lemmens, K., Liu, J., Spahiu, K., Ekeroth, E., Casas, I., de Pablo, J., Watson, C., Robinson, P., Hodgkinson, D. (2010) MICADO, Model uncertainty for the mechanism of dissolution of spent fuel in nuclear waste repository. Final activity report. European Commission, Brussels, Belgium.
- Johnson, L. and Shoesmith, D.W. (1988) Spent Fuel in Radioactive Waste Forms for the Future. W. Lutze and R.C. Ewing, Eds. (North-Holland, Amsterdam), 635-698.
- Johnson, L., Ferry, C., Poinssot, C., Lovera, P. (2004) Estimates of the Instant Release Fraction for UO<sub>2</sub> and MOX fuels at t=0. Nagra Technical Report 04-08.
- Kamikura, K. (1992) FP gas release behaviour of High Burn-up MOX fuel for Thermal Reactors. Proceedings of Technical Committee Meeting on Fission Gas release and Fuel Rod Chemistry Related to Extended Burnup. IAEA-TEDOC-697.

Metz, V., Loida, A., González-Robles, E., Bohnert, E., Kienzler, B. (2012) Characterization of irradiated PWR UOX fuel (50.4 GWd/t<sub>HM</sub>) used for leaching experiments. Proceedings of 7<sup>th</sup> EC FP – FIRST-Nuclides 1<sup>st</sup> Annual Workshop (Budapest, Hungary).

Poinssot, C., Ferry, C., Kelm, M., Grambow, B., Martínez Esparza, A., Johnson, L., Andriambololona, Z., Bruno, J., Cachoir, C., Cavedon, J. M., Christensen, H., Corbel, C., Jegou, C., Lemmens, K., Loida, A., Lovera, P., Miserque, F., De Pablo, J., Poulesquen, A., Quiñones, J., Rondinella, V. V., Spahiu, K. and Wegen, D. (2005) Final report of the European project Spent Fuel Stability under repository conditions. CEA Report, CEA-R-6093.

Shoesmith, D.W. (2000) Fuel corrosion process under waste disposals. *Journal of Nuclear Materials*, 282, 1-31.

Shoesmith, D.W. (2007) Used Fuel and Uranium dissolution studies - A review. NWMO Technical Report, NWMO-TR-2007-03.

Wegen, D.H., Papaioannou, D., Nasyrow, R., Gretter, R., de Weerd, W. (2012) Non-destructive analysis of segment N0204 of the spent fuel pin SBS1108 (in prep.).





# CHARACTERIZATION OF SCK•CEN FUEL SAMPLES USED FOR LEACH TESTS IN FIRST-NUCLIDES

Kevin Govers\*, Marc Verwerft, Wouter Van Renterghem, Karel Lemmens, Thierry Mennecart, Christelle Cachoir, Lesley Adriaensen, Andrew Dobney, Mireille Gysemans

Studiecentrum voor Kernenergie (SKN-CEN), BE

\* Corresponding author: kgovers@sckcen.be

## Abstract

In the framework of the FIRST-Nuclides program, SCK•CEN will conduct leaching experiments on a PWR UOX fuel, taken from the Belgian Tihange 1 reactor, with a rod average burnup of 50 MWd/kg<sub>HM</sub> in order to determine the rapid release of some of the most critical radionuclides. Considering the influence of the irradiation parameters on the actual location of fission products at the beginning of the leaching test, the interpretation of the experimental results highly relies on a good characterization of the fuel samples. This article will deal with the characterization of the fuel rod and samples that will be used for the leach tests performed at SCK•CEN.

## Introduction

As one of the partners of FIRST-Nuclides with a hot-cell infrastructure and the required analytical laboratories, SCK•CEN will perform leach tests on spent fuel samples with a relatively high burn-up. For this purpose, a fuel rod was selected from the spent fuel stock available at SCK•CEN for which the characteristics are known and can be made public.

In the past, several fuel rods irradiated under high duty conditions in Tihange 1 PWR reactor, have been extracted from their assembly to perform post-irradiation experiments at SCK•CEN laboratories. These fuel rods and relevant results of the previous post-irradiation examination (PIE) campaign are available for further research. These fuel rods are therefore good candidates for correlating leach tests measurements to FGR results.

The present article provides the characteristics of the fuel rod that will be used for the leach tests at SCK•CEN (Mennecart, et al., 2012). It is a PWR UOX fuel from the Belgian Tihange 1 reactor irradiated about 12 years ago during cycles 20 and 21 up to an average burnup of about 50 MWd/kg<sub>HM</sub>.

We show the scheme according to which the samples will be cut for further characterization and for the leach tests. Detailed irradiation data are not available yet and will be reported at a later stage. In the meantime pellet average isotopic composition has been estimated based on the calculated burnup.

## **Fuel rod characteristics**

### *Fuel rod history*

The Tihange 1 NPP, located in Belgium, is a PWR reactor loaded with 15×15 fuel assemblies usually operated at an elevated linear power. Two fuel rods located at symmetrical positions (D05 and E12) in the assembly have been extracted from assembly FT1X57 for non-destructive and destructive analyses in the SCK•CEN laboratories (Sannen and Pathoens, 2003). Fuel rod D05 has been selected for use in FIRST-Nuclides and will be further characterized in this paper.

Details about the power history at rod and sample level will be reconstructed by the operator during the first phase of the FIRST-Nuclides project, based on reactor power history and power distribution mapping of the core. At present, generic data are available: the final rod-average burnup, estimated as 50.0 MWd/kg<sub>HM</sub> for rod D05, was achieved in two cycles of 18 months each. The intermediate burnup was about 28.1 MWd/kg<sub>HM</sub>.

### *Rod fabrication data*

The geometry of assembly FT1X57 consists of a 15×15 array of fuel rods with 21 unfuelled locations (guide tubes) for potential insertion of control rods or instrumentation. The cladding material is M5. Nominal data about the fuel rod design can be found in **Table 1**. Batch data relative to rod dimensions and fuel composition are reported in **Table 2**.

**Table 1:** Nominal (design) data – rod D05, fuel assembly FT1X57

<b>Assembly type</b>		<b>AFA 2G</b>
Assembly geometry		15 × 15
# of fuel rods per assembly		204
Rod pitch	(mm)	14.3
<b>Fuel</b>		
Type		UO <sub>2</sub>
Enrichment (nominal)	(% U <sup>235</sup> /U <sub>tot</sub> )	4.25
Density (nominal)	(% TD)	96
Average grain size	(µm)	10
<b>Cladding</b>		
Type		M5 recrystallized
Composition		Nominal M5
• Nb	(wt.%)	0.8 – 1.2
• Fe	(wt.%)	0.015 – 0.06
• O	(wt.%)	0.09 – 0.12
• Zr	(wt.%)	balance
External diameter	(mm)	10.720
Thickness	(mm)	0.618
Internal diameter	(mm)	9.484

### Cutting scheme definition

Fuel rods D05 and E12 were cut, after non-destructive tests, into four segments of about 1 m length each. The samples for the leach tests will be taken from the second segment (from the bottom) of rod D05, internally referred to as FT1X57-D05/R4. The burnup profile between the end of the first span up to the end of the fifth span is indeed relatively constant, as shown by the  $\gamma$ -activity measurement (see **Figure 1**), except close to grid locations. Activity peaks are observed at regular intervals in the central zone, indicating volatile product migration to colder zones at inter-pellet locations. A large contribution to the signal originates from Cs isotopes. There is, however, no indication of major redistribution of volatile fission products along the fuel rod, which would be characterized by a slightly depleted signal at the centre and higher activity in the bottom and top parts.

The samples to be used for the leach tests will consist of two pellets. The samples are cut from mid-pellet to mid-pellet in order to keep a representative inventory of the volatile elements that relocate at pellet-pellet interfaces. Two other samples are taken for fuel characterization. The first one is used for radiochemical analysis (RCA) of the fission product and actinides inventory; enabling the average pellet burnup to be determined. The second one is used for optical microscopy (OM) and

determination of the local element composition by electron-probe micro-analysis (EPMA). An additional spare sample is also foreseen. The proposed cutting scheme is illustrated in **Figure 2**. Signal peaks, regularly spaced by about 11.8 mm, were exploited to identify pellet-pellet interfaces. The samples are located in the flat  $\gamma$ -activity zone, far enough away from the grid locations. Although the axial burnup is expected to be homogeneous over the sampling zone, leach test samples are proposed to be flanked by the sample used for burnup determination by RCA and the sample used for OM / EPMA. The spare sample is located the closest to the third grid location, next to the OM / EPMA sample.

**Table 2:** Batch data – rod D05

<b>Fuel rod</b>		
Rod total length	(mm)	3861.9
Active fuel stack length	(mm)	3634.9
Plenum length	(mm)	205.1
Diametrical pellet-clad gap	( $\mu\text{m}$ )	190
He filling pressure	(bar)	20
<b>Fuel characteristics</b>		
Material		UO <sub>2</sub>
Density	(% TD)	96.44
Mass metal/oxide	(g <sub>U</sub> / g <sub>UO<sub>2</sub></sub> )	88.13
U isotopic composition		
<sup>234</sup> U / U <sub>tot</sub>	(wt%)	0.038
<sup>235</sup> U / U <sub>tot</sub>	(wt%)	4.251
<sup>236</sup> U / U <sub>tot</sub>	(wt%)	0.001
<sup>238</sup> U / U <sub>tot</sub>	(wt%)	95.71
Impurities / additives		Not available yet
<b>Pellet dimensions</b>		
Diameter	(mm)	9.294
Length	(mm)	11.15
Dish		
• Depth	(mm)	0.34
• Spherical radius	(mm)	16.70
Chamfer		
• Height	(mm)	0.20
• Width	(mm)	0.57

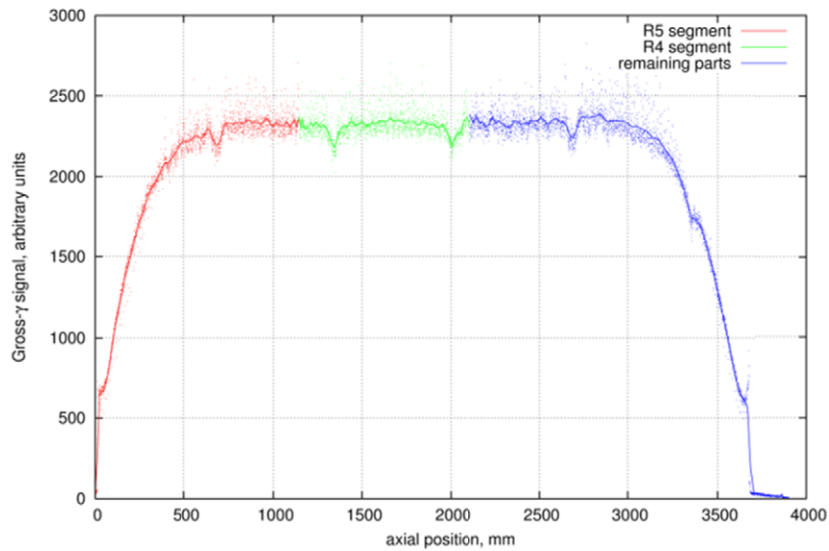


**Figure 1:** Gross- $\gamma$  scanning of rod D05. Measurements were acquired every 0.5 mm using a collimator. The line (a guide for the eye) clearly identifies the activity drop due to support grids. The flat activity profile over most of fuel rod length is characteristic of high burnup fuel.

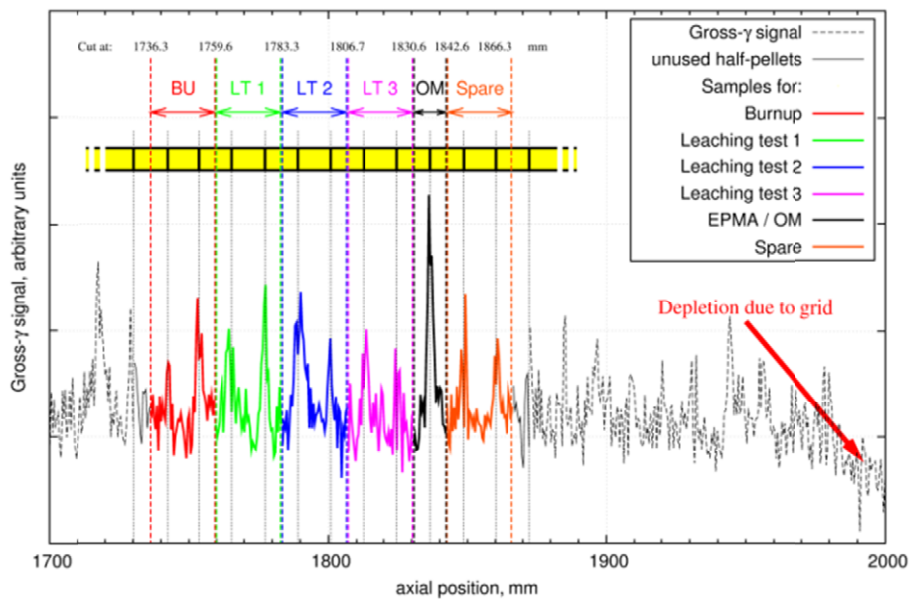


**Figure 2:** Proposed cutting scheme of segment FT1X57-D05/R4. Three samples are intended for leaching experiments. One sample will be used for burnup determination and another one for optical microscopy and EPMA. An additional spare sample is currently being considered.

### Estimated isotopic inventory

Although the detailed power history has not yet been provided by the reactor operator and the burnup is still approximate, fuel composition can be estimated using robust tools. The following results have

been derived using the ORIGEN-ARP module available in SCALE 6.1 (ORNL, 2011). It contains pre-compiled cross-section libraries for several LWR fuel assembly designs, among which the PWR 15 × 15 lattice. Variations in fuel composition, burnup and moderator density are handled through interpolation of the library data.

A simplified, constant, power history has been postulated over 2 cycles of 500 days each, reflecting the 18 months cycles of the selected high duty fuel rods. A shutdown period of 50 days has been assumed between both cycles and a storage time of 10 years after the irradiation.

The power level has been varied (see **Figure 3**) to examine the sensitivity of the fuel composition to the burnup after 10 years storage, which is representative of the specimen considered in the present study. Two burnup levels are highlighted in **Figure 4** and **Figure 5** corresponding respectively to the rod average burnup and sample burnup. One should keep in mind that values calculated with neutronic codes reflect isotopic production and decay but do not model fission product redistribution (migration).

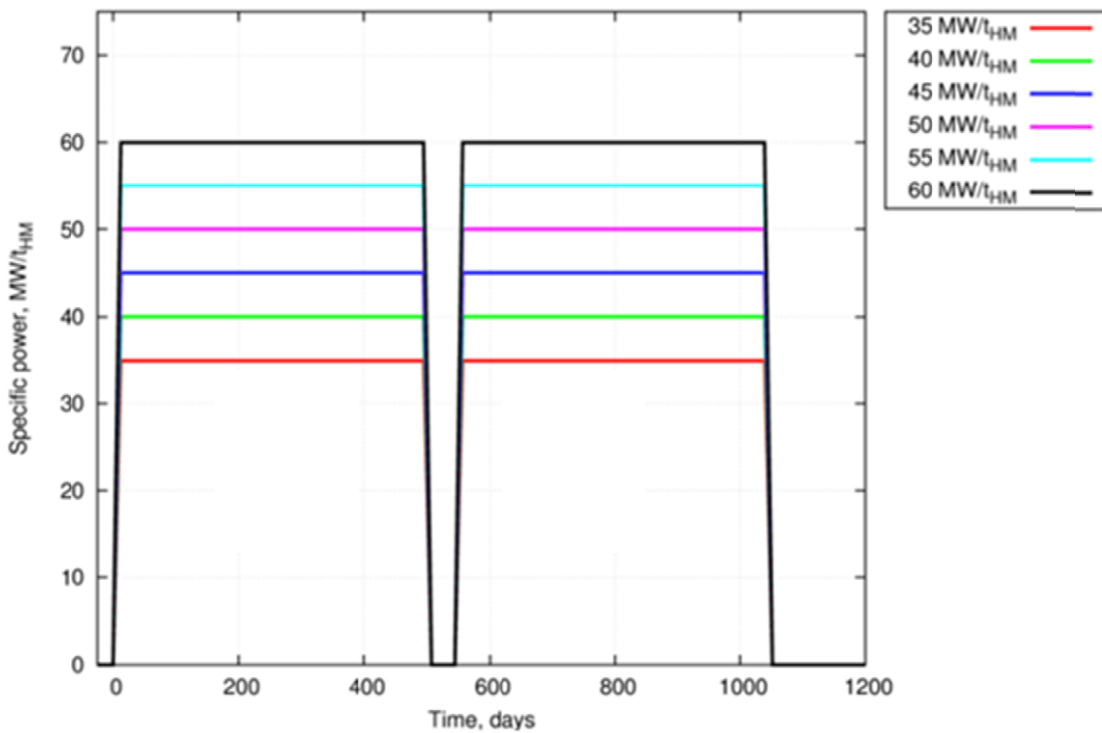


**Figure 3:** Simplified power history for the various burnup cases. We have assumed 2 cycles of 500 days at constant power. Additional calculations will be performed once the detailed power history is available.

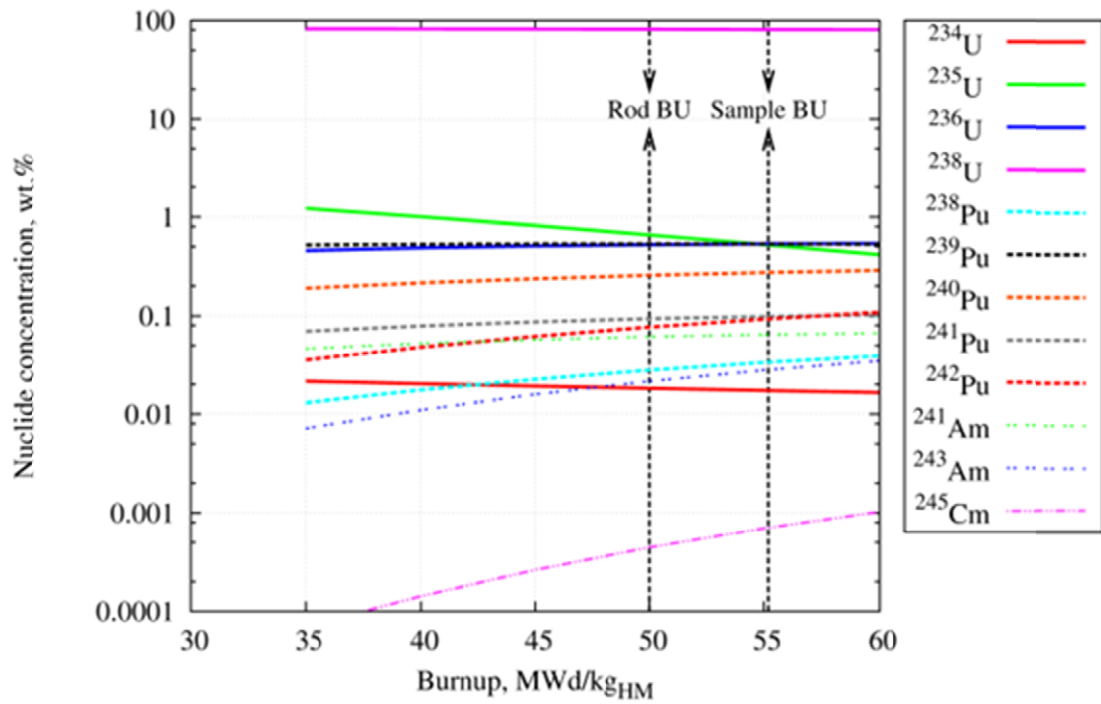


**Figure 4:** Actinide inventory evolution with disposal burnup, after 10 years of decay. Vertical arrows indicate the approximate rod and sample burnups.

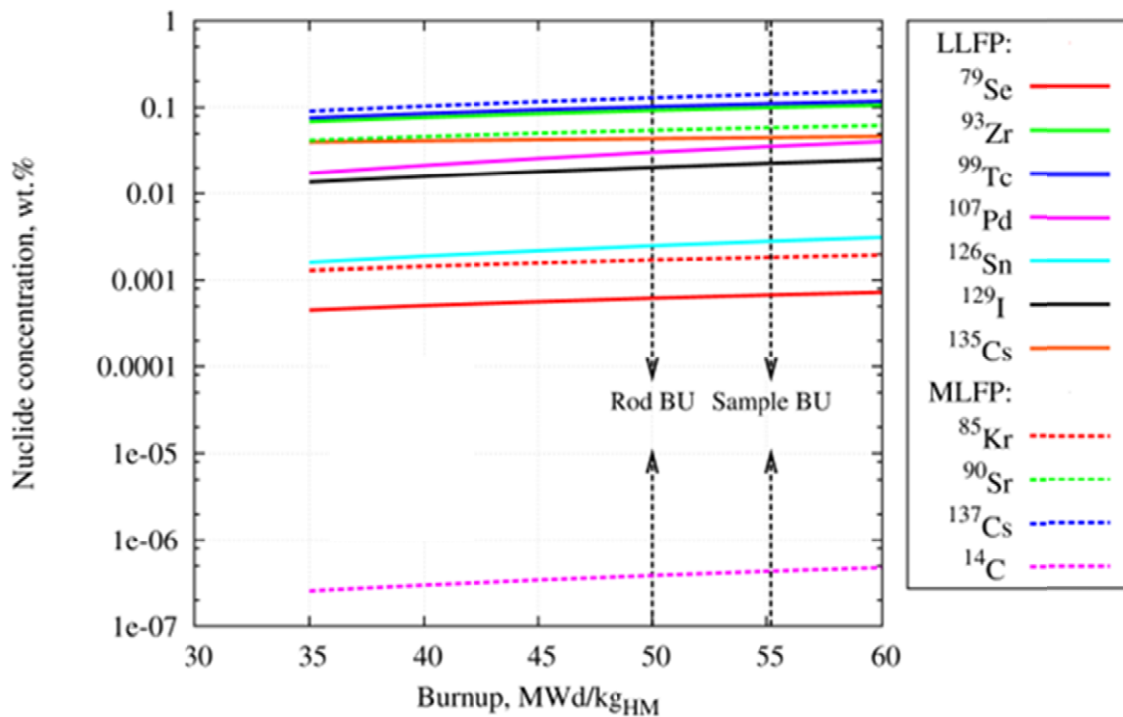


**Figure 5:** Relevant (in terms of the leaching test experiments) long- and medium-lived radioisotope inventory evolution with disposal burnup, after 10 years of decay. Vertical arrows indicate the approximate rod and sample burnups.

## Conclusions and Future work

This article summarizes the fabrication data currently available for dissemination amongst First-Nuclides partners. It will be complemented later by the detailed power history of the rod (i.e. including axial profile) for which calculations by the plant operator should become available in the coming weeks. Further characterization of the sample will be made using optical microscopy, radiochemical analysis and electron-probe microanalysis.

## Acknowledgement

The authors wish to thank Areva (fuel manufacturer), Electrabel (plant operator) and Tractebel (engineering office, support to operator) for providing agreement to use the fuel for additional research.

*The research leading to these results has received funding from the European Union's European Atomic Energy Community's (Euratom) Seventh Framework Programme FP7/2007-2011 under grant agreement n° 295722 (FIRST-Nuclides project).*

## References

- Mennecart, T., Lemmens, K., Govers, K., Adriaensen, L., Cachoir, C., Dobney, A. (2012) Concept of leach test for the experimental determination of IRF radionuclides from Belgian high burnup spent nuclear fuel in First-Nuclides. Budapest, Hungary.
- ORNL. (2011) Scale: A Comprehensive Modeling and Simulation Suite for Nuclear Safety Analysis and Design. Available from Radiation Safety Information Computational Center at Oak Ridge National Laboratory as CCC-785.
- Sannen, L., and Parthoens, Y. (2003) R-3788 - Framatome – Tihange 1: Assembly FT1X57 – Rods E12 and D05 – Non-destructive evaluation, Puncture, H<sub>2</sub> analysis. Mol, Belgium: SCK-CEN.



# SELECTION OF HIGH BURN-UP FUEL SAMPLES FOR LEACH EXPERIMENTS AND SPECTROSCOPICAL STUDIES AT PSI

Ines Günther-Leopold\*, Hans-Peter Linder, Annick Froideval Zumbiehl, Enzo Curti

Paul Scherrer Institut (PSI), CH

\* Corresponding author: ines.guenther@psi.ch

## Abstract

The selection of suitable high burn-up spent nuclear fuel samples available in the Hot Laboratory of the Paul Scherrer Institut (PSI) that will be used for leach experiments and XRF/XAS studies to investigate the instant release fraction (IRF) and the redox state of relevant radionuclides in the frame of the FIRST Nuclides project is described in this report. The data required for the characterization of fuel and cladding were collected and compiled.

## Introduction

WP3 “Dissolution based release” of the FIRST Nuclides project targets the quantification of the fast release of gaseous and non-gaseous activation and fission products into the aqueous phase during spent nuclear fuel leach tests. The present report describes the characteristics of the high burn-up fuel samples selected for leach experiments foreseen to be carried out in the Hot Laboratory of PSI.

The experiments will cover high burn-up  $\text{UO}_2$  and mixed oxide (MOX) spent nuclear fuels from boiling water reactor (BWR) and pressurized water reactor (PWR) having burn-up in the range of 57 to 64  $\text{GWd/t}_{\text{HM}}$ . Special emphasis will be given to the determination of IRF values of Cs, I, Se and  $^{14}\text{C}$  as well as to the Se redox state. The results from these leaching experiments on fuel samples with and without cladding, as well as cladding fragments alone, should help gaining insight into the contribution of the cladding material onto the  $^{14}\text{C}$  IRF values.

## Characteristics of the selected fuel samples

PSI is able to perform leach experiments on maximum nine fuel samples in parallel in the “Dissolution box” of the Hot Laboratory. The test matrix was defined by selecting three samples (cladded fuel,

cladding and fuel fragments) from an  $\text{UO}_2$  fuel rod irradiated in the Leibstadt BWR (KKL), as well as six samples (cladded fuel, fuel fragments, cladding with and without fuel residues) from the Gösgen PWR (KKG), of which four originate from an  $\text{UO}_2$  fuel rod and two from a MOX fuel rod. In addition to a previously published study (Johnson et al., 2012) fuel fragments and cladding of this MOX fuel rod will be leached separately in order to complete the available data set for this material.

The information given in this paper is also compiled within the Deliverable 1.1 (“Characterisation of spent nuclear fuel samples to be used in FIRST-Nuclides – relevance of samples for the Safety Case”, issued June 2012).

*High burn-up UO<sub>2</sub> fuel from BWR*

Details on the selected UO<sub>2</sub> BWR fuel rod from KKL are given in **Table 1**.

**Table 1:** Characterisation data of the UO<sub>2</sub> BWR fuel selected for PSI investigations

<b>Data category</b>	<b>Parameter</b>
Reactor	Leibstadt NPP, Switzerland Boiling Water Reactor
Fuel assembly design information	10 x 10 Lattice SVEA96 Optima, fuel assembly AIA003, rod position H6, Node 4
Assembly / cladding material composition	Zircaloy-2, designation LK3/L
Fuel rod data	Fission gas release: 2.26% Rod length as fabricated: 4146.6 Rod length after irradiation: 4163.3 Internal rod pre-pressure: 7 bar
Fuel material (pellet) data	UO <sub>2</sub> , initial enrichment: 3.9% <sup>235</sup> U Pellet diameter (as fabricated): 8.77 ± 0.013 mm Pellet length: 10.7 ± 0.8 mm Density (spec) 10.52 ± 0.19 g/cm <sup>3</sup> Density as fabricated 10.48 – 10.54 g/cm <sup>3</sup> Grain size 6 ≤ x ≤ 25 μm
Fuel sample data	Sample position 455 mm to 520 mm from BEP
Cladding sample data	Zircaloy-2 with liner, designation LK3/L Cladding outer diameter: 10.30 ± 0.04 mm Cladding inner diameter: 8.94 ± 0.04 mm Liner Thickness 70 ± 40 μm
Irradiation data	Rod average burnup: 57.5 GWd/t <sub>U</sub> , exp. determined local burnup: 6.1% FIMA Number of cycles: 7 Date of loading: August 1998 Date of unloading: April 2005 Duration of irradiation: 2400 days Average linear power: ~ 160 W/cm Max. linear power: 270 W/cm

*High burn-up UO<sub>2</sub> fuel from PWR*

Details on the selected UO<sub>2</sub> PWR fuel rod from KKG are given in **Table 2**.

**Table 2:** Characterisation data of the UO<sub>2</sub> PWR fuel selected for PSI investigations

<b>Data category</b>	<b>Parameter</b>
Reactor	Gösgen NPP, Switzerland PWR
Fuel assembly design information	KKG-14B-4021-01-0129 Lattice geometry: 15x15, 48 assemblies with 20 control rods/assembly Fuel rod diameter: 10.765 mm Fuel rod diameter after irradiation: 10.697 mm
Assembly / cladding material composition	Zircaloy 4, DX HPA4 (0.6Sn)
Fuel rod data	Test rod Fission gas release: 13.2%, 51.5 bar Internal rod pre-pressure: 22 bar Rod length as fabricated: 3860 mm Rod length after irradiation: 3879 mm Active length: 3550 mm
Fuel material (pellet) data	UO <sub>2</sub> , initial enrichment: 4.3% <sup>235</sup> U Fuel density (as fabricated): 10.45 g/cm <sup>3</sup>
Fuel sample data Cladding sample data	Sample position 2620 mm to 2695 mm from BEP Cladding outer diameter: 10.75 ± 0.05 mm Cladding inner diameter: max. 9.45 mm Max. Oxide: 36 µm
Irradiation data	Rod average burnup: 62.2 GWd/t <sub>U</sub> , exp. determined local burnup: to be performed Number of cycles: 4 Date of loading: 28.7.1999 Date of unloading: 28.6.2003 Duration of irradiation: 1324.43 days

*High burn-up MOX fuel from PWR*

Details on the selected MOX PWR fuel rod from KKG are given in **Table 3**.

**Table 3:** Characterisation data of the MOX PWR fuel selected for PSI investigations

<b>Data category</b>	<b>Parameter</b>
Reactor	Gösgen NPP LPWR
Fuel assembly design information	KKG-13-5024-10-676 Lattice geometry: 15x15 48 assemblies with 20 control rods/assembly Fuel rod diameter: 10.76 mm (measured) Fuel rod diameter after irradiation: 10.736 mm
Assembly / cladding material composition	Duplex ELS0.8b
Fuel rod data	Test rod Fission gas release: 26.7%, 76.4 bar Internal rod pre-pressure: 22 bar Rod length as fabricated: 3859.0 mm Rod length after irradiation: 3886.1 mm Active length: 3550 mm
Fuel material (pellet) data	MOX, initial enrichment: 5.5% Pu <sub>fiss</sub> Fuel density (as fabricated): 10.45 ± 0.15 g/cm <sup>3</sup> Fuel density after irradiation: 9.903 g/cm <sup>3</sup> Pellet diameter (as fabricated): 9.13 ± 0.013 mm
Fuel sample data	Sample position 2030 mm to 2070 mm from BEP
Cladding sample data	Cladding outer diameter: 10.75 ± 0.05 mm Cladding inner diameter: 9.30 ± 0.04 mm Max. Oxid: 36 µm
Irradiation data	Rod average burnup: 63.0 GWd/t <sub>U</sub> , exp. determined local burnup: 7.3% FIMA Number of cycles: 4 Date of loading: 30.06.1997 Date of unloading: 07.07.2001 Duration of irradiation: 1368 days Average linear power: 306 W/cm (average fuel rod power in 4 cycles) Max. linear power: approx. 430 W/cm

## Cutting plans

For each of the selected fuel rods one suitable fuel segment with a maximum length of 70 cm (due to pre-cutting for emplacement in the PSI Hot Laboratory dry storage facility) was selected and a segment cutting plan was compiled, similar to the one shown in **Figure 1** for the UO<sub>2</sub> PWR fuel sample. The actual sampling position of the sub-samples for the leach experiments are given in Tables 1 to 3. The cutting plans were forwarded to the Hot Cell group of the Hot Laboratory. The retrieval of the fuel samples from the dry storage facility, the cutting of the segments and the further sample treatment in view of generating isolated cladding samples and fuel fragments are scheduled for spring 2013.

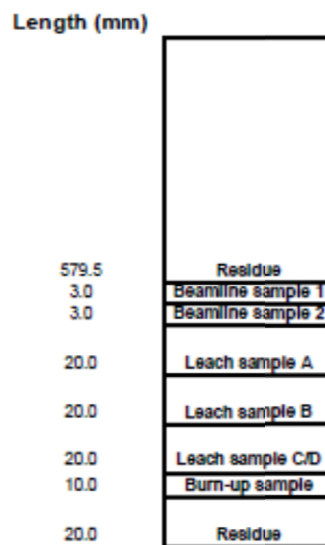


**Figure 1:** Cutting plan for the selected high burn-up UO<sub>2</sub> PWR fuel segment

## Leach equipment

Since the handling of the leaching equipment has to be performed with manipulators in the shielded dissolution box of the Hot Laboratory, the design has to be as simple as possible. For the experimental setup it was decided to use the same design as the one already used in an earlier study (Lawrence et al., 2012). The experimental setup consists of glass columns (total volume approx. 250 ml) with a sealed outlet cock for sampling and an integrated glass filter in order to prevent the clogging of the cock by solid particles. The equipment used in the above mentioned previous study is shown in **Figure 2**. Technical discussions with SCK•CEN have resulted in the agreement that both laboratories will use the same design for the experimental studies in the frame of the FIRST-Nuclides project.

The glass components for the leach equipment are already ordered, whereas the pistons will be manufactured in-house. The experimental setup will be manufactured till end of 2012.

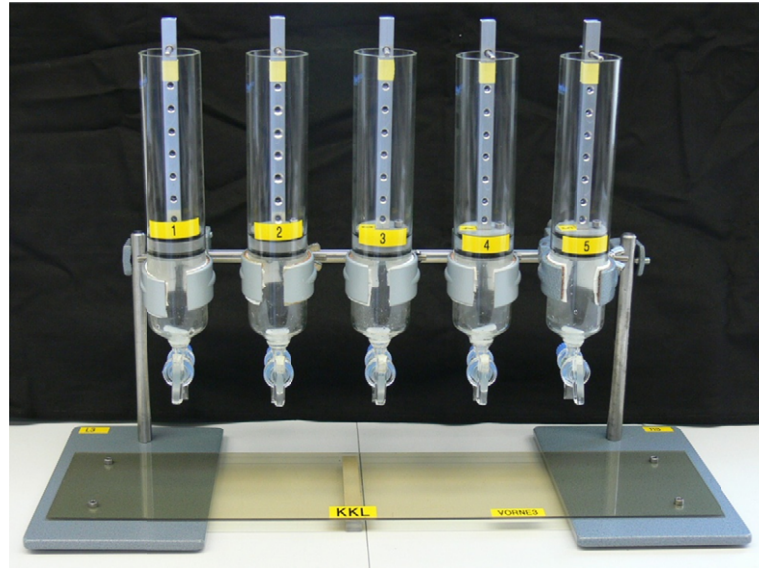


**Figure 2:** *Assembly of five glass columns with pistons designed and used for earlier PSI leaching experiments*

### **Acknowledgement**

The support and recommendations of L. Johnson (Nagra) concerning the sample selection are greatly acknowledged. The authors thank M. Martin (AHL/PSI) for technical and scientific advices in view of sample preparations for the proposed measurement campaigns at the INE (ANKA, KIT, Germany) and microXAS (SLS, PSI) beamlines.

*The research leading to these results has received funding from the European Union's European Atomic Energy Community's (Euratom) Seventh Framework Programme FP7/2007-2011 under grant agreement n° 295722 (FIRST-Nuclides project).*

### **References**

Johnson, L., Günther-Leopold, I., Kolber Waldis, J., Linder, H.P., Low, J., Cui, D., Ekeroth, E., Spahiu, K., Evins, L.Z. (2012) Rapid aqueous release of fission products from high burn-up LWR fuel: Experimental results and correlations with fission gas release. *Journal of Nuclear Materials*, 420, 54-62.





# CHARACTERISATION OF SPENT VVER-440 FUEL TO BE USED IN THE FIRST-NUCLIDES PROJECT

Zoltán Hózer\*, Emese Slonszki

Magyar Tudományos Akadémia Energiatudományi Kutatóközpont (MTA EK), HU

\* Corresponding author: zoltan.hozer@energia.mta.hu

## Abstract

Dissolution rates of different isotopes from VVER fuel will be determined in the FIRST-Nuclides project based on activity measurements at the Paks NPP. The present report summarizes the design and operational characteristics of fuel that were stored in the given periods in the spent fuel storage pool of the power plant. The isotope inventories are also included in order to facilitate the calculation of fractional release rates.

## Introduction

In the framework of the FIRST-Nuclides project the MTA Centre for Energy Research will produce fuel dissolution data on VVER fuel. There were two series of measurements at the Paks NPP that can be used for the evaluation of fuel dissolution in wet environment:

- a) In 2003 thirty fuel assemblies were damaged at the power plant during a cleaning tank incident. The integrity of fuel cladding was lost and most of the fuel pellets had direct contact with the coolant. The damaged fuel was stored in a special service area of the spent fuel storage pool for almost four years. During this period the activity concentration was regularly measured. Using the measured data the dissolution rates of different isotopes can be calculated.
- b) In 2009 a leaking fuel assembly was identified at the NPP. The assembly was removed from the reactor core and the placed in the spent fuel storage pool. The power plant decided to launch a special measurement programme for the investigation of activity release from the leaking fuel rod in wet storage conditions. The measured data allows us to produce dissolution rates for these conditions, too.

As a first step of analyses the fuel assemblies have to be characterised. In the present report the main geometrical, design and operational data will be summarised for both damaged and leaking VVER–440 fuel assemblies.

## 1. Characterisation of damaged fuel

On 10 April 2003 severe damage of fuel assemblies took place during an incident at Unit 2 of Paks Nuclear Power Plant in Hungary (Hózer et al., 2010; NEA/CSNI/R, 2008; Slonszki et al., 2010; Hózer et al., 2009). The assemblies were being cleaned in a special tank below the water level of the spent fuel storage pool in order to remove crud buildup. That afternoon, the chemical cleaning of assemblies was completed and the fuel rods were being cooled by circulation of storage pool water. The first sign of fuel failure was the detection of some fission gases released from the cleaning tank during that evening. The cleaning tank cover locks were released after midnight and this operation was followed by a sudden increase in activity concentrations. The visual inspection revealed that all 30 fuel assemblies were severely damaged. The first evaluation of the event showed that the severe fuel damage happened due to inadequate coolant circulation within the cleaning tank.

The damaged fuel assemblies were removed from the cleaning tank in 2006 and are stored in special canisters in the spent fuel storage pool of the Paks NPP.

Following several discussions between expert from different countries and international organisations the OECD–IAEA Paks Fuel Project was proposed.

The Project will focus on the numerical simulation of the most important aspects of the incident. A database necessary for the code calculations was collected. This data is available for the FIRST-Nuclides project.

### 1.1. Design characteristics of VVER-440

The fuel assembly data were collected from open literature (Solonin et al., 1997). The main data is listed below. The list includes both working and follower type VVER-440 assemblies. Both types can be found among the damaged assemblies.

Length of (working) fuel assembly	3217 mm
Length of (follower) fuel assembly	3200 mm
Shroud material	Zr 2,5%Nb
Cladding material	Zr 1%Nb

Number of fuel rods	126
Fuel assembly key size	144 mm
Lattice pitch	12.2 mm
Fuel rod length	2550 mm
Fuel column length (working assembly)	2420 mm
Fuel column length (follower assembly)	2320 mm
Outer cladding diameter	9.15 mm
Cladding thickness	0.65 mm
Pellet diameter	7.57 mm
Central hole diameter	1.2-1.8 mm
Pellet-cladding gap	0.15-0.26 mm
Pellet shape	chamfered
Pellet height	9-12 mm
Pellet density	10.4-10.8 g/cm <sup>3</sup>
Pellet densification max.	0.4%
Helium pressure	0.5 MPa
Free fuel element volume	15 cm <sup>3</sup>
Number of spacer grids	10

Some material properties of E110 (Zr1%Nb) cladding material has collected from open literature (Smirnov et al., 1997).

Cladding yield strength at 20 °C	400-420 MPa
Cladding yield strength at 350 °C	180-190 MPa
Cladding ultimate strength at 20 °C	430-450 MPa
Cladding ultimate strength at 350 °C	200-210 MPa
Cladding uniform elongation at 20 °C	10%
Cladding uniform elongation at 350 °C	15%
Cladding total elongation at 20 °C	34-38%
Cladding total elongation at 350 °C	42-47%
Irradiated cladding yield strength at 20 °C	500-580 MPa
Irradiated cladding yield strength at 350 °C	340-370 MPa
Irradiated cladding ultimate strength at 20 °C	460-510 MPa

Irradiated cladding ultimate strength at 350 °C	305-335 MPa
Irradiated cladding uniform elongation at 20 °C	2-5%
Irradiated cladding uniform elongation at 350 °C	4-6%
Irradiated cladding total elongation at 20 °C	14-24%
Radiated cladding total elongation at 350 °C	18-24%
Number of perforations at the bottom of the shroud (working assemblies)	12
Number of perforations at the top of the shroud (working assemblies)	12
Diameter of perforations	9 mm

### 1.2. Operational data of damaged fuel assemblies

The operational data of fuel assemblies has been collected in order provide burnup specific data for each fuel assembly that was cleaned in the cleaning tank. Such data are necessary for the definition of initial fuel state (before start of cleaning operation).

This part of database collection included several calculations, which were based on real fuel cycles of each assembly.

The power histories of fuel assemblies are included in the database, so participants can carry out their own calculations (e.g. with fuel behaviour codes) if they consider it necessary.

Operational data for Unit 2 and cycles 16-19 were provided by the Paks NPP. They included:

- load map of archives for cycle 16 describing the burnup distribution at the beginning of cycle,
- power distributions and histories for cycles 16-19,
- refuelling matrices between 16-19 cycles.

The burnup distribution in 10 axial nodes for each assembly was calculated using the GLOBUSKA module of the KARATE programme system (Hegedűs et al., 2002).

The decay heat of each node of each assembly was calculated using power distribution and considering the storage time between reactor shutdown and the incident. The ORIGEN and TIBSO codes were applied for this purpose. The reactor-physics calculations were performed at the Reactor Analysis Department of the Atomic Energy Research Institute, Budapest.

The fuel assemblies with similar power histories and of the same type (follower or working) were grouped into 6 groups and only one representative assembly was calculated for each group. Later all

fuel assemblies were assigned to their given values. This approach was applied in the following calculations, too.

The assemblies groups are listed below with the factory No.:

- 1. assembly group (1.-6.): 60465, 60466, 60467, 60468, 60469, 60470 (standard assemblies with 10.8 MWd/kg<sub>U</sub> burnup)
- 2. assembly group (7.-11.): 53906, 53873, 53994, 53930, 53878 (standard assemblies with 26.7 MWd/kg<sub>U</sub> burnup)
- 3. assembly group (12.): 57033(follower assembly with 10.1 MWd/kg<sub>U</sub> burnup)
- 4. assembly group (13.-18.): 58734, 59741, 59738, 59742, 59743, 59739 (follower assemblies with 21.1 MWd/kg<sub>U</sub> burnup)
- 5. assembly group (19.-24.): 61039, 61040, 61040, 61042, 61043, 61046 (follower assemblies with 13.3 MWd/kg<sub>U</sub> burnup)
- 6. assembly group (25.-30.): 61048, 61049, 61050, 60577, 60575, 60576 (follower assemblies with 13.1 MWd/kg<sub>U</sub> burnup)

The burnup dependent parameters of each assembly were determined using the reactor-physics data and fresh fuel parameters with the TRANSURANUS (Lassmann, 1992) code, where slice 1 correspondes to node 10. We used for our calculation averaged data on geometries. **Table 1** the data on geometries are summarized. Please note that some differences may exist between these data (used for the present calculations) and the fuel data published in open literature (and given in previous chapter).

**Table 2** contains the main parameters of fuel assemblies at the end of cycle 19. The maximum value of calculated parameters and the minimum gap size, furthermore the calculated rod internal pressure at 20 °C, 60 °C and 260 °C are presented.

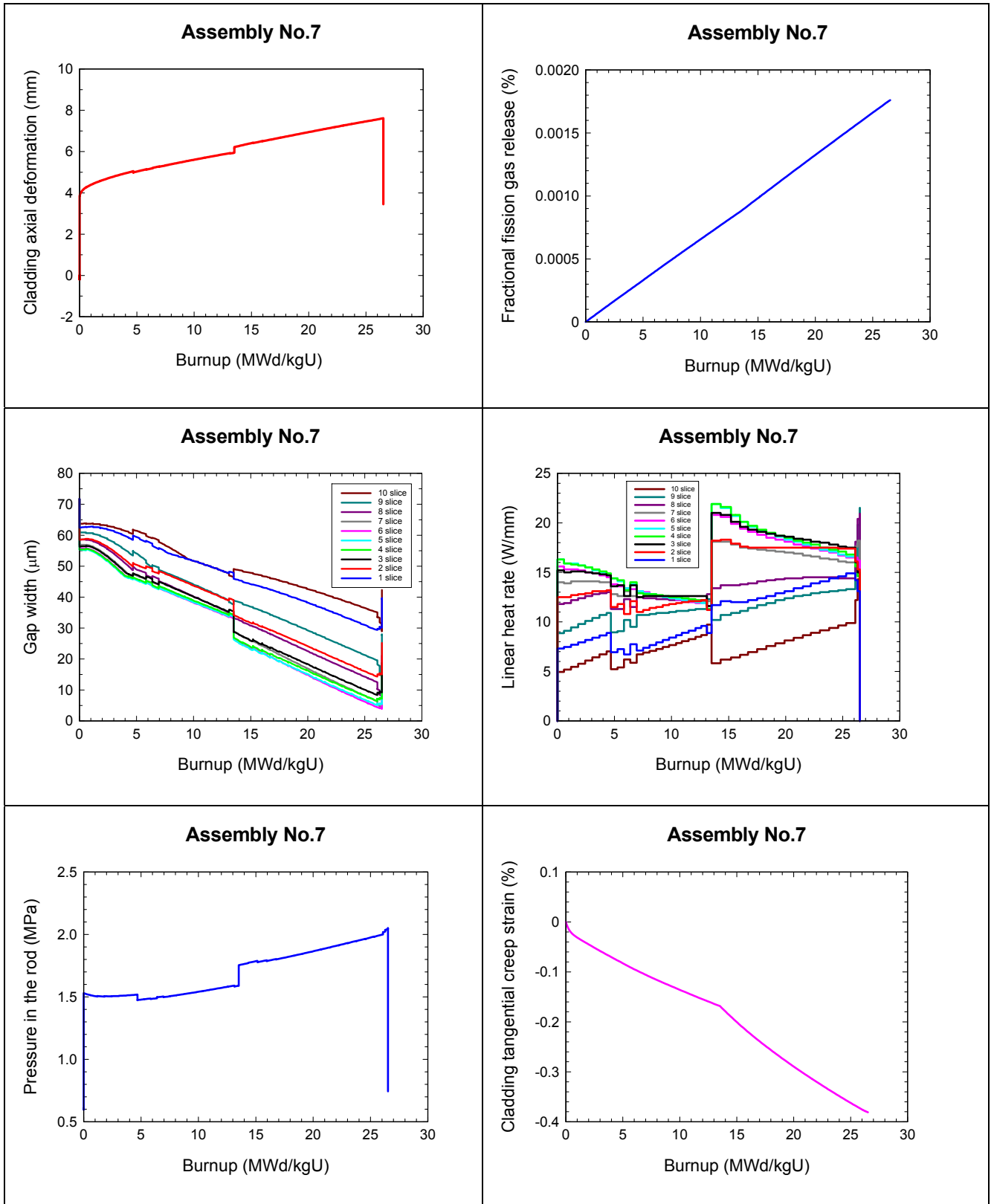
The calculated cladding axial deformation, fractional fission gas release, gap width, linear heat rate, pressure in the rod, tangential creep strain, fuel temperature, average fuel temperature, cladding tangential stress and the power history and profile of all assemblies are shown in for assembly No.7 (53906) in **Figure 1** as an example.

**Table 1:** Geometrical parameters of fresh assemblies

Parameter	Assembly	Assemblies	Assemblies	Assemblies	Assemblies	Assemblies
	No. 12	No. 7-11	No. 13-18	No. 19-24	No. 25-30	No. 1-6
Friction coefficient between fuel and cladding: static friction	8.00E-01	8.00E-01	8.00E-01	8.00E-01	8.00E-01	8.00E-01
Friction coefficient between fuel and cladding: sliding friction	8.00E-01	8.00E-01	8.00E-01	8.00E-01	8.00E-01	8.00E-01
Height of axial slice 1-10 [mm]	2.32E+02	2.42E+02	2.32E+02	2.32E+02	2.32E+02	2.42E+02
Height of axial slice 11 [mm]	9.00E+01	9.00E+01	9.00E+01	9.00E+01	9.00E+01	9.00E+01
Inner fuel radius [mm]	7.25E-01	7.25E-01	7.25E-01	7.25E-01	7.25E-01	7.25E-01
Outer fuel radius [mm]	3.78E+00	3.78E+00	3.78E+00	3.78E+00	3.78E+00	3.78E+00
Inner cladding radius [mm]	3.88E+00	3.88E+00	3.88E+00	3.88E+00	3.88E+00	3.88E+00
Outer cladding radius [mm]	4.55E+00	4.55E+00	4.55E+00	4.55E+00	4.55E+00	4.55E+00
Surface roughness fuel [mm]	1.80E-03	1.80E-03	1.80E-03	1.80E-03	1.80E-03	1.80E-03
Surface roughness clad [mm]	1.00E-03	1.00E-03	1.00E-03	1.00E-03	1.00E-03	1.00E-03
Fillgas pressure [MPa]	6.00E-01	6.00E-01	6.00E-01	6.00E-01	6.00E-01	6.00E-01
Fillgas temperature [°C]	2.00E+01	2.00E+01	2.00E+01	2.00E+01	2.00E+01	2.00E+01
Upper plenum volume (maximum) [mm <sup>3</sup> ]	4.26E+03	4.26E+03	4.26E+03	4.26E+03	4.26E+03	4.26E+03
Gap volume (maximum) [mm <sup>3</sup> ]	5.73E+03	5.97E+03	5.73E+03	5.73E+03	5.73E+03	5.97E+03
Volume of central void (maximum) [mm <sup>3</sup> ]	3.83E+03	4.00E+03	3.83E+03	3.83E+03	3.83E+03	4.00E+03
Total free volume [mm <sup>3</sup> ]	1.38E+04	1.42E+04	1.38E+04	1.38E+04	1.38E+04	1.42E+04
Friction coefficient between fuel and cladding: static friction	8.00E-01	8.00E-01	8.00E-01	8.00E-01	8.00E-01	8.00E-01

**Table 2:** Collected values of assemblies at the end of cycle 19

Parameter	Assemblies	Assemblies	Assembly	Assemblies	Assemblies	Assemblies
	No. 7-11	No. 13-18	No. 12	No. 19-24	No. 25-30	No. 1-6
Max. cladding axial deformation [mm]	7.62E+00	6.95E+00	5.61E+00	6.32E+00	6.26E+00	5.79E+00
Max. bumup [MWd/kgU]	3.14E+01	2.74E+01	1.61E+01	1.61E+01	1.59E+01	1.26E+01
Average bumup [MWd/kgU]	2.65E+01	2.19E+01	1.04E+01	1.38E+01	1.36E+01	1.07E+01
Max. fractional fission gas release [%]	1.76E-03	1.53E-03	9.38E-04	8.92E-04	8.80E-04	6.92E-04
Min. gap size [ $\mu$ ]	3.89E+00	4.47E+00	2.26E+01	2.50E+01	2.57E+01	3.63E+01
Max. linear heat rate [W/mm]	2.19E+01	2.06E+01	2.24E+01	2.28E+01	2.21E+01	1.75E+01
Max. pressure in the rod [MPa]	2.05E+00	1.92E+00	1.76E+00	1.76E+00	1.75E+00	1.60E+00
Rod internal pressure at 20 °C [MPa]	7.43E-01	7.09E-01	6.41E-01	6.53E-01	6.51E-01	6.28E-01
Rod internal pressure at 60 °C [MPa]	8.46E-01	8.06E-01	7.29E-01	7.42E-01	7.40E-01	7.15E-01
Rod internal pressure at 260 °C [MPa]	1.38E+00	1.32E+00	1.19E+00	1.21E+00	1.20E+00	1.16E+00
Cladding tangential creep strain [%]	-3.81E-01	-3.14E-01	-1.49E-01	-2.59E-01	-2.49E-01	-1.53E-01
Max. fuel temperature [°C]	9.10E+02	9.12E+02	9.76E+02	9.87E+02	9.64E+02	8.06E+02
Max. average fuel temperature [°C]	6.90E+02	7.17E+02	7.55E+02	7.62E+02	7.48E+02	6.51E+02



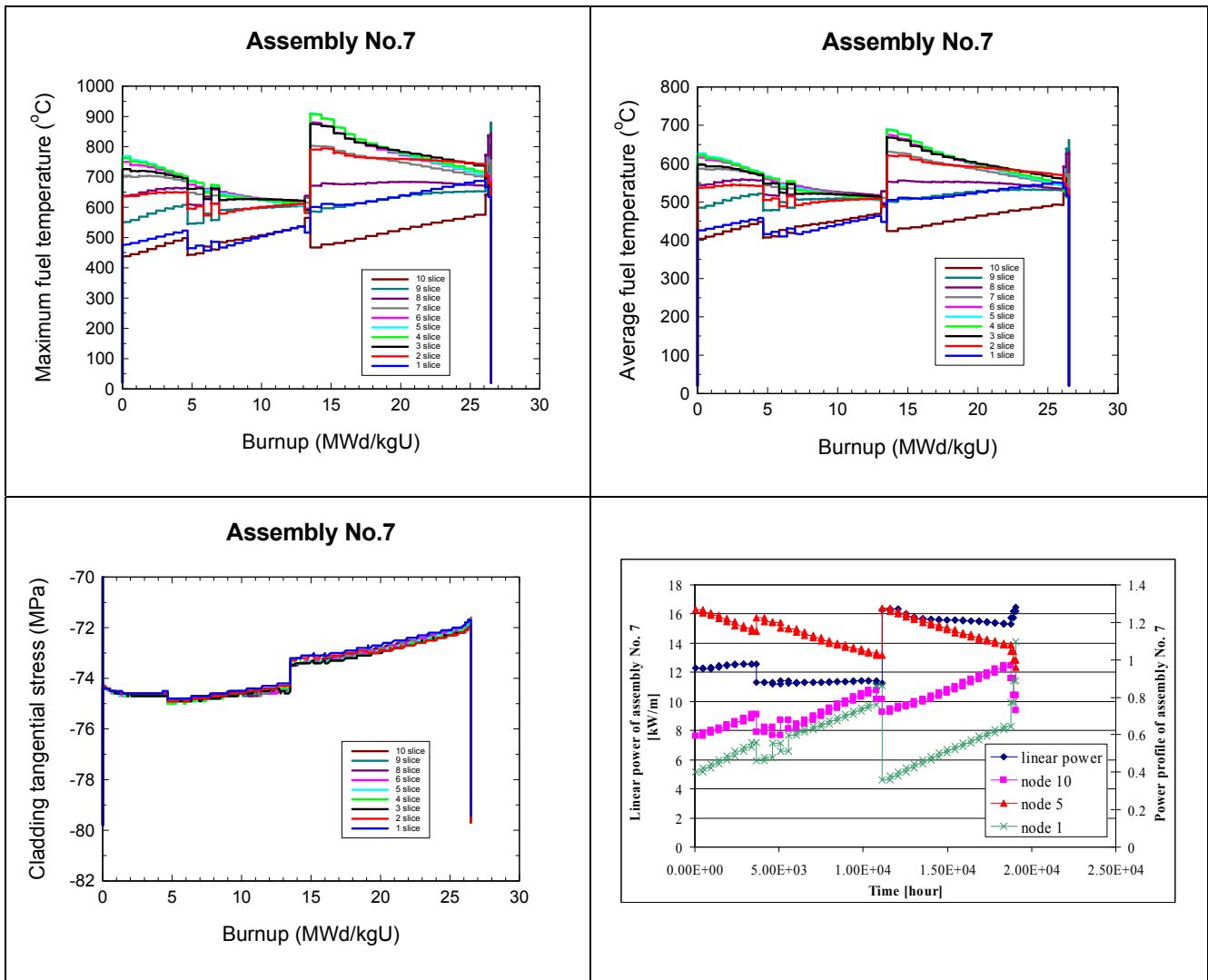


**Figure 1:** Representation of the calculated burnup dependent parameters, power history and profile for assembly No. 7.

### 1.3. Isotope inventory

The isotope inventory of the 30 assemblies was calculated using the ORIGENARP module of the SCALE4.4a program system. The calculations yielded the concentrations and activities of isotopes for the six assembly groups. The data was assigned to the each fuel assembly.

The typical material composition was considered in the calculations with following isotopes and elements:  $^{234}\text{U}$ ,  $^{235}\text{U}$ ,  $^{236}\text{U}$ ,  $^{238}\text{U}$ , Hf, Nb, Sn, Zr. The calculations were done with 44 energy groups gamma and neutron spectrum directory from time of shutdown of Unit 2 of Paks NPP for the next calculated calendar days: 0 (day of shutdown), 3, 10, 13 (day of incident), 30, 60, 120, 240, 365 and 760. The database includes 138 isotopes in the above 10 times for each assembly.



The data of 6 assemblies were used to characterise the assemblies (e.g. fission product content). It could be seen that the order of activities of assemblies were very close to each other after shutdown. The calculations were carried out at the Reactorphysics Department of Paks NPP. The total activities of 30 assemblies is shown in **Table 3**.

The total activity of assemblies and assemblies groups after shutdown were determined by 3 main groups like light elements (activated structural materials of assemblies – assembly claddings, spacer grids, rod claddings), actinides and fission products.

The light elements are monotonous decreasing in time and their activity was significant part of the total activity of assembly at the time of the incident. These elements are  $^{91}\text{Zr}$ ,  $^{92}\text{Zr}$ ,  $^{94}\text{Zr}$ ,  $^{96}\text{Zr}$ ,  $^{93}\text{Nb}$ ,  $^{119}\text{Sn}$ ,  $^{120}\text{Sn}$ .

The activity of actinides is important in all examined periods compared to total activity of calculated assemblies. It includes the  $^{234}\text{U}$ ,  $^{235}\text{U}$ ,  $^{236}\text{U}$ ,  $^{238}\text{U}$ ,  $^{237}\text{Np}$ ,  $^{235}\text{Np}$ ,  $^{239}\text{Pu}$ ,  $^{240}\text{Pu}$ ,  $^{241}\text{Pu}$ ,  $^{242}\text{Pu}$ ,  $^{241}\text{Am}$ ,  $^{243}\text{Am}$ ,  $^{242}\text{Cm}$ ,  $^{244}\text{Cm}$ . The release of these elements with all probability can be taken place only if they dissolve from pellets.

Activity of fission products are decreasing in time and their contribution to the total activity is important only at the beginning period after the incident. Their activities will converge to a saturation value, which represents a considerable part of the release at the incident.

## **2. Characterisation of the 70873 leaking fuel assembly**

The No. 70873 fresh follower fuel assembly was loaded into position No. 33 of cycle 22 of Unit 4 at the Paks NPP. The enrichment of U was 3,82%. The design characteristics of this assembly are the same as that of damaged fuel described in chapter 1.1.

### *2.1. Operational data of leaking fuel assembly*

The operational history of the assembly was provided by the power plant.

The assembly was operated for one year and was removed from the core during the refueling period. For this reason the assembly reached only 14 MWd/kg<sub>U</sub> burnup.

According to the analyses of primary coolant activities, this assembly had only one single leaking fuel rod, the other 125 rods were intact.

**Table 3:** Isotope inventory of 30 damaged fuel assemblies at the reactor shutdown

Isotope	Activity [Bq]	Isotope	Activity [Bq]	Isotope	Activity [Bq]
<sup>239</sup> Np	2,30E+18	<sup>131</sup> I	1,23E+17	<sup>127</sup> Te	8,90E+15
<sup>133</sup> I	2,61E+17	<sup>88</sup> Rb	1,06E+17	<sup>133m</sup> Xe	8,05E+15
<sup>133</sup> Xe	2,51E+17	<sup>131</sup> Te	1,06E+17	<sup>241</sup> Pu	7,67E+15
<sup>135</sup> I	2,47E+17	<sup>105</sup> Ru	1,05E+17	<sup>137</sup> Cs	7,22E+15
<sup>140</sup> La	2,45E+17	<sup>88</sup> Kr	1,04E+17	<sup>129m</sup> Te	7,11E+15
<sup>99</sup> Mo	2,37E+17	<sup>91m</sup> Y	1,03E+17	<sup>137</sup> Ba	6,90E+15
<sup>140</sup> Ba	2,35E+17	<sup>105</sup> Rh	9,78E+16	<sup>90</sup> Y	6,53E+15
<sup>95</sup> Zr	2,33E+17	<sup>147</sup> Nd	8,55E+16	<sup>90</sup> Sr	5,90E+15
<sup>95</sup> Nb	2,30E+17	<sup>135</sup> Xe	7,44E+16	<sup>134</sup> Cs	5,75E+15
<sup>97</sup> Nb	2,25E+17	<sup>237</sup> U	7,12E+16	<sup>111m</sup> Ag	5,09E+15
<sup>97</sup> Zr	2,23E+17	<sup>149</sup> Pm	6,36E+16	<sup>111</sup> Pd	5,08E+15
<sup>141</sup> Ce	2,16E+17	<sup>135m</sup> Xe	5,17E+16	<sup>111</sup> Ag	5,04E+15
<sup>141</sup> La	2,15E+17	<sup>129</sup> Sb	3,78E+16	<sup>136</sup> Cs	3,08E+15
<sup>97m</sup> Nb	2,12E+17	<sup>106</sup> Rh	3,73E+16	<sup>242</sup> Am	2,48E+15
<sup>99m</sup> Tc	2,09E+17	<sup>85m</sup> Kr	3,66E+16	<sup>244</sup> Am	1,71E+15
<sup>143</sup> Ce	2,06E+17	<sup>129</sup> Te	3,58E+16	<sup>242</sup> Cm	9,69E+14
<sup>143</sup> Pr	2,00E+17	<sup>106</sup> Ru	3,20E+16	<sup>125</sup> Sb	5,77E+14
<sup>92</sup> Y	1,86E+17	<sup>153</sup> Sm	3,07E+16	<sup>181</sup> Hf	4,86E+14
<sup>92</sup> Sr	1,85E+17	<sup>105m</sup> Rh	2,99E+16	<sup>154</sup> Eu	2,33E+14
<sup>91</sup> Y	1,83E+17	<sup>109</sup> Pd	2,89E+16	<sup>155</sup> Eu	1,22E+14
<sup>132</sup> I	1,81E+17	<sup>131m</sup> Te	2,25E+16	<sup>110m</sup> Ag	1,09E+14
<sup>132</sup> Te	1,78E+17	<sup>151</sup> Pm	2,22E+16	<sup>122</sup> Sb	8,19E+13
<sup>91</sup> Sr	1,78E+17	<sup>83</sup> Br	1,70E+16	<sup>180m</sup> Hf	4,37E+13
<sup>103</sup> Ru	1,72E+17	<sup>83m</sup> Kr	1,70E+16	<sup>239</sup> Pu	3,62E+13
<sup>103m</sup> Rh	1,72E+17	<sup>147</sup> Pm	1,69E+16	<sup>124</sup> Sb	3,35E+13
<sup>89</sup> Sr	1,46E+17	<sup>238</sup> Np	1,65E+16	<sup>3</sup> H	3,18E+13
<sup>145</sup> Pr	1,39E+17	<sup>148</sup> Pm	1,49E+16	<sup>240</sup> Pu	3,06E+13
<sup>93</sup> Y	1,38E+17	<sup>156</sup> Eu	9,60E+15	<sup>244</sup> Cm	2,30E+13
<sup>144</sup> Pr	1,25E+17	<sup>243</sup> Pu	9,30E+15	<sup>175</sup> Hf	1,88E+13
<sup>144</sup> Ce	1,23E+17	<sup>127</sup> Sb	9,20E+15	<sup>242</sup> Am	4,68E+12

The power of axial nodes of the assembly was calculated using the power normalized power distribution and the power of assembly. The power of axial nodes of assembly was divided by 126 (total number of fuel rods) and by the length of nodes that determined the linear heat rate of one rod.

The FUROM code (Kulacsy, 2011) was applied for the calculation of the coolant temperature from the inlet temperature of core for each axial nodes. The fast neutron flux was determined by the FUROM, too. The initial data for FUROM calculations are given in **Table 4**.

**Table 4:** Technological parameters of fuel rod used in the calculations

Parameter		Value of parameter
inner fuel radius	[mm]	0.675
outer fuel radius	[mm]	3.7925
surface roughness fuel	[ $\mu\text{m}$ ]	2
inner cladding radius	[mm]	3.88
outer cladding radius	[mm]	4.55
surface roughness clad	[ $\mu\text{m}$ ]	1
active length of rod	[m]	2.36
enrichment	[%]	3.82
Relative density of fresh fuel	[-]	0.962
relative density after densification	[-]	0.97
fuel grain size	[ $\mu\text{m}$ ]	14
He fillgas pressure	[bar]	6
plenum volume	[ $\text{cm}^3$ ]	8.5
coolant inlet temperature	[ $^{\circ}\text{C}$ ]	266

**Figure 2** shows the linear heat rate versus time for each of axial nodes. While the power of some nodes increased, some others decreased, but the total power of rods in the follower assembly decreased during the cycle.

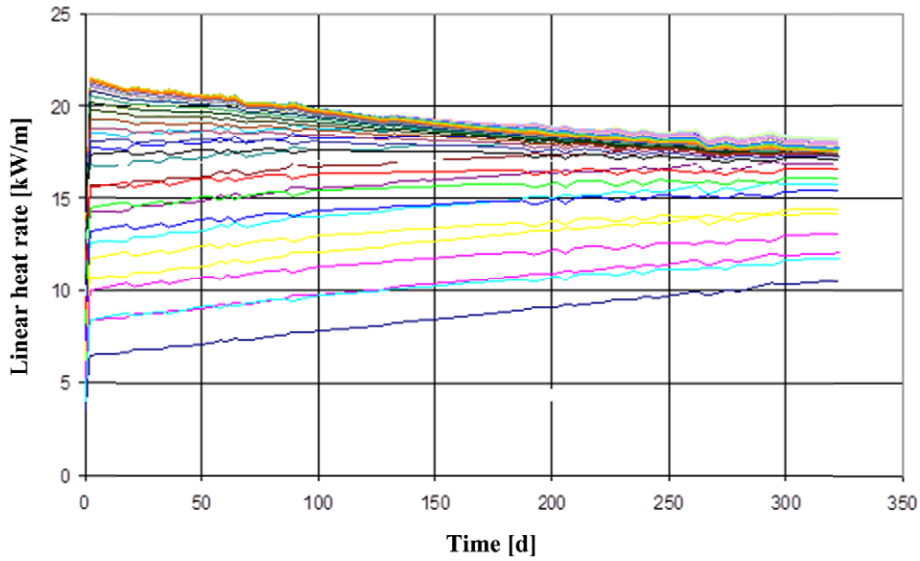


Figure 2: Linear heat rate of 39 axial nodes of rod versus time

2.2. Isotope inventory of 70873 assembly

The 70873 assembly contained 114,837 kg U, from which the mass of <sup>235</sup>U was 4,405 kg. Cycle 22 of Unit 4 operated for near nominal power (1485 MW) after the third effective day (Figure 3).

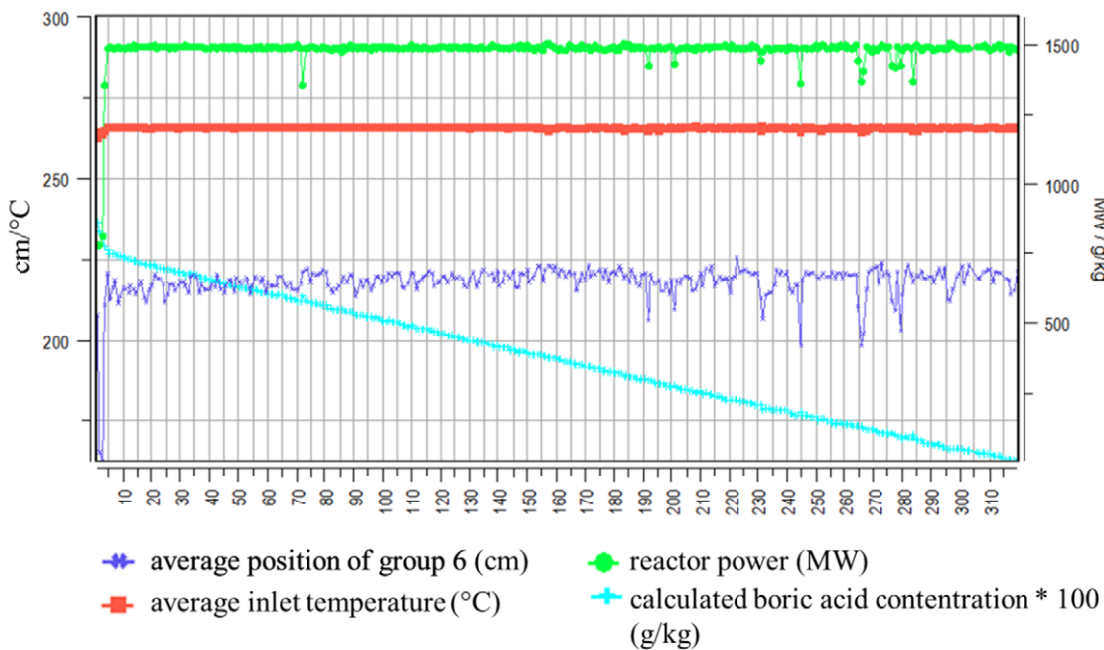


Figure 3: Reactor parameters of cycle 22 of Unit 4

Cycle 22 of Unit 4 was 319,95 effective operational days based on measured data. The cycle started at 30.05.2008 and finished at 24.04.2009. Calculated burnup of 70873 assembly was 14,137 MWd/kg<sub>U</sub>, so the calculated power was 5,097 MW. The isotope inventory of 70873 assembly during the operation and the storage was calculated based on these data by ORIGEN-ARP 5.01 program (**Table 5.**). The time steps in the calculations were: 0.3, 1, 3, 10, 30, 90, 150, 250, 300, 319.95 during the operation and 1, 3, 10, 30, 90, 150, 250, 350, 400, 450 during the storage.

**Table 5:** Isotope inventory of one fuel rod in the leaking 70873 fuel assembly at the reactor shutdown

Isotope	Mass [g]	Activity [Bq]
<sup>239</sup> Np	8,31	5,67E+14
<sup>140</sup> La	0,47	7,86E+13
<sup>95</sup> Zr	11,77	7,40E+13
<sup>95</sup> Nb	6,35	7,31E+13
<sup>141</sup> Ce	8,12	6,80E+13
<sup>99</sup> Mo	0,42	5,88E+13
<sup>99m</sup> Tc	0,04	5,32E+13
<sup>103</sup> Ru	5,54	5,24E+13
<sup>89</sup> Sr	5,49	4,69E+13
<sup>144</sup> Ce	36,38	3,41E+13
<sup>97</sup> Nb	0,00	2,73E+13
<sup>97</sup> Zr	0,05	2,72E+13
<sup>106</sup> Ru	7,74	7,61E+12
<sup>137</sup> Cs	62,21	1,59E+12
<sup>90</sup> Sr	32,14	1,30E+12
<sup>134</sup> Cs	2,82	1,08E+12
<sup>136</sup> Cs	0,04	8,06E+11
<sup>125</sup> Sb	0,37	1,12E+11
<sup>242</sup> Cm	0,08	7,74E+10
<sup>154</sup> Eu	0,51	3,74E+10
<sup>239</sup> Pu	552,90	2,48E+10
<sup>155</sup> Eu	0,16	2,35E+10
<sup>110m</sup> Ag	0,01	1,77E+10
<sup>240</sup> Pu	97,59	1,61E+10
<sup>3</sup> H	0,00	1,12E+10
<sup>122</sup> Sb	0,00	9,68E+09
<sup>124</sup> Sb	0,00	7,67E+09
<sup>244</sup> Cm	0,04	1,04E+09
<sup>241</sup> Am	0,62	6,25E+08

### 3. Conclusions

The main characteristics of the damaged and leaking fuel VVER-440 fuel assemblies have been collected. The fuel damage took place in an incident after reactor shutdown, while the leaking fuel was detected during normal operation.

There were no special examination of the fresh fuel assemblies before loading them into the reactor core, for this reason factory data are used to characterise the fuel. The operational parameters were derived using power histories of from the NPP. The calculations were carried out with fuel behavior codes FUROM and TRANSURANUS.

The isotope inventories were determined using the real power histories of each fuel assembly for almost one thousand isotopes. For future evaluation only the long lived isotopes will be used. The inventory is important for the determination of fractional releases.

30 fuel assembly were stored in the same pool when fuel was damaged. The activity release resulted from all assemblies. The calculation of dissolution rates should use some averaged values.

From the leaking fuel assembly only one out of 126 fuel rods was in contact with water, but the leaking rod was not identified. The averaged values from this assembly can be used for the characterization of a source rod and for the evaluation of activity data from this type of assembly.

### Aknowledgement

*The research leading to these results has received funding from the European Union's European Atomic Energy Community's (Euratom) Seventh Framework Programme FP7/2007-2011 under grant agreement n° 295722 (FIRST-Nuclides project).*

### References

Hegedűs C., Hegyi G., Hordósy G., Keresztúri A., Makai M., Maráczy C., Telbisz F., Temesvári E., Vértés P. (2002) The KARATE Program System. PHYSOR 2002.

Hózer, Z., Szabó, E., Pintér, T., Baracska Varjú I., Bujtás, T., Farkas, G., Vajda, N. (2009) Activity release from damaged fuel during the Paks-2 cleaning tank incident in the spent fuel storage pool. Journal of Nuclear Materials, 392, 90-94.

Hózer, Z., Aszódi, A., Barnak, M., Boros, I., Fogel, M., Guillard, V., Győri, Cs., Hegyi, G., Horváth, G. L., Nagy, I., Junninen, P., Kobzar, V., Légrádi, G., Molnár, A., Pietarinen, K.,

Pernecky, L., Makihara, Y., Matejovic, P., Perez-Feró, E., Slonszki, E., Tóth, I., Trambauer, K., Tricot, N., Trosztel, I., Verpoorten, J., Vitanza, C., Voltchek, A., Wagner, K. C., Zvonarev, Y. (2010) Numerical analyses of an ex-core fuel incident: Results of the OECD-IAEA Paks Fuel Project. *Nuclear Engineering and Design*, 240, 538-549.

Kulacsy, K. (2011) Fuel behaviour calculations with version 2.0 of the code FUROM, 9th International Conference on VVER Fuel Performance Proceedings, Modelling and Experimental Support.

Lassmann, K. (1992). TRANSURANUS: a fuel rod analysis code ready for use. *Journal of Nuclear Materials*, 188, 295-302.

NEA/CSNI/R (2008)2. OECD-IAEA Paks Fuel Project Final Report.

Slonszki, E., Hózer, Z., Pintér, T., Baracska Varjú, I. (2010) Activity release from the damaged spent VVER-fuel during long-term wet storage. *Radiochimica Acta*, 98, 231-236.

Solonin, M., Bibilashvili, Y., Loltoukhovsky, A., Medvedev, A., Novikov, V., Nikishov, A., Nikulina, A., Sokolov, N., Sokolov, F., Lunin, G., Proselkov, V., Panyushkin, A., Tsiboulia, V., Afanasiev, V., Rozhkov, V., Enin, A., Samoylov, O., Vasilchenko, I., Tsikanov, V., Golovanov, V., Ovchinikov, V., Smirnov, V., Smirnov, A. (1997) VVER Fuel Performance and Material Development for Extended Burnup in Russia. Proc. Second Int. Seminar on VVER Fuel Performance, Modelling and Experimental Support.

Smirnov V., Smirnov V., Kanashov B., Kuzmin V., Bibilashvili Y., Novikov V., Enin A., Rozhkov V., Tzibulya V., Bek E. (1997) Behaviour of VVER-440 and VVER-1000 in a Burnup Range of 20-48 MWd/kg<sub>U</sub>. 2<sup>nd</sup> International Seminar on VVER Fuel Performance Proceedings, Modelling and Experimental Support.





# MODELLING OF BOUNDARY AND INITIAL CONDITIONS FOR UPSCALING MIGRATION / RETENTION PROCESSES OF FISSION PRODUCTS IN THE SPENT NUCLEAR FUEL STRUCTURE

Bernhard Kienzler<sup>\*</sup>, Christiane Bube, Ernesto González-Robles Corrales, Volker Metz

Karlsruher Institute fuer Technology (KIT), DE

\* Corresponding author: [bernhard.kienzler@kit.edu](mailto:bernhard.kienzler@kit.edu)

## Abstract

To prepare the modelling studies on the initial speciation of fission and activation products of low concentrations in high burn-up LWR fuel, important initial and boundary conditions were derived. These include the burn-up history and decay of fission products, temperatures during irradiation in the reactor and during storage in the laboratory, properties of the rim structure, such as thickness, rim burn-up, xenon concentrations and porosity.

## Introduction

In safety assessments for disposal of spent nuclear fuel in deep underground repository, failure of canisters and loss of the integrity of fuel rods is considered in the long term. Some of the radionuclides within the spent fuel material will be directly exposed to water contact after the barrier failure. The modelling studies performed at KIT aim on the speciation of activation and fission products of low concentrations in high burn-up LWR fuel before contact to water. This information is a prerequisite for a multi-scale modelling of the migration / retention processes of activation and fission products in the spent nuclear fuel, in the cladding, and for estimation of the fission product total release. In order to develop and apply such models for scale-up of release processes from the micro-scale level to the fuel-rod scale, boundary and initial conditions are required. In this context KIT is going to calculate the initial speciation of radionuclides of the instant / fast release fraction as function of irradiation history, temperature and other critical parameters of the 50.4 GWd/t<sub>HM</sub> PWR fuel, used in experimental studies at KIT.

Following calculations were performed to provide for the initial and boundary conditions:

- Calculation of the burn-up and decay history using the webKorigen software package (Nucleonica GmbH, 2011).
- Calculation of the rim zone burn-up
- Calculation of the rim zone thickness
- Calculation of the porosity

### Characteristic data of the KIT fuel

The studied 50.4 GWd/t<sub>HM</sub> PWR Gösigen fuel consists of pure UO<sub>2</sub>, fabricated by Kraftwerk Union AG using the NIKUSI process (Stratton, 1991). The fuel rod was irradiated in the PWR Gösigen (KKG), Switzerland. The data given in **Table 1** characterize the studied N0204 KKG-BS fuel rod segment and are used for the modelling.

**Table 1:** Characteristic data of the fuel rod segment N0204 KKG-BS studied by KIT

Property	Value
initial enrichment:	3.8% <sup>235</sup> U
pellet diameter:	9.3 mm
pellet density	10.41 g/cm <sup>3</sup>
rod diameter:	10.75 ± 0.05 mm
zircaloy wall thickness:	0.725 mm
initial radial gap:	0.17 mm
number of cycles:	4
average burn-up:	50.4 GWd/t <sub>HM</sub>
av. linear power:	260 W/cm
max. linear power:	340 W/cm
discharge date:	27. May 1989
duration of irradiation	1226 days
storage time	23 years

## Fission Product Inventories

The fissions per initial metal atom (FIMA) provide a measure for the burn-up of spent nuclear fuel. There are various approaches to calculate FIMA. In the present study the approach of (Nakahara et al., 1990) was applied, which is described in equation (1):

$$\text{FIMA}(\%) = \frac{\left( \frac{100 \cdot {}^{148}\text{Nd}}{\text{U} \cdot \gamma_{148}} \right)}{\left( 1 + \frac{\text{Pu}}{\text{U}} + \frac{{}^{148}\text{Nd}}{\text{U} \cdot \gamma_{148}} \right)} \quad \text{eq.1}$$

U, Pu,  ${}^{148}\text{Nd}$  denote the molar fractions of the respective radioelements / radionuclides,  $\gamma_{148}$  denotes the fission yield for the mass 148. All these isotopes decay to the stable isotope  ${}^{148}\text{Nd}$ . Based on an effective energy release of 205.4 MeV per fission, the burn-up (GWd/t<sub>HM</sub>) is then obtained by multiplying the FIMA (%) by the conversion factor 9.60.

Calculations of the burn-up and the decay history of the 50.4 GWd/t<sub>HM</sub> PWR Gösgen fuel were performed using the webKorigen software package (Nucleonica GmbH, 2011). The code was applied via the web portal [www.nucleonica.net](http://www.nucleonica.net). Input parameters were the initial enrichment, the final average burn-up, the number of reactor cycles and the decay time. The output included activities, amount of radionuclides (in gram and mol) and decay heat per radionuclide and selected decay time. More options were available, but these were not relevant for the present modelling study.

## Boundary conditions for the temperature history of the 50.4 GWd/t<sub>HM</sub> fuel rod segment

The central temperature of a fuel rod was calculated according to following equations:

$$\Delta T = Q \cdot R^2 / (4 \cdot \lambda) \quad \text{eq.2}$$

or alternatively

$$\Delta T = \text{linear power rate} / (4\pi \cdot \lambda) \quad \text{eq.3}$$

where Q denotes the heat production rate, R the radius of the fuel rod and  $\lambda$  the heat conductivity. The heat conductivity varies as a function of the burn-up between 5 W m<sup>-1</sup> K<sup>-1</sup> for fresh UO<sub>2</sub> fuel and 2.5 W m<sup>-1</sup> K<sup>-1</sup> for irradiated fuel (Lucuta et al., 1996). Using equations (2) and (3) and the data of the 50.4 GWd/t<sub>HM</sub> PWR Gösgen fuel (**Table 1**),  $\Delta T$  values in the range of 827 to 1000 K were calculated. The coolant's temperature in the Gösgen PWR was 325°C. Therefore, the maximal temperature during irradiation of the studied N0204 KKG-BS fuel rod segment was estimated to be above 1300°C.

Up to present, the fuel rod segment was stored over a period of 23 years. The radioactive decay reduced the heat production rate to  $9.39 \cdot 10^{-4}$  W/g corresponding to  $9.77 \cdot 10^{-4}$  W/cm<sup>3</sup>. The heat rate was controlled by inserting the N0204 KKG-BS fuel rod segment into a thermal insulation package and measuring the temperature at the surface of the rod segment. Measurements and calculations correspond well, under the assumption that 82% of the total decay heat remained in the rod segment. The result shows that not only the total calculated  $\alpha/\beta$  decay heat, but also 40 % of the  $\gamma$  decay heat remains in the UO<sub>2</sub> matrix. The heat development in the insulated rod was simulated using the *FLEXPDE* code; data for heat capacity of UO<sub>2</sub> fuel was taken from IAEA TECDOC-949 (IAEA, 1997).

### Calculated rim zone burn-up and thickness of the 50.4 GWd/t<sub>HM</sub> fuel

Properties of the rim zone were analyzed by many authors, e.g. (Bremier et al., 2002; Koo et al., 2001; Manzel and Walker, 2000; Matzke and Spino, 1997; Roudil et al., 2009; Spino et al., 1996; Une et al., 1992). Koo et al. (2001) reviewed published literature with respect to the effect of burn-up on the rim thickness and on the fission gas content. Based on the analysis of these data, the mean local burn-up within the entire rim region is estimated to be 1.33 times the average pellet burn-up. This finding is consistent with local neodymium profile measurements. The best fit was represented by eq. 4,

$$R_t = 3.55 BU_R - 185 \quad \text{eq.4}$$

where  $R_t$  is the rim thickness ( $\mu\text{m}$ ) and  $BU_R$  is the rim burn-up (GWd/t<sub>HM</sub>). A pessimistic function that bounds all the data is also given in (Koo et al., 2001) by

$$R_t = 5.28 BU_R - 178 \quad \text{eq.5}$$

However, use of the latter expression suggests that significant rim thicknesses exist even in fuels with burn-ups in the range of 30 GWd/t<sub>HM</sub>. Since this seems completely inconsistent with microstructural studies, a revised expression was developed, given by Johnson (Johnson et al., 2005):

$$R_t = 5.44 BU_R - 281 \quad \text{eq.6}$$

Using the data of the 50.4 GWd/t<sub>HM</sub> PWR fuel, following results were obtained:

Rim zone burn-up:	67.0 GWd/t <sub>HM</sub>
Rim zone thickness:	83.7 $\mu\text{m}$

### Calculated Xenon concentrations in the rim zone of a 50.4 GWd/t<sub>HM</sub> fuel pellet

Koo (Koo et al., 2001) quoted an expression derived by Lassmann et al. (1995) for calculating the concentration of fission gas (Xe) in the rim zone.

$$Xe_m = c \cdot \left[ \frac{1}{a} + \left( BU_{rim}^0 - \frac{1}{a} \right) e^{-a(BU_{rim} - BU_{rim}^0)} \right] \quad \text{eq.7}$$

where  $c$  denotes the Xe production rate (wt% per unit burn-up ( $1.46 \cdot 10^{-2}$  wt.% per GWd/t<sub>HM</sub>),  $a$  denotes a fitting constant (0.0584,  $BU_{rim}$  is the rim burn-up and  $BU_{rim}^0$  is the threshold burn-up for rim formation (30 GWd/t<sub>HM</sub>). The Xe present in rim pores is calculated by

$$Xe_{pores} = c \cdot BU_{rim} - Xe_m \quad \text{eq.8}$$

For the 50.4 GWd/t<sub>HM</sub> PWR Gösgen fuel, following results were calculated:

Xenon in the matrix of rim	Xe	0.026 wt.%
Xe in the rim pores	Xe <sub>pores</sub>	0.953 wt.%

The result shows that almost the complete Xe inventory of the rim is located in pores.

### Calculated rim porosity of the 50.4 GWd/t<sub>HM</sub> fuel

The thermal conductivity of UO<sub>2</sub> fuel has been investigated since many years, as it represents the most important property influencing the fuel operating temperature, and in turn affecting directly fuel performance and behaviour, particularly its fission-gas release and swelling. Therefore, the factors influencing the thermal conductivity have been analyzed. Very important in this context is the porosity of the UO<sub>2</sub> matrix (Lucuta et al., 1996). Spino (Spino et al., 1996) investigated the rim microstructure in PWR fuels in the burn-up range 40 to 67 GWd/t<sub>HM</sub> and provided for tabulated data on burn-up, radial position and measured porosity, and pore sizes in 2D and 3D. Spino also presented an equation allowing the calculations of the burn-up – porosity relation:

$$\text{Porosity} = (\text{burn-up} - BU_o) \times d_1 + \exp(-d_2 + d_3 \times r/r_0) \quad \text{eq. 9}$$

$BU_o$ ,  $d_1$ ,  $d_2$ ,  $d_3$  denote fit parameters,  $r$  the radius and  $r_0$  represents the maximum pellet radius.  $BU_o$  is the lowest burn-up for which eq.9 is valid. The data of (Spino et al., 1996) and eq.9 were used to fit their data in order to obtain the following values for the  $d_1$ ,  $d_2$ ,  $d_3$  fit parameters.

$BU_o$	22 GWd/t <sub>HM</sub>
$d_1$	$1.23 \times 10^{-1}$

$d_2$	37
$d_3$	39.6

Using these fit parameters, for 50.4 GWd/t<sub>HM</sub> PWR Gösgen fuel following data were obtained:

Rim porosity ( $r/r_0 = 0.9$ ):	3.8 %
Rim porosity ( $r/r_0 = 1$ ):	17.0 %
average rim porosity ( $0.9 \leq r/r_0 \leq 1$ ):	6.2 %

## Outlook

For modelling the speciation of activation and fission products, information on different available databases was compiled. This included the *HSC Chemistry 7.0* software program for process flow-sheet simulation, which contains specific calculation modules and twelve databases together with extensive thermo-chemical, heat transfer and mineralogical data.

Furthermore, the *MTDATA* base is considered, which provides for a very extensive thermodynamic database for oxide systems. The *MTDATA* base is available via the web portal <http://resource.npl.co.uk/mtdata/NPLOxideDatabase.htm>. It includes full coverage of Zr and partial data for U oxides. However, this database contains only limited data for fission products. Since further development of *MTDATA* is integrated in a European project with Rudy Konings (JRC-ITU, Karlsruhe) on data for nuclear fuels and their interaction, data for most of the fission products will be acquired in future.

Another promising option for modelling the speciation of activation and fission products is the *GEMS* code and database developed by D. Kulik (PSI, Villigen). *GEMS* is applicable for thermodynamic modelling of aquatic (geo)chemical systems by Gibbs Energy Minimization and is available via the web portal <http://gems.web.psi.ch/>.

## Acknowledgement

*The research leading to these results has received funding from the European Union's European Atomic Energy Community's (Euratom) Seventh Framework Programme FP7/2007-2011 under grant agreement n° 295722 (FIRST-Nuclides project).*

## References

- Bremier, S., Walker, C. T., Manzel, R. (2002) Fission gas release and fuel swelling at burn-ups higher than 50 MWd/kg<sub>U</sub>. Fission Gas Behaviour in Water Reactor Fuels, Seminar Proceedings, 93-106.
- IAEA (1997) Thermophysical properties of materials for water cooled reactors. IAEA TECDOC - 949.
- Johnson, L., Ferry, C., Poinssot, C., Lovera, P. (2005) Spent fuel radionuclide source-term model for assessing spent fuel performance in geological disposal. Part I: Assessment of the instant release fraction. Journal of Nuclear Materials, 346, 56-65.
- Koo, Y.H., Lee, B.H., Cheon, J.S., Sohn, D.S. (2001) Pore pressure and swelling in the rim region of LWR high burnup UO<sub>2</sub> fuel. Journal of Nuclear Materials, 295, 213-20.
- Lassman, K., Walker, C.T., van de Laar, J., Lindström, F. (1995) Modelling the high burnup UO<sub>2</sub> structure in LWR fuel. Journal of Nuclear Materials, 226, 1-8.
- Lucuta, P. G., Matzke, H., Hastings, I. J. (1996) A pragmatic approach to modelling thermal conductivity of irradiated UO<sub>2</sub> fuel: Review and recommendations. Journal of Nuclear Materials, 232, 166-80.
- Manzel, R. and Walker, C.T. (2000) High burnup fuel microstructure and its effect on fuel rod performance. ANS International Topical Meeting on Light Water Reactor Fuel Performance (Park City, Utah, April 10-13, 2000).
- Matzke, H. and Spino, J. (1997) Formation of the rim structure in high burnup fuel. Journal of Nuclear Materials, 248, 170-79.
- Nakahara, Y., Suzuki, T., Gunji, K., Kohno, N., Sonobe, T., Ohnuki, M., Itoh, M., Takano, H., Adachi, T. (1990) Actinide and Fission Productnuclides Accumulated in PWR Spent Fuels. OECD-NEA Information Exchange Programme on Actinide and Fission Product Separation and Transmutation First Meeting, (Mite, Japan, 6-8 November 1990).
- Nucleonica GmbH (2011) Nucleonica Nuclear Science Portal [www.nucleonica.com](http://www.nucleonica.com), Version 3.0.11 [online text].
- Roudila, D., Jegoua, C., Broudica, V., Tribeta, M. (2009) Rim instant release radionuclide inventory from French high burnup spent UOX fuel. MRS Proceedings, 1193, 627.
- Spino, J., Vennix, K., Coquerelle, M. (1996) Detailed characterisation of the rim microstructure in PWR fuels in the burn-up range 40–67 GWd/t<sub>M</sub>. Journal of Nuclear Materials, 231, 179-90.

Stratton, R.W. (1991) A comparative irradiation test of UO<sub>2</sub> sphere-pac and pellet fuel in the Goesgen PWR. Int. Topical Meeting on LWR Fuel Performance, 174-83.

Une, K., Nogita, K., Kashibe, S., Imamura, M. (1992) Microstructural change and its influence on fission gas release in high burnup UO<sub>2</sub> fuel. Journal of Nuclear Materials, 188, 65-72.



# CONCEPT OF LEACH TESTS FOR THE EXPERIMENTAL DETERMINATION OF IRF RADIONUCLIDES FROM BELGIAN HIGH-BURNUP SPENT NUCLEAR FUEL IN FIRST-NUCLIDES

Thierry Mennecart, Karel Lemmens, Kevin Govers, Adriaensen Lesley, Christelle Cachoir, Dobney Andrew, Gysemans Mireille, Van Renterghem Wouter, Verwerft Marc

Studicentrum voor Kernenergie (SCK-CEN), BE

\* Corresponding author: [thierry.mennecart@sckcen.be](mailto:thierry.mennecart@sckcen.be)

## Abstract

In the framework of the FIRST-Nuclides program, SCK•CEN will conduct leaching experiments on a PWR UOX fuel, taken from the Belgian Tihange 1 reactor, with an rod average burnup of 50 MWd/kg<sub>HM</sub> in order to determine the rapid release of some of the most critical radionuclides. The main experimental parameters have been defined, i.e. the type of fuel, the number of tests and the sample preparation, the experimental setup, the leach test conditions (medium, atmosphere), the sampling scheme and the surface and solution analyses. Preparations are on-going, with the start of leach tests planned for early 2013. The average pellet burnup of the samples tested will be determined analytically, together with a detailed characterization of the microstructure.

## Introduction

As one of the partners of FIRST-Nuclides with a hot-cell infrastructure and the required analytical laboratories, SCK•CEN will perform leach tests on spent fuel samples with a relatively high burn-up. For this purpose, a fuel rod was selected from the spent fuel stock available at SCK•CEN for which the characteristics are known and can be made public.

The selected fuel samples originate from a PWR UOX fuel from the Belgian Tihange 1 reactor with an average burnup of 50 MWd/kg<sub>HM</sub>. More information about this fuel is given in the paper from SCK•CEN's contribution to WP1 of FIRST-Nuclides (Govers et al., 2012).

The results obtained from leach tests depend on how the fuel samples are prepared before leaching commences. Cladded fuel segments and decladded fuel fragments, or fragments from the centre or the periphery of the pellet will exhibit different leaching behaviours. A combination of differently

prepared samples provides the most complete information, but for budgetary reasons, the number of tests with different samples has been limited to two at SCK•CEN.

In the following sections, we describe the sample preparation, the sample pre-test characterization, the experimental setup, the leachate composition and the solution analyses, before ending with our conclusions and future work. The details of the methods presented may have to be changed if difficulties occur when they are applied.

### **Sample preparation**

Two fuel segments, about 2.5 cm long, including one whole and two half pellets, will be taken from the central part of the fuel rod (Govers et al., 2012), and prepared as samples for leach testing.

As agreed with the other partners in WP3, every participating laboratory should perform at least one test with an intact clad fuel segment. So the first segment will be used as it is after cutting, without any further treatment. For a second test, the cladding will be cut open longitudinally on opposite sides of the fuel segment. The two cladding halves with the attached fuel will be separated from each other by applying force with a simple tool (e.g. screwdriver). The fuel attached to the cladding halves will not be detached. The leach test will be done with the two cladding halves, the attached fuel, and the fuel fragments that may come loose during the sample preparation, all in one leach vessel.

A third, adjacent segment will be cut in order to determine the burnup by means of radiochemical analysis.

A fourth, shorter segment, will be cut for the microstructural characterization of the fuel before leaching. That same sample will also be analysed by electron-probe microanalysis (EPMA) to determine the local concentration of various elements.

### **Sample pre-test characterization**

Although fabrication data and detailed irradiation history will be available for the project, a cross-check between these estimations and experimental observations of the state of the irradiated fuel is needed in order to reduce uncertainties on e.g. available free surfaces for leaching and on fission product inventory and location at the end of the irradiation. Good agreement between experiments and theoretical models for the behaviour of "observable" fission products would allow us to make firm hypotheses about the location of the few isotopes for which the experimental sensitivity is too low.

### *Burnup analyses*

The average pellet burnup will be determined by radiochemical analysis (RCA) of a small fuel segment (equivalent of 2 pellets) cut in the vicinity of the test samples. The proposed cutting scheme specifies a cutting from mid-pellet to mid-pellet in order to keep a relevant inventory of Cs, bearing in mind the relocation of Cs to the pellet-pellet interface observed upon  $\gamma$ -scanning. The burnup determination is based on the measurement of various burnup indicators, mainly Nd isotopes, by TIMS, and confirmed by  $^{137}\text{Cs}$  and  $^{144}\text{Ce}$ , using  $\gamma$ -spectrometry. Other relevant isotopes in terms of the fast / instant release fraction will also be measured, within the range permitted by the technique.

### *Microstructure analysis*

A segment (1 pellet height, cut from mid-pellet to mid-pellet) of the rod fuel will be examined using different surface analysis techniques. After polishing, optical microscopy and Scanning Electron Microscopy (SEM) will be used to observe the surface state and the different zones before the leach test. This will provide information about the microstructure of the fuel, such as e.g. the cracking pattern or the radial extent of the high burnup structure zone. Inspection of the outer part of the pellet will determine whether contact was established between the pellet and the cladding, and the extent of the interaction layer. A Telatom 3 optical microscope and a JEOL JSM-6310 SEM are installed inside a hot cell and licensed for the analysis of irradiated fuel pellets.

### *Electron-probe microanalysis*

That very same sample used for microstructure analysis will also be subjected to electron-probe microanalysis (EPMA). A CAMECA SX-100R instrument, installed inside a hot cell, is available at SCK•CEN. The instrument has four shielded spectrometers and can analyse all elements from C to Cm. The shielding of the spectrometers protects the detectors from the direct radiation of the sample and allows the analysis of radioactive samples. The EPMA technique enables the quantitative determination of the local concentration of selected elements with a detection limit up to 100 ppm. Contrary to the radiochemical burnup analysis, which provides isotopic information, EPMA concerns only the elemental content. It can, however, sample much smaller zones (typically of the order of hundreds of micrometers) and provide local information. The radial distribution of Xe, Cs and Nd (together with U and Pu) will be measured using this technique. Local inventory in a grain is also possible and would indicate the extent of depletion of some elements close to grain boundaries. These measurements will be performed directly inside the hot cell.

## Experimental setup

The experiments will be performed inside a hot cell under an air atmosphere.

Since SCK•CEN did not, at the start of FIRST-Nuclides, possess leaching equipment suitable for use inside a hot cell, our experimental setup was selected by comparing the advantages and disadvantages of the various setups employed by the other partners. Finally the setup used at PSI for similar purposes was chosen (**Figure 1**). It consists of glass tubes, used as leaching vessels, each equipped with a piston that fits tightly in the glass tube. After filling the tube with the leachant previously deaerated by bubbling with Ar, the air in the headspace is pushed out by the piston via an overflow. Because there will be little or no further exchange between the solution in the vessel and the air in the hot cell, fuel oxidation by atmospheric oxygen should be limited during the leaching test. At the bottom of each glass tube, a glass frit prevents the loss of spent fuel fragments during sampling. A moderate pressure on the piston is sufficient to force the solution through the frit. The sample volume at each sampling point depends on the number and height of the perforations in the metal rod that fixes the piston at the desired height.

Three parallel leach tests will be conducted: one leach unit will contain an intact fuel segment, a second unit will contain a partially decladded sample (see 'sample preparation'), and a third unit will be filled only with the leachate, as a blank test to estimate the cross contamination.



**Figure 1:** Experimental setup used by PSI for the leaching of the spent fuel, and applied also at SCK•CEN [Courtesy of PSI]

## Leachate composition

The leachate composition can have an influence on the leaching behaviour of specific radionuclides, if their release is solubility controlled. Leachants of different pH can thus result in different leaching or different stability in solution of the leached components (e.g.  $^{14}\text{C}$  in carbonate form can volatilize if the pH is too low). In the case of redox sensitive radionuclides, such as Se and Tc, the redox potential of the medium is even more important. The oxidation of the fuel will cause a faster release of radionuclides from the fuel matrix, and may increase the solubility of Se and Tc, if they are originally present in reduced form.

To eliminate the uncertainty linked to the use of different leachates when the tests with different fuels are compared, there is agreement within WP3 to use a standard leachant, consisting of 19 mM NaCl + 1 mM  $\text{NaHCO}_3$ . The pH of this solution is around 7.4. No pH buffer will be added to the solution, because important pH changes are not expected.

## Solution analyses

All leaching vessels will be sampled simultaneously at four different points in time, the final sampling being planned for one year after the start of the tests.

Only the most relevant radionuclides will be measured, using either mass-spectrometry or radioanalytical techniques.

The concentration of  $^{238}\text{U}$  will be used to estimate the dissolution rate of the fuel and will be measured by means of ICP-MS.

ICP-MS will permit the determination of the concentrations of  $^{93}\text{Zr}$ ,  $^{129}\text{I}$ ,  $^{135}\text{Cs}$ ,  $^{137}\text{Cs}$ ,  $^{99}\text{Tc}$ ,  $^{107}\text{Pd}$  and  $^{126}\text{Sn}$  releases into solution during the dissolution of the fuel. Some of these radionuclides (especially  $^{107}\text{Pd}$ ,  $^{129}\text{Sn}$  and  $^{99}\text{Tc}$ ) may have concentrations close to the detection limit.

The concentrations of  $^{59}\text{Ni}$ ,  $^{94}\text{Nb}$  and  $^{137}\text{Cs}$  will be measured by  $\gamma$ - or X-ray-spectrometry. The concentrations of  $^{14}\text{C}$ ,  $^{63}\text{Ni}$  and  $^{90}\text{Sr}$  will be determined using liquid scintillation counting (LSC).

In some cases, prior to the analyses, a separation will be required to avoid interference with others radionuclides. This will be the case for  $^{14}\text{C}$ ,  $^{59}\text{Ni}$ ,  $^{63}\text{Ni}$ ,  $^{94}\text{Nb}$  and  $^{90}\text{Sr}$ .

Although the measurement of the  $^{14}\text{C}$ -,  $^{59}\text{Ni}$ -,  $^{63}\text{Ni}$ - and  $^{94}\text{Nb}$ -content of waste matrices is performed routinely at SCK•CEN, their analysis in a spent fuel and/or in leachates thereof has not previously been performed at SCK•CEN. An evaluation and optimization of existing methodologies will have to be performed.

Analyses of  $^{79}\text{Se}$  are not planned.

### **Conclusions and Future work**

The main parameters of the experiments to be performed by SCK•CEN have been fixed. The equipment for the leaching experiments has been ordered and should be delivered before the end of 2012. In the meantime, the accessory equipment is being prepared, including for the longitudinal cutting, and the analytical scheme is being worked out in detail. The cutting of the fuel segments is planned for the end of 2012 or January 2013, depending on the exact availability of the cutting equipment and hot cell.

The leaching tests are expected to start in the first months of 2013, such that the analytical results from the last sample (after one year) will be available mid-2014. The first analytical results will be available in the course of 2013. The average pellet burnup analysis is planned in parallel in 2013.

### **Acknowledgement**

*The research leading to these results has received funding from the European Union's European Atomic Energy Community's (Euratom) Seventh Framework Programme FP7/2007-2011 under grant agreement n° 295722 (FIRST-Nuclides project).*

This work was performed as part of the programme of the Belgian Agency for Radioactive Waste and Enriched Fissile Materials (NIRAS/ONDRAF) on the geological disposal of high level/long-lived radioactive waste. The authors gratefully acknowledge the technical support from Ben Gielen and the analytical service of the SCK•CEN as well as AREVA, Electrabel and Tractebel for the data related to the fuel rod.

### **References**

Govers, K., Verwerft, M., Lemmens K. (2012) Characterization of SCK•CEN fuel samples used for leaching test experiments in the framework of FIRST-Nuclides. 7<sup>th</sup> EC FP – FIRST-Nuclides 1<sup>st</sup> Annual Workshop Proceedings.

# CHARACTERIZATION OF IRRADIATED PWR UOX FUEL (50.4 GWd/THM) USED FOR LEACHING EXPERIMENTS

Volker Metz\*, Andreas Loida, Ernesto González-Robles, Elke Bohnert, Bernhard Kienzler

Karlsruher Institute of Technology (KIT), DE

\* Corresponding author: volker.metz@kit.edu

## Abstract

A high burn-up UOX fuel, discharged from the *KKG* pressurized water reactor (PWR Gösgen, Switzerland) was chosen for leaching experiments, which will be conducted at KIT-INE to determine the instant / fast release fraction of safety relevant radionuclides. The studied fuel rod segment achieved an average burn-up of 50.4 GWd/t<sub>HM</sub> and a maximal linear power of 340 W/cm during reactor operation. Besides the burn-up and linear power rate, the instant / fast release fraction of the spent nuclear fuel depends on various parameters related to the manufacturing and irradiation history, which are documented in the present communication. Characteristics of the selected spent nuclear fuel sample are compared to characteristics of other high burn-up fuels studied within the FIRST-Nuclides project.

## Introduction

In safety assessments for disposal of spent nuclear fuel (SNF) in deep underground repository, failure of canisters and loss of the integrity of fuel rods is considered in the long term. Some of the radionuclides within the SNF material will be directly exposed to water contact after the barrier failure. Experimental studies performed at KIT-INE aim on the fast / instant release of activation and fission products from a high burn-up (HBU) fuel upon contact with water. This information is a prerequisite for a reliable assessment of the migration / retention processes of activation and fission products in the spent nuclear fuel, in the cladding, and for estimation of the fast / instant release fraction (IRF). The IRF depends on critical characteristics of the SNF such as manufacturing process, burn-up history and fuel temperature history and storage time.

For the experimental and theoretical studies within the FIRST-Nuclides project, KIT-INE provides a HBU-SNF rod segment in the ownership of KIT, where all data and findings can be published without

restrictions. The fuel rod was irradiated during four cycles in the PWR Gösgen (*KKG*), Switzerland, and discharged in May 1989. During reactor operation an average burn-up of 50.4 GWd/t<sub>HM</sub> was achieved. Characteristic data of the *KKG* fuel sample were collected, dealing with the fuel manufacturing, fuel assembly design and irradiation history. With respect to the cladding, the characterization covers the composition, cladding thickness and the initial radial gap width between pellet and cladding. The information regarding the fuel material comprises the initial enrichment, pellet dimensions, density and specifics of the production process. The irradiation history covers the burn-up, the irradiation time and the number of cycles as well as the maximum and average linear power rate.

The selected fuel rod segment (**Figure 1**) was transported to JRC-ITU in March 2012 for characterisation, gas sampling, cutting and sampling of fuel pellets. Results of the non-destructive characterisation and gas sampling, conducted in the following weeks, are given in reports of JRC-ITU and KIT-INE (Wegen et al., 2012a; Wegen et al., 2012b; Wegen et al., 2012c; González-Robles et al., 2012, respectively). After puncturing and successive cutting of the fuel rod segment, gas samples and fuel pellets were returned to KIT-INE for further investigations.



**Figure 1:** 50.4 GWd/t<sub>HM</sub> PWR fuel rod segment after removal from the lead shield storage tube at the shielded box-line of KIT-INE before transport to JRC-ITU



### Characteristics of the selected 50.4 GWd/t<sub>HM</sub> PWR fuel

The data given in **Table 1** characterize the studied segment N0204 of the KKG-BS fuel rod SBS1108. The studied HBU-SNF consists of pure UO<sub>2</sub>, fabricated by Kraftwerk Union AG using the *NIKUSI* sintering process (Stratton et al., 1991). *NIKUSI* is a short-term fast sintering process under controlled oxidizing condition at a temperature (< 1300 °C) below the temperature range of conventional UO<sub>2</sub> pellet sintering processes (Kutty et al., 2004). Stratton et al. (1991) reported an UO<sub>2</sub> stoichiometry of U/O = 2.002. Generally, the fuel pellets of the segment had been initially enriched with 3.8% <sup>235</sup>U. Two pellets adjacent to the upper and lower isolation pellets were made of U<sub>nat</sub> (**Figure 2**). The cladding material is Zircaloy-4 (DX ESL 0.8) with an external and internal diameter of 10.75 ± 0.05 mm and about 9.3 mm, respectively; the wall thickness is specified as 0.725 mm (Kernkraftwerk Gösgen, 2010; Stratton et al., 1991).

The lattice geometry of the fuel assembly consisted of a 15×15 array of fuel rods. 205 of the 225 positions per assembly were occupied with fuel rods, the 20 remaining positions were available for control rods (Kernkraftwerk Gösgen, 2010). The final rod-average burn-up was estimated as 50.4 GWd/t<sub>HM</sub> for the fuel rod SBS1108, which had been achieved in four cycles of 1226 days total irradiation duration. A rim zone burn-up of 67.0 GWd/t<sub>HM</sub> and a maximal temperature during irradiation above 1300 °C was estimated based on the data of **Table 1** (Kienzler et al., 2012). The average and maximal linear power was calculated as 260 and 340 W/cm, respectively.

**Table 1:** Characteristic data of 50.4 GWd/t<sub>HM</sub> fuel rod segment discharged from PWR Gösgen

Data category	Information category	Parameter
Reactor	essential	PWR Gösgen, Switzerland light water coolant
Fuel assembly design information	essential	Lattice geometry: 15x15 48 assemblies with 20 control rods per assembly External fuel rod diameter: 10.75 ± 0.05 mm Fuel rod # SBS 1108, Segment N 0204
Fuel rod data	essential	Test fuel rod Internal rod pre-pressure: 21.5 ± 1 bar He
Fuel material data	essential	UO <sub>2</sub> fuel, initial enrichment 3.8% <sup>235</sup> U, U <sub>nat</sub> , resp. O/U = 2.002; fuel fabrication without additives Pellet dimensions: Ø = 9.2 mm, height = 11 mm Calculated radionuclide inventory given in Grambow et al. (2000) Fuel density (as fabricated): 10.41 g/cm <sup>3</sup>
	supplemental	Measured radionuclide inventory given in Grambow et al. (2000)
Cladding data	essential	Zircaloy-4, DX ESL 0.8 Wall thickness: 0.725 mm Initial radial gap fuel / cladding: <0.17 mm
Irradiation data	essential	Calculated burn-up: 50.4 GWd/t <sub>HM</sub> Number of cycles: 4 Average linear power: 260 W/cm Maximal linear power: 340 W/cm Discharge: 27. May 1989 Irradiation duration: 1226 days

### Comparison of selected 50.4 GWd/t<sub>HM</sub> PWR fuel to other HBU-SNF samples

In a recent report regarding the characterisation of 13 spent nuclear fuel samples to be used in the FIRST-Nuclides project, it was shown that these HBU-SNF samples were irradiated at a wide range of operational conditions (Metz et al., 2012). The initial <sup>235</sup>U enrichment versus the average discharge burn-up of the selected fuel rods are compared to average values for irradiated BWR and PWR fuel assemblies reported by the NEA (2006). As shown in **Figure 3**, most of the high burn-up fuels selected for investigations in the project FIRST-Nuclides are on or close to trend-lines for present high burn-up fuels. The data point of the PWR Gösgen fuel rod segment plots on the trend line of PWR fuel with

4-batch-refuelling scheme and is characterized by a relatively low burn-up compared to the other PWR and BWR fuels selected for studies within FIRST-Nuclides. At the present state, the characterisation of the selected 13 HBU-SNF samples leads to the conclusion that these samples are relevant to high burn-up fuels which need to be disposed of in European repositories (Metz et al., 2012).

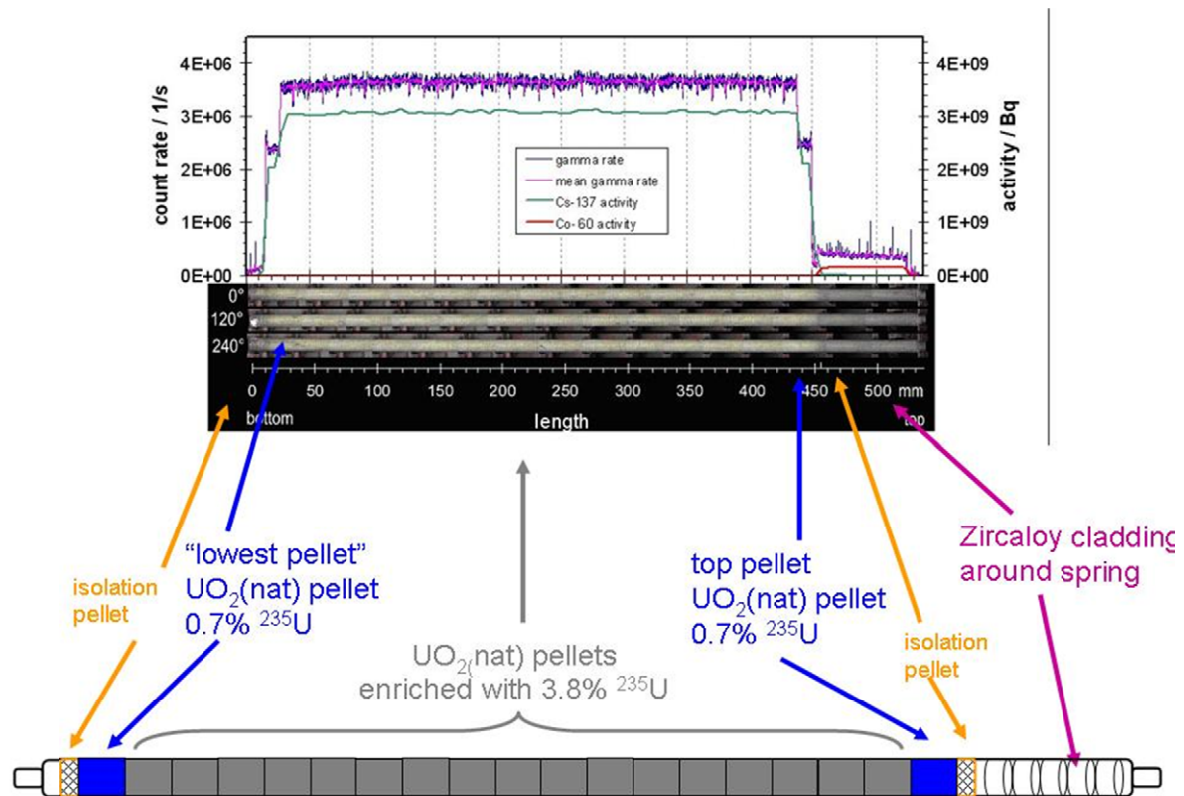


**Figure 2:** Schematic cross section of the Gösgen 50.4 GWd/t<sub>HM</sub> fuel rod segment and  $\gamma$ -scan of the segment showing the total  $\gamma$ -rate and the activities of <sup>137</sup>Cs and <sup>60</sup>Co along the segment. The  $\gamma$ -scan was measured by JRC-ITU and the inserted image is taken from Wegen et al. (2012a).

## Summary and Future work

KIT-INE provides a spent nuclear fuel rod segment in the ownership of KIT, where all data and findings can be published without restrictions. The studied 50.4 GWd/t<sub>HM</sub> PWR fuel belongs to a group of 13 HBU-SNF samples, considered as representative to some extent to high burn-up SNF which need to be disposed of in European repositories. Data on the fuel rod manufacturing and irradiation history are documented in the present communication. The fuel rod segment was transported to JRC-ITU for characterization, gas sampling, cutting and sampling of fuel pellets. Results of the non-destructive characterization, of the leaching behaviour, studied in previous experimental series, will be

documented and interpreted to complete the available data-set for the studied fuel rod segment. Within the FIRST-Nuclides project, pellets of the fuel rod segment will be used in leaching experiments to determine fast / instant release fraction under reducing conditions.

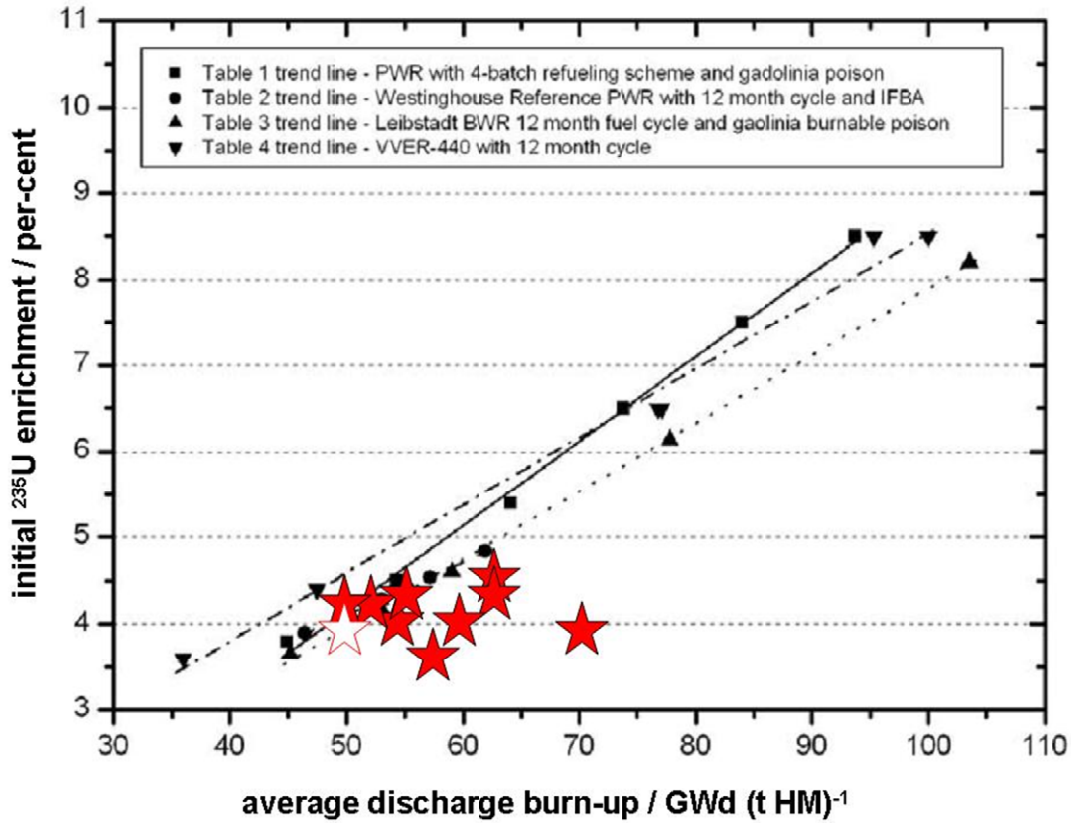


**Figure 3:** Initial  $^{235}\text{U}$  enrichment versus discharge burn-ups averaged per fuel assemblies (modified after NEA Nuclear Science Committee, 2006). Data of selected BWR and PWR fuel rods, to be used in the FIRST-Nuclides project, are shown as stars. The data point of the 50.4 GWd/t<sub>HM</sub> PWR fuel is denoted by an open star.

**Acknowledgements**

The authors would like to thank our colleagues at JRC-ITU, in particular to Ralf Gretter, Ramil Nasyrow, Dimitrios Papaioannou, Wim de Weerd and Detlef Wegen for performing the non-destructive analysis of the 50.4 GWd/t<sub>HM</sub> PWR fuel segment as well as for cutting the segment and further activities related to the characterization of the samples. The reviews by Daniele Boulanger (ONDRAF-NIRAS) and Lawrence Johnson (NAGRA) are gratefully acknowledged.

*The research leading to these results has received funding from the European Union's European Atomic Energy Community's (Euratom) Seventh Framework Programme FP7/2007-2011 under grant agreement n° 295722 (FIRST-Nuclides project).*

## References

- González-Robles, E., Bohnert, E., Loida, A., Müller, N., Lagos, M., Metz, V., Kienzler, B. (2012) Fission gas measurements and description of leaching experiments with of KIT's irradiated PWR fuel rod segment (50.4 GWd/t<sub>HM</sub>). 7<sup>th</sup> EC FP – FIRST-Nuclides 1<sup>st</sup> Annual Workshop Proceedings (Budapest, Hungary).
- Grambow, B., Loida, A., Martínez-Esparza, A., Díaz-Arocas, P., de Pablo, J., Paul, J.-L., Marx, G., Glatz, J.-P., Lemmens, K., Ollila, K., and Christensen, H. (2000) Long-term safety of radioactive waste disposal: source term for performance assessment of spent fuel as a waste form. Final report. Source term for performance assesment of spent fuel as a waste form. European Commission, Nuclear Science and Technology Series. Forschungszentrum Karlsruhe Wissenschaftliche Berichte, FZKA 6420.
- Kernkraftwerk Gösgen (2010) Technik und Betrieb – Technische Hauptdaten. Kernkraftwerk Gösgen-Däniken AG, Däniken (Solothurn, Switzerland).
- Kienzler, B., Bube, C., González-Robles, E., Metz, V. (2012) Modelling of boundary conditions for upscaling migration / retention processes of fission products in the spent nuclear fuel structure. 7<sup>th</sup> EC FP – FIRST-Nuclides 1<sup>st</sup> Annual Workshop Proceedings (Budapest, Hungary).
- Kutty, T.R.G., Hegde, P.V., Khan, K.B., Jarvis, T., Sengupta, A.K., Majumdar, S., Kamath, H.S. (2004) Characterization and densification studies on ThO<sub>2</sub>-UO<sub>2</sub> pellets derived from ThO<sub>2</sub> and U<sub>3</sub>O<sub>8</sub> powders. *Journal of Nuclear Materials*, 335, 462-470.
- Metz, V., Bohnert, E., Bube, C., González-Robles, E., Kienzler, B., Loida, A., Müller, N., Carbol, P., Glatz, J. P., Nasyrow, R., Papaioannou, D., Rondinella, V. V., Serrano Purroy, D., Wegen, D., Curtius, H., Klinkenberg, H., Günther-Leopold, I., Cachoir, C., Lemmens, K., Mennecart, T., Vandendorre, J., Casas, I., Clarens, F., de Pablo, J., Sureda Pastor, R., Hózer, Z., Slonszki, E., Ekeröth, E., Roth, O. (2012) Fast / Instant Release of Safety Relevant Radionuclides from Spent Nuclear Fuel (FIRST-Nuclides): Characterisation of spent nuclear fuel samples to be used in FIRST-Nuclides – relevance of samples for the Safety Case. Deliverable No 1.1. European Commission, Brussels.
- NEA (2006) Very High Burn-ups in Light Water Reactors. OECD Nuclear Energy Agency, NEA publication no. 6224, ISBN 92-64-02303-8.
- Stratton, R.W., Botta, F., Hofer, R., Ledergerber, G., Ingold, F., Ott, C., Reindl, J., Zwicky, H.U., Bodmer, R., Schlemmer, F. (1991) A comparative irradiation test of UO<sub>2</sub> sphere-pac and pellet fuel in

the Goesgen PWR. International Topical Meeting on LWR Fuel Performance “Fuel for the 90’s”(Avignon, France), p. 174-83.

Wegen, D.H., Papaioannou, D., Nasyrow, R., Rondinella, V.V., Glatz, J.P. (2012a) Non-destructive analysis of a PWR fuel segment with a burn-up of 50.4 GWd/t<sub>HM</sub> – Part I: Visual examination and  $\gamma$ -scanning. 7<sup>th</sup> EC FP – FIRST-Nuclides 1<sup>st</sup> Annual Workshop Proceedings (Budapest, Hungary).

Wegen, D.H., Papaioannou, D., Nasyrow, R., Rondinella, V.V., Glatz, J.P. (2012b) Non-destructive analysis of a PWR fuel segment with a burn-up of 50.4 GWd/t<sub>HM</sub> – Part II: Defect determination. 7<sup>th</sup> EC FP – FIRST-Nuclides 1<sup>st</sup> Annual Workshop Proceedings (Budapest, Hungary).

Wegen, D.H., Papaioannou, D., Gretter, R., Nasyrow, R., Rondinella, V.V., Glatz, J.P. (2012c) Preparation of samples for IRF investigations and Post Irradiation examinations from 50.4 GWd/t<sub>HM</sub> PWR fuel. 7<sup>th</sup> EC FP – FIRST-Nuclides 1<sup>st</sup> Annual Workshop Proceedings (Budapest, Hungary).

# MODELLING OF SPENT FUEL SATURATION WITH WATER – APPROACH, PRELIMINARY RESULTS AND POTENTIAL IMPLICATIONS

Marek Pȩkala<sup>\*</sup>, Andr s Idiart , Lara Duro, Olga Riba

Amphos 21 Consulting S.L. (AMPHOS21), ES

\* Corresponding author: [marek.pekala@amphos21.com](mailto:marek.pekala@amphos21.com)

## Introduction

Disposal in a deep underground repository is currently considered by several countries as the preferred option for the long-term management of spent nuclear fuel (SNF). For regulatory reasons the safety of such a disposal facility must be demonstrated quantitatively through Performance Assessment (PA) calculations. One of the factors that have the potential to significantly influence the results of PA is the radionuclide release rate from the waste upon contact with groundwater. In current PA calculations the radionuclide release from the SNF is typically represented by a two-stage process: (i) an instantaneous release of a fraction of the inventory immediately upon contact with water (the *instant release fraction* – IRF), followed by (ii) a relatively slow release rate of the inventory confined in the SNF matrix over a long period of time. PA calculations indicate that instant release is important for the overall safety assessment of the facility, but there are significant uncertainties about the nature of this phenomenon and how it should be represented in PA. The First Nuclides project has been initiated with the aim to provide better, both conceptual and quantitative, understanding of the processes involved in the instant release of radionuclides from SNF.

In the context of IRF, the knowledge of the rate of SNF saturation with water is key as the release of some radionuclides is conditioned upon wetting of the grain surfaces of the fuel by water. Therefore, the instant release rate of these radionuclides depends, among others, on the rate of SNF saturation with water. An improved understanding of the rate of saturation with water will help to elucidate radionuclide instant release both under repository conditions and with regard to laboratory experiments conducted on the SNF under near-room conditions.

## Conceptual Approach

### *Background and Motivation*

Under repository conditions water saturation of the SNF would be contingent upon breaching of the surrounding cladding, which provides a water-tight barrier. This could happen as a result of a number of physico-chemical processes (Rothman, 1984; Pescatore et al., 1989). Depending on the gas pressure within the intact fuel rod, a local failure (e.g. a pin-hole or a small crack) of the cladding under fully saturated conditions in the near-field could allow water ingress into the rod (if the hydrostatic pressure is higher than the gas pressure in the rod) until the gas pressure within the rod established equilibrium with the hydrostatic pressure. The amount of water flowing into the rod (and therefore the SNF portion directly exposed to water) would depend on the initial gas pressure in the rod and on the hydrostatic pressure (which under fully saturated conditions is a function of the repository depth). Should the initial gas pressure be above the hydrostatic pressure, after the excess gas has escaped the rod, direct water inflow into the rod would be prevented due to pressure equilibration between the inside and outside of the rod. From a conceptual viewpoint, modelling of SNF water saturation under the above-described scenarios would require a dual-phase (coupled water-gas flow) approach, where the two partial differential equations (PDE) describing the flow of the two phases are coupled and solved simultaneously. Such an approach poses a significant computational challenge, therefore as a first attempt a simplifying assumption was made according to which the cladding had undergone extensive damage allowing all gas contained within the fuel rod to escape. This approach eliminates the need to account for the coupled behaviour of the gas in the system. Consequently, a computationally simpler approach for unsaturated water flow described by the Richards equation could be used, which relies on the assumption that gas has sufficiently low viscosity to allow it to move (as it is replaced by water) without significant pressure build-up (Pinder and Celia, 2006). Therefore, in this approach it is assumed that there is no gas pressure gradient. This model represents therefore a worst-case scenario, whereby groundwater can contact the entire external surface of the SNF pellet stack within the rod. It is further assumed, that the process of water saturation of the entire SNF pellet stack can be adequately approximated by the saturation of a single pellet. Therefore, the calculation results represent the saturation with water of a single SNF pellet. This approach has the additional benefit that it resembles saturation of a single uncladded SNF pellet under laboratory conditions (if account is taken of the appropriately lower boundary water pressure values, which are near atmospheric). Hence, the results of these calculations may be useful in elucidating the results of radionuclide release rate studies conducted under laboratory conditions.



### *Interconnected Pellet Voidage Available for Saturation with Water*

Fluid saturation of a medium is the process of filling up of interconnected voids within the medium by the fluid. It has been suggested that, during the saturation with water of SNF, very slow water vapour diffusion along boundaries of individual  $\text{UO}_2$  grains composing the fuel pellet may occur (Marchetti et al., 2010). However, as a first approximation, in this work it has been assumed that this (matrix) “porosity” is inaccessible to liquid water. Although a significant increase of porosity occurs in the SNF pellet rim as a result of recrystallization processes during irradiation in the reactor, these are assumed to be non-connected, and therefore were excluded from the model (Spino et al., 1996). Fuel pellets suffer a varying degree of cracking due to thermo-mechanical constraints while irradiated in the reactor (e.g. Faya, 1981). This is due to a sharp thermal gradient that is established radially within a pellet and the resulting differential expansion. The degree of cracking (aperture geometry and crack patterns) depends on the reactor operating conditions and can be somewhat correlated with the degree of burn-up (Oguma, 1983; Williford, 1984). In the water saturation calculations presented here, only cracks are assumed to provide continuous passage (connected “porosity”) to inflowing water, and are therefore the only pathways included in the model.

### *Conceptualisation of the Pellet*

For modelling purposes an idealised *Reference Pellet* representing relatively high linear power and burn-up conditions (around 60 kW/m) was defined (**Figure 1**). It was assumed that the pellet consists of completely impervious matrix (i.e. zero interconnected porosity) and is cross-cut by cracks.

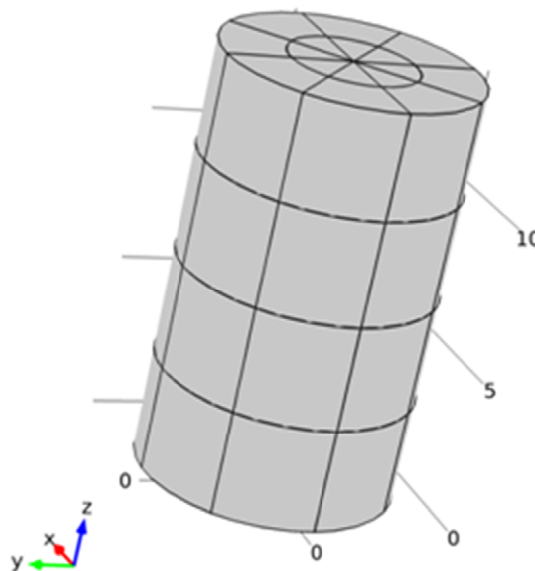


**Figure 1:** The Reference Pellet with idealised crack pattern. Pellet dimensions are in millimetres (height = 13.5 mm, diameter = 8.19 mm).

The crack characteristics of the *Reference Pellet* were defined based on literature relating mean pellet crack aperture (20  $\mu\text{m}$ ) and crack pattern (regularly distributed cracks: 3 axial, 3 radial and 1 circumferential) with power applied to rod in the reactor (Oguma, 1983; Williford, 1984). Thereafter, the saturation with water of these cracks was modelled as saturation of a network of discrete cracks. It was further assumed that the pellet is at room temperature, therefore no heat transfer or high temperature effects are accounted for.

In addition to the *Reference Pellet* calculations (water saturating major cracks), another set of calculations was carried out to test the influence of sub-micrometre scale cracks (present within sectors of the pellet bounded by the major cracks). 1D calculations over a reference distance of 1 mm were performed assuming an arbitrarily small (due to lack of reliable data) mean fracture aperture of 0.1  $\mu\text{m}$  and employing the concept of porous-equivalent medium (which assumes that the cracks are sufficiently small and well-connected so as to be adequately approximated by a porous medium). Also the interconnected voidage for these calculations was assumed to be 0.1 (where by *voidage* is meant the ratio of volume of void space within the pellet and the total volume of the pellet).

The rationale for splitting the calculations into two separate models of different scales was based on the expected distinct time-scales required for the saturation of the major and small crack systems (which was expected to be much faster in case of the larger cracks).

#### *Mathematical Description of Saturation with Water*

The modelled process is variably-saturated flow of water in cracks. The simplest mathematical model for such a problem is based on the Richards equation (Bear and Cheng, 2010), which constitutes an extension of the empirical Darcy's Law to unsaturated conditions. Although originally developed to model variably-saturated flow in soils, the Richards approach has been further extended to other porous and fractured materials (Finsterle, 2000; Liu and Bodvarsson, 2001). The Richards equation is a PDE that can be solved for water (moisture) pressure (or equivalently for water content) as a function of time and space. The solution of the Richards equation must however be conducted simultaneously with a coupled set of constitutive algebraic equations describing water retention and relative permeability properties of the medium. In this study the commonly used van Genuchten model (van Genuchten, 1980) is used in conjunction with the Richards flow equation. In the model, the dependence of permeability on the degree of water saturation results in significant non-linearity, especially at low water content (dry) conditions, which may render the problem numerically difficult (instability and convergence problems – Forsyth et al., 1995).

### *Parameterisation of the Model*

Two parameters ( $n$  and  $\alpha$ ) are required for the van Genuchten model. These are typically derived from laboratory water saturation experiments. However, to the authors' knowledge, this data is not available for SNF. Therefore, retention curves for the pellet were estimated based on a model derived from statistical considerations of the cracks apertures (Fredlund and Xing, 1994; Zhang and Fredlund, 2003). The retention curve was calculated assuming a mean value of crack aperture (20  $\mu\text{m}$  for the Reference Pellet calculations and 0.1  $\mu\text{m}$  for the small-scale cracks calculations), a relative standard deviation of the apertures (50% and 100%) and assuming that the crack apertures follow a log-normal distribution. No data is available on the relative standard deviations for SNF crack apertures, therefore intermediate values from the study of Keller (1997) on fracture statistics from rock cores were used as first approximations. The van Genuchten parameters were then fitted to the retention curves by means of non-linear optimisation. The interconnected voidage in the *Reference Pellet* (volume of fractures over bulk volume, 0.02) was estimated from the assumed mean fracture aperture and the fracture geometry. In the case of the small-scale cracks calculations, an arbitrary value of 0.1 was assumed for their porosity. The saturated permeability was estimated according to the cubic law, which relates the permeability with the cube of the aperture (Marsily, 1986). Zero compressibility for the fractures was assumed. The residual water content was also assumed to be zero.

### **Numerical Implementation**

The model was implemented in the finite element code *Comsol Multiphysics* using the *Fracture Flow Interface* (for the *Reference Pellet*) and the *Richards Interface* (for the sub-micrometre scale crack apertures – porous-equivalent approach). The *Fracture Flow Interface* was modified by manually implementing a storage-retention term and the van Genuchten constitutive equations so as to account for variably-saturated flow within the fractures. The pressure is the state variable of the model. The finite element mesh (consisting of 10,500 triangular elements) used in calculations for the *Reference Pellet* is shown in **Figure 2**. Mesh-independence of the solution was verified by running select calculations with a refined mesh of 50,000 elements. In the case of sub-micrometre cracks, calculations were carried out using 1D geometry over a reference distance of 1 mm discretised by 1000 elements, and with the cracks represented as an effective porous medium (*Richards Interface*). MUMPS direct solver was used to solve the set of linear algebraic equations resulting from problem discretisation, while the solution was progressed in time using the BDF solver. Linear finite elements were used and gravity effects were ignored.

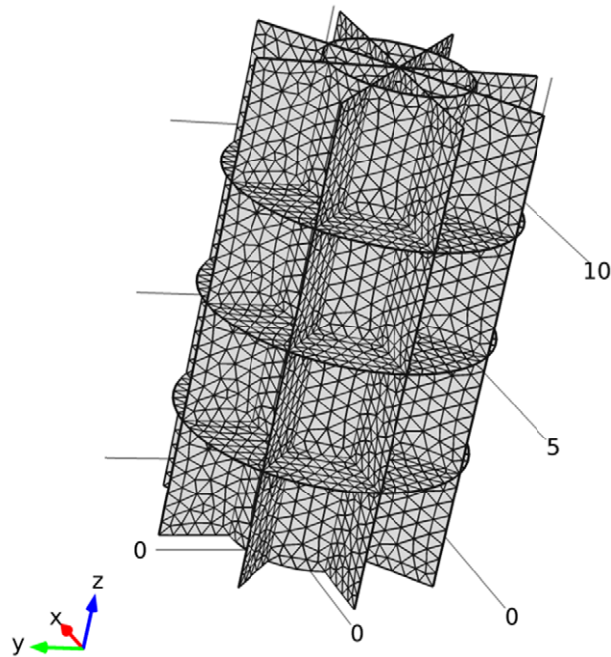


**Figure 2:** The finite element mesh of the Reference Pellet. Dimensions are in millimetres.

## Calculation Cases and Results

### *Boundary Conditions*

The preliminary calculation efforts presented below focused on low boundary pressures (corresponding to 5 cm water column), which may be thought of as representative of laboratory ambient conditions (i. e. water saturation of an uncladded pellet in a beaker), in contrast with hydrostatic pressures at repository depth (e.g. 400-500 m). The boundary pressure (constant in time) was applied to all external crack boundaries, as shown in **Figure 3**.

### *Initial Conditions*

The initially dry conditions in the pellet were represented by a low water saturation degree; two values were tested: 1‰ and 0.1‰. An example of the initial and boundary state of the Reference Pellet corresponding to about 1‰ water saturation is shown in **Figure 3**.

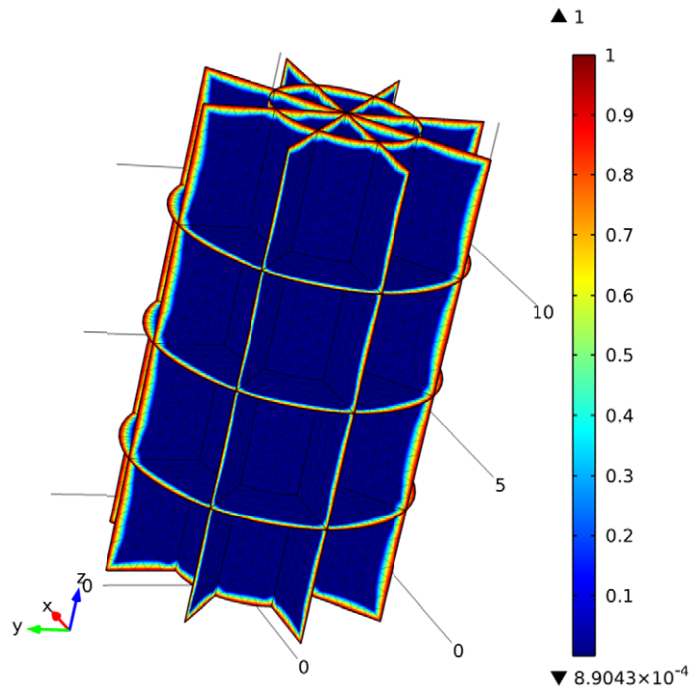


**Figure 3:** Example of the initial and boundary conditions applied to the Reference Pellet in a typical calculation. Colours represent degree of saturation with water (fraction of unity). Boundary water pressure (corresponding to 5 cm water column) is applied the external edges of cracks (full water saturation). The initial suction pressure corresponds to just below 1‰ water saturation. Pellet dimensions are in millimetres.

*Calculation Cases*

Two calculation cases were considered: (**Table 1**) saturation of the Reference Pellet through a network of interconnected discrete fractures (*Case 1*), and (**Table 2**) saturation of a network of sub-micrometre cracks (*Case 2*). Preliminary results of these calculations are shown in **Tables 1** and **2** for the *Case 1* and *Case 2* calculations, respectively.

**Table 1:** Preliminary results for *Case 1*: approximate time to full water saturation in the Reference Pellet (mean fracture aperture 20 μm). RSD – relative Standard Deviation of fracture aperture assumed in calculating water retention, Initial S – initial degree of water saturation of the fracture system (initial condition). Boundary pressure corresponds to a 5 cm water column (near atmospheric conditions).

RSD (%)	Initial S = 1‰	Initial S = 0.1‰
50	1 second	1 minute
100	1 minute	2 hour

**Table 2:** Preliminary results for Case 2: approximate time to full water saturation of the sub-micrometre scale fractures (mean aperture  $0.1 \mu\text{m}$ ) over a distance of 1 mm. RSD – relative Standard Deviation of fracture aperture assumed in calculating water retention curve, Initial S – initial degree of water saturation of the fracture system (initial condition). Boundary pressure corresponds to a 5 cm water column (near atmospheric conditions).

RSD (%)	Initial S = 1‰	Initial S = 0.1‰
50	5 second	1 minute
100	2 hour	1 year

## Discussion

### *Main Uncertainties in the Model*

The results presented are preliminary and are underpinned by a number of important assumptions, which in the absence of literature or experimental data had to be made. Therefore, the water saturation times presented should be regarded with a degree of caution.

On a conceptual level, although the proposed approach has been applied to variably-saturated flow in fractured rocks (Finsterle, 2000; Liu and Bodvarsson, 2001), there exists some concern as to the validity of applying retention parameters derived from bulk scale properties to flow within individual, discrete cracks. This could be particularly the case if the extent of cracks is large relative to the modelled domain (the pellet). To circumvent this problem it is argued that retention properties of the pellet result predominantly from variation of crack apertures on a microscopic scale within individual cracks (rather than from the presence of cracks characterised by different, but relatively constant, apertures).

Considerable uncertainty exists regarding the parameterisation of the model. In particular, as the water retention curve of the pellet has not been determined experimentally and had to be approximated using geometric considerations, the resulting van Genuchten fitting parameters depend crucially on the crack network statistics. This information however is scarce and, to a large extent, had to be assumed. Two crack parameters are of special importance: the mean aperture and the standard deviation of the apertures. The latter parameter is especially important for the performance of the model (the calculated water saturation time) as can be seen from the results shown in **Tables 1** and **2**. Moreover, the initial degree of dryness (which defines the initial suction pressure in the crack network) has an important impact on the calculated time to full saturation with water. For example, if the initial degree of water saturation was much lower, the calculated saturation times would increase.

### *Potential Implications*

Due to the presence of cracks in the pellet of distinctly different apertures we expect that the water saturation of the SNF pellet will proceed in two stages. First the larger cracks will be saturated relatively quickly (possibly in a matter of minutes to hours) followed by saturation with water of the smaller (sub-micrometre) cracks, which may be a much longer process (operating over a time scale of many days to months). If any additional voids (aside cracks) were thought to participate in the saturation process (such as grain boundaries) this would make the saturation time significantly longer (perhaps on the scale of many years) depending on their hydraulic properties. Such a two-stage water saturation regime could have implications for the interpretation of SNF leaching experiments. In such experiments it has been observed that radionuclide release proceeds in two distinct phases: (i) a rapid release phase (over a period of minutes and hours) followed by (ii) an extended period of radionuclide release at a much slower rate (over periods of at least several hundreds of days – e.g. González-Robles (2011)). This pattern has been explained by distinct fuel dissolution rates operating during the two phases (González-Robles, 2011). However, the two-stage water saturation process described above could also exert a similar effect on the radionuclide release rate. The two mechanisms (dissolution and surface wetting) could be complementary. This hypothesis will be studied in more detail with the model developed in this work.

## **Conclusions and Future Work**

### *Conclusions*

A preliminary model for simulating the saturation with water of a single SF pellet has been proposed and tested. The pellet was conceptualised to be composed of a completely impervious matrix (with no interconnected porosity) cross-cut by a network of interconnected fractures. The fractures are idealised to belong to two separate populations differing in their mean aperture (20  $\mu\text{m}$  and 0.1  $\mu\text{m}$ ). Saturation with water proceeds through the cracks network due to water pressure gradient. The Richards approach to modelling variably-saturated flow within the crack was employed and the model was implemented in *Comsol Multiphysics*. Although considerable uncertainties remain regarding the parameterisation of the model (particularly with respect to the water retention properties of the pellet) preliminary results indicate that (under near atmospheric conditions) the larger cracks would saturate relatively quickly (within hours at most), while the smaller cracks may take much longer to become fully saturated (months to years). This may have implications for the interpretation of laboratory SNF leaching experiments on radionuclide release.

### *On-going and Future Work*

This work is under active development. It is expected that the uncertainties currently present in the model and affecting the results will be reduced as more experimental data becomes available. Using the current approach it is straightforward to include the effect of presence of partial cladding on the SF pellet (by adjusting the boundary conditions) as may be the case in some laboratory experiments. Similarly, extrapolation to repository conditions (of the water saturation of a single uncladded pellet) would pose no significant difficulty. An extension of the model to include the entire rod under repository conditions is possible but would cause a significant increase in the complexity of the model (dual-phase coupled flow of gas and water).

An alternative and more detailed approach to modelling variably-saturated flow in cracks could be based on the work of Or and Tuller (2000) who developed a model for surface liquid retention on rough fracture surfaces due to adsorptive and capillary forces. This approach however would require detailed knowledge on the crack surface geometry. Such information could be obtained, for example, by means of X-Ray Computer Tomography (CT).

### **Acknowledgement**

*The research leading to these results has received funding from the European Union's European Atomic Energy Community's (Euratom) Seventh Framework Programme FP7/2007-2011 under grant agreement n° 295722 (FIRST-Nuclides project).*

### **References**

- Bear, J. and Cheng, A. H-D. (2010) Modelling groundwater flow and contaminant transport. Theory and Applications of Transport in Porous Media Volume 23. Springer Science+Business Media B.V.
- Faya, S. C. S. (1981) A survey on fuel pellet and healing phenomena in reactor operation. Instituto de Pesquisas Energéticas e Nucleares, Centro de Engenharia Nuclear, Report OUTUBRO/1981.
- Finsterle, S. (2000) Using the continuum approach to model unsaturated flow in fractured rock. Water Research Resources, 36, 2055-2066.
- Forsyth, P. A., Wu, Y. S., Preuss, K. (1995) Robust numerical methods for saturated-unsaturated flow with dry initial conditions in heterogenous media. Advances in Water Resources, 18, 25-38.
- Fredlund, D. G. and Xing, A. (1994) Equations for the soil-water characteristic curve. Canadian Geotechnical Journal, 31, 521-532.



- van Genuchten, M. Th. (1980) A closed-form equation for predicting the hydraulic conductivity of unsaturated soils. *Soil Science Society of America Journal*, 44, 892–898.
- González-Robles Corrales, E. (2011) Study of radionuclide release in commercial UO<sub>2</sub> spent nuclear fuels. Effect of burn-up and high burn-up structure. Ph. D. Thesis, Universitat Politècnica de Catalunya.
- Keller, A. A. (1997) High resolution CAT imaging of fractures in consolidated materials. *International Journal of Rock Mechanics and Mining Sciences*, 34, 358.
- Liu, H-H. and Bodvarsson, G. S. (2001) Constitutive relations for unsaturated flow in a fracture network. *Journal of Hydrology*, 252, 116-125.
- Marchetti, I., Belloni, F., Himbert, J., Carbol, P., Fanghänel, Th. (2010) 2010 Spent Nuclear Fuel Workshop presentation. Barcelona, 3 November 2010.
- de Marsily, G. (1986) *Quantitative Hydrogeology*. Academic Press, San Diego.
- Oguma, M. (1983) Cracking and relocation behaviour of nuclear fuel pellets during rise to power. *Nuclear Engineering and Design*, 76, 35.
- Or, D. and Tuller, M. (2000) Flow in unsaturated fractured porous media: Hydraulic conductivity of rough surfaces. *Water Resources Research*, 36, 1165-1177.
- Pescatore, C., Cowgill, M. G., Sullivan, T. M. (1989) Zircaloy cladding performance under spent fuel disposal conditions. Brookhaven National Laboratory, Progress Report BNL-52235.
- Pinder, G. F. and Celia, M. A. (2006) *Subsurface Hydrology*. John Wiley & Sons, Inc.
- Rothman, A. J. (1984) Potential corrosion and degradation mechanisms of zircaloy cladding on spent nuclear fuel in a tuff repository. Lawrence Livermore National Laboratory, UCID-20172.
- Spino, J., Vennix, K., Coquerelle, M. (1996) Detailed characterisation of the rim microstructure in PWR fuels in the burn-up range 40-67 GWd/t<sub>M</sub>. *Journal of Nuclear Materials*, 231, 179-190.
- Tokunaga, T. K. and Wan, J. (1997) Water film flow along fracture surfaces of porous rock. *Water Resources Research*, 33, 1357-1367.
- Willford, R. E. (1984) A cracked-fuel constitutive equation. *Nuclear Technology*, 67, 208.
- Zhang, L. and Fredlund, D. G. (2003) Characteristics of water retention curves for unsaturated fractured rocks. Second Asian Conference on Unsaturated Soils, UNSAT-ASIA 2003, Osaka, Japan.



# MODELLING OF SPENT FUEL SATURATION WITH WATER –SELECTION OF MATERIALS, PREPARATIONS AND EXPERIMENTAL SET-UP

Olivia Roth\* and Anders Puranen

Studsvik Nuclear AB (STUDSVIK), SE

\* Corresponding author: olivia.roth@studsvik.se

## Abstract

This paper describes the selection of six high burn-up SNF samples for leaching experiments and laser ablation studies and the preparations made for the start of the experiments as well as the start-up of two leaching experiments and laser ablation studies.

The main focus of the investigations is to explore the effects of additives and dopants on the fast/instant release of fission products such as Cs and I. Experiments will also be performed to investigate the feasibility of measuring fast/instant release of Se and  $^{14}\text{C}$ .

Furthermore, laser ablation experiments will be performed to study the radial distribution of I, Xe and Cs and to explore any correlation to the fission gas release (FGR) and instant release leach rates of the corresponding fuel samples.

## Introduction

This paper describes ongoing efforts at Studsvik Nuclear AB within the EURATOM FP7 Collaborative Project "Fast / Instant Release of Safety Relevant Radionuclides from Spent Nuclear Fuel (CP FIRST-Nuclides)".

The aim with the project is to study the fraction of fission and activation products that is fast/instantly released from spent nuclear fuel upon contact with aqueous media. The fraction consists of readily soluble phases in the gap between fuel and cladding, cracks and grain boundaries. Some of these fission and activation products have a long half-life and are for this reason important for the safety assessment of deep repositories for spent nuclear fuel.

At the Studsvik Hot Cell laboratory, spent fuel leaching studies have been conducted since around 1980. During 1990-1996 a comprehensive research program was initiated aiming at mapping the most

important parameters influencing the stability of spent nuclear fuel in water (Forsyth, 1997). Since then the program has been extended with leaching experiments of high burn-up fuel and instant release experiments (Johnson et al., 2011; Zwicky et al., 2011).

In these previous experiments, standard  $\text{UO}_2$  fuel has been used. Today new fuel types with additives and dopants are taken into use in commercial reactors. The additives and dopants effects properties such as grain size and fission gas release which in turn may affect the instant release behavior of the fuel. The main objective of this study is to investigate how these changes in the fuel matrix affect the instant release process.

### Sample selection and preparation

The main focus of the investigation is to explore the effects of additives and dopants on the fast/instant release of fission products such as Cs and I. For this reason six high burn-up fuels were chosen for the studies. The selected fuels are listed in **Table 1**.

*Table 1: Fuels selected for investigation at Studsvik*

Sample name	Reactor type	Fuel type	FGR [%]	Calculated BU (rod average) [MWd/kgU]
D07	BWR	Std $\text{UO}_2$	~1.6	50.2
L04	BWR	Std $\text{UO}_2$	~3.1	54.8
5A2	BWR	Std $\text{UO}_2$	~2.4	57.1
C1	BWR	Al/Cr doped $\text{UO}_2$	~1.4	59.1
VG81	PWR	Gd doped $\text{UO}_2$	~2.2	54.4
AM2K12	PWR	Std $\text{UO}_2$	~4.9	70.2

The fuels have previously been characterized by measuring the fission gas release (FGR). The method for FGR measurements is described in section 1.1. The calculated burn-up (average) for the rods are provided from the core calculations of the power stations that irradiated the rods. All samples will undergo gamma scanning (either gross gamma scan or digital gamma scan) before experimental start-up. The method for this is described in section 1.2.

### *Method for analysis of fission gas release 1.1*

The fission gas release was measured by puncturing the rods at the plenum, collecting the internal gas in a standard volume and determining the pressure. Samples of the gas were collected and analysed by mass spectrometry.

The total internal free volume of the rod was determined by the backfill method, using argon at constant pressure. The amount of released gas was calculated from the puncturing pressure and the volume of the puncturing system and from the gas composition.

Using the UO<sub>2</sub> content of the rod, the average burn-up of the rod and fission yields of Xe and Kr (interpolated from standard calculations with the Origen code) the amount of generated fission gas can be determined.

The fission gas release (i.e. fraction of released gas relative to generated gas) was obtained from the measured amount of released Xe and Kr isotopes, and the predicted amount of generated Xe and Kr.

### *Method for gamma scanning 1.2*

Gamma scanning is performed by moving the sample past a Ge detector with a 0.5 mm collimator. The signal from the detector can be recorded in analog or digital mode. Analog recording of the signal gives the total energy detected as a function of the axial position on the rod i.e. the gross gamma spectrum. Digital recording records the energy from each nuclide separately and a spectrum for each nuclide is given.

The gamma spectra gives information on the positions of pellet-pellet interfaces as well as the burn-up profile. By scanning a reference sample with known burn-up in sequence with the sample, the local burn-up of the sample can be calculated from the digitally recorded <sup>137</sup>Cs signal.

## **Spent fuel leaching studies**

### *Sample preparation 2.1*

Spent fuel leaching studies are performed using samples from 6 different fuel rods. Before the start of the leaching experiment each fuel segment is gamma scanned to identify pellet-pellet interfaces, thereafter samples are cut from the segment. The samples are cut at mid-pellet positions as shown in **Figure 1**. Each sample consists of approximately 2 fuel pellets including cladding.

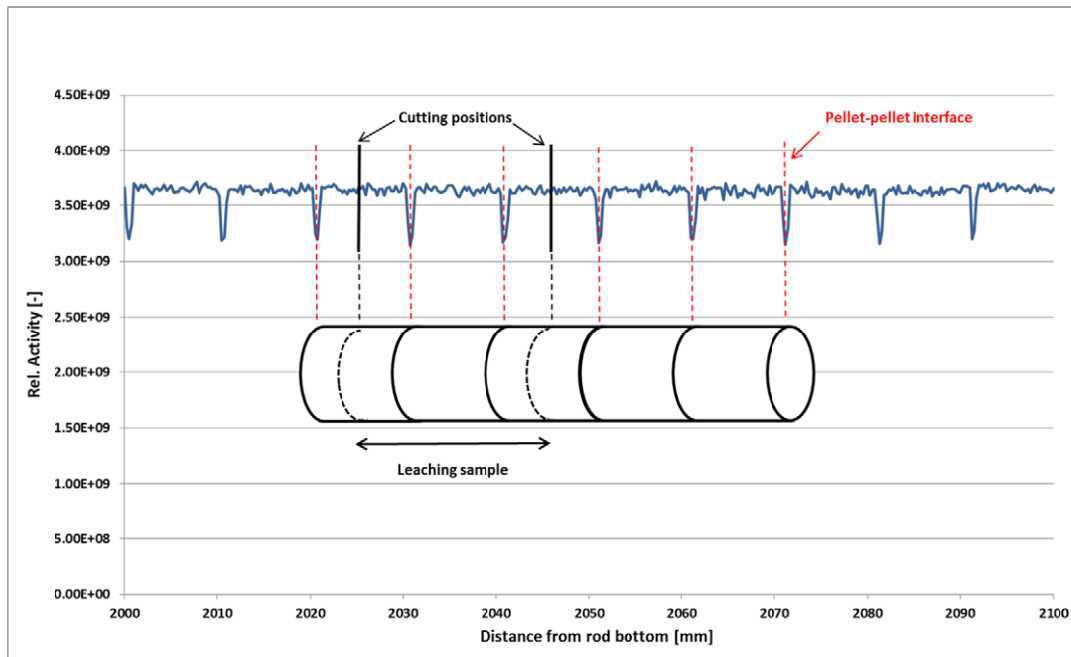


**Figure 1:** Schematic picture of leaching sample position relative to gamma spectrum

The samples are leached as cladded fuel segments, fuel fragments + separated cladding or fuel powder. The fuel segments are weighed before the start of the leaching experiments. To obtain the samples consisting of fuel fragments + separated cladding, the cladding is cut vertically and bent open which causes the fuel fragments to detach from the cladding. The fuel fragments are collected and leached together with the cladding (and any remaining fuel still sticking to the inside of the cladding).

In a next step the leaching of powdered specimens will be performed using a simultaneous grinding and leaching technique described by (Stroes-Gascoyne et al., 1995). The objective of this method is to expose the grain boundaries by grinding the fuel down to the same size range as the individual fuel grains. This would ideally make the entire grain boundary inventory available for leaching. By combining the grinding and leaching into one wet grinding step surface oxidation and temperature effects (from the friction of grinding) can be minimized.

### *Experimental Setup 2.2*

The leaching experiments are performed in a Hot Cell at the Studsvik Hot Cell laboratory. Leaching of cladded fuel segments and fuel fragments + separated cladding is performed in glass flasks. Each flask contains 200 ml leaching solution (10 mM NaCl + 2 mM NaHCO<sub>3</sub>). Cladded fuel segments are placed in a 'basket' made of platinum wire. Fuel fragments + separated cladding are placed in glass baskets

with filter bottom. The baskets are attached to stop cocks and immersed in the leaching solution. The experiments are performed under aerated, stagnant conditions (no stirring).

The leaching is performed in a cumulative way in which the leaching solution is completely exchanged at every sampling interval. After 1 d, 7 d, 21 d, 63 d, 92 d and 182 d (resulting in a cumulative leaching time of 365 d), the stopcock and fuel basket is transferred to a new leaching flask containing a freshly made leaching solution. Samples of the old leaching solutions are withdrawn from the used leaching flasks and analysed by ICP-MS and gamma analysis ( $^{137}\text{Cs}$ ). In order to calculate the leached fraction of the fuel inventory up to a given leaching time the analysed concentrations are thus added to the results of the prior samplings.

In August 2012, the leaching of two fuel samples (cladded fuel segments) was started. Two exchanges of leaching solutions (1 day and 7 days) have been successfully performed. The analysed data is under evaluation. **Figure 2** shows the general procedure for the leaching experiments.

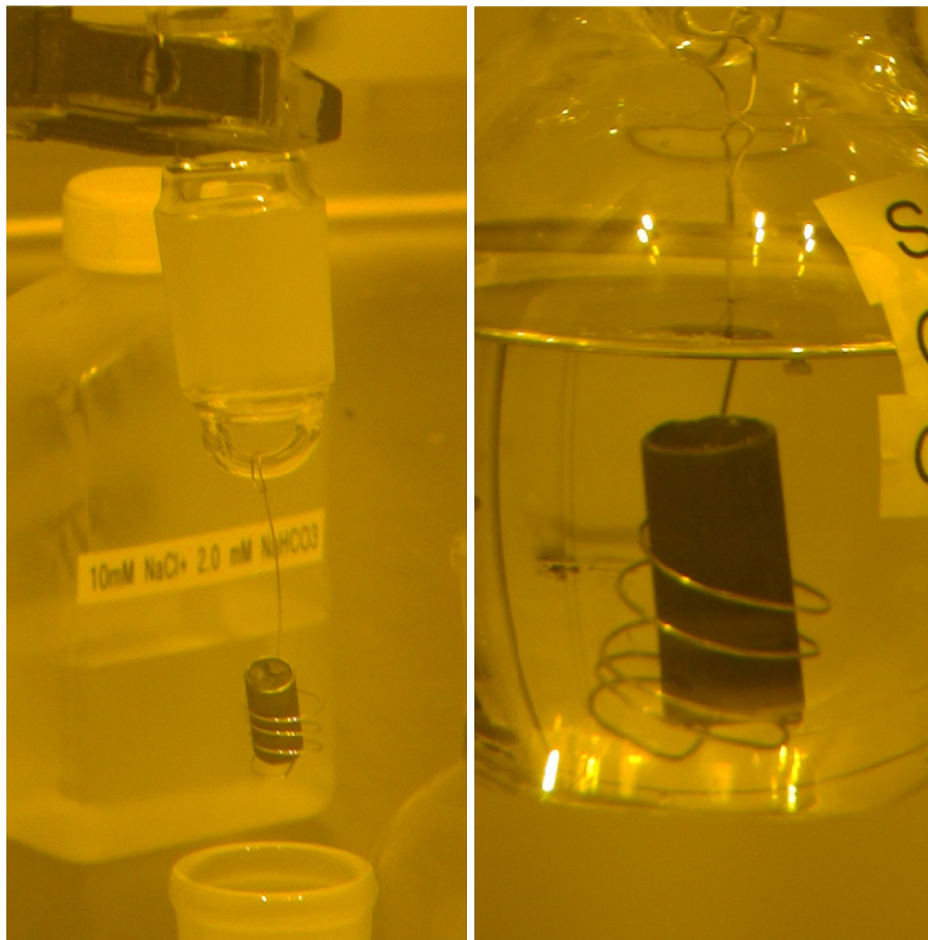


**Figure 2:** General pictures of leaching experiments a) cladded fuel in Pt-basket, b) Pt-basket with cladded fuel immersed in leaching solution

As mentioned above, leaching of powdered specimens will be performed using a simultaneous grinding and leaching technique described by (Stroes-Gascoyne et al., 1995).

For this purpose a rotary pestle and mortar mill will be used. Using this mill, powders with a final grain size of 10-20  $\mu\text{m}$  should be achieved. Approximately 1 g of fuel will be grinded and simultaneously leached in 100 ml leaching solution (10 mM NaCl + 2 mM NaHCO<sub>3</sub>).

Before the start of the combined leaching and grinding experiment the grinding method will be tested by grinding fuel in different time intervals and evaluate the achieved grain size by sieving and SEM analysis.

The cladding from the powdered fuel sample will be leached separately using the same experimental set up as for fuel fragments + separated cladding with contact periods 1 day and 7 days.

All aqueous samples from the leaching studies are removed from the hot cell and transported to the chemistry laboratory where the samples are centrifuged (and filtered if necessary in the case of powdered samples) and analysed for Cs and I with ICP-MS.

A method for analysis of Se and <sup>14</sup>C will be tested. Se analysis will be performed using hydride generation ICP-MS. If convincing Se isotopic ratios consistent with a fissiogenic origin are obtained, efforts to determine the Se speciation in the leaching solution will also be made (by control of the Se redox state and hydride generation or by chromatography). Preliminary results on the first leaching samples analysed by ICP-MS indicate fissiogenic <sup>82</sup>Se levels close to the detection limit (without modifications for specific analysis of Se). Analysis of <sup>14</sup>C will be performed using a method with liquid scintillation.

### **Laser ablation**

Laser ablation will be used to study the radial distribution of I, Xe and Cs. Taking the circular geometry of the fuel cross section into account the average fuel content can also be obtained from the data. The results will be used to investigate any correlation to the FGR, and to the instant release rates of the corresponding fuel samples. The samples to be studied are cross sections (transversal cut, perpendicular to the axial direction of the rod) from a standard UO<sub>2</sub> fuel and an Al/Cr-additive fuel (5A2 and C1 in **Table 1**). The sample preparation is underway with the laser ablation cross sections to be analysed taken at mid pellet position from a neighbour pellet to the fuel sample for the leaching investigation.



The ablation equipment consists of a New-Wave UP-213 floating<sup>2</sup> Nd:YAG laser in connection to an ablation chamber that is housed in a hot cell (**Figure 3**). The transport gas (He or Ar) from the ablation cell is injected into a Perkin Elmer Elan 6100 DRC II Inductively Coupled Plasma Mass Spectrometer (ICP-MS), installed in a glove box. The ablating laser operates at a wavelength of 213 nm with a pulse length of < 4 ns. The spot size can be varied between 5-160  $\mu\text{m}$  with an ablation frequency between 1-20 Hz. For scans across a fuel pellet cross section line speeds of 10-30  $\mu\text{m}/\text{s}$  are commonly employed.



**Figure 3:** The laser ablation hot cell and the sample transfer cask

Optimisation and calibration of the system is performed by ablation on SRM NIST glass standards (Pearce et al., 1997). For investigations of spent fuel the data is normalized as fractions of  $^{238}\text{U}$ . The results of this method have been shown to be in good agreement with determinations by dissolution analysis and the results of theoretical calculations (Granfors et al., 2012).

### **Future work**

The study will continue with three leaching experiments using fuel fragments + separated cladding and one experiment using the simultaneous grinding leaching method. The testing of methods for analysis of Se and  $^{14}\text{C}$  will continue and the laser ablation experiments will be finalized.

Further efforts will be made to make more data from previous characterizations of the spent fuel available to the project (such as microscopy results). If necessary, such data will be produced.

---

<sup>2</sup> The laser is mounted on a motorized X-Y-Z stage with < 1  $\mu\text{m}$  resolution

## Acknowledgement

*This project is funded by The Swedish Nuclear Fuel and Waste Management Co. (SKB) , Posiva Oy and the European Union's European Atomic Energy Community's (Euratom) Seventh Framework Programme FP7/2007-2011 under grant agreement n° 295722 (FIRST-Nuclides project).*

## References

Forsyth, R. (1997) The SKB Spent Fuel Corrosion Program – An evaluation of results from the experimental program performed in the Studsvik Hot Cell Laboratory. Skb Technical Report SKB TR 97-25.

Granfors, M., Puranen, A., Zwicky, H-U. (2012) Radial profiling and isotopic inventory analysis of irradiated nuclear fuel using laser ablation ICP-MS. Proc. Top Fuel 2012. In press.

Johnson, L., Günther-Leopold, I., Kobler, Waldis, J., Linder, H.P., Low, J., Cui, D., Ekeroth, E., Spahiu, K., Evins, L.Z. (2011) Rapid aqueous release of fission products from high burn-up LWR fuel: Experimental results and correlations with fission gas release. Journal of Nuclear Materials, 420, 54-62.

Pearce, N., Perkins, W., Westgate, J., Gorton, M., Jackson, S., Neal, C., Chenery, S. (1997) A Compilation of New and Published Major and Trace Element Data for NIST SRM 610 and NIST SRM 612 Glass Reference Materials. The Journal of Geostandards and Geoanalyses. 21, 115-144.

Stroes-Gascoyne, S., Moir, D.L., Kolar, M., Porth, R.J., McConnell, J.L., Kerr, A.H. (1995) Measurement of gap and grain-boundary inventories of  $^{129}\text{I}$  in used CANDU fuels. MRS Proceedings, 353, 625-631.

Zwicky, H-U., Low, J., Ekeroth, E. (2011) Corrosion studies with high burnup light water reactor fuel; Release of nuclides into simulated groundwater during accumulated contact time of up to two years. SKB Technical Report SKB TR-11-03.

## **WP3. DISSOLUTION BASED RELEASE JOINT CONTRIBUTION ITU-CTM**

Daniel Serrano-Purroy<sup>1\*</sup>, Laura Aldave de las Heras<sup>1</sup>, Jean Paul Glatz<sup>1</sup>, Vincenzo V. Rondinella<sup>1</sup>,  
Frederic Clarens<sup>2</sup>, Joan de Pablo<sup>2</sup>, Ignasi Casas<sup>3</sup>, Rosa Sureda<sup>2</sup>

<sup>1</sup> Joint Research Centre – Institute for Transuranium Elements (JRC-ITU), European Commission

<sup>2</sup> Funadaió Centre Tecnologic (CTM), ES

<sup>3</sup> Universitat Politècnica de Catalunya · Barcelona Tech (UPC), ES

\* Corresponding author: [daniel.serrano-purroy@ec.europa.eu](mailto:daniel.serrano-purroy@ec.europa.eu)

### **Abstract**

A summary of the work to be carried out at ITU in the frame of WP3 by ITU and CTM as well as an updated work program are reported. In addition some effort was dedicated to the development of an improved method of ICPMS Sr determination and preliminary results are also reported. The study of Sr, although being a short-living radionuclide and therefore not important for IRF, is an aspect of special interest due to some contradictory literature findings. Although it has been traditionally considered as matrix release indicator recent experimental work carried out at ITU has shown that Sr dissolves faster than the matrix. In order to clarify this statement a more precise evaluation method is being developed in the frame of this project. Similar methodologies will also be applied for other radionuclides of interest like Se.

### **Dissolution based fast radionuclide release**

In the following months several corrosion experiments will be carried out at ITU by dedicated ITU and CTM personnel. The aim of these experiments is the determination of the IRF of commercial spent UO<sub>2</sub> nuclear fuels. Different samples will be used, see WP1, and the experiments will be carried out using cladded segments and two different powder fuel fractions: one prepared from the centre of the pellet (CORE) and another one from the fuel pellet periphery (OUT), enriched with the so-called High Burn-Up Structure (HBS).

## 1. *Experimental set-up*

### 1.1. *Powder samples*

Approximately 0.25 g of SNF powder will be placed in in 50 ml borosilicate glass test tubes of (150 x 25) mm with plastic screw cap (Schütt Labortechnik GmbH, Göttingen, Germany) with 50 ml of the selected leaching solution. The tubes will be placed on a rotator stirrer to avoid concentration gradients. The rotator stirrer is made in polymethacrylate over a stainless steel framework, using an electrical motor with a nominal speed of 30 rpm; enough to ensure that the SNF is kept in suspension and to assure a perfect contact with the solution.

The experiments will be performed in air equilibrated solutions. To minimize the possibility of uranium saturation and secondary phase formation the solution will be completely replenished after each sampling. All aliquots taken will be acidified with 1M HNO<sub>3</sub> and measured by a sector field ICP-MS (Inductively Coupled Plasma Mass Spectrometry) (Thermo Element2, Thermo Electron Corporation, Germany). If other measuring methodologies, for example for iodine or selenium, are developed during the course of the project, they will also be applied.

The pH, Eh and temperature will be measured at given intervals with an Orion 525A+ pH-meter and a gel pH Triode L/M, (9107BN, Thermo-Electron, USA) and platinum Redox electrodes, (97-78-00, Thermo-Electron, USA). The pH electrode will be calibrated with commercial pH buffer solutions (METTLER TOLEDO Inc., USA; pH 4.01 (Ref. 501307069), pH 7.00 (Ref.51302047), pH 9.21 (Ref. 51302070)). Commercial pH 7.00 buffer solution will be used to calibrate the redox electrode.

### 1.2. *Cladded segments*

Samples of approximately 2 mm of cladded segment will be placed in a (50 ± 1) ml flask with 50 ml of the selected leaching solution in equilibrium with air leaving a head space gas of about 10 ml. The solution will be shaken daily to avoid the build up of concentration gradients in the liquid phase. Samples will be hanged in a Pt wire in order to facilitate de sampling. Again, solution will be completely replenished after each sampling.

Sampling treatment will be the same as the one explained in section 1.1.1.

### 1.3. *Leaching solution*

The selected leaching solution will be 19 mM NaCl + 1.0 mM NaHCO<sub>3</sub>.

#### 1.4. Solution analysis results

The total released or cumulative moles in solution for element  $i$ ,  $mols(i)$ , will be calculated considering the total amount of radionuclide removed in each sampling (Equation 1):

$$mols(i) = \sum_0^n mols_{sample}(n,i) \quad \text{eq. 1}$$

where  $mols_{sample}(n,i)$  correspond to the moles in solution before each complete replenishment  $n$  (mols).

The Fraction of Inventory of an element  $i$  released in the Aqueous Phase ( $FIAP_i$ ) will be given by Eq. 2.

$$FIAP_i = \frac{m_{i,aq}}{m_{i,SNF}} = \frac{c_i V_{aq}}{m_{SNF} H_i} \quad \text{eq. 2}$$

where  $m_{i,aq}$  is the mass of element  $i$  in the aqueous phase (g),  $m_{i,SNF}$  the mass of element  $i$  in the SNF sample (g),  $m_{SNF}$  the mass of SNF used in the experiment (g),  $H_i$  corresponds to the fraction of inventory for the nuclide  $i$  (g/g),  $c_i$  is the concentration of element  $i$  in solution (g/ml) and  $V_{aq}$  is the volume of solution (ml).

The Fractional Release Rate for an element  $i$  ( $FRR_i$ ) in  $d^{-1}$  will be given by Eq. 3:

$$FRR_i = \frac{\Delta FIAP_i}{\Delta t} \quad \text{eq. 3}$$

where  $t$  is the time (d).

The Fractional Release for an element  $i$  Normalised to the total Surface area ( $FNS_i$ ) will be:

$$FNS_i = \frac{FIAP_i}{S} \quad \text{eq. 4}$$

where  $S$  is the total surface area ( $m^2$ ).

And the Fractional Release Normalised to Uranium for an element  $i$  ( $FNU_i$ ) is given by Eq. 5.

$$FNU_i = \frac{FIAP_i}{FIAP_U} \quad \text{eq. 5}$$

where  $FIAP_i$  and  $FIAP_U$  are the FIAP of element  $i$  and Uranium, respectively.

## Method development for quantitative analysis

### 2. Determination of $^{90}\text{Sr}$ at ultratrace levels using the TRUFAST system and ICPMS detection

The method utilizes an automated on-line system (see **Figure 1**) for the determination of  $^{90}\text{Sr}$  at ultratrace levels in natural samples by ICPMS. The TRUFAST system uses two high purity valves to take up an aliquot of sample, retain and concentrate Sr removing the matrix on a PFA column packed with Sr<sup>®</sup>-Spec resin. The pre-concentrated Sr is eluted by backpressure into a PFA nebulizer attached to the ICPMS spray chamber.

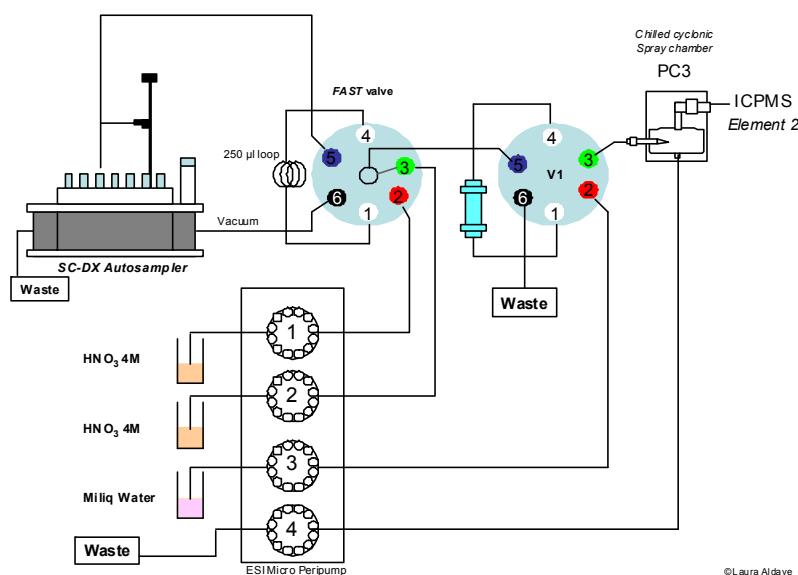


**Figure 1:** System diagram for the determination of  $^{90}\text{Sr}$  by preconcentration and matrix removal

#### 2.1. Results

In **Figure 2** the elution profiles obtained for solutions 4 mol/L HNO<sub>3</sub> containing 10, 25, 50 and 100 pg/g of  $^{90}\text{Sr}$  are reported. As can be seen,  $^{90}\text{Sr}$  is eluted in a total time of 120 s.

A calibration curve was obtained by using the peak area of  $^{90}\text{Sr}$  versus the total  $^{90}\text{Sr}$  concentration. Linear regression was calculated using the Least squares linear regression method. The calibration curve is also shown in **Figure 2**. A fit for purpose curve is obtained which does not introduce an extra uncertainty component. The method shows potential for the determination of  $^{90}\text{Sr}$  in natural samples in this concentration range.

The detection limit of  $^{90}\text{Sr}$  was calculated by means of repeated measurements of the blank and according to Currie (Currie, 1968). The detection limit is 1.6 pg/g, taking into account that the

injection volume is 250  $\mu\text{l}$  that represents an absolute amount of 0.25 pg (5 Bq) of  $^{90}\text{Sr}$ . The precision of the method, based on the relative standard deviation of the peak area calculated on the basis of three repetitions is always less than 2% in this concentration range.

However, the detection limit, accuracy and precision of  $^{90}\text{Sr}$  determination by ICPMS are mainly affected by the occurrence of isobaric atomic and molecular ions at  $m/z = 90$  (see **Table 1**). Moreover, the peak tailing of the highly abundant  $^{88}\text{Sr}$  isotope, the concentration of natural strontium in the sample is usually in the low  $\mu\text{g/g}$  range, will also disturb the  $^{90}\text{Sr}$  determination.

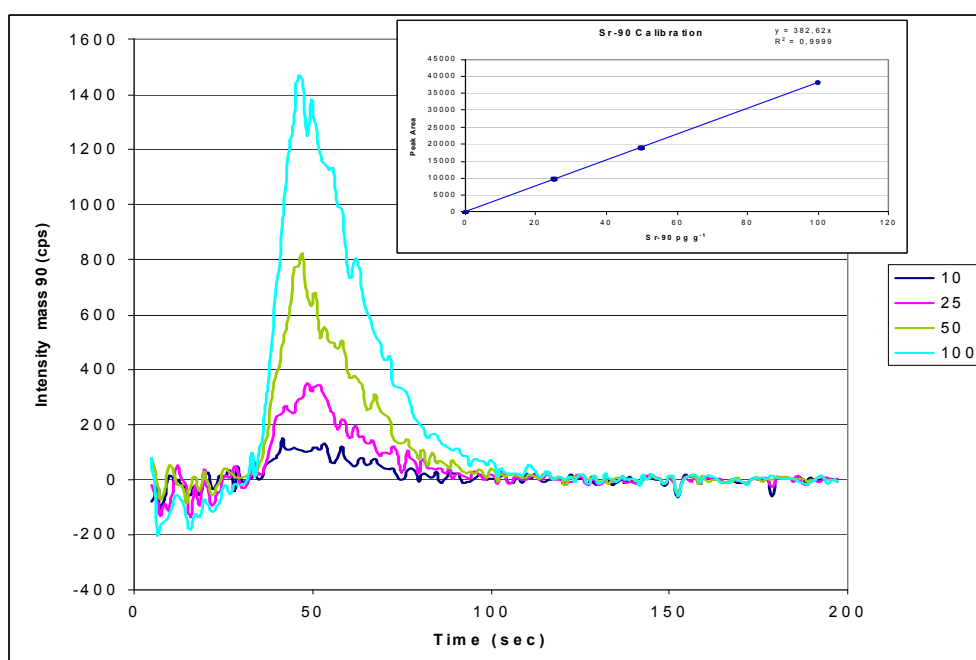


**Figure 2:** Elution Chromatograms of solutions containing 10, 25, 50 and 100 pg/g of  $^{90}\text{Sr}$

**Table 1:** Possible interferences for  $^{90}\text{Sr}$  and required mass resolution

Nuclide	Molecular ions	Required mass resolution ( $m/\Delta m$ )
$^{90}\text{Sr}$	$^{180}\text{W}_2^+$	1370
	$^{180}\text{Hf}_2^+$	1372
	$^{58}\text{Ni}_{16}\text{O}_2^+$	2315
	$^{74}\text{Ge}^{16}\text{O}^+$	10765
	$^{52}\text{Cr}^{38}\text{Ar}^+$	19987
	$^{50}\text{V}^{40}\text{Ar}^+$	49894
	$^{54}\text{Fe}^{36}\text{Ar}^+$	155548
	$^{50}\text{Ti}^{40}\text{Ar}^+$	158287
	$^{90}\text{Zr}^+$	29877

Artificial ground waters samples adjusted to 4 mol/L HNO<sub>3</sub> were prepared and analysed in order to determine the impact of possible interferences in the m/z 90 due to the presence in the water of the elements described in **Table 1**. Two series of samples were prepared with and without natural strontium, in order to study both the interferences formation and the peak tailing of <sup>88</sup>Sr on m/z 90. The concentration of natural strontium in the artificial ground water samples used was between 2 to 6 ng/g. However, concentrations up to 150 ng/g are possible in natural waters. **Figure 3** shows that the peak tailing of the <sup>88</sup>Sr isotope is not disturbing the peak area of <sup>90</sup>Sr when the concentration of Sr is around 5 ng/g.

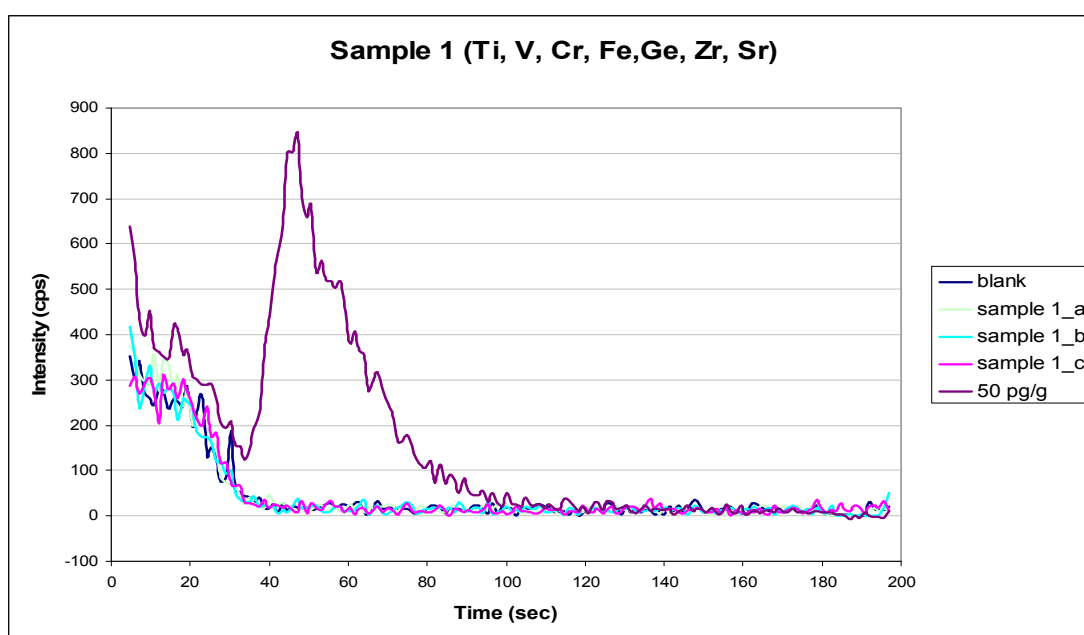


**Figure 3:** Elution Chromatograms of artificial ground waters with a concentration of 5 ng/g of natural strontium

Further studies are ongoing to determine the lowest natural Sr concentration that increases the background signal in the peak area of <sup>90</sup>Sr. Operating the ICPMS in medium resolution could remove the peak tailing of <sup>88</sup>Sr on the m/z 90, reducing, however sensitivity and increasing the detection limits of <sup>90</sup>Sr.

## 2.2. Conclusions

The TRUFAST system offers easy and efficient determination of low pg/g levels of <sup>90</sup>Sr in natural water. Moreover, with its automated and versatile sample uptake and introduction capabilities, reduces sample preparation time while achieving good detection limits.



Applicability of the TRUFAST system for the analysis of leachates of spent fuel in ground water has been preliminary studied. In **Table 2** are summarized the total inventory of Sr isotopes in a UO<sub>2</sub> fuel. With a burn-up of 40 GWd/t<sub>HM</sub> irradiated in a PWR with 4 cycles of 1 year and a cooling time of 4 years. In addition, the concentrations of some elements affecting the quantitative determination of <sup>90</sup>Sr and the theoretical concentration of Sr released in ground water using the IRF of Cera et al. (2000) are also shown.

**Table 2:** Spent fuel total theoretical inventory and Sr concentrations released using IRF estimates<sup>3</sup> for strontium and potential interfering elements

Nuclide	µg/g fuel <sup>1</sup>	fuel dissolution <sup>2</sup> µg/g	% released <sup>3</sup>	µg/g in leachates
<sup>90</sup> Sr	147.5	2.95	3	0.0885
<sup>88</sup> Sr	102.5	2.05	3	0.0615
<sup>90</sup> Zr	23.5	0.47		
<sup>90</sup> Y	0.0375	7.5E-04		
<sup>74</sup> Ge	0.015	3.0E-04		
<sup>89</sup> Sr	1.35E-08	2.7E-10	3	8.1E-12

1 UO<sub>2</sub> fuel. Burnup 40 GWd/t<sub>HM</sub> irradiated in a PWR, 4 cycles of 1 year. Cooling time 4 years.  
2 Dissolution of a small sample 0.25 g. Final volume 50 ml  
3 Cera et al. (2003)

Considering the analytical figures of the TRUFAST system coupled to ICPMS and the values summarised in **Table 2**, it is clear that the method developed can be applied for the determination of Sr in leachates of spent fuel in ground water. In spite of the presence of some elements interfering at m/z 90, those elements are not retained in the column and have no impact on the quantitative determination of <sup>90</sup>Sr. The influence of the abundance sensitivity of <sup>88</sup>Sr will only depend of the total concentration of natural Sr in the ground water used for the leaching experiments. Indeed, the concentration of <sup>88</sup>Sr in the spent fuel is of the same order of magnitude as <sup>90</sup>Sr.

## Updated Work Program

ID	Task Name	2012				2013				2014			
		Qtr 1	Qtr 2	Qtr 3	Qtr 4	Qtr 1	Qtr 2	Qtr 3	Qtr 4	Qtr 1	Qtr 2	Qtr 3	Qtr 4
1	<b>Workpackage 3 (Dissolution based release)</b>												
2	<b>D3.1 Dissolution fast/instant release studies</b>					■	■	■	■	■	■	■	■
3	Experiments with segments					■	■	■	■				
4	Experiments with powder					■	■	■	■				
5	SEM									■	■	■	■
6	Knudsen Cell									■	■	■	■
7	Data treatment									■	■	■	■
8	<b>Method development for quantitative analysis</b>	■	■	■	■	■	■	■	■	■	■	■	■
9	Sr					■	■	■	■				
10	Se					■	■	■	■				
11	I									■	■	■	■
12	<b>Deliverables</b>					■	■	■	■	■	■	■	■
13	Contribution to D3.1					■							
14	Contribution to D3.1									■			
15	Contribution to D3.1												■

## Acknowledgement

*The research leading to these results has received funding from the European Union's European Atomic Energy Community's (Euratom) Seventh Framework Programme FP7/2007-2011 under grant agreement n° 295722 (FIRST-Nuclides project).*

## References

- Cera, E., Merino, J., Bruno, J., Clarens, F., Giménez, J., de Pablo, J., Martínez-Esparza, A. (2003) ENRESA 2003. AGP arcilla. Modelo de alteración del combustible nuclear gastado. Enviro.
- Currie, L.A. (1968) Limits for quantitative detection and quantitative determination. Analytical Chemistry, 40, 586.

# PREVIOUS INVESTIGATIONS ON THE INSTANT RELEASE FRACTION AND GENERAL DESCRIPTION OF THE PROJECT

Alba Valls<sup>1\*</sup>, Olga Riba<sup>1</sup>, Lara Duro<sup>1</sup>, Ernesto González-Robles Corrales<sup>2</sup>, Bernhard Kienzler<sup>2</sup>,  
Volker Metz<sup>2</sup>

<sup>1</sup> Amphos 21 Consulting S.L. (SP)

<sup>2</sup> Karlsruhe Institute of Technology (KIT), Institut für Nukleare Entsorgung (INE) (DE)

\* Corresponding author: alba.valls@amphos21.com

## Abstract

The State-of-the-Art report on fast / instant release of activation and fission products from spent nuclear fuel is documented by a summary of results obtained from more than 100 published experiments. All authors refer to a definition of the fast / instant release as a fraction of the inventory of some segregated radionuclides that may be rapidly released from the fuel and fuel assembly materials at the time of canister breaching. In the context of safety analysis, the time of mobilization of this fraction can be considered as an instantaneous release of some radionuclides at the containment failure time, even when the real release occurs during few weeks, months or years.

## Introduction

The Collaborative Project “Fast / Instant Release of Safety Relevant Radionuclides from Spent Nuclear Fuel (FIRST-Nuclides)” contributes to the progress towards implementing of geological disposal in line with the Vision Report and the Strategic Research Agenda (SRA) of the “Implementing Geological Disposal – Technology Platform (IGD-TP)”. It falls within the 7<sup>th</sup> Framework Programme Topic Fission-2011-1.1.1. FIRST-Nuclides project started in January 2012 and extends over three years.

The consortium consists of 10 beneficiaries, six of which can provide with experimental facilities having specialized installations and equipment for working with highly radioactive materials and the other four are organizations having specific knowledge. 8 institutions have joined the project as associated groups and the end-user group is created by 6 members.

The fast / instant release fraction of radionuclides from spent fuel was investigated in the frame of national research programmes and in previous European projects: SFS (Poinssot et al., 2005; Johnson et al., 2004), NF-PRO (Sneyers, 2008) and MICADO (Grambow et al., 2010). There are still some remaining open issues derived from these investigations. Actually during the MICADO project, the following information was described as missing:

- Understanding of the distribution of fission gas release (FGR) and deriving more realistic relationships between FGR and release of various fission products.
- Relationships between the FGR and iodine release for LWR fuel.
- Quantification and modelling of long-term retention of fission products on grain boundaries.
- Quantification of the IRF for high burn-up fuel.
- Chemical speciation of the relevant elements especially chemical form of  $^{14}\text{C}$ .

### **Objectives of FIRST-Nuclides**

The objectives of FIRST-Nuclides are defined considering the outcomes of the previous European projects and publications. Thus, the main objective of the present collaborative project is to improve the understanding of the fast / instant release of radionuclides from high burn-up spent  $\text{UO}_2$  fuels from LWRs in geological repositories.

The overall objectives of CP FIRST-Nuclides are the following:

- To provide for improved data for the fast/instant release fraction for high burn-up spent  $\text{UO}_2$  fuel
- To establish correlations between the experimental FGR and the fast/instant release of non-gaseous fission products, in particular  $^{129}\text{I}$ ,  $^{79}\text{Se}$  and  $^{135}\text{Cs}$
- To reduce uncertainties with respect to the fast/instant release of  $^{129}\text{I}$  and  $^{14}\text{C}$
- To determine the chemical form of the relevant elements in order to evaluate retention processes

### **Description of the fuel**

The spent nuclear fuel of interest in the investigations of FIRST-Nuclides project is  $\text{UO}_2$  fuel with a burn-up of around  $60\text{GWd}/t_{\text{HM}}$ . The selected fuels, representative for present PWRs and BWR, have grain sizes of 10-20  $\mu\text{m}$ , densities of 10.0-10.8  $\text{g}/\text{cm}^3$  and pore sizes in the range of 5 to 80  $\mu\text{m}$ .

In the following table, the characteristics of the fuel that will be used in the FIRST-Nuclides investigations are detailed.

**Table 1.** Fuel data under investigation from PWR and BWR

		PWR	BWR
<b>Discharge (manufacturer)</b>		1989 (AREVA)	-2008 2005 – 2008 (AREVA/Westinghouse)
<b>Cladding</b>	Material	Zry-4-M5	Zyr 2
	Diameter	9.50 - 10.75	9.84 - 10.2
	Thickness (mm)	0.62 - 0.73	
<b>Pellet</b>	Enrichment(%)	2.8 - 4.3	3.5 - 4.25 %
	Grain size ( $\mu\text{m}$ )	5 - 40	6 - 25
	Density ( $\text{g/cm}^3$ )	10.41	10.52
<b>Irradiation</b>	BU (GWd/t)	45 - 70.2	50.2 – 59.1
	Cycles	2 - 14	5 - 7
<b>Linear Power</b>	Average (W/cm)	186 - 306	160 -200
<b>FGR</b>	(%)	4.9 – 26.7	1.4 – 3.1

### Structural and chemical processes in nuclear fuel

The Fast /Instant release fraction is highly affected by processes occurring in the fuel pellet during the irradiation period and its storage, determining both the micro and macrostructure of the spent fuel rod. Once the water reaches the spent fuel pellet, the proportion of radionuclide release will be influenced by their location in the pellet and their chemical form.

During the irradiation period, the pellet suffers several structural changes:

- **Macroscopic fragmentation** of the **pellet** (in ~15 fragments) due to steep thermal gradients developed under irradiation and because of low thermal conductivity (Ferry et al., 2006). During irradiation the pellet temperature can be as high as 1700°C at the center of the pellet,

decreasing to about 400°C (regulatory guidance limit (NRC, 2003)) at its rim or outer boundary.

- **Decrease of pellet/cladding gap** as a result of retention of fission products in the fuel matrix that causes swelling of the fuel pellet. The volume gap for pellet is  $\sim 0.07 \text{ cm}^3$  and this can be reduced down to  $0.01 \text{ cm}^3$  with  $\text{BU} = 40 \text{ MWd/kg}_U$  and even disappear for  $\text{BU} > 47 \text{ MWd/kg}_U$  causing pellet-clad mechanical interaction (PCMI) (Forsyth, 1997).
- **Radial zonation** of the pellet with the formation of a rim structure due to higher local BU for average pellet  $\text{BU} > 40 \text{ MWd/Kg}_U$  with thickness from  $\sim 40$  to  $\sim 250 \mu\text{m}$  (Martínez-Esparza et al., 2009). Due to the greater amount of fission products and defects generated in the pellet rim, a recrystallization process takes place resulting in an structure with smaller grain sizes (0.1 to  $0.5 \mu\text{m}$ ), high porosity (15%) and smaller lattice parameter making the structure fairly resistant to fracturing despite the high porosity (Spino and Papaioannou, 2008).
- **Longitudinal zonation** due to heterogeneous burn up along the rod presenting lower BU at the endings of the rod (Dehaut et al., 2000).

The chemical stability of the fission products in equilibrium with  $\text{UO}_{2\pm x}$ , can be classified into four main groups (Kleykamp, 1985):

- Elements soluble in the spent fuel matrix including actinides, lanthanides, rare earth elements and elements forming soluble oxides, such as Zr, Nb, Sr.
- Elements forming insoluble oxides in the matrix: Rb, Cs, Ba, Zr, Nb, Mo, Te.
- Fission products that form metallic precipitates: Mo, Tc, Ru, Rh, Pd, Ag, Cd, In, Sn, Sb, Te.
- Fission gases (Kr, Xe, He) and volatile fission products (I, Br, Rb, Cs, Te)

The distribution of fission products in the spent fuel rod is determined by the radiological inventory and by the structural changes. In terms of fast/instant release fraction, it is important to know those radionuclides incompatible with the matrix and located in the gap and grain. Experimental determinations show that fission gases, volatile fission products and other fission products such as Mo, Tc and Sr are mainly in these areas. Thus, when water contacts these radionuclides they will be rapidly released.

### Investigations on fast/instant release fraction

Data obtained from different leaching experiments with spent fuel ( $\text{UO}_2$  and MOX) performed during the last 30 years are compiled in the FIRST-Nuclides deliverable D5.1 (Kienzler et al., 2012).

Initially, investigations on fast/instant release fraction were done with spent nuclear fuel with a maximum burn up of around 50 GWd/t<sub>U</sub>. It has been observed that the average burn up of SNFs used in those studies is progressively increasing with time (**Figure 1**). Last investigations have been performed mainly using SNF with burn up higher than 45 GWd/t<sub>U</sub>.

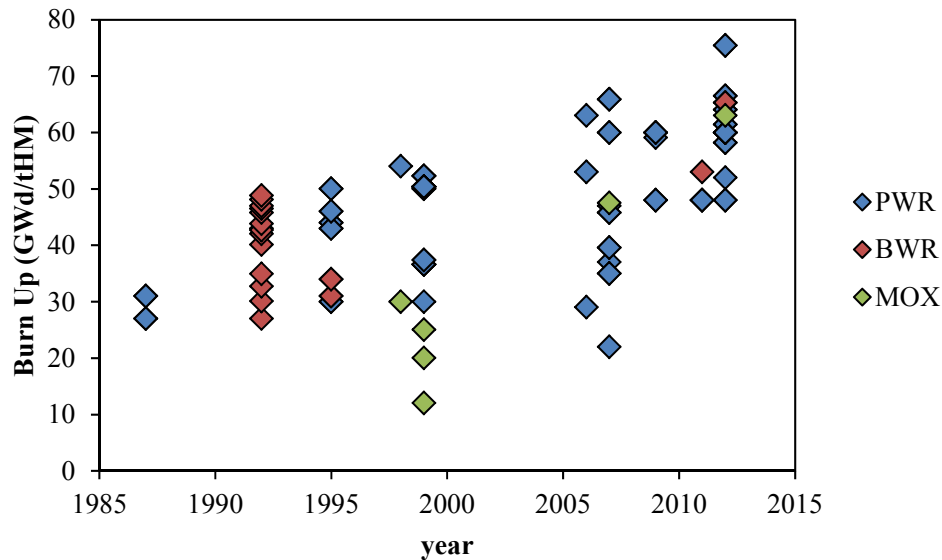


**Figure 1:** Spent fuel burn up used in leaching experiments during the last 30 years

About 100 experiments have been compiled in the review and most of them have been done with PWR spent fuels with burn up between 41 and 50 GWd/t<sub>U</sub> (**Figure 2**). There is relatively less measurements of fast/instant release for MOX spent fuel. All these experimental data have been reported in 30 different publications. Therefore, the scarcity of data concerning high burn up fuel highlights the need to study these fuels currently being discharged from nuclear power stations.

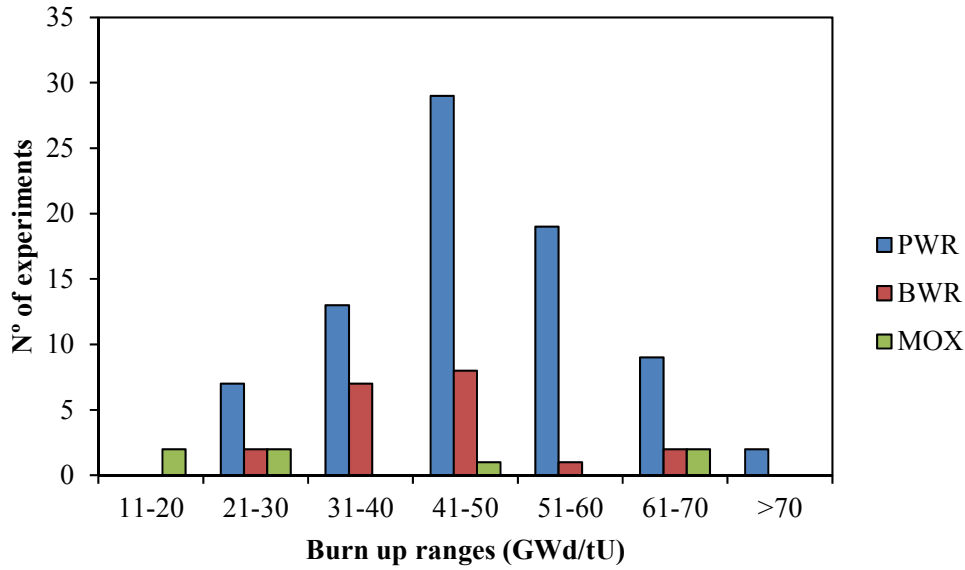


**Figure 2:** Number of experiments performed with different SNF and BU

Radionuclides considered in that review exercise are rubidium, caesium, strontium, iodine, molybdenum and technetium. In the following figure (**Figure 3**), it is represented the amount of measurements reported in the reviewed publications for each radionuclide taking into account if the measurement stands for the release from the gap or from the grain boundaries (gb).

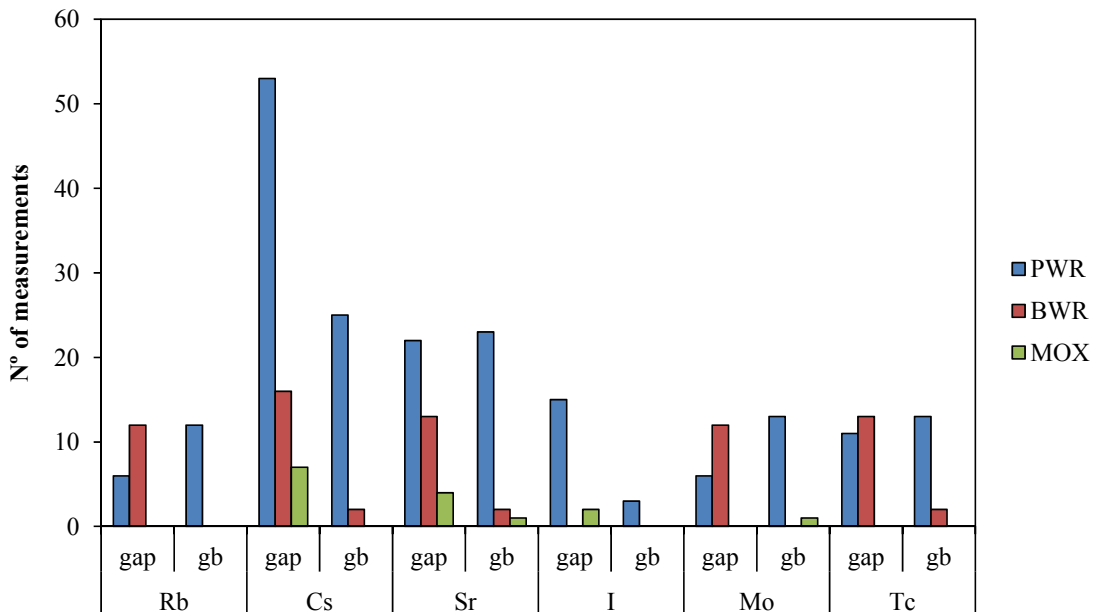


**Figure 3:** Number of measurements of IRF of different radionuclides from the gap and the grain boundaries (gb)



**Figure 3** shows that most of measurements are focused on the release of caesium from the gap although several experiments have measured the instant release of strontium from both the gap and grain boundaries. As most of the studies have been performed with PWR spent fuels, IRF data are also mostly for this kind of fuels. Only few data of IRF are obtained from MOX spent fuels.

## Conclusions

Significant improvements in the understanding of the performance of spent fuel under repository conditions have taken place. However, most of the published data on fast/instant release fractions relates to fuel with burn-up values below 45 GWd/t<sub>U</sub>. Over the next years the average burn-up will increase, reaching average values of about 60 GWd/t<sub>U</sub>. For that reason, FIRST-Nuclides focus on improving the understanding of the fast/instant release of radionuclides from high burn-up spent fuels. Further steps consist on update the present database with data produced in the FIRST-Nuclide project to improve the database of IRF for fission and activation products and to correlate fission gas release measurements with other fission products considered to be low confined in the spent fuel matrix

## Aknowledgements

*The research leading to these results has received funding from the European Union's European Atomic Energy Community's (Euratom) Seventh Framework Programme FP7/2007-2011 under grant agreement n° 295722 (FIRST-Nuclides project).*

## References

- Kienzler, B., Metz, V., González-Robles, E., Montoya, V., Valls, A., Duro L. (2012) State of the art report. Deliverable D5.1 of the FIRST-Nuclides Project.
- Dehaut, P., Dubois, S., Maguin, J.C., Huet, F., Pelletier, M., Lacroix, B., Pasquet, B., Guérin, Y., Hourdequin, N., Salot, R., Desgranges, L., Delette, G., Struzik, C. (2000) Le combustible nucléaire et son état physico-chimique à la sortie des réacteurs. CEA report, CEA-R-5923.
- Ferry, C., Poinssot, C., Cappelaere, C., Desgranges, L., Jegou, C., Miserque, F., Piron, J.P., Roudil, D., Gras, J.M. (2006) Specific outcomes of the research on the spent fuel long-term evolution in interim dry storage and deep geological disposal. Journal of Nuclear Materials, 352, 246-253.

Forsyth, R. (1997) An evaluation of results from the experimental programme performed in the Studsvik Hot Cell Laboratory. The SKB Spent Fuel Corrosion Programme. SKB Technical Report, TR-97-25.

Grambow, B., Bruno, J., Duro, L., Merino, J., Tamayo, A., Martin, C., Pepin, G., Schumacher, S., Smidt, O., Ferry, C., Jegou, C., Quiñones, J., Iglesias, E., Villagra, N.R., Nieto, J.M., Martínez-Esparza, A., Loida, A., Metz, V., Kienzler, B., Bracke, G., Pellegrini, D., Mathieu, G., Wasselin-Trupin, V., Serres, C., Wegen, D., Jonsson, M., Johnson, L., Lemmens, K., Liu, J., Spahiu, K., Ekeröth, E., Casas, I., de Pablo, J., Watson, C., Robinson, P., Hodgkinson, D. (2010) Final Report of the Project MICADO: Model uncertainty for the mechanism of dissolution of spent fuel in nuclear waste repository.

Johnson, L., Poinssot, C., Ferry, C., Lovera, P. (2004) Estimates of the instant release fraction for UO<sub>2</sub> and MOX fuel at t=0. A Report of the Spent Fuel Stability (SFS) Project.

Kleykamp, H. (1985) The chemical state of the fission products in oxide fuels. *Journal of Nuclear Materials*, 131, 221-246.

Martínez-Esparza, A., Clarens, F., Gonzalez-Robles, E., Gimenez, F.J., Casas, I., De Pablo, J., Serrano, D., Wegen, D., Glatz, J.P. (2009) Effect of burn-up and high burn-up structure on spent nuclear fuel alteration. ENRESA publicación técnica 04-2009.

NRC (2003) NRC ISG-11. Interim Staff Guidance – 11, Rev. 3.

Poinssot, C., Ferry, C., Kelm, M., Grambow, B., Martínez, A., Johnson, L., Andriambolona, Z., Bruno, J., Cachoir, C., Cavendon, J.M., Christensen, H., Corbel, C., Jégou, C., Lemmens, K., Loida, A., Lovera, P., Miserque, F., de Pablo, J., Poulesquen, A., Quiñones, J., Rondinella, V., Spahiu, K., Wegen, D.H. (2005) Spent fuel stability under repository conditions. Final report of the European (SFS) project.

Sneyers, A. (2008) Understanding and Physical and Numerical Modelling of the Key Processes in the Near Field and their Coupling for Different Host Rocks and Repository Strategies. Report of the NF-PRO project.

Spino, J. and Papaioannou, D. (2008) Lattice contraction in the rim zone as controlled by recrystallization: Additional evidence. *Journal of Nuclear Materials*, 372, 416-420.

# RADIOLYTIC CORROSION OF GRAIN BOUNDARIES ONTO THE UO<sub>2</sub> TRISO PARTICLE SURFACE

Johan Vandenberg<sup>1\*</sup>, Ali Traboulsi<sup>1</sup>, Guillaume Blain<sup>1</sup>, Jacques Barbet<sup>2</sup>, Massoud Fattahi<sup>1</sup>

<sup>1</sup> Centre National de la Recherche Scientifique (CNRS), FR

<sup>2</sup> Cyclotron ARRONAX, FR

\* Corresponding author: johan.vandenberg@subatech.in2p3.fr.

## Abstract

This work is dealing with the understanding of the corrosion mechanisms at solid/solution interface and taking into account for the <sup>4</sup>He<sup>2+</sup> ions irradiation effects on these mechanisms. These corrosion and <sup>4</sup>He<sup>2+</sup> ions radiolysis phenomena appear at solid/solution interface and will be studied at a μmetric scale by the Raman spectroscopy. Moreover, a <sup>4</sup>He<sup>2+</sup> ions irradiation affects a small low volume and allows us to control the irradiated area (solution, solid or interface). For the solid, the chemical species induced by <sup>4</sup>He<sup>2+</sup> ions radiolysis of water are reactive and are involved in classical corrosion mechanisms of UO<sub>2</sub>. Moreover, we want to study the impact of the <sup>4</sup>He<sup>2+</sup> ions radiolysis of water layers physisorbed into the surface onto corrosion mechanisms. That is the reason why we want to use a local irradiation, allowed by the <sup>4</sup>He<sup>2+</sup> ions ion beam provided by the ARRONAX cyclotron (E = 64.7 MeV). In this work an experimental apparatus will be performed in order to characterize solid/solution interface at μmetric scale by Raman spectroscopy under <sup>4</sup>He<sup>2+</sup> ions irradiation provided by the cyclotron ARRONAX facility. The leaching experiments under irradiation will be performed for a short time in order to study the parameters during the fast instant release step. The grain boundaries effect will be studied by the comparison between one TRISO particles set (solids with grain boundaries) and one TRISO particles set previously washed by one acid solution (solid without grain boundaries). The role of H<sub>2</sub> will be studied by the comparison between experiments under Ar or Ar/H<sub>2</sub> atmosphere. The dose rate range will be between 0 and 100 Gy/min by using the alpha ion beam which let us control the dose set down into the sample. For all these experiments, measurements will be performed by the *in situ* Raman spectroscopy during the irradiation in order to follow the formation/consumption of the secondary phases formed onto the solid. The SEM will be performed in order to characterize the grain boundaries and the secondary phases formed by the leaching/irradiation experiments. The μGC is used to measure the P<sub>H<sub>2</sub></sub> into the irradiation cell to follow the

production/consumption of this gaseous species formed by the water radiolysis and consumed by the leaching process.

## Introduction

This paper deals with the radiolytic corrosion at the  $\text{UO}_2$  surface. We study the impact of the water radiolysis on the corrosion of the grain boundaries (GB) detected at the TRISO particle surface. Moreover, the  $\text{H}_2$  influence onto the corrosion is studied. In more details, the conditions of these experiments are described below:

- $\text{UO}_2$  TRISO particle natural: This work deals with the impact of the GB present at the  $\text{UO}_2$  TRISO particle surface. We want to study the effect of the GB onto the dissolution (It has been already shown that for  $\text{ThO}_2$  TRISO particles it is the GB which control the solubility (Vandenborre et al., 2010). Moreover, information provided on the GB impact on the  $\text{UO}_2$  TRISO particle dissolution can be relevant for the instant release fraction because IRF is linked to the GB phase onto the Spent Fuel surface.
- Pure water irradiated: We want to study the effect of the radiolysis, classically induced by the high burn-up spent  $\text{UO}_2$  fuel, by an external alpha beam with a large scale of dose rate (between 0 and 100 Gy/min) in order to study the radiolytic dissolution of  $\text{UO}_2$  and its secondary phases. Moreover, the dose rate of about 25 Gy/min corresponds to the dose rate delivered by the high burn-up spent  $\text{UO}_2$  fuel (Grambow et al., 2010). Then, we study the solid surface dissolution by the water radiolysis coming not from the high burn-up spent  $\text{UO}_2$  fuel but by a controlled alpha beam. This alpha beam is controlled for the dose rate, the localisation of the 30  $\mu\text{m}$  layer irradiated (in water, onto the surface, into the GB...) in order to determine the impact of this localisation onto the IRF. Moreover, the water radiolysis produces molecular species such as  $\text{H}_2\text{O}_2$  which play a non negligible role into the  $\text{UO}_2$  corrosion mechanism as described in the literatura (Corbel et al., 2001; Ekeroth et al., 2006; Jégou et al., 2005; Jonsson et al., 2004; Roth and Jonsson, 2008; Suzuki et al., 2006).
- $\text{H}_2$  effect: This is studied either induced by the water radiolysis or initially merged in the system during the dissolution of the GB. In fact, we are able to measure the  $\text{H}_2$  produced or consumed by the radiolysis/dissolution mechanisms and to bring information onto the reactivity of the IRF vs. the  $\text{H}_2$ , in particular at 0.02 M (=0.16 bar) corresponding to experimental conditions performed in previous European Projects (MICADO, SFS). Moreover, the  $\text{H}_2$  quantity implied during the dissolution of GB phases can be measured.

- UO<sub>2</sub> secondary phases characterization and evolution can be followed by *in situ* Raman spectroscopy. The kinetics (from a few minutes to a few days) of formation/consumption of the secondary phases onto the UO<sub>2</sub> surface (with a localization at the GB by  $\mu$ -Raman technique) give data onto the formation/consumption of the instant release fractions. Raman experiments have been successfully performed onto the UO<sub>2</sub> surface with good results for the determination of schoepite and studtite phases at the UO<sub>2</sub> surface as described in the literatura (Amme et al., 2002; Biwer et al., 1990; Carbol et al., 2005; Corbel et al., 2006; Eary and Cathles, 1983; Hanson et al., 2005; He and Shoesmith, 2010; Sattonnay et al., 2001).

Also, this work can answer to the GB formation, depletion, evolution, reactivity vs. alpha external dose rate, [H<sub>2</sub>] at the UO<sub>2</sub> surface for the FIRST-Nuclides Project. Moreover, it seems relevant for the retention process to know the secondary phases formation/depletion by the radiolytic chemical reactions and the effect of H<sub>2</sub> onto these phases.

## Material and Methods

### *Samples*

UO<sub>2</sub> TRISO particles are purchased by Pr. Fachinger from FZJ and the synthesis detailed in (Brähler et al., 2012) with, in particular, a calcination step which was performed at 1600°C for UO<sub>2</sub> crystallization. Physico-mechanical characterization and first solubility tests have been performed (Bros et al., 2006; Grambow et al., 2008; Titov et al., 2004).

Solid analysis is performed by SEM (scanning electron microscopy, JEOL 5800 SV with a 15 kV voltage) and the SEM samples were covered by a Pt layer in order to improve electron conduction and increase the picture resolution. Mechanical separation of C-layers from the UO<sub>2</sub> spheres is performed in order to analyse the sphere (**Figure 2**). **Table 1** shows the properties of the UO<sub>2</sub> spheres after the separation step. Moreover, we have checked by EDX that the chemical composition of the sphere surface is only UO<sub>2</sub>.

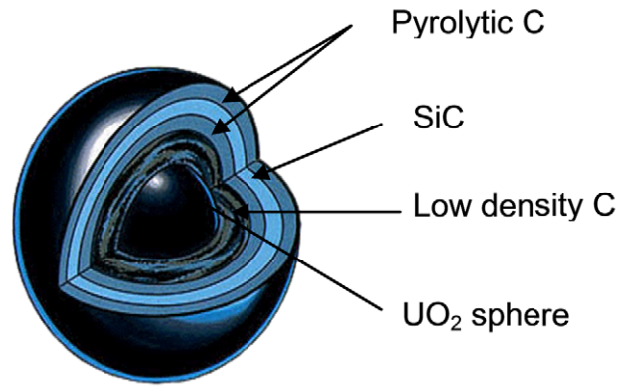


**Figure 1:** UO<sub>2</sub> spheres with different C-layers from (Brähler et al., 2012)

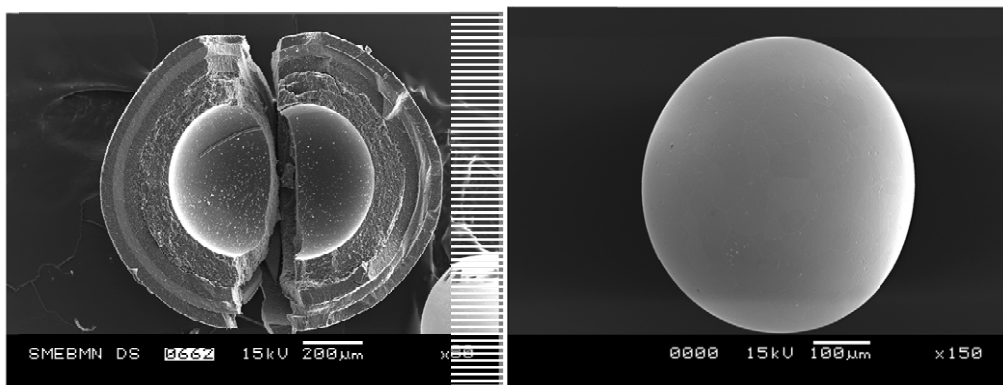


**Figure 2:** SEM picture of UO<sub>2</sub> TRISO particle after the separation step, Left: C-Layers, Right: UO<sub>2</sub> sphere

**Table 1:** Properties determined for the UO<sub>2</sub> sphere

Sphere	UO <sub>2</sub> (cr)
Diameter (mm)	0.50
Weight (mg)	0.76
Density (g/cm <sup>3</sup> )	10.96
Geometric Surface Area (m <sup>2</sup> /g)	1.05E-3

The pre-washing batch experiments were performed exposing unirradiated UO<sub>2</sub> TRISO particles to an aqueous solution in undersaturated conditions. A HDPE (High Density poly-ethylene) reaction vessel is used, containing 15 ml of a 0.1 mol/L HCl solution under continuous stirring during 15 days in order to deplete the GB phases.

### *Irradiation experiments*

$^4\text{He}^{2+}$  ions irradiations are provided by the ARRONAX cyclotron facility (Saint-Herblain, France) onto a vertical beam-line. Experiments are carried out within the ARRONAX cyclotron at 64.7 MeV. The intensity of the particles beam, measured on an internal Faraday cup located one meter upstream, is maintained at 70 nA. The uncertainty of that current measurement is about 10%. Fricke dosimetry (Fricke and Hart, 1996) is used in this study in order to determine the dose deposited into the samples. This method is based on the oxidation of  $\text{Fe}^{2+}$  to  $\text{Fe}^{3+}$  by the species produced by the water radiolysis reactions. The concentration of ferric ions is monitored by UV-Vis measurements at 304 nm ( $\epsilon = 2197 \text{ L}\cdot\text{mol}^{-1}\cdot\text{cm}^{-1}$ , 298 K) with a spectrophotometer CARY4000 (VARIAN). These measurements are carried out on samplings few minutes after irradiation. Super Fricke solutions are prepared by dissolving the desired quantity of Mohr's salt ( $[\text{Fe}^{2+}] = 10 \text{ mmol/L}$ ) and NaCl (1 mmol/L) in aerated aqueous 0.4 mol/L  $\text{H}_2\text{SO}_4$  solutions. All reagents are analytical grade or equivalent. NaCl is added in order to avoid any organic impurities. The irradiation time is a few minutes for ARRONAX experiments. The dose rates were measured at 7500 Gy/min during irradiation in the ARRONAX facility using the ferric ion radiolytic yield extrapolated from the literature (Costa et al., 2012) ( $G(\text{Fe}^{3+}) = 5.0 \cdot 10^{-7} \text{ mol/J}$  for  $E = 5.0 \text{ MeV}$  and  $G(\text{Fe}^{3+}) = 11.7 \cdot 10^{-7} \text{ mol/J}$  for  $E = 64.7 \text{ MeV}$ ).

At the ARRONAX cyclotron, 2 ml of solution is introduced into the irradiation cell. Due to the small penetration depth of  $^4\text{He}^{2+}$  ions in water, the irradiated volume fraction is small.

### *In situ Raman experiments*

The Raman system is purchased from the HORIBA Jobin-Yvon Company. Raman spectra are recorded with an iHR550 spectrometer equipped with two optic fibers (diameter = 100  $\mu\text{m}$ , length = 20 m). The detector is a charged coupled device (CCD) cooled by Peltier effect (203 K). Raman spectra are excited with a laser beam at 632.8 nm emitted by a He/Ne Laser. The laser beam is weakly focused on samples with a diameter of about 1 mm and a power of about 14 mW for a working distance of 40 mm on the sample and an acquisition time of 2 minutes. The Raman backscattering is collected through an objective system and dispersed by 1200 groves/mm gratings to obtain 5  $\text{cm}^{-1}$  spectral resolution for Raman stokes spectra excited at 632.8 nm. The wavenumber accuracy was checked and considered better than 0.5  $\text{cm}^{-1}$ .

With the Raman spectroscopic device (laser excitation and back scattering Raman) described before, *in situ* experiments have been performed onto the solid samples in contact with ultrapure water. **Figure 3** displays the device installed onto the  $^4\text{He}^{2+}$  beam line. The  $^4\text{He}^{2+}$  ions beam is provided by the ARRONAX cyclotron facility with  $E = 64.7 \text{ MeV}$ . The average length of the  $^4\text{He}^{2+}$  particle for this

energy is determined at about 2.5 mm in the ultrapure water solution by the SRIM 2008 simulation code (Ziegler et al., 2010). Thus, we could have checked experimentally that for a volume solution of 2 ml, with a solid/ $^4\text{He}^{2+}$ -beam distance of 5 mm, the  $^4\text{He}^{2+}$  ions irradiation direct effects occur onto the solution and not onto the solid surface. So, with this *in situ* experimental device experiment under irradiation, this work can be devoted to study the effect of the water radiolysis species onto the solid corrosion and the direct irradiation consequences onto the solid surface.

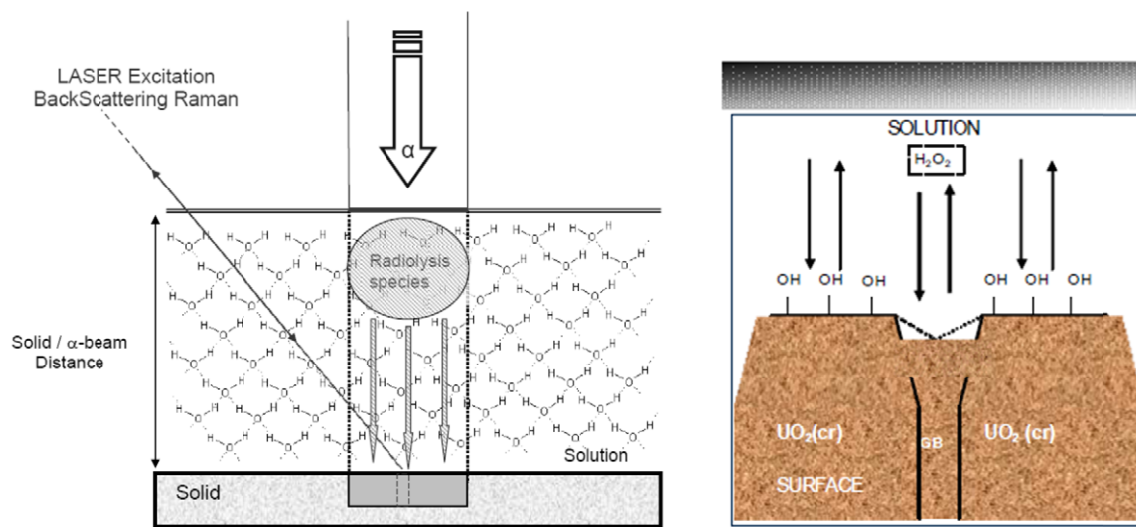


**Figure 3:** Left: *In situ* Raman spectroscopic device experiment under  $^4\text{He}^{2+}$  ions beam irradiation onto the ARRONAX facility vertical beam line, Right: Zoom at the  $\text{UO}_2$  TRISO particle surface with  $\text{UO}_2(\text{cr})$  and GB phases

## Results

### 1. WPI Results

#### 1.1 Irradiation cell development

First test experiments of *in situ* Raman analysis have been performed with a first version of our irradiation cell, which permits analysis of the surface with Raman spectroscopy (See **Figure 4**). However, we are developing a new version in order to analyze respectively, during the alpha irradiation, the solid by the Raman spectroscopy and the solution by the UV-VIS spectrophotometry. Moreover, with the cell we will be able to measure the hydrogen in the system by  $\mu$ -Gas Chromatography (See **Figure 5**). This complete analytic system will be useful in order to determine the uranium speciation at the surface, in the solution during the irradiation and to measure the hydrogen produced or consumed by the chemical system.



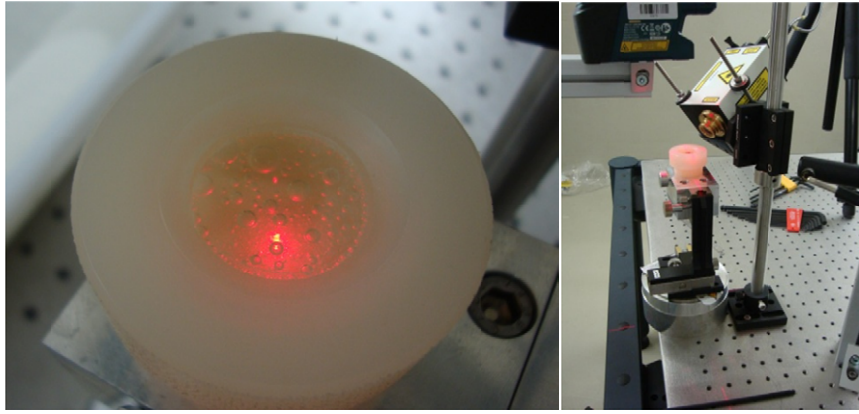


**Figure 4:** Left: Irradiation cell with  $H_2$  bubbles produced by the water radiolysis, Right: In situ Raman spectroscopic device experiment under  $^4He^{2+}$  ions beam irradiation onto the ARRONAX facility vertical beam line



**Figure 5:** Left: New measurement cell with UV-VIS probe, Right: Schematic picture of the new In situ Raman spectroscopic cell

## 1.2 SEM pictures

A pre-washing experiment has been performed in order to study  $UO_2$  TRISO particle with and without GB. By this way, we will determine the impact of the GB onto the radiolytic dissolution process of the  $UO_2$  TRISO particle. First SEM pictures analysis were performed onto two samples. The  $UO_2$  TRISO particle surfaces were analyzed before and after the pre-washing step (Respectively **Figure 6** and **Figure 7**).

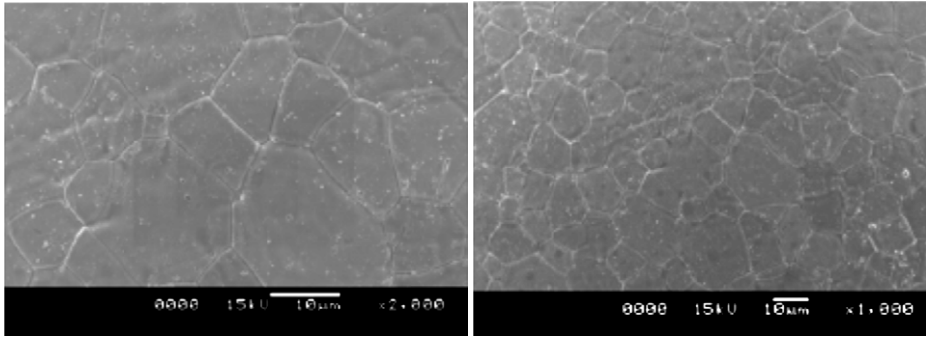


**Figure 6:** SEM pictures of the  $UO_2$  TRISO particle BEFORE the pre-washing step

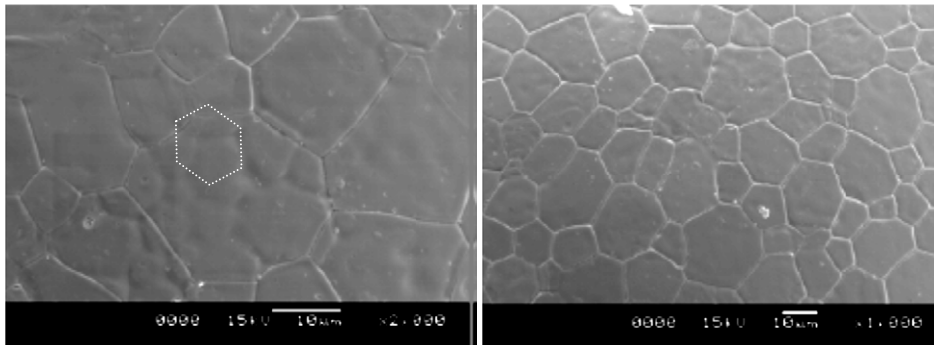


**Figure 7:** SEM pictures of the  $UO_2$  TRISO particle AFTER the pre-washing step

From these pictures, the grain size average can be determined about  $15 \pm 5 \mu\text{m}$ . Moreover, the pre-washing process involves a dissolution of the C-layers remained at the  $UO_2$  surface. Moreover, new grains, with GB too, occur at the  $UO_2$  surface with a lower grain size average.

The next step of this work is to analyze, by  $\mu$ -Raman spectroscopy, the surface with  $UO_2(\text{cr})$  grain and GB(I), from the solid sintering, and GB(II), from the pre-washing process.

## 2. WP2 Results

The spectra of the first tests of *in situ* Raman experiment under alpha irradiation were shown in **Figure 8**. The spectra have been monitored versus the irradiation time (1 to 6 min). We can recognize the typical fundamental UO stretch Raman band at  $443 \text{ cm}^{-1}$  of the  $UO_2$ . Nevertheless, the sensitivity is too low to permit determining of the evolution of the Raman spectra versus the irradiation time. So we are not yet able to detect accurately the  $UO_2$  secondary phases such as shoenite or studite in the Raman spectra are at  $800\text{-}870 \text{ cm}^{-1}$  (Amme et al., 2002; Aubriet et al., 2006; Biber et al., 1990; Hoekstra and Siegel, 1973; Sobry, 1973). That is the reason why, in the next step of this task, we will install a new

powerful LASER with a higher excitation wavelength of 532 nm in order to increase the sensitivity of our experimental device.

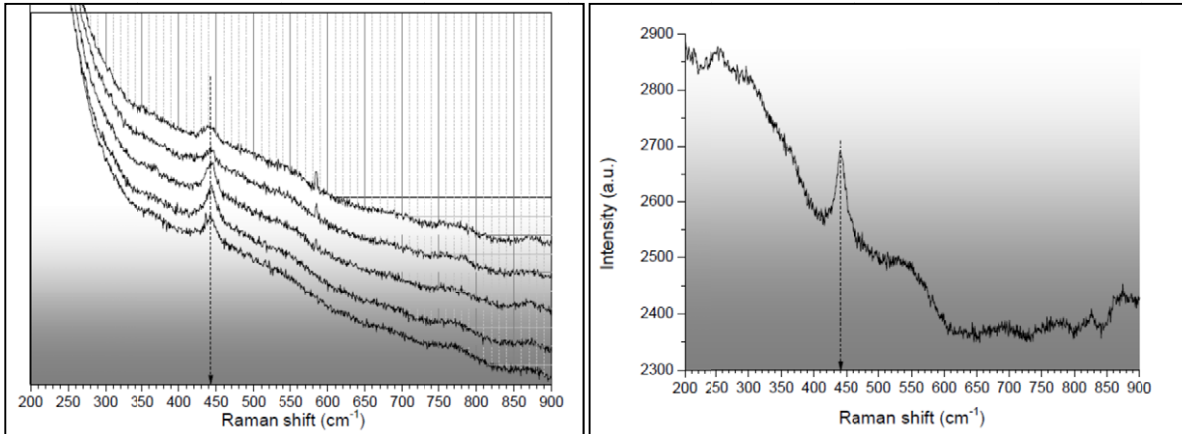


**Figure 8:** Raman spectra of the  $\text{UO}_2$  TRISO particle, Left: For irradiation times from 1 to 5 min, Right: For irradiation time of 6 min

## Conclusions and Future work

The future works planned for this task:

- A complete Uranium speciation during the radiolytic corrosion respectively into the solution by UV-VIS Spectrophotometry and at the solid surface by Raman analysis.
- Improvement of the Raman detection in order to increase the sensitivity by a green excitation LASER (532 nm), a higher time resolution for the mechanisms kinetics determination at a higher spatial scale for the discrimination between the  $\text{UO}_2(\text{cr})$  grain and the GB analysis.
- A Hydrogen impact study onto the radiolytic corrosion by the control and the measurement of the atmosphere in the irradiation cell in order to determine the part of  $\text{H}_2$  which occurs into the radiolytic corrosion process.
- Finally, after the FIRST-Nuclides Project, the same system will be used into an Irradiated TRISO particle in order to study a more realistic system close to the Spent Nuclear Fuel. Thus this work is the first step of the complete study.

## Acknowledgement

We acknowledge B. Humbert and J.Y. Mevellec from the IMN laboratory for support in Raman measurements and N. Stephant for SEM measurements. The authors acknowledge ARRONAX staff for the efficient performing of irradiation runs onto the cyclotron facility.

*The research leading to these results has received funding from the European Union's European Atomic Energy Community's (Euratom) Seventh Framework Programme FP7/2007-2011 under grant agreement n° 295722 (FIRST-Nuclides project).*

## References

Amme, M., Renker, B., Schmid, B., Feth, M.P., Bertagnolli, H., Döbelin, W. (2002) Raman microspectrometric identification of corrosion products formed on UO<sub>2</sub> nuclear fuel during leaching experiments. *Journal of Nuclear Materials*, 306, 202-212.

Aubriet, H., Humbert, B., Perdicakis, M. (2006) Interaction of U(VI) with pyrite galena and their mixtures a theoretical and multitechnique approach. *Radiochimica Acta*, 94, 657-663.

Biwer, B.M., Ebert, W.L., Bates, J.K. (1990) The Raman spectra of several uranyl-containing minerals using a microprobe. *Journal of Nuclear Materials*, 175, 188-193.

Brähler, G., Hartung, M., Fachinger, J., Grosse, K.H., Seemann, R. (2012) Improvements in the fabrication of HTR fuel elements. *Nuclear Engineering and Design*, 251, 239-243.

Bros, P., Mouliney, M.H., Millington, D., Sneyers, A., Fachinger, J., Vervondern, K., Roudil, D., Cellier, F., Abram, T.J. (2006) Raphael project- HTR specific waste characterization programme. *Proceedings HTR2006: 3<sup>rd</sup> International Topical Meeting on High Temperature Reactor Technology*, B00000162.

Carbol, P., Cobos-Sabate, J., Glatz, J.P., Ronchi, C., Rondinella, V., Wegen, D.H., Wiss, T., Loida, A., Metz, V., Kienzler, B., Spahiu, K., Grambow, B., Quinones, J., Martinez Esparza Valiente, A. (2005) The effect of dissolved hydrogen on the dissolution of <sup>233</sup>U doped UO<sub>2</sub>(s), high burn-up spent fuel and MOX fuel, in: Co, S.N.F.a.W.M. (Ed.), Report. SFS EU-Project, Stockholm.

Corbel, C., Sattonnay, G., Guilbert, S., Garrido, F., Barthe, M.F., Jegou, C. (2006) Addition versus radiolytic production effects of hydrogen peroxide on aqueous corrosion of UO<sub>2</sub>. *Journal of Nuclear Materials*, 348, 1-17.

- Corbel, C., Sattonnay, G., Lucchini, J.-F., Ardois, C., Barthe, M.-F., Huet, F., Dehaut, P., Hickel, B., Jegou, C. (2001) Increase of the uranium release at an  $\text{UO}_2/\text{H}_2\text{O}$  interface under  $\text{He}^{2+}$  ion beam irradiation. *Nuclear Instruments and Methods in Physics Research Section B: Beam Interactions with Materials and Atoms*, 179, 225-229.
- Costa, C., Vandenborre, J., Crumière, F., Blain, G., Essehli, R., Fattahi, M. (2012) Chemical Dosimetry during alpha irradiation: A specific system for UV-Vis in situ measurement. *American Journal of Analytical Chemistry*, 3, 6-11.
- Eary, L. and Cathles, L. (1983) A kinetic model of  $\text{UO}_2$  dissolution in acid,  $\text{H}_2\text{O}_2$  solutions that includes uranium peroxide hydrate precipitation. *Metallurgical and Materials Transactions B*, 14, 325-334.
- Ekeroth, E., Roth, O., Jonsson, M. (2006) The relative impact of radiolysis products in radiation induced oxidative dissolution of  $\text{UO}_2$ . *Journal of Nuclear Materials*, 355, 38-46.
- Fricke, H. and Hart, E.J. (1966) *Chemical dosimetry, Radiation Dosimetry*. Attix F.H. et Roesch W.C, New York, USA.
- Grambow, B., Abdelouas, A., Guittonneau, F., Vandenborre, J., Fachinger, J., von Lensa, W., Bros, P., Roudil, D., Perko, J., Marivoet, J., Sneyers, A., Millington, D., Cellier, F. (2008) The Backend of the Fuel Cycle of HTR/VHTR Reactors. *ASME Conference Proceedings*, 649-657.
- Grambow, B., Bruno, J., Duro, L., Merino, J., Tamayo, A., Martin, C., Pepin, G., Schumacher, S., Smidt, O., Ferry, C., Jegou, C., Quinoñes, J., Iglesias, E., Rodriguez Villagra, N., Nieto, J.M., Martinez-Esparza, A., Loida, A., Metz, V., Kienzler, B., Bracke, G., Pellegrini, D., Mathieu, G., Wasselin-Trupin, V., Serres, C., Wegen, D., Jonsson, M., Johnson, L., Lemmens, K., Liu, J., Spahiu, K., Ekeroth, E., Casas, I., De Pablo, J., Watson, C., Robinson, P., Hodgkinson, D. (2010) Final Activity Report : Project MICADO Model for Uncertainty for the mechanism of dissolution of spent fuel in nuclear waste repository in: Commission, E. (Ed.), Report.
- Hanson, B., McNamara, B., Buck, E., Friese, J., Jenson, E., Krupka, K., Arey, B. (2005) Corrosion of commercial spent nuclear fuel.1. Formation of studtite and metastudtite. *Radiochimica Acta*, 93, 159-168.
- He, H. and Shoesmith, D. (2010) Raman spectroscopic studies of defect structures and phase transition in hyper-stoichiometric  $\text{UO}_{2+x}$ . *Physical Chemistry Chemical Physics*, 12, 8108-8117.

Hoekstra, H.R. and Siegel, S. (1973) The uranium trioxide-water system. *Journal of Inorganic and Nuclear Chemistry*, 35, 761-779.

Hoekstra, H.R. and Siegel, S. (1973) The uranium trioxide-water system. *Journal of Inorganic and Nuclear Chemistry*, 35, 761-779.

Jégou, C., Muzeau, B., Broudic, V., Peugeot, S., Poulesquen, A., Roudil, D., Corbel, C. (2005) Effect of external  $\gamma$  irradiation on dissolution of the spent  $\text{UO}_2$  fuel matrix. *Journal of Nuclear Materials*, 341, 62-82.

Jonsson, M., Ekeröth, E., Roth, O. (2004) Dissolution of  $\text{UO}_2$  by one and two electron oxidants. *MRS Proceedings*, 807, 77-82.

Roth, O. and Jonsson, M. (2008) Oxidation of  $\text{UO}_2(\text{s})$  in aqueous solution. *Central European Journal of Chemistry*, 6, 1-14.

Sattonnay, G., Ardois, C., Corbel, C., Lucchini, J.F., Barthe, M.F., Garrido, F., Gosset, D. (2001)  $\gamma$ -radiolysis effects on  $\text{UO}_2$  alteration in water. *Journal of Nuclear Materials*, 288, 11-19.

Sobry, R. (1973) Etude des "uranates" hydrates--II: Examen des propriétés vibrationnelles des uranates hydrates de cations bivalents. *Journal of Inorganic and Nuclear Chemistry*, 35, 2753-2768.

Suzuki, T., Abdelouas, A., Grambow, B., Menecart, T., Blondiaux, G. (2006) Oxidation and dissolution rates of  $\text{UO}_2(\text{s})$  in carbonate-rich solutions under external  $\alpha$  irradiation and initially reducing conditions. *Radiochimica Acta*, 94, 567-573.

Titov, M.M., Fachinger, J., Bukaemskiy, A.A. (2004) Investigation of physico-mechanical properties of ceramic oxide kernels for nuclear applications. *Journal of Nuclear Materials*, 328, 21-30.

Vandenborre, J., Grambow, B., Abdelouas, A. (2010) Discrepancies in Thorium Oxide Solubility Values: Study of Attachment/Detachment Processes at the Solid/Solution Interface. *Inorganic Chemistry*, 49, 8736-8748.

Ziegler, J.F., Ziegler, M.D., Biersack, J.P. (2010) SRIM The stopping and range of ions in matter (2010) *Nuclear Instruments and Methods in Physics Research Section B: Beam Interactions with Materials and Atoms*, 268, 1818-1823.

# NON-DESTRUCTIVE ANALYSIS OF A PWR FUEL SEGMENT WITH A BURN-UP OF 50.4 GWD/THM – PART I: VISUAL EXAMINATION AND $\gamma$ -SCANNING

Detlef H. Wegen<sup>\*</sup>, Dimitrios Papaioannou, Ramil Nasyrow, Vincenzo V. Rondinella,  
Jean-Paul Glatz

Joint Research Centre – Institute for Transuranium Elements (JRC-ITU), European Commission

\* Corresponding author: Detlef.Wegen@ec.europa.eu

## Abstract

Non-destructive analysis is an essential set of analyses for validation of the fuel rod safety and provides a valuable basis of information to plan and implement successful sampling. In a first step the pin was inspected visually for defects. These results were complemented by  $\gamma$ -spectrometric measurements along the fuel pin. This provided first information about the actual pellet positions in the pin and the burn-up axial profile.

## Introduction

During reactor operation a fuel rod is exposed to conditions which lead to complex alterations in the fuel, but also in the cladding material. Heat and fission products (FP) are produced by nuclear fission in the fuel. Due to the high temperature the cladding can creep and the generated FP cause a swelling of the fuel (Olander, 1976; Franklin et al., 1983). New isotopes are created by neutron activation not only in the fuel but, also in the structural materials. Hydrogen and irradiation can cause embrittlement of the cladding (Bertolino et al., 2002; Daum et al., 2001). As a consequence of these solicitations defects can be generated in the rod. The first step in analysis of spent fuel rods is the non-destructive testing (NDT). NDT is an essential set of analyses that allows to consistently acquire reliable data needed for validation of the safety and efficient performance of the fuel rod in pile and to provide a valuable basis of information to plan and implement successful destructive post irradiation examination (PIE) (Papaionnau et al., 2012) In the following, the NDT performed on a PWR (Gösgen, Switzerland) UOX fuel segment with a burn-up of 50.4 GWd/t<sub>HM</sub> is described. Details of the irradiation are given in (Metz et al., 2012). The examinations have been carried out in the hot cells of JRC-ITU (Wegen et al., 2012a).

## Visual Examination

The aim is to examine the state of the outer cladding surface and to detect possible defects or abnormalities. Visual examination of outer cladding surface of irradiated fuel rods is performed by means of a CCD colour camera installed in a hot cell.

### *Procedure of the examination*

The fuel rod is put horizontally on the metrology bench and pushed at a defined depth into the fixing mandrel centring. With a known speed (2.494 mm/s) the fuel rod is translated in front of a CCD digital video camera at a focal length of ca. 20 cm. A digital video film of the complete length of the fuel rod is recorded and characteristic zones of normal or abnormal states are reported in an examination form indicating the corresponding axial position. This procedure is repeated along 3 axes generators at 120° to each other.

### *Photographs*

The engraved label of the pin segment was checked by optical examination (**Figure 1**).

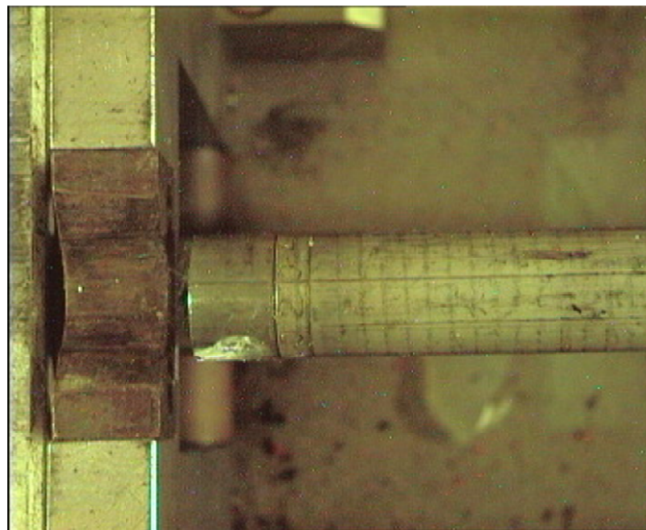


**Figure 1:** Macrograph showing the label of segment N0204

The optical examination of the segment at the three positions (0°, 120°, 240°) (**Figure 2**) shows no large defects, but helical tracks around the pin. These tracks have been formed before the actual NDT



analysis at ITU. One can assume that they origin from analyses performed at the reactor site. The longitudinal scratches were most likely formed during the removal of the pin from the bundle.

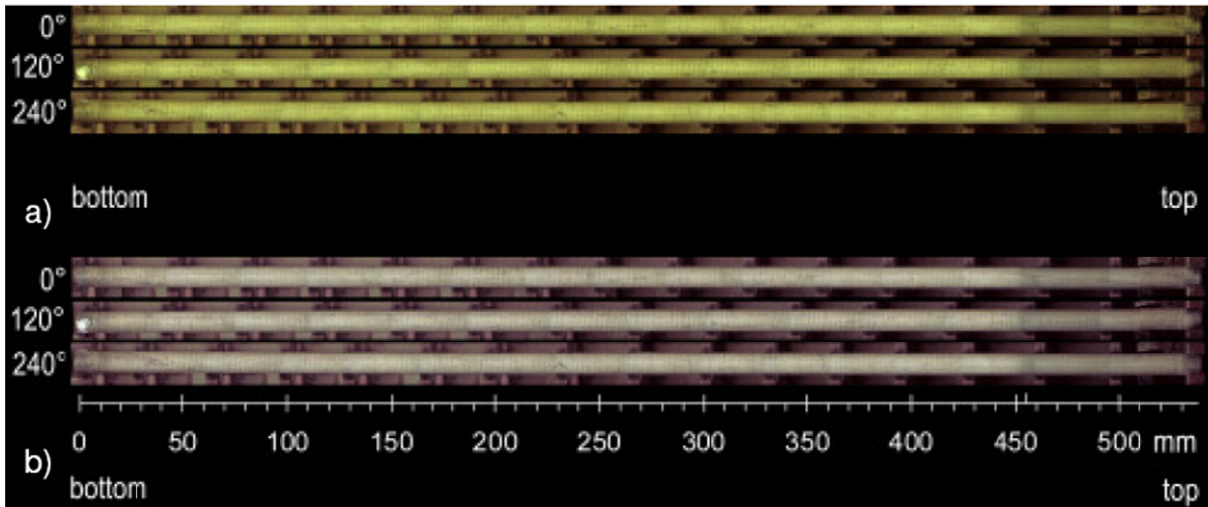


**Figure 2:** Montage of 46 single pictures extracted from three digital video films showing segment N0204 at three positions. (a) as recorded inside the hot cell; (b) with colour correction.

In the centre of the segment, at the position corresponding to the location of the fuel pellets, the cladding looks brighter than at the bottom and top end. The boundary between these areas is relatively sharp. The rod thus seems to be less oxidised at the top and bottom end. The slight distortion of the spiral track and the slight change of the colour intensity is an artefact resulting from the montage of 46 single pictures (perspective displacement and slightly inhomogeneous illumination).

### Gamma Scanning

The recording of the  $\gamma$ -ray emission spectrum along the axis of a fuel rod allows fission products to be qualitatively and quantitatively analysed. The overall purpose is the determination of the axial distribution of  $\gamma$ -emitters from irradiated fuel rod. This technique enables:

- the observation of volatile fission product migration (for instance Cs),
- an estimation of the fuel's average burn up and
- the estimation of the power experienced by the rod during a power transient.

The fuel rod is translated during the measurement in front a collimator and a Ge-detector; the collimator aperture is 1.2 mm.

Analyses of a fixed energy range corresponding to a particular emission energy are associated with a nuclide (for example the 661.6 keV line for  $^{137}\text{Cs}$ ) for its qualitative and quantitative determination.

The impulses provided by the Ge-counter are analysed simultaneously

by a multi channel spectrometer,

by a rate meter provided with an analogue output proportional to the counting rate of the detector.

### *Experimental Procedure*

#### Background

Before or after each measurement, keeping exactly the same conditions, the background spectrum is obtained and the total  $\gamma$ -ray intensity is counted. These are subtracted from the raw data for the rod to calculate the real (net) pin data.

#### Energy Calibration

The  $\gamma$ -spectroscopy system is calibrated using  $^{137}\text{Cs}$  and  $^{152}\text{Eu}$  sources at the beginning of each measurement series or when a measurement parameter is changed (e.g. amplification gain, displacement of the detector, use of other collimator aperture). Three known energy lines (for instance the  $^{152}\text{Eu}$  lines at 344, 778 and 1408 keV) covering the whole range are measured and put on the graph “measured vs. reference” peak positions. If the standard deviation of the linear regression does not exceed 2 keV, the calibration is accepted. Otherwise the calibration is repeated.

#### Efficiency Calibration

The efficiency calibration is carried out with a known, certified source  $^{137}\text{Cs}$  with homogeneous surface activity distribution, with same form, geometry and similar chemical composition (to guarantee identical absorption effects) as the fuel pin. The quantitative determination of the isotope is performed after subtracting the background signal.

### Control of measurements

Before the measurement of a fuel rod, it is necessary to control the following measuring conditions:

- i) Reproducibility of the data acquisition system using a calibrated  $^{137}\text{Cs}$ -source (with activity of  $1.113 \cdot 10^9$  Bq).
- ii) Preliminary identification of the spectrum peaks and expected intensity, so that no overflow of the detection system takes place during the measurement. The  $\gamma$ -counting rate should not exceed 15,000 counts/sec. If necessary, the counting rate can be attenuated.

The measurements cover the energy range 50 to 2200 keV.

### Procedure of the measurement

The fuel rod is placed horizontally on the metrology bench and pushed at a defined depth in the fixing mandrel centring. The fuel rod is translated during the measurement in front of the collimator (with aperture of 1.2 mm) and the Ge-detector. The impulses generated by the detector's Ge crystal are treated simultaneously:

- by a multi-channel spectrometer for nuclide identification. The  $\gamma$ -spectrum is obtained for 150 s time intervals and corresponds to a pin length of 5 mm.
- by a rate meter. Here it is measured the total  $\gamma$ -ray intensity for the complete wavelength range to determine the axial distribution of  $\gamma$ -emitters. The length-relevant resolution of the measurement depends on the collimator aperture. The analogue output of the rate meter is measured continuously with a multi-meter; an ADC changes this output to digital and the signal is also recorded on the hard disk of a computer. The scanning rate of the digital signal was one value per second and the translation speed of the fuel rod 2 mm/min. The modifying factor of the rate meter is 3000 with an analogue output range from 0–5 V.

For every isotope choice the axial distribution of the corresponding activity is recorded on the hard disk of a computer.

During the measurement no changes in the cell environment that could affect the  $\gamma$ -background level are permitted.

Laser length measurement is carried out in parallel with a precision of  $\pm 0.01$  mm and the reproducibility of  $\pm 0.05$  mm.

*Experimental Results*

The measured total  $\gamma$ -scan rate (**Figure 3**) in the region of the bottom end (plug and insulation pellet) is very low. It shows higher values at the position of the first natural UO<sub>2</sub>-pellet. The next sharp increase marks the start of the enriched UO<sub>2</sub>-pellet stack. Along this stack the <sup>137</sup>Cs activity remains remarkably constant indicating a homogeneous burn-up distribution along the stack, with a small decrease below 100 mm. Small sharp drops in this region are seen at the pellet/pellet interfaces. The pellets have dished ends where the specific activity and therefore also the  $\gamma$ -rate are lower. Volatile fission products can migrate to these locations and increase the specific activity at the pellet/pellet interfaces. This has not or only to a small amount occurred here that was not enough to reach the specific activity level of the fuel pellets. The peaks can be used for position analysis of single fuel pellets.

Near the top end the rate drops at the position of the second natural UO<sub>2</sub>-pellet. The following drop marks the position of the second insulation pellet. Then the total  $\gamma$ -rate increases because of an increase of the <sup>60</sup>Co-activity resulting from the neutron activation of cobalt as component of the steel spring. Towards the top end plug the  $\gamma$ -rate levels out.

The comparison with the optical picture of the segment shows that the brighter area exactly corresponds to the fuel stack positions and length.

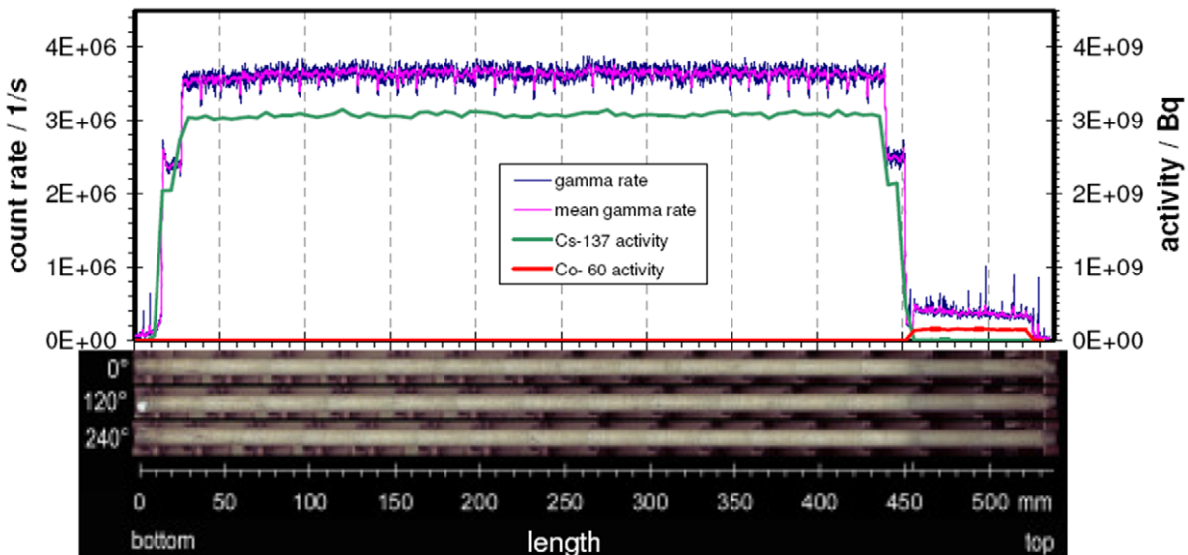


**Figure 3:**  $\gamma$ -scan of segment N0204 showing the total  $\gamma$ -rate and the activities of <sup>137</sup>Cs and <sup>60</sup>Co along the segment

A detailed analysis of the  $\gamma$ -scan rate was carried out and provided length data of the pellets after irradiation. They are summarised in **Table 1**. The average pellet length (mean peak distance) was 11.3 mm for the “natural”  $\text{UO}_2$  and 11.5 mm for the “enriched”  $\text{UO}_2$ .

The fuel properties are given by Metz et al. (Metz et al., 2012). The pellet length before irradiation can be estimated from the length of the fuel stack plus the length of the isolation pellets which is given with  $(439 \pm 0.5)$  mm in the technical drawing of this fuel rod segment by the fuel manufacturer. The length of the bottom side isolation pellet is given with 3 mm. We assumed an uncertainty of 0.5 mm. The length of the top end isolation pellet (iso1) is adjusted so that the total length of  $(439 \pm 0.5)$  mm is obtained. The length of iso1 is  $(4.9 \pm 0.5)$  mm (see **Table 1**) and a total fuel stack length of  $(431.1 \pm 0.9)$  mm is deduced. There are 38 pellets in the stack i.e. an average length of 11.3 mm per pellet before irradiation. Assuming the same length for natural and enriched pellets, the enriched fuel stack length is  $(408 \pm 1)$  mm.

**Table 1:** Determination of pellet positions of segment N0204 from  $\gamma$ -scanning data

calculated results:	
number of gaps found:	39
number of pellets (enriched U):	36
number of pellets (natural U):	2
total fuel stack length:	435.0 mm
enriched U fuel stack length:	412.4 mm
mean peak distance(PD) enriched U:	11.5 mm
mean peak distance(PD) natural U:	11.3 mm

description	position(bot end=0) mm	distance mm
pin top end	538.3	2.8
1st data point measured at pin top end	535.5	10.0
spring	525.5	69.2
iso1 (measured REFERENCE POINT)	456.3	4.9
fuel stack top end	451.4	---
natural UO2 II	440.0	11.3
enriched UO2 36	428.9	11.2
35	417.5	11.4
34	405.9	11.6
33	394.7	11.3
32	383.0	11.6
31	371.5	11.5
30	359.9	11.7
29	348.5	11.3
28	337.1	11.4
27	325.6	11.6
26	314.3	11.3
25	303.0	11.3
24	291.3	11.6
23	279.7	11.6
22	268.3	11.4
21	256.9	11.4
20	245.3	11.6
19	233.7	11.6
18	222.2	11.5
17	210.9	11.3
16	199.4	11.5
15	187.9	11.5
14	176.1	11.8
13	165.0	11.1
12	153.6	11.4
11	142.1	11.6
10	130.7	11.4
9	119.3	11.4
8	107.6	11.6
7	96.1	11.5
6	84.7	11.4
5	73.3	11.5
4	61.9	11.4
3	50.3	11.6
2	38.9	11.4
1	27.7	11.2
natural UO2 I	16.4	11.3
fuel stack bottom end	16.4	---

For PWR fuel rods with a burn-up of 50.4 GWd/t<sub>HM</sub> the expected volume swelling is in the range of 3.0 to 3.5% considering a volume swelling rate between 0.06 and 0.07 %/GWd/t<sub>HM</sub> (Guérin, 1999). The linear fuel swelling calculated from the “enriched” UO<sub>2</sub> fuel stack lengths before and after irradiation (**Table 1**) is (1 ± 0.2)% or expressed as volume swelling (3.0 ± 0.7)%, which matches the expectation. The natural UO<sub>2</sub> fuel pellets remain in the range of ±0.2 mm unchanged.

### Conclusions and Future work

Visual inspection of the fuel segment has shown no larger defects, but some helicoidal and longitudinal scratches on the cladding. At the positions of the fuel pellets, a colour change is visible in the cladding, which can be attributed to increased cladding oxidation in this area.  $\gamma$ -scanning has shown a homogeneous burn-up along the pin with a very small decrease towards the bottom end. Furthermore, the positions and the number of fuel pellets as well as the spring in the plenum were determined.

Further examinations of this segment are described in (Wegen et al., 2012b).

### Acknowledgement

*The research leading to these results has received funding from the European Union's European Atomic Energy Community's (Euratom) Seventh Framework Programme FP7/2007-2011 under grant agreement n° 295722 (FIRST-Nuclides project).*

### References

- Bertolino, G., Meyera, G., Perez Ipinab, J. (2002) Degradation of the mechanical properties of Zircaloy-4 due to hydrogen embrittlement. *Journal of Alloys and Compounds*, 330–332, 408-413.
- Daum, R.S., Majumdar, S., Bates, D.W., Motta, A.T., Koss, D.A., Billone, M.C. (2001) On the Embrittlement of Zircaloy-4 Under RIA-Relevant Conditions. *Zirconium in the Nuclear Industry: Thirteenth International Symposium*, Annecy, France, June 10-14, 2001, ASTM Special Technical Publication 1423.
- Franklin, D.G., Lucas, G.E., Bement, A.L. (1983) Creep of zirconium alloys in nuclear reactors. ASTM special technical publication 815, Baltimore, United States.

Guérin Y. (1999) In-Reactor Behaviour of Fuel Materials, in: Bailly, H., Ménessier, D., Prunier, C. (eds.), The Nuclear Fuel of Pressurized Water Reactors and Fast Reactors. Commissariat à l'Énergie Atomique (CEA).

Metz, V., Loida, A., González-Robles, E., Bohnert, E., Kienzler, B. (2012) Characterization of irradiated PWR UOX fuel (50.4GWd/t<sub>HM</sub>) used for leaching experiments. 7<sup>th</sup> EC FP – FIRST-Nuclides 1<sup>st</sup> Annual Workshop Proceedings (Budapest, Hungary).

Olander, D.R. (1976) Fundamental aspects of nuclear reactor fuel elements. California Univ. Technical Report TID-26711-P1, Berkeley, United States.

Papaioannou, D., Nasyrow, R., De Weerd, W., Bottomley, D., Rondinella, V.V. (2012) Non-destructive examinations of irradiated fuel rods at the ITU hot cells. 2012 Hotlab conference, 24-27 September 2012, Marcoule, France.

Wegen, D.H., Papaioannou, D., Nasyrow, R., Gretter, R., de Weerd, W. (2012) Non-destructive testing of segment N0204 of the spent fuel pin SBS1108 - Contribution to WP1 of the collaborative project FIRST Nuclides. JRC75272, European Atomic Energy Community, Karlsruhe, Germany.

Wegen, D.H., Papaioannou, D., Nasyrow, R., Rondinella, V.V., Glatz, J.P. (2012) Non-destructive analysis of a PWR fuel segment with a burn-up of 50.4 GWd/t<sub>HM</sub> – Part II: Defect determination. 7<sup>th</sup> EC FP – FIRST-Nuclides 1<sup>st</sup> Annual Workshop Proceedings (Budapest, Hungary).



# NON-DESTRUCTIVE ANALYSIS OF A PWR FUEL SEGMENT WITH A BURN-UP OF 50.4 GWD/THM – PART II: DEFECT DETERMINATION

Detlef H. Wegen<sup>\*</sup>, Dimitrios Papaioannou, Ramil Nasyrow, Vincenzo V. Rondinella,  
Jean-Paul Glatz

Joint Research Centre – Institute for Transuranium Elements (JRC-ITU), European Commission

\* Corresponding author: Detlef.Wegen@ec.europa.eu

## Abstract

The fuel segment is examined for deformations and other defects of the cladding. The oxide thickness along the segment's cladding is determined and it is shown that the results are in good agreement with  $\gamma$ -scanning data. Assumptions about the temperature profile along the segment are derived.

## Introduction

As pointed out elsewhere (Papaioannou et al., 2012) non-destructive testing (NDT) is an essential set of analyses that allows to consistently acquire reliable data needed for validation of the safety and efficient performance of the fuel rod in pile and to provide a valuable basis of information to plan and implement successful destructive post irradiation examination (PIE). During reactor operation a fuel rod is exposed to conditions which lead to complex alterations in the fuel, but also in the cladding material. Heat and fission products (FP) are produced by nuclear fission in the fuel. Due to the high temperature the cladding can creep and the generated FP cause a swelling of the fuel (Olander, 1976; Franklin et al., 1983). Hydrogen and irradiation can cause embrittlement of the cladding (Bertolino et al., 2002; Daum et al., 2001). As a consequence of these solicitations defects can be generated in the rod. In the following, the defect determination performed on one of five segments of a segmented PWR (Gösgen, Switzerland) UOX fuel rod with a burn-up of 50.4 GWd/t<sub>HM</sub> is described. The fuel stack consists of 36 “enriched” UO<sub>2</sub>-pellets plus one natural UO<sub>2</sub> pellet at top and bottom end (Wegen et al., 2012b). Details of the irradiation are given in (Metz et al., 2012). The examinations have been carried out in the hot cells of JRC-ITU (Wegen et al., 2012a).

## Profilometry

Profilometry is used to quantify the combined effects of cladding creep and fuel swelling as well as the evaluation of rod ovalization and detection of any geometrical anomaly. The measurements are generally made using inductive transducers following calibration on certified standards in the diameter range of interest.

For this purpose the fuel rod is put horizontally on the metrology bench and pushed at a defined depth into the fixing mandrel centring. The fuel rod is simultaneously translated and rotated during the measurement and crossed through the knife edge contacts of the LVDT (linear variable differential transformer) gauge. Following parameters are used:

Spiral rotation:	2 mm advance per rotation
Translation speed:	1000 mm per hour
Measurement precision:	$\pm 3 \mu\text{m}$

Complementary this measurement was repeated two times without rotation with the same translation speed, the angular position of the knife edge were changed by 90 degrees to one another.

The outputs of the LVDT gauge (diameter measurement) are recorded continuously via data logger on the connected computer and stored in electronic media. Scanning rate of the data logger was one value per 0.25 s.

Reference standards with diameter similar to the nominal value (10.5, 10.6, 10.67, 10.70, 10.75, 10.8 and 10.85 mm) were used for the calibration of the LVDT gauge.

Laser length measurement is carried out parallel to profilometry, defect and oxide thickness determination with a precision of  $\pm 0.01$  mm and the reproducibility of  $\pm 0.05$  mm.

### *Results of the examination*

The measured diameter of the segment and the pellet positions are shown in **Figure 1a**. A creep down of the zircaloy cladding is visible. An overview about in-reactor creep of zirconium alloys is given in (Adamson et al., 2009). The diameter before irradiation was 10.75 mm the measured average diameter along the fuel stack is about 10.71 mm. The mean diameter is smaller at the fuel stack ends than in the middle of the stack (**Table 1**). The measured curve shows a periodical change of the diameter along the fuel stack. The positions of the maxima of the averaged diameter curve (average of 80 data points) match very well with the positions of the pellet/pellet interfaces obtained from  $\gamma$ -scanning. The minima are always located at the centre of a pellet (**Table 1**). The difference between minimal and maximal

diameter is along the stack of the originally enriched UO<sub>2</sub> pellets in the range of 13 to 20 µm. At the position of the natural UO<sub>2</sub> pellets the average cladding diameter decreases about 20 to 30 µm. The profiles along the fuel stack of the average minimal and of the maximal diameter reach a maximum 250 to 350 mm from the bottom end of the segment. Here the diameter is 25 to 30 µm larger compared to the positions of the first and last "enriched" UO<sub>2</sub> pellets. The segment shows a slight ovalization.

## Defect Determination

Eddy current examinations are carried out to detect defects present in the cladding, such as cracks, variable thickness, corrosion, etc. Geometrical or structural heterogeneities in the cladding (crack, corrosion, etc.) modify the eddy current path. These variations of the eddy current generated in the examined part by the alternating field of a coil are assessed.

### *Experimental procedure*

The fuel rod is put horizontally on a metrology bench and pushed at a defined depth in the fixing mandrel centring. The fuel rod is translated during the measurement at a speed of 100 mm/min and moved through an encircling coil. The standard coil frequency of 300 kHz can be preferably adjusted depending on the depth of the detected defect.

The measurement is calibrated using standards of the same material under examination with following pre-set defects:

- 1, 2, 4 holes of 1 mm diameter
- internal groove 0.1 mm thick
- outer groove 0.1 mm thick
- swelling 0.1 mm

A calibration is made before each measurement (**Figure 1a**).

As can be seen are the phase shift of the X- and Y-signals (see Lissajous pattern in **Figure 1a**) affected by the type of the simple standard defects while the amplitude gives information about the defect size. The defect length can be derived from the position of the minima and maxima of the signals along the tube length. The characterisation of "natural" defects from measured data is complex (Auld and Moulder, 1999).

The X- and Y-outputs of the encircling coil (test signal equals X- plus Y-outputs) are continuously acquired and stored via data logger in a computer file.

### Results

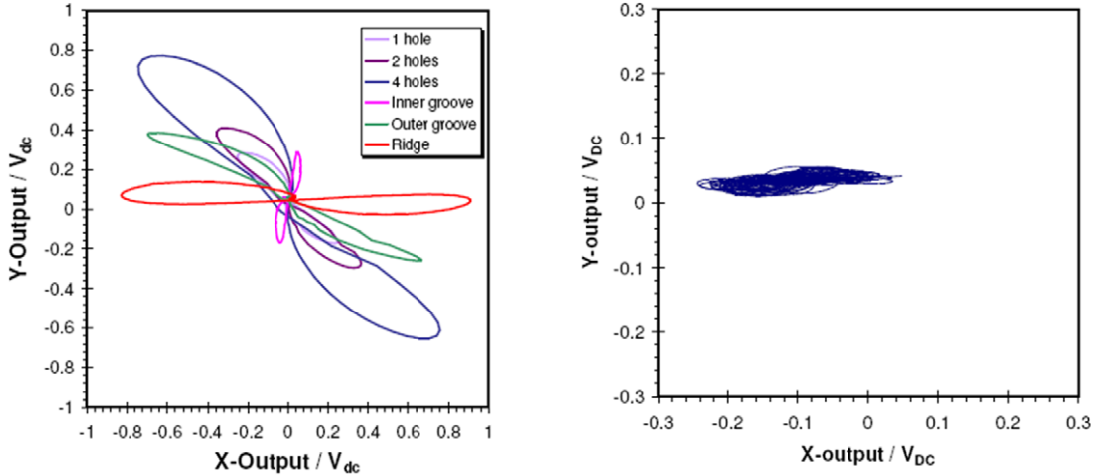


**Figure 1:** Eddy current Lissajous pattern of (a) standard defects and (b) measured along the fuel stack

**Figure 2b** shows the measured eddy current, the total  $\gamma$ -scanning and the pellet positions. From the measurement no larger defects could be detected. A small periodical change is visible which correlates with the pellet/pellet interfaces. This effect reflects the small change in diameter found in the profilometry investigations because the relationship between the segments diameter and the diameter of the encircling coil is not maintained constant (IAEA, 2011). It is less pronounced at the fuel stack ends than in the centre. In the Lissajous pattern no other defects than a series of ridges is visible (**Figure 1b**). In general the results fit with those obtained from  $\gamma$ -scanning and profilometry. They are summarized in **Table 1**. The defect locations determined from eddy current testing match with those obtained from  $\gamma$ -scanning and profilometry. The measured diameter differences along the pin are also in agreement with the profilometry data taking into account an uncertainty of  $\sim 40\%$  resulting from the accuracy of the ridge standard of  $(140 \pm 60) \mu\text{m}$ .

### Outer Oxide Layer Thickness

High frequency eddy current measurements are suitable to determine coating/substrate associations (nonmagnetic/ferromagnetic, insulator/conductor). The magnetic force lines are modified in the vicinity of a ferromagnetic material. The density of force lines in the material varies with the distance

of the probe from the ferromagnetic material. This effect is used to measure the layer thickness at the surface of fuel rods after calibration with tubes, identical in geometry and nature to the rod cladding.

#### *Procedure of the measurement*

The fuel rod is put horizontally on a metrology bench and pushed at a defined depth in the fixing mandrel centring. The fuel rod is simultaneously translated and rotated during the measurement, which is carried out by means of eddy current using a punctual coil unit touching the outer surface of the cladding.

Spiral rotation: 5 mm advance per rotation

Translation speed: 20 mm per minute

Scanning rate of the data logging was one value per second.

The measuring system is calibrated using standards consisting of oxidized rods of the same material under examination. The thickness of the standard's oxide layer is certified by the manufacturer (AREVA-NP).

Calibration control is carried out before each fuel rod examination. The precision of the translation is  $\pm 0.05$  mm/metre and  $\pm 5^\circ$  for the rotation. The precision of the oxide layer thickness measurement is  $\pm 2$   $\mu\text{m}$ .

The outputs of the eddy current coil (outer oxide layer thickness) and axial position are continuously acquired by a PC.

#### *Results of the oxide thickness measurement*

The measured oxide profile is given together with the total  $\gamma$ -scanning and the pictures of the segment in **Figure 2c**. The oxide profile matches with the optical appearance of the pin. Thicker oxide (35 to 45  $\mu\text{m}$ ) is found in the light grey zone of the pin while at the darker grey zones at both ends the thickness is below 17  $\mu\text{m}$ . The maximal thickness is found on the pin between 250 and 350 mm from the bottom end.

Temperature is beside exposure time, water chemistry, neutron flux and others a main parameter controlling the oxide growth (Garzarolli and Garzarolli, 2012). Looking at the measured oxide profile it can be assumed that despite a relatively constant burn-up (Wegen et al., 2012b) the temperature at the cladding surface was lower towards both ends of the pin.

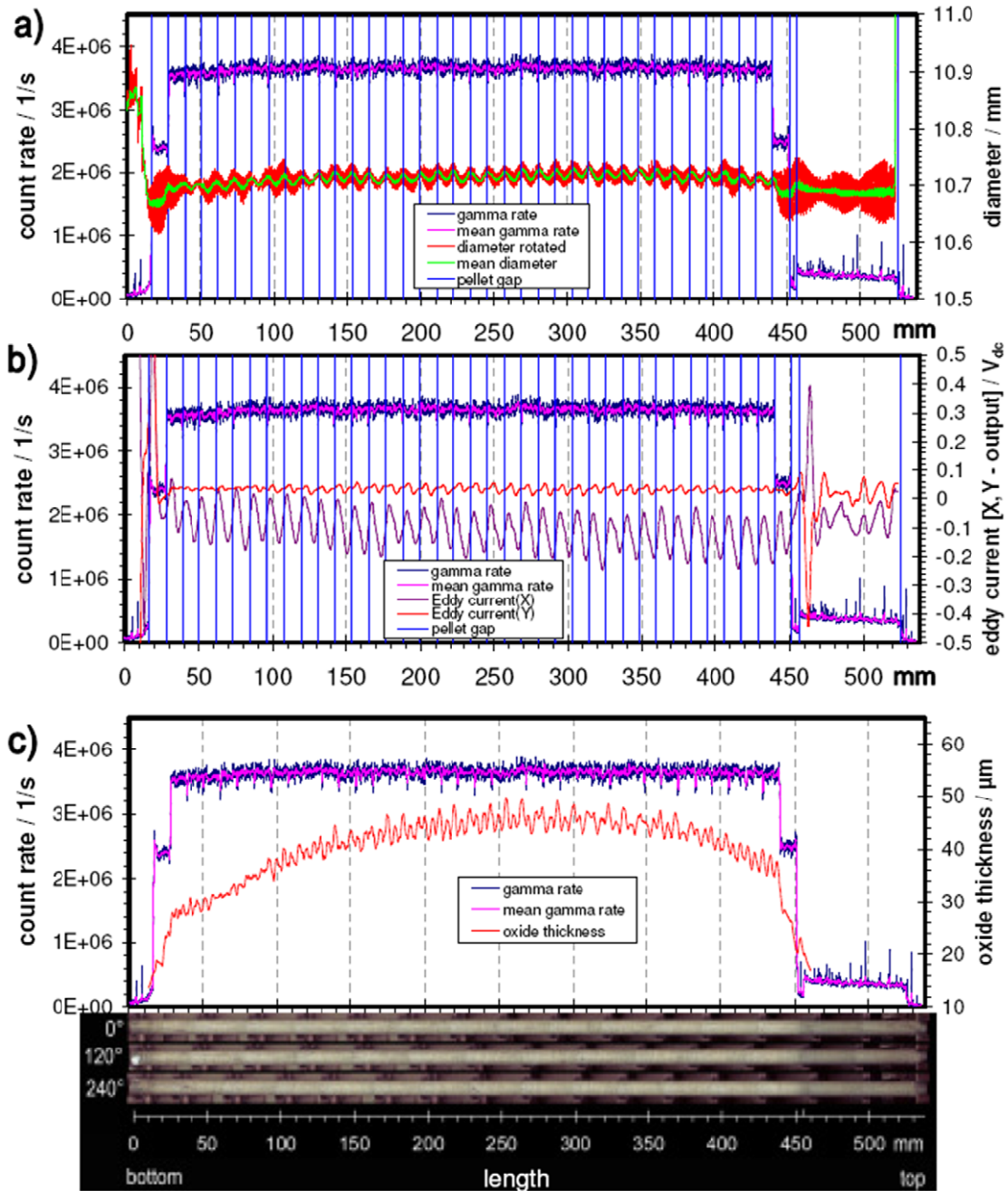


**Figure 2:** Results of NDT. (a) Diameter and mean diameter (rotated) along segment N0204 together with  $\gamma$ -scan and pellet positions. (b) Defect determination via eddy current measurement.  $\gamma$ -scan and pellet positions are also shown. (c) Outer oxide layer thickness along segment N0204.

### Conclusions and Future work

NDT has been successfully carried out on a PWR UOX fuel rod with a burn-up of 50.4 GWd/t<sub>HM</sub>. The examined segment N0204 shows no major defects. Ridges were identified with profilometry and eddy

current testing at the pellet/pellet gap locations. The obtained results are in good agreement with those obtained from  $\gamma$ -scanning (Wegen et al., 2012b).

The measured oxide thickness profile matches well with the visual nature of the outer cladding (Wegen et al., 2012b). Despite a homogeneous burn-up it seems that the maximum temperature of the cladding water interface was between 250 and 350 mm from the bottom end of the segment. This is supported by slight variations measured with profilometry and eddy current in the same zone.

**Table 1:** Comparison of  $\gamma$ -scanning (Wegen et al., 2012a; Wegen et al., 2012b), profilometry and eddy current data

description	Y-scanning: pellet gap position <sup>1</sup> mm	profilometry:		calculated mean diameter difference $\mu$ m	Y-scanning: pellet centre position <sup>1</sup> mm	profilometry:		eddy current defect position <sup>1</sup> mm	eddy current diameter difference $\mu$ m
		max. diameter position <sup>1</sup> mm	mean diameter rotated (max) mm			min. diameter position <sup>1</sup> mm	mean diameter rotated (min) mm		
fuel stack top end	451.4	451.4	10.683 <sup>2</sup>					452.5	17 <sup>2</sup>
natural UO <sub>2</sub> II	440.0	440.2	10.713	23 <sup>2</sup>	445.7	445.8	10.682 <sup>2</sup>	441.4	15 <sup>2</sup>
enriched UO <sub>2</sub> 36	428.9	429.7	10.714	13	434.5	436.9	10.699	430.0	14
35	417.5	417.9	10.718	14	423.2	423.2	10.705	418.4	14
34	405.9	406.0	10.724	18	411.7	412.4	10.704	406.4	12
33	394.7	395.3	10.721	14	400.3	400.5	10.707	395.5	13
32	383.0	383.6	10.722	16	388.8	388.9	10.708	383.9	16
31	371.5	371.7	10.724	17	377.3	377.2	10.706	371.8	12
30	359.9	359.9	10.726	17	365.7	366.2	10.708	360.8	14
29	348.5	349.2	10.727	17	354.2	354.4	10.710	349.1	13
28	337.1	337.4	10.726	15	342.8	342.8	10.711	337.7	10
27	325.6	325.6	10.724	14	331.3	331.9	10.711	326.3	14
26	314.3	314.8	10.731	20	319.9	320.2	10.709	315.0	13
25	303.0	303.0	10.729	18	308.6	308.5	10.714	303.2	13
24	291.3	292.1	10.729	19	297.1	297.5	10.708	291.8	13
23	279.7	280.4	10.729	19	285.5	285.7	10.710	280.2	14
22	268.3	268.6	10.728	20	274.0	274.0	10.709	268.9	13
21	256.9	256.8	10.724	16	262.6	263.2	10.706	257.0	10
20	245.3	245.9	10.725	18	251.1	251.5	10.708	245.5	13
19	233.7	234.2	10.723	18	239.5	239.7	10.706	233.6	13
18	222.2	222.5	10.726	19	228.0	228.0	10.705	222.4	11
17	210.9	210.7	10.725	17	216.6	216.8	10.710	211.1	12
16	199.4	199.9	10.722	17	205.2	205.3	10.706	199.3	10
15	187.9	188.1	10.721	17	193.7	193.6	10.705	188.1	9
14	176.1	176.2	10.719	16	182.0	182.7	10.703	176.2	15
13	165.0	164.8	10.722	19	170.6	171.0	10.701	164.7	14
12	153.6	153.7	10.724	19	159.3	159.3	10.703	153.2	13
11	142.1	141.9	10.725	20	147.9	148.3	10.705	141.9	14
10	130.7	130.0	10.721	17	136.4	136.5	10.703	130.4	12
9	119.3	118.7	10.717	15	125.0	125.0	10.704	118.5	13
8	107.6	106.6	10.720	21	113.5	113.1	10.699	106.9	14
7	96.1	96.6	10.717	18	101.9	102.1	10.699	95.7	12
6	84.7	84.4	10.713	17	90.4	90.1	10.699	84.4	16
5	73.3	72.4	10.713	22	79.0	78.8	10.693	72.7	15
4	61.9	60.5	10.708	19	67.6	67.9	10.691	60.6	16
3	50.3	50.0	10.703	13	56.1	55.9	10.688	49.6	12
2	38.9	37.7	10.705	14	44.6	44.0	10.693	38.3	9
1	27.7	27.7	10.703		33.3	33.2	10.690	28.5	11 <sup>2</sup>
natural UO <sub>2</sub> I	16.4	15.7	10.672 <sup>2</sup>		22.0	22.2	10.662 <sup>2</sup>	15.9	92 <sup>2</sup>
fuel stack bottom end	16.4								
average value(1...36)			10.721	17			10.704		13

<sup>1)</sup> Positions relative to the bottom end of the segment <sup>2)</sup> Not included in average value

The results achieved by NDT were used for the preparation of samples for further destructive examinations at JRC-ITU and IRF determinations at KIT-INE (Wegen et al., 2012c).

## Acknowledgement

*The research leading to these results has received funding from the European Union's European Atomic Energy Community's (Euratom) Seventh Framework Programme FP7/2007-2011 under grant agreement n° 295722 (FIRST-Nuclides project).*

## References

Adamson, R., Garzarolli, F., Patterson, C. (2009) In-Reactor Creep of Zirconium Alloys. Advanced Nuclear Technology International, Skultuna, Sweden.

Auld, A. and Moulder, J.C. (1999) Review of Advances in Quantitative Eddy Current Nondestructive Evaluation. Journal of Nondestructive Evaluation, 18, 3-36.

Bertolino, G., Meyera, G., Perez Ipinab, J. (2002) Degradation of the mechanical properties of Zircaloy-4 due to hydrogen embrittlement. Journal of Alloys and Compounds, 330–332, 408–413.

Daum, R. S., Majumdar, S., W. Bates, D., Motta, A. T., Koss, D. A., Billone, M. C. (2001) On the Embrittlement of Zircaloy-4 Under RIA-Relevant Conditions. Zirconium in the Nuclear Industry: Thirteenth International Symposium, Annecy, France, June 10-14, 2001, ASTM Special Technical Publication 1423.

Franklin, D.G., Lucas, G.E., Bement, A.L. (1983) Creep of zirconium alloys in nuclear reactors. ASTM special technical publication 815, Baltimore, United States.

Garzarolli F. and Garzarolli M. (2012) PWR Zr Alloy Cladding Water Side Corrosion. Advanced Nuclear Technology International, Mölnlycke, Sweden.

International Atomic Energy Agency (2011) Eddy Current Testing at Level 2: Manual for the Syllabi Contained IAEA-TECDOC-628/Rev. 2 ‘Training Guidelines for Non-Destructive Testing Techniques’.

Metz, V., Loida, A., González-Robles, E., Bohnert, E., Kienzler, B. (2012) Characterization of irradiated PWR UOX fuel (50.4GWd/t<sub>HM</sub>) used for leaching experiments. 7<sup>th</sup> EC FP – FIRST-Nuclides 1<sup>st</sup> Annual Workshop Proceedings (Budapest, Hungary).

Olander, D.R. (1976) Fundamental aspects of nuclear reactor fuel elements. California Univ. Technical Report TID-26711-P1, Berkeley, United States.



Papaioannou, D., Nasyrow, R., De Weerd, W., Bottomley, D., Rondinella, V. V. (2012) Non-destructive examinations of irradiated fuel rods at the ITU hot cells. 2012 Hotlab conference (Marcoule, France).

Wegen, D.H., Papaioannou, D., Nasyrow, R., Gretter, R., de Weerd, W. (2012) Non-destructive testing of segment N0204 of the spent fuel pin SBS1108 - Contribution to WP1 of the collaborative project FIRST Nuclides. JRC75272, European Atomic Energy Community, Karlsruhe, Germany.

Wegen, D.H., Papaioannou, D., Nasyrow, R., Rondinella, V.V., Glatz, J.-P. (2012) Non-destructive analysis of a PWR fuel segment with a burn-up of 50.4 GWd/t<sub>HM</sub> – Part I: Visual inspection and  $\gamma$ -scanning. 7<sup>th</sup> EC FP – FIRST-Nuclides 1<sup>st</sup> Annual Workshop Proceedings (Budapest, Hungary).

Wegen, D.H., Papaioannou, D., Gretter, R., Nasyrow, R., Rondinella, V.V., Glatz, J.-P. (2012) Preparation of samples for IRF investigations and post irradiation examinations from 50.4 GWd/t<sub>HM</sub> PWR fuel. 7<sup>th</sup> EC FP – FIRST-Nuclides 1<sup>st</sup> Annual Workshop Proceedings (Budapest, Hungary).



# PREPARATION OF SAMPLES FOR IRF INVESTIGATIONS AND POST IRRADIATION EXAMINATIONS FROM 50.4 GWd/t<sub>HM</sub> PWR FUEL

Detlef H. Wegen<sup>\*</sup>, Dimitrios Papaioannou, Ralf Gretter, Ramil Nasyrow, Vincenzo V. Rondinella, Jean-Paul Glatz

Joint Research Centre – Institute for Transuranium Elements (JRC-ITU), European Commission

\* Corresponding author: Detlef.Wegen@ec.europa.eu

## Abstract

Samples for leaching experiments at KIT-INE have been prepared from a PWR fuel segment at the hot cell facility of JRC-ITU. The specimens were carefully examined and some features relevant for future investigations were identified.

## Introduction

The aim was to prepare samples for leaching experiments at KIT-INE from a PWR fuel segment with a burn-up of 50.4 GWd/t<sub>HM</sub> (Metz et al., 2012). For this purpose it was envisaged to cut whole pellets with cladding from the segment. Of special interest were natural UO<sub>2</sub> pellets located at the top and bottom end of the fuel stack (first and last pellet of the fuel stack). Ideally, the segment was to be cut at the positions of the pellet/pellet gaps formed by the pellets dishings.

## Experimental procedure

The sample preparation was carried out after non-destructive testing of the pin (Wegen et al., 2012a; Wegen et al., 2012b) in the hot cells of ITU (under nitrogen atmosphere with a typical oxygen contents < 1%). A cutting machine equipped with a diamond wafering blade (Buehler Isomet ® series 15HC) was used for the sectioning of the segment. The dry cutting was performed slowly without any cooling liquid.

To find the exact positions of the pellet/pellet gaps a reference must be found. Therefore, the top end of the segment containing the spring was cut-off approximately 10 mm before the isolation pellet at the top end. Then the length of the top end section was measured as well as the distance from the cut to the

isolation pellet inside the cladding. The positions for all the cuttings needed were calculated from this reference point considering a cut width of 0.4 mm and fixed in a cutting plan (see **Figure 1**).

The lengths of the specimens were measured and a picture of each cut was taken. From these data the cutting positions relative to the  $\gamma$ -scan were calculated (**Figure 2**).

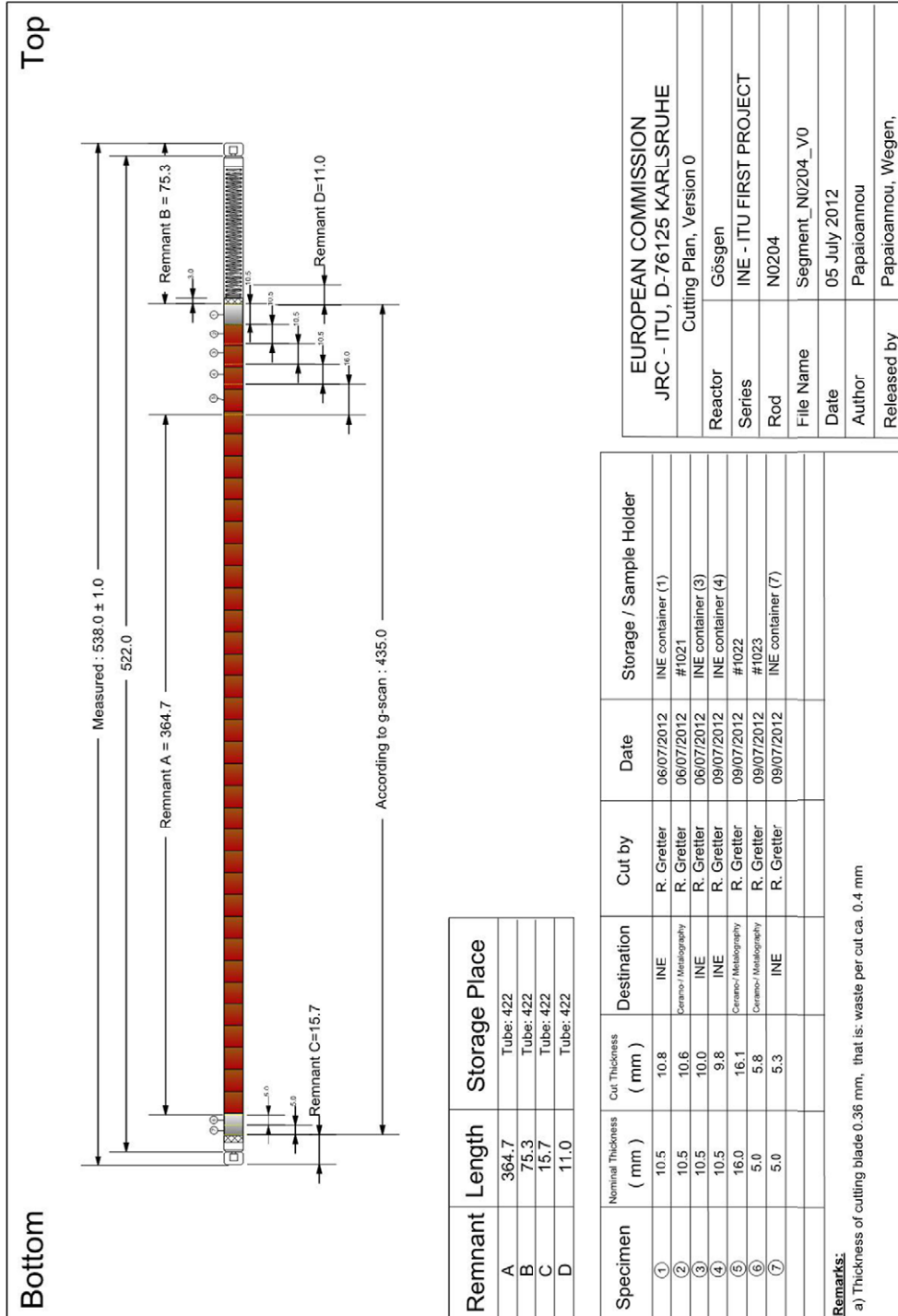
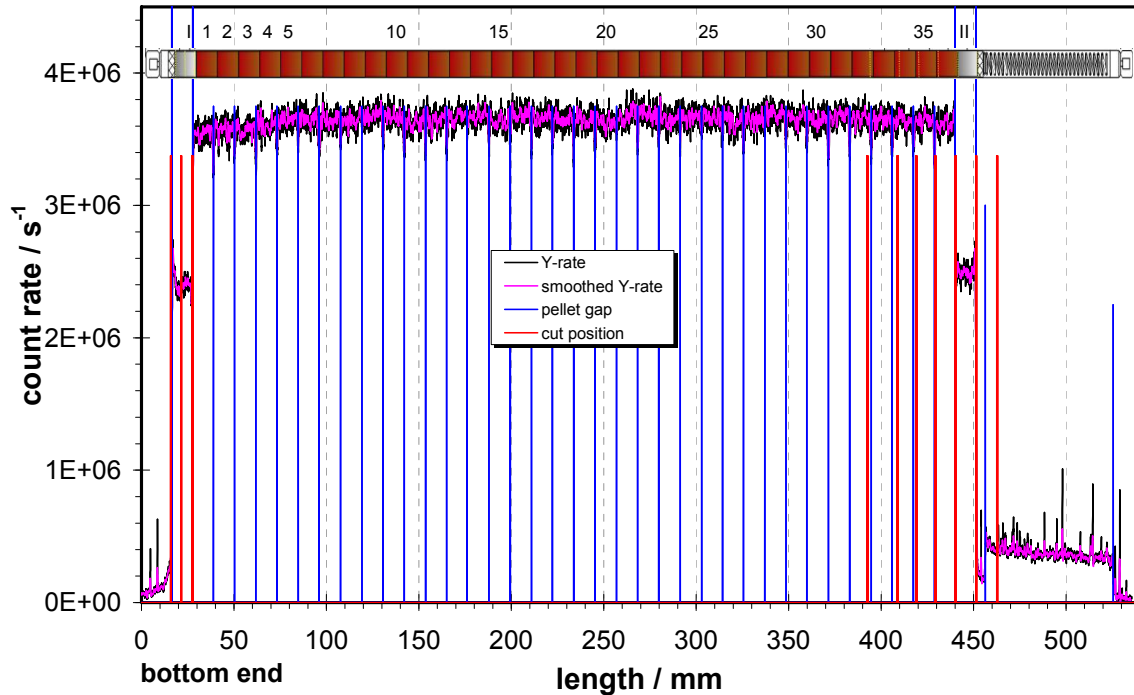


Figure 1: Cutting plan of segment N0204



**Figure 2:**  $\gamma$ -scan of segment N0204 showing pellet-pellet interfaces (blue) and cut positions (red). For illustration a sketch of the fuel segment is also included (I and II: “natural”  $\text{UO}_2$ ; 1, 2, ..., 36: enriched  $\text{UO}_2$ ).

### Description of the specimen

The samples were designated in the sequence of their preparation (1 to 7). To distinguish between top and bottom side the specimens were marked with a small notch in the cladding. Specimens 1 to 5 were marked at the top side while specimen 6 and 7 were marked at the bottom side. The cut positions relative to the  $\gamma$ -scan and the appearance of the samples are shown in **Figure 3** and **Figure 4**.

#### *Specimen 1*

Specimen 1 was cut exactly at the pellet/pellet gap. Parts of the pellet dishing can be seen on the top and bottom side of the sample. Referring to **Figure 2** it contains the “natural”  $\text{UO}_2$  pellet II.

#### *Specimen 2*

This specimen contains the last enriched  $\text{UO}_2$  pellet 36 from the bottom end (**Figure 2**). The top side shows parts of the dishing while at the bottom side the cut is tight at the dishing and it is cut-off.

*Specimen 3*

The photograph from the top side of the enriched pellet 35 (**Figure 2**) shows a nearly complete dishing but at the bottom side the cut goes through the pellet and therefore the dishing is removed from the pellet.

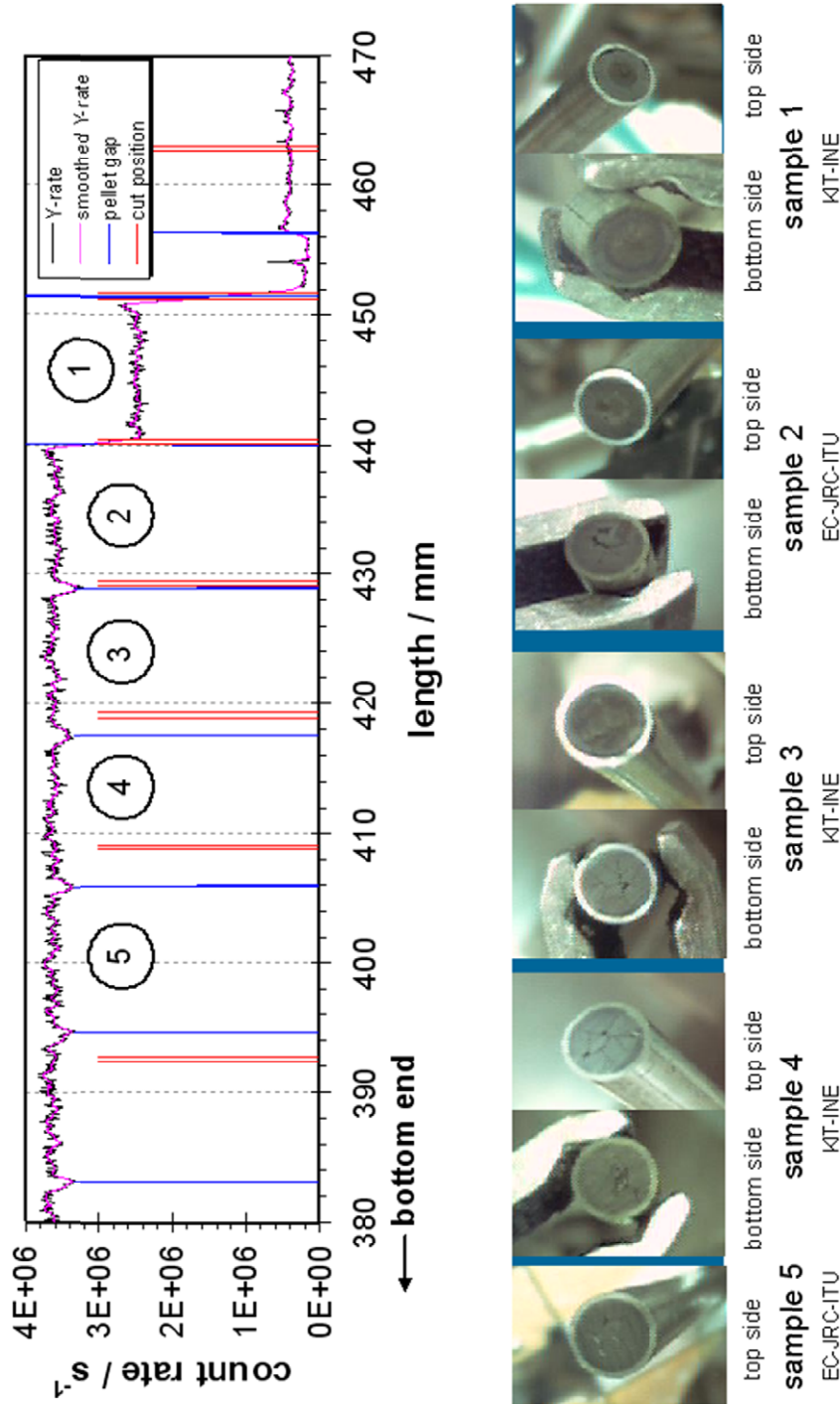


**Figure 3:** Cut positions in relation to  $\gamma$ -scan and photographs of samples 1 to 5

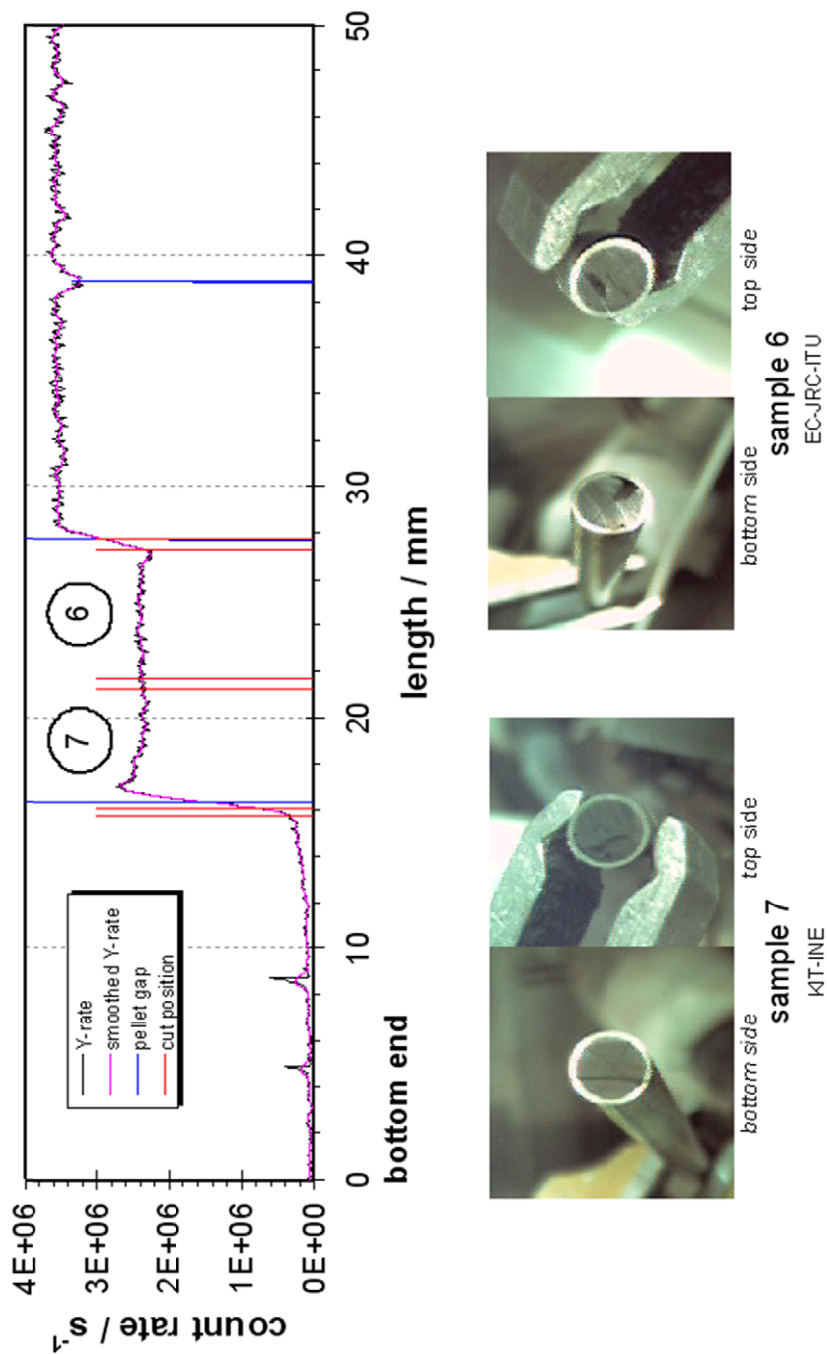


**Figure 4:** Cut positions in relation to  $\gamma$ -scan and photographs of samples 6 and 7

*Specimen 4*

Comparing the cut positions and  $\gamma$ -scanning data, and looking at the photographs of top and bottom side both showing no dishing leads to the conclusion that specimen 4 contains at its top end ~1.5 mm of pellet 35 including the complete pellet/pellet gap and at the bottom end ~8.3 mm of the top end of

pellet 34 (**Figure 2**). This sample is very special for leaching experiments because of the volatile fission product inventory in the hidden gap near the top end of specimen 4.

### *Specimen 5*

Specimen 5 is foreseen for longitudinal ceramography of the whole pellet 33. It contains also ~3 mm of pellet 34 and ~2 mm of pellet 32.

### *Specimen 6 and 7*

These specimens are attributed to the “natural” UO<sub>2</sub> pellet I (**Figure 2**). The cut position match with those of the pellet/pellet gaps obtained from  $\gamma$ -scanning but on the photographs no dishing can be seen. The lengths of the samples (**Figure 1**) are 5.8 and 5.3 mm respectively. Considering a cut width of 0.4 mm a total length for both of 11.5 mm is obtained. In **Table 1** in (Wegen et al., 2012a) the length of pellet I is listed with 11.3 mm which is 0.2 mm shorter than the distance between the cuts. This gives rise to the assumption that the top end of specimen 6 could contain a small part of the enriched pellet 1. This finding has to be taken into account planning future examinations.

## **Preparation for transport**

Specimen 1, 3, 4 and 7 were foreseen to be transported back to KIT-INE while specimen 2, 5 and 6 remain at ITU for further examinations. For the transport, the samples were placed in a steel capsule as cut and separated by aluminum plates as shown in **Figure 5**. Before closure the capsule was purged inside the hot cell with argon. The transport of samples to KIT-INE has taken place in July 2012.

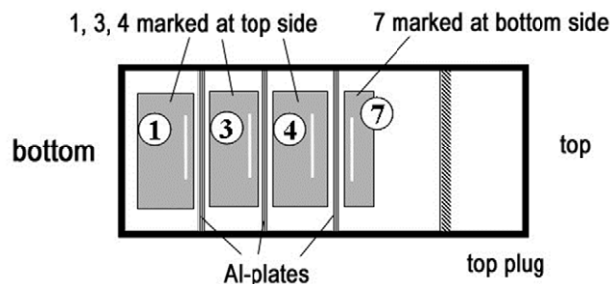


**Figure 5:** Loading of samples in transport container (schematic)



## Conclusions and Future work

A reference point was successfully fixed after the cut-off of the segments top end which enables together with the total  $\gamma$ -scan of the segment an exact determination of the cut positions. This information together with photographs taken from the various cuts made a further characterisation of the specimen possible and some possible; specific features to be taken into account for future investigations were identified.

The specimen 2, 5 and 6 are foreseen for further destructive analyses e.g. ceramography etc.

## Acknowledgement

*The research leading to these results has received funding from the European Union's European Atomic Energy Community's (Euratom) Seventh Framework Programme FP7/2007-2011 under grant agreement n° 295722 (FIRST-Nuclides project).*

## References

- Metz, V., Loida A., González-Robles, E., Bohnert, E., Kienzler, B. (2012) Characterization of irradiated PWR UOX fuel (50.4GWd/t<sub>HM</sub>) used for leaching experiments. 7<sup>th</sup> EC FP – FIRST-Nuclides 1<sup>st</sup> Annual Workshop Proceedings (Budapest, Hungary).
- Wegen, D.H., Papaioannou, D., Nasyrow, R., Rondinella, V.V., Glatz, J.-P. (2012) Non-destructive analysis of a PWR fuel segment with a burn-up of 50.4 GWd/t<sub>HM</sub>, 7<sup>th</sup> EC FP – FIRST-Nuclides 1<sup>st</sup> Annual Workshop Proceedings (Budapest, Hungary).
- Wegen, D.H., Papaioannou, D., Nasyrow, Gretter, R., de Weerd, W. (2012) Non-destructive testing of segment N0204 of the spent fuel pin SBS1108 - Contribution to WP1 of the collaborative project FIRST Nuclides. JRC75272, European Atomic Energy Community, Karlsruhe, Germany.



# FISSION GAS RELEASE MEASUREMENT ON ONE 50.4 GWd/t<sub>HM</sub> PWR FUEL SEGMENT

Detlef H. Wegen\*, Dimitrios Papaioannou, Wim De Weerd, Vincenzo V. Rondinella,  
Jean-Paul Glatz

Joint Research Centre – Institute for Transuranium Elements (JRC-ITU), European Commission

\* Corresponding author: Detlef.Wegen@ec.europa.eu

## Abstract

Fission gas release measurements have been performed on one of five short UOX fuel segments of a segmented PWR fuel rod with a burn-up of 50.4 GWd/t<sub>HM</sub> at the hot cell facilities of JRC-ITU. The free volume and the normal fission gas volume were determined while the isotopic composition could not be obtained.

## Introduction

The determination of fission gas release to the plenum of a fuel pin as well as the isotopic composition of the gas and the measurement of the free volume of the fuel rod is important to evaluate the overall fuel rod behaviour during irradiation. Furthermore, it plays an important role in the context of final waste storage to estimate the instant release fraction (IRF) of volatile fission products at times when the waste after a canister failure comes in contact with groundwater (Carbol et al., 2012).

The measurement device in operation developed at JRC-ITU consists of two main parts: i) the puncturing device installed inside a hot cell consisting of a drilling machine, a system of standard volumes and calibrated pressure gauges (**Figure 1**); ii) a quadrupole mass spectrometer installed outside the hot cell (**Figure 2**).

## Experimental

The measurement procedure is as described in (Hoffmann et al., 2005) and in (Papaioannou et al., 2012).

The PWR fuel rod with a burn-up of 50.4 GWd/t<sub>HM</sub> consisted of five closed segments which were mounted together. The segments were separated without opening them before the fission gas release measurement. For measurement the ~0.5 m long segment is introduced plenum first into the chamber of the puncturing station, via an aperture that is sealed with a flat rubber seal. Two expansion chambers with known volumes ( $V_{e1}$  and  $V_{e2}$ ) are connected to the evacuated drilling chamber with the fuel rod inside. They are filled with a known pressure of neon, since neon is not present in the fission gas. One expansion chamber is opened and the neon gas will now equilibrate between the two chambers while temperature and pressure change are measured. The volume of the drilling chamber ( $V_d$ ) less the volume of the rod inside the chamber can be calculated using the law of Boyle – Marriot. Then the chambers are evacuated.

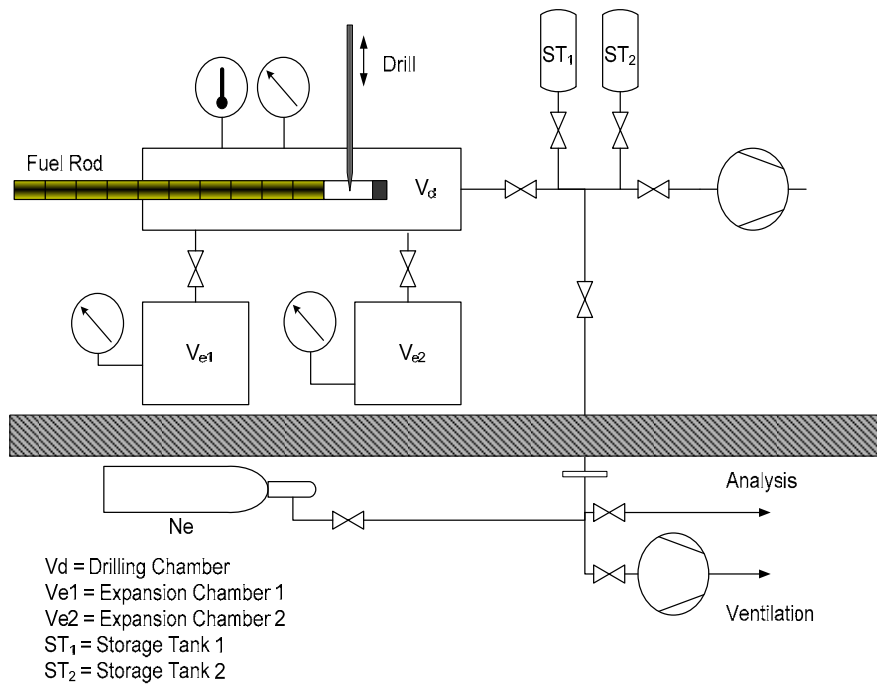


**Figure 1:** Scheme of the puncturing device

The pin is punctured with the drilling machine and the fission gas under the internal pressure of the fuel rod is released into the evacuated drilling chamber ( $V_d$ ), where temperature and pressure are measured. In case of a large amount of released gas the expansion chambers are used to lower the gas pressure below 1 bar for measurement. To allow a complete outgassing the pressure data are taken after waiting for ~2 hours. The gas can be stored in the storage tanks ( $ST_1$ ,  $ST_2$ ). Additional pumping completes the gas removal from the rod.

The mass spectrometer is calibrated using gas standards with known composition of Xe, Kr at a concentration level as close as possible to the expected concentration. Since neon is not present in fission gas, it is used as purge gas to clean the lines after calibration in three cycles of evacuation and purging. Then the lines are evacuated to approximately 3 mbar and the gas from the drilling chamber is fed into the quadrupole mass spectrometer in order to determine the isotopic composition of the fission gas.

To determine the free gas volume of the rod, neon is released from the pre-pressurized expansion volumes ( $V_{e1}$ ,  $V_{e2}$ ) to the purged and evacuated drilling chamber with the punctured rod still inside. The neon will now equilibrate between the two chambers and also fill the free gas volume of the punctured rod. By means of the pressure drop of the chamber and the prior measured drilling chamber volume the free gas volume of the rod is calculated.

For the fission gas release determination of the PWR fuel rod SBS 1108, Segment N 0204 irradiated at Gösgen (Metz et al., 2012) it was foreseen to share the gas sample between KIT-INE and JRC-ITU. For this purpose a gas sampling outlet was installed outside the hot cell (**Figure 2**). A gas mouse can be attached to the sampling outlet to collect a gas sample. The modified system was tested and worked without problems.

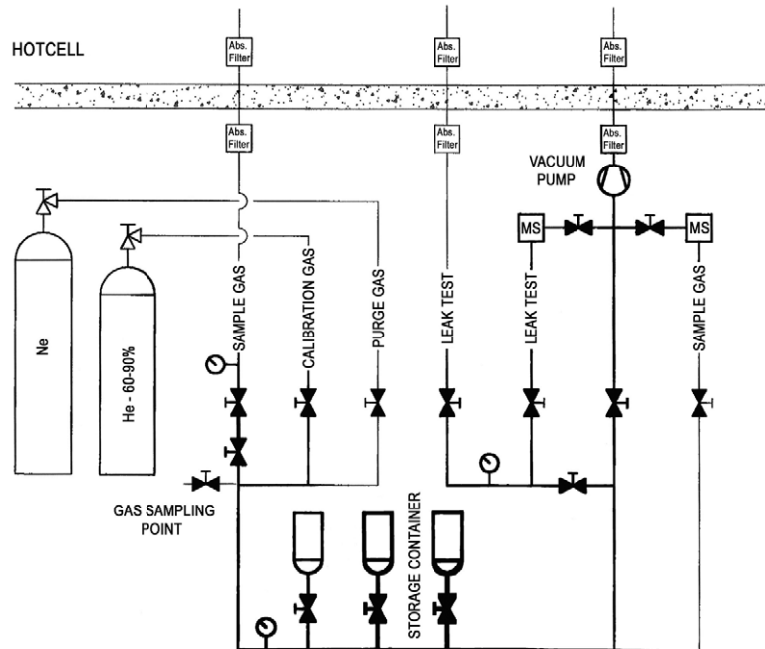


**Figure 2:** Simplified scheme of the fission gas sampling station installed outside the hot cell

**Results**

The measurement was carried out in the second half of May 2012. The results of the pressure and volume determinations are summarized in **Table 1** and in (Wegen et al., 2012). Because of the short length of the segment (~0.5 m) the fission gas volume was small compared to a normal LWR rod with a length of ~4 m. From the totally available 147 cm<sup>3</sup> fission gas three batches were sampled in gas mice before composition determination and transferred to KIT-INE for further analysis.

**Table 1:** Results of the fission gas release measurements at ITU. The volumes given are referred to a temperature of  $T_o = 273.15\text{ K}$  and a pressure of  $p_o = 1013.25\text{ mbar}$ .

Date:	22.5.12	Temperature:	22 °C
Operator:	W.W.	Leak Rate:	3.02E-03 mbar·L·s <sup>-1</sup>
Reactor:	KKGg		
Pin No.:	07-63/07-47 SBS 1108//G09/G09		
<b>IRRADIATION DATA:</b>			
Average Burn-up:	50.4	GWd/t(U)	
<b>RESULTS:</b>			
Free volume of the pin:	4.2 cm <sup>3</sup>		
Pressure before puncturing:	37.2 bar		
Normal gas volume:	142 cm <sup>3</sup>		

At JRC-ITU the composition of the remaining gas was measured by mass spectrometry. Careful data analysis and cross checking of the results showed that the results obtained were not significant. The reasons for this are most probably technical problems triggered by a too small amount of available fission gas.

More reliable results concerning the gas composition should be obtainable by mass spectrometry analysis of the gas sample sent to KIT-INE (Bohnert et al., 2012).

**Conclusions**

The fission gas volume and the free volume of the fuel segment investigated were determined successfully. The sampled gas was shared between KIT-INE and JRC-ITU. Because the amount of available gas was too small the determination of the isotopic composition was not possible using the setup installed in ITU.

## Acknowledgement

*The research leading to these results has received funding from the European Union's European Atomic Energy Community's (Euratom) Seventh Framework Programme FP7/2007-2011 under grant agreement n° 295722 (FIRST-Nuclides project).*

## References

- Bohnert, E., González-Robles, E., Herm, M., Kienzler, B., Lagos, M., Metz, V. (2012) Determination of Gaseous Fission and Activation Products Released from 50.4 GWd/t PWR Fuel. 7<sup>th</sup> EC FP – FIRST-Nuclides 1<sup>st</sup> Annual Workshop Proceedings (Budapest, Hungary).
- Carbol, P., Wegen, D.H., Wiss, T., Fors, P. (2012) Spent Fuel as Waste Material. R.J.M. Konings, (ed.) Comprehensive Nuclear Materials, 5, 389-420.
- Hoffmann, P.B., de Weerd, W., Toscano, E.H. (2005) Post-irradiation examination of high burnup BWR fuel rods: Techniques and results, Jahrestagung Kerntechnik 2005, 10-12 May 2005, Nürnberg, Germany.
- Metz, V., Loida, A., González-Robles, E., Bohnert, E., Kienzler, B. (2012) Characterization of irradiated PWR UOX fuel (50.4GWd/t<sub>HM</sub>) used for leaching experiments, 7<sup>th</sup> EC FP – FIRST-Nuclides 1<sup>st</sup> Annual Workshop Proceedings (Budapest, Hungary).
- Papaioannou, D., Nasyrow, R., De Weerd, W., Bottomley, D., Rondinella, V. V. (2012) Non-destructive examinations of irradiated fuel rods at the ITU hot cells, 2012 Hotlab conference (Marcoule, France).
- Wegen, D.H., Papaioannou, D., Nasyrow, R., Gretter, R., de Weerd, W. (2012) Non-destructive testing of segment N0204 of the spent fuel pin SBS1108 - Contribution to WP1 of the collaborative project FIRST Nuclides. JRC75272, European Atomic Energy Community, Karlsruhe, Germany.





# **POSTERS**



7th Framework Programme Collaborative Project:

Fast / Instant Release of Safety Relevant Radionuclides from Spent Nuclear Fuel (FIRST-Nuclides)



Objectives

Understanding the fast / instant release of radionuclides from high burn-up spent UO<sub>2</sub> fuels in geological repositories.

- Experimental investigations of irradiated fuel.
- Provide for improved data for the fast/instant release fraction for high burn-up spent UO<sub>2</sub> fuel.
- Study correlations between the Fission Gas Release and non-gaseous fission products, in particular <sup>129</sup>I, <sup>79</sup>Se and <sup>135</sup>Cs.
- Reduce uncertainties with respect <sup>129</sup>I, and <sup>14</sup>C releases.
- Determine the chemical form of the relevant elements.
- Discuss the impact of the results on the peak-dose.

Consortium

The project is implemented by a consortium with 10 Beneficiaries from 7 EURATOM Signatory States, and the EC Institute for Transuranium Elements:



Associated Groups: Groups participating in the project at their own costs with specific RTD contributions or particular information exchange functions. End-User Group: Waste Management / Regulating Organizations.

Structure of the project

- WP 1: Samples and tools:** Selection, characterization and preparation of materials and set-up of tools.
- WP 2: Gas release + rim and grain boundary diffusion:** Experimental determination of fission gases release. Rim and grain boundary diffusion experiments.
- WP 3: Dissolution based release:** Dissolution based fast/instant radionuclide release.
- WP 4: Modelling:** Modelling of migration/retention processes of fission products in the spent fuel structure.

- WP 5: Knowledge, reporting and training:** Knowledge Management, State-of-the-Art report, general reporting, documentation up-date, dissemination and training.
- WP 6: Project management.**

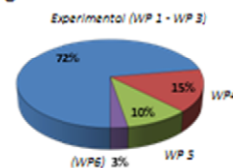


Figure 1. Use of staff resources committed for different types of activities within the project.

Details of the experimental programme (WP 1-WP 3):

- Chemical form, specifically for fission gases, <sup>135</sup>Cs, <sup>129</sup>I, <sup>14</sup>C compounds, <sup>79</sup>Se, <sup>99</sup>Tc and <sup>126</sup>Sn.
- Determination of gap and grain boundary inventories.
- Dependency of fast/instant release on
  - UO<sub>2</sub> fuel and the respective manufacturing process,
  - evolution of higher burn-up and burn-up history,
  - linear power and fuel temperature history, ramping processes, and storage time.
- Accessibility / transport properties on grain boundaries.
- Exchange processes along the grain boundaries.
- Transition between instant/fast release and radiolytically driven matrix corrosion.

Table 1. Fuel data under investigation from PWR and BWR

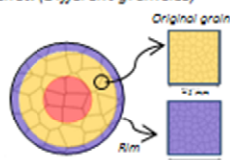
	PWR	BWR
<b>Discharge (manufacturer)</b>	1989 -2008 (AREVA)	2005 - 2008 (AREVA/ Westinghouse)
<b>Cladding</b>		
Material/diameter/thickness (mm)	Zry-4-M5 / 9.50 - 10.75 / 0.62-0.73	Zyr 2 / 9.84 - 10.2
<b>Pellet</b>		
Enrich.(%) / grain size (µm) / den. (g·cm <sup>-3</sup> )	2.8 - 4.3 / 5 - 40 / 10.41	3.5 - 4.25 % / 6 - 25 / 10.52
<b>Irradiation</b>		
BU (GWd/t) / cycles	45 - 70.2 / 2 - 14	50.2 - 59.1 / 5 - 7
Lin. Power (W/cm)	186 - 306	160 - 200
FGR (%)	4.9 - 26.7	1.4 - 3.1

Enrich = enrichment, den = density, BU = burn up, Lin = linear

Modelling (WP 4)

- Fission product migration on grain boundaries.
- Effects of fractures in the pellets.
- Effects of holes/fractures in the cladding.
- Chemical state of relevant elements.

Figure 2. Microstructure of the pellet. (Different grain size)



Dissemination, Mgt\* and Training (WP 5-WP6):

Duration of the CP: 01 Jan. 2012 to 31 Dec. 2014  
 Funding: Total Costs: 4 741 261 €  
 EC Contribution: 2 494 513 €  
 Events: 2<sup>nd</sup> Annual Workshops: (October 2013)

\*Mgt = Management

CONTACT: Coordinator: [bernhard.kienzler@kit.edu](mailto:bernhard.kienzler@kit.edu) (KIT-INE) and Coordination Secretariat: [alba.valls@amphos21.com](mailto:alba.valls@amphos21.com) (AMPHOS21)

Acknowledgement: "This research leading to this results has received funding from the European Atomic Energy Community's Seventh Framework Programme (FP7/2007-2011) under grant agreement no. 295722, the FIRST-Nuclides project". For more information visit: [www.firstnuclides.eu](http://www.firstnuclides.eu)





## **TOPICAL SESSIONS**



# THERMODYNAMICS OF FISSION PRODUCTS IN SPENT NUCLEAR FUEL<sup>3</sup>

Ondřej Beneš

Joint Research Centre – Institute for Transuranium Elements (JRC-ITU), European Commission

The behaviour of spent nuclear fuel (SNF) as well as the fast release of safety relevant radionuclides are controlled by various phases formed under the conditions during the use of the fuel in a nuclear power plant. Important parameters are (i) the temperature, (ii) the composition of the fuel and (iii) the oxygen potential of oxide-fuel. In an ideal case, the thermodynamics should be able to describe the behaviour of SNF. As basis for understanding the behaviour of fission products (FP) in the fuel, the phase diagrams of the binary systems “U-O” and “U-Pu” as well as the ternary system “U-Pu-O” were discussed. For fresh nuclear fuel (U-Pu-O system), the phase diagrams are well elaborated, but that is not case for the complex system SNF, in which all FPs are present. A full description of phase diagrams including all FPs of interest is not available. Presently, the primary interest is on the volatile FPs and their solid/gas equilibrium.

Thermodynamics provide information on the chemical state of FPs which influences the physical properties of the fuel itself, such as thermal conductivity, melting temperature, deformations, and swelling as well as determine the physico-chemical properties of the FP mainly their volatility and solubility in water. Temperature and the oxygen potential of the fuel (determined by O/M ration in  $\text{UO}_2$ ) are the key parameters with respect to thermodynamics. However, kinetics especially diffusion processes of the FPs is another driving force for the phase formation. As example, the Cs – I system was discussed in details and thermodynamic considerations were compared to Knudsen cell experiments. According to thermodynamics, CsI is the stable compound at  $T = 900\text{K}$ , however, the temperature varies by more than 500 K over the radius of a fuel pin in a nuclear power plant.

The chemical state of a series of FPs was given including metal precipitates, molybdenum, zirconium, and iodine. The stable form of iodine is CsI, but due to kinetic reasons I or  $\text{I}_2$  can also be formed. Reaction sites where CsI can be formed are bubbles and microstructures in the  $\text{UO}_2$  matrix. At low burn-up ( $<5 \text{ GWd/t}$ ), such structures are not available, therefore the formation of CsI is not likely. The generation of other iodides is also possible such  $\text{ZrI}_4$  or  $\text{MoI}_4$ . Due to the excess of caesium in comparison to iodine ( $\text{Cs/I} \sim 10$ ), it is expected that almost all iodine will be in the form of CsI located at grain boundaries, cracks and/or fission gas bubbles. Remaining caesium reacts with zirconium,

---

<sup>3</sup> Abstract summarized by the coordination team

forming  $\text{Cs}_2\text{MoO}_4$  as stable Cs phase. Cs does not react with  $\text{UO}_2$  forming uranate phases, such as  $\text{Cs}_2\text{UO}_4$ , instead it reacts with  $\text{ZrO}_2$ :  $2 \text{Cs (s)} + \text{ZrO}_2\text{(s)} + 0.5 \text{O}_2\text{(g)} \rightarrow \text{Cs}_2\text{ZrO}_3\text{(s)}$ .

This compound is in equilibrium with  $\text{Cs}_2\text{MoO}_4$ . Neither of these compounds is volatile. At oxygen potentials below -440 kJ/mol, tellurium reacts with Cs molybdate forming  $\text{Cs}_2\text{Te(s)}$  and free oxygen according to  $\text{Te(l)} + \text{Cs}_2\text{MoO}_4\text{(s)} \rightarrow \text{Cs}_2\text{Te(s)} + \text{O}_2\text{(g)} + \text{MoO}_2\text{(s)}$ .

Rare earth elements are highly soluble in the solid  $\text{UO}_2$  matrix, forming  $\text{UO}_2\text{-R}_2\text{O}_3$  solid solutions. Significant deformation of the  $\text{UO}_2$  crystals are not observed by the presence of  $\text{R}_2\text{O}_3$ . Both FPs Ba and Sr are present in an oxidized form reacting either with  $\text{UO}_2$  or  $\text{ZrO}_2$  to give  $\text{BaZrO}_3$  and  $\text{SrZrO}_3$  which is found as a solid solution  $(\text{Ba,Sr})\text{ZrO}_3$ . Above 1000 K,  $\text{BaUO}_3$  is formed, but no  $\text{SrUO}_3$ . Sr is found in so called "grey phase" consisting of  $(\text{Ba,Sr})(\text{U,Pu,Zr})\text{O}_3$  solid solution. At oxygen potentials above 400 kJ/mol and in the presence of  $\text{MoO}_2$ ,  $\text{BaMoO}_4$  becomes stable.



# CHARACTERISTICS OF SPENT NUCLEAR FUEL

Christoph Gebhardt and Wolfgang Goll

AREVA FUEL Business Unit (FDM-G), FR

The talk provided information on management of UO<sub>2</sub> fuel for Pressurized Water Reactor (PWR) and Boiling Water Reactor (BWR) fuels, including neutron-physical aspects which are basis of an optimal usage of the fuel. The distribution of spent nuclear fuel in relation to their burn-up - as reported by the utilities - was presented, as well as the histories of the bundle power for some reactors. These bundle powers depend on the reactor operation and on the number of cycles. The radial and axial burn-up distribution was demonstrated for a modern 18x18 fuel assembly with 60 MWd/kg<sub>U</sub> average burn-up. In this context the pellet centerline temperatures as a function of the rod's linear heat rate and the temperature of the coolant were discussed for BWR and PWR fuel elements.

The fuel pellet manufacturing processes and typical inventories of additives and impurities of fuel pellets were explained. Special attention was given to the typical Al (~100 ppm) and Cr (~800 ppm) contents in the fuel pellets. In the following discussion it was questioned whether trivalent Al and Cr might interact with trivalent actinides under repository conditions. With respect to the cladding, typical PWR and BWR fuel rod cladding materials were described and their irradiation induced alterations in regard to corrosion and hydrogen uptake was quantified. It was shown that an increase in burn-up causes both an increase in hydrogen incorporation and an extension of the Zircaloy oxide thickness. The lecture included the corrosion relevant compositions of PWR and BWR cladding alloys and the behaviour of modern cladding materials such as M5, where the component Sn is replaced by Nb which shows significantly lower corrosion rates under the temperature regime of reactors. In this material, also the hydrogen uptake is lower.

Furthermore, defect mechanisms under interim and final storage were discussed. During handling, transport, discharge operations and interim storage it is required that systematic failures of fuel rods will not occur and the mechanical integrity of the fuel assembly structure is retained. Systematic cladding failures can be avoided by limiting stress and strain of the material. If defective fuel rods are present, these rods need special treatment and/or confinement.

Under disposal conditions, temperatures and, hence, stresses are further reduced excluding systematic failure. Defects under thermal creep conditions are limited to small cracks leading to a prompt loss of rod inner pressure. In the long term, effects from He production, delayed hydride cracking and other post-irradiation processes may become relevant.

# IMPACT OF THE IRRADIATION HISTORY OF NUCLEAR FUELS ON THE CORROSION BEHAVIOUR IN A DISPOSAL ENVIRONMENT

Dani Serrano-Purroy and Jean-Paul Glatz

Joint Research Centre – Institute for Transuranium Elements (JRC-ITU), European Commission

Nuclear fuel becomes a very heterogeneous material during irradiation both from a structural and from a compositional point of view. The degree of heterogeneity due essentially to a very high temperature gradient (e.g. 1000°C in the pellet centre, 500°C at the fuel periphery corresponding to a distance of app. 5 mm) increases with burn-up and linear power. For MOX produced by a master mix blend technique (MIMAS), Pu-rich (25% Pu) agglomerates up to 150 µm diameter are present already before irradiation.

Also the composition, i.e. the content of higher actinides formed by neutron capture and the fission product content increases with burn-up. Furthermore the fission events are taking place more and more at the fuel pellet periphery, where Pu formed by neutron capture of  $^{238}\text{U}$  takes over from  $^{235}\text{U}$  as fissile material. Higher actinides, essentially Pu, Np, Am and Cm are produced in always higher amounts as the burn-up increases. For MOX where Pu is the fissile material from the beginning the built-up of higher actinides is even more significant (almost 10 times more compared to  $\text{UO}_2$  at the same burn-up). Depending on their thermophysical properties, the fission products migrate in the thermal gradient to the fuel grain boundaries or for the most volatile elements like fission gases Xe, Kr but also Cs or I to the fuel periphery and depending on the irradiation conditions a more or less important part of these elements are even found in the fuel pin plenum after irradiation.

Detailed post irradiation examination using optical, scanning or transmission electron microscopy, electron microprobe analysis, Knudsen cell, gamma scanning but also chemical analysis, allow to characterise the fuel changes during irradiation. Among others the development of thermal cracks, porosity, radiation defects due to strong  $\alpha, \beta, \gamma$  radiation are identified. The grain subdivision at the fuel pellet periphery (RIM effect) or the precipitation of 5 metal (Ru, Rh, Pd, Mo, Tc) particles' at the grain boundaries is being observed.

It was shown that the irradiation history and here first of all the linear power reached in the fuel, is the dominating cause of the above mentioned phenomena, e.g. fuels run at high linear power, even if the burn-up is moderate, show very high release of volatiles to the fuel rod plenum.

It is obvious that all these modification affect the fuel corrosion behaviour in a repository in the situation of failure of all retention barriers, i.e. when the fuel gets in contact with ground water. Especially the instant release fraction, i.e. the release of highly soluble elements (Cs, I, Se, Te, Rb...) with a large part of the inventory transported to the fuel periphery during irradiation, can considerably depend on the fuel irradiation history.

# THE POTENTIAL OF THE TRANSURANUS CODE FOR SOURCE TERM CALCULATION OF SPENT NUCLEAR FUEL

Paul Van Uffelen

Joint Research Centre – Institute for Transuranium Elements (JRC-ITU), European Commission

TRANSURANUS is a computer program for the thermal and mechanical analysis of fuel rods during various operating conditions, generally referred to as a fuel performance code. Emphasis lies on assessing both the temperature and the stress levels in a fuel pin, since they are linked to the crucial safety criteria, set by the regulators, to be fulfilled during the entire in-pile lifetime of the fuel rod. The code has been transmitted to various industrial partners, research organisations, as well as, safety authorities and universities across Europe. The corresponding know-how is also being transferred via international summer schools, training courses and workshops organised by JRC-ITU, as well as, advanced courses at several universities within the European Union.

The TRANSURANUS code solves the equations for the radial heat transfer, the radial displacement along with the stress distribution in both the fuel and the surrounding cladding, and describes the fission product behaviour as a function of time. The equations embody the following phenomena:

- Thermal performance: heat conduction, radiation and convection;
- Mechanical performance: elastic deformation, creep, densification, thermal expansion, pellet cracking and relocation, swelling;
- Actinide behaviour: depletion and build-up of main U, Np, Pu, Am and Cm nuclides, impact on the radial power profile;
- Fission product behaviour of Xe, Kr, Cs, Nd, and He

The lecture will treat the main equations and the associated limitations with the focus on fission product behaviour. More precisely, the following mechanisms will be considered in greater detail: recoil, knock-out & sputtering, lattice diffusion, trapping, irradiation re-solution, thermal re-solution, thermal diffusion, grain boundary diffusion, grain boundary sweeping, bubble migration, bubble interconnection and sublimation or vaporisation. For each of these mechanisms, a brief description will be provided along with a discussion of its domain of application. Following a description of the main relevant mechanisms, the various models for fission gas release and swelling in the open literature will be reviewed, including those which have been implemented in the TRANSURANUS code.

Once the behaviour of the fuel rod is computed in each axial slice, they are coupled in the code via balance equations for stresses and gas composition. For this reason standard fuel performance codes are so-called 1.5 D codes, while 2D (3D) codes solve the equations (for heat removal and stresses) simultaneously in two (three) dimensions.

The TRANSURANUS code has a clearly defined mechanical–mathematical framework, in which new material properties and models can easily be incorporated. The code has a comprehensive material data bank for oxide, mixed oxide, carbide and nitride fuels, Zircaloy and steel claddings and several different coolants (water, sodium, potassium, lead, bismuth). Besides its flexibility for fuel rod design, the code can deal with a wide range of different situations, with time scales from milliseconds to years. Hence, TRANSURANUS can be used as a single code system for simulating both long-term irradiations under normal operating conditions as well as transient tests. In this way the code can be applied to a fuel pin segment from a commercial fuel rod that is re-irradiated in an experimental reactor after instrumentation, like in the Halden Boiling Water Reactor. The 'restart' mode allows simulating re-fabricated fuel rods, i.e. where the fill gas has been completely changed. TRANSURANUS also allows simulating cladding tubes without fuel submitted to heating burst tests in out-of-pile conditions. Finally, thanks to the restart option, the code has also occasionally been used to simulate storage conditions. Nevertheless, this requires the appropriate material properties for such conditions to be implemented, such as the expression for cladding creep in the temperature range of interest.

Once the main models of the code have been presented, the verification and validation procedure of the code will be outlined and illustrated. More precisely, the verification of models in a stand-alone environment on the basis of either analytical or more complex and accurate numerical solutions obtained by means of more-dimensional finite element solutions will be presented. In a second step, the validation relies on experimental data, when available, such as, the local thermal conductivity of nuclear fuel as a function of burn-up and temperature, the radial concentrations of fission products measured after irradiation by means of electron probe micro-analysis or secondary ion mass spectrometry, or cladding tube diameters after burst tests that correspond to conditions during a loss of coolants accident. The final step of the code validation consists of a comparison against integral experimental data, as well as a comparison with other code predictions. Excellent opportunities for benchmark exercises like FUMEX-III are organised by the IAEA, or the LOCA benchmark organised by the OECD-NEA.

The widely used mechanistic approach described above leads, in many cases, to discrepancies between theoretical predictions and experimental evidence because some of the physical processes are of stochastic nature. The mechanistic approach has therefore been augmented by statistical analyses that apply basic probabilistic methods, such as the Monte Carlo method, in order to better understand uncertainties and their consequences.

A combination of a restart and Monte Carlo statistics may be used to perform a probabilistic analysis only after the restart. This option may thus also be helpful for the analysis a long base irradiation of a fuel rod in a reactor followed by the simulation of the same rod during a transient or long term storage.





## **PRESENTATIONS BY ASSOCIATED GROUPS**



# LONG TERM BEHAVIOUR OF SPENT AGR FUEL IN REPOSITORY

David Hambley

Spent Fuel Management and Disposal, Fuel Cycle Solutions, National Nuclear Laboratory (NNL), UK

## Background

The majority of nuclear power production in the UK is from Advanced Gas-Cooled Reactors. The spent fuel from these reactors is currently being reprocessed, however the reprocessing facility is due to close within the next 10 years and it is anticipated that future arisings will be sent to a geological disposal facility towards the end of this century. The siting and development of a geological disposal facility is under way and incorporates spent fuel.

## AGR Fuel

The AGR and its fuel are unique to the UK. Whilst the fuel in both AGR and most LWRs is uranium dioxide, there are many significant differences:

- AGR fuel pellets are annular, whilst in LWR systems the pellets are solid,
- the fuel cladding is stainless steel (20/25/Nb), whereas most power reactor system use zirconium alloy cladding;
- the cladding temperature in operation is higher, up to 825°C, but peak fuel temperatures and radial temperature gradients are similar;
- differences in the neutron spectrum leads to a lower rim/average Pu profile.
- the coolant in AGRs is carbon dioxide, which produces some deposition of carbon on the fuel pin surfaces, this is substantially different from the 'crud' formed on LWR fuel pins and can lead to much higher fission gas release in a small proportion of the fuel pins.

The peak fuel element burn-up is currently around 40 GWd/teU, which is somewhat lower than many LWRs and is unlikely to exceed 45 GWd/teU.

## Current Programme

The UK Nuclear Decommissioning Agency are interested in investigating whether the differences between AGR and LWR fuel result in significantly different fuel behaviour under repository

conditions. This programme is being conducted via 6 PhDs at Cambridge University, Lancaster University and Imperial College.

Inactive simulants of active FPs have been incorporated into SIMfuel replicating species at 100 years cooling, which have been characterised with optical and SEM microscopy and X-ray diffraction. All key phases have been identified and analyses are continuing. This will be followed by annealing at 300°C and 825°C to compare effects on FP distributions with LWR fuels.

Modelling of the fission product distribution in AGR UO<sub>2</sub> at elevated temperatures is currently under way to be followed by modelling of radiation damage in U secondary mineral phases and solubility of FPs.

Work is underway to induce radiation damage in SIMfuel samples and examine the effects of the damage on dissolution behaviour.

Two separate investigations are underway into UO<sub>2</sub> corrosion. They are investigating the effects of cladding and cladding corrosion products on dissolution and whether a fenton cycle could be initiated. Other aspects include investigation of the formation and stability of UO<sub>2</sub> secondary phases on UO<sub>2</sub> and their impact on corrosion.

Finally the radiation stability of secondary phases (particularly for alpha recoil damage) will be examined using XRD and <sup>17</sup>O MASNMR, this will be followed by examination of the actinide substitution process: i.e. solid solubility and possible partitioning of Np or Pu.

# SOURCE TERM MODELLING FOR SPENT FUEL ELEMENTS IN PERFORMANCE ASSESSMENT

Artur Meleshyn<sup>1</sup>, Jens Wolf<sup>1</sup>, Ulrich Noseck<sup>1</sup>, Guido Bracke<sup>2</sup>

Gesellschaft für Anlagen- und Reaktorsicherheit (GRS) mbH, DE

<sup>1</sup> Brunswick, Germany

<sup>2</sup> Cologne, Germany

Integrated performance assessment models of deep geological repositories for high-level radioactive waste (HLW) and spent nuclear fuel include a source term which describes the release of radionuclides from HLW or spent fuel elements (SFE) from failed containers into the contacting aqueous solution. The chemical release rate depends on time (kinetics), solubility of radionuclides in the solution (thermodynamics), and temperature. The general source term can be represented in the form:  $A_i(t) = n_c(t) \cdot \sum A_{X,i}(t) \cdot r_X$ , where  $n_c(t)$  is the fraction of the failed containers at time  $t$ ,  $A_{X,i}(t)$  is the inventory of radionuclide  $i$  in component  $X$  at time  $t$ , and  $r_X$  is the chemical release rate for component  $X$ . GRS currently utilizes two databases to model the source term with respect to the definition of the components and their characteristic release rates and, correspondingly, the relative inventories of radionuclides in the components.

In the project Scientific Basis for the Assessment of the Long-Term Safety of Repositories, four SFE-components are currently defined: Zircaloy, structural parts, fuel matrix, and instant release fraction (IRF) with the characteristic isotope-independent release rates of 0.0036, 0.002,  $1.0 \cdot 10^{-6}$ , and  $1.0 \text{ a}^{-1}$ , respectively. In comparison to the previously used SPA source term with only three SFE components (Lührmann et al., 2012) this source term results in significant changes in the calculated effective dose rate. The degree of these changes indicates also a strong dependence on the applied solubility limits, which were assumed for the geochemical environment of a repository, as well as on relative inventories of dose-determining radionuclides  $^{36}\text{Cl}$ ,  $^{129}\text{I}$ ,  $^{135}\text{Cs}$ ,  $^{226}\text{Ra}$ ,  $^{233}\text{U}$ , and  $^{237}\text{Np}$  in the components of SFE.

Only three SFE-components were defined in the Preliminary Safety Analysis of Gorleben site: Zircaloy (including tubes and structural materials), fuel matrix, and IRF with the characteristic isotope-independent release rates of 0.00003, 0.00365, and  $1.0 \text{ a}^{-1}$ , respectively (Larue et al., 2012). The IRF of fission gas,  $^{14}\text{C}$ ,  $^{36}\text{Cl}$ ,  $^{90}\text{Sr}$ ,  $^{99}\text{Tc}$ ,  $^{107}\text{Pd}$ ,  $^{129}\text{I}$ ,  $^{135}\text{Cs}$ , and  $^{137}\text{Cs}$  is provided for burn-ups of 41, 48, 60, 75 GWd/t<sub>HM</sub>. Solubility limits in highly-saline brines are provided for Zr, Tc, Sm, Th, U, Np, Pu, and Am and were derived from experimental and analogue studies (Kienzler et al., 2012). Solubility data

for other elements with radionuclides is not available. This is considered presently to be unimportant for performance assessment calculations (Larue et al., 2012).

The source term used in performance assessment calculations acts directly on effective dose rate and performance indicators (e.g., radiotoxicity flux from repository compartments) of a repository. These safety and performance indicators can be used to assess the effect of high burn-up fuel on selected scenarios. GRS can contribute to the outcome of FIRST-Nuclides project by performance assessment calculations for generic repositories for HLW/SF in rock salt and claystone applying an improved source term using parameters for high burn-up SFE provided or derived from data by the beneficiaries of FIRST-Nuclides.

## References

Kienzler, B., Altmaier, M., Bube, C., Metz, V. (2012) Radionuclide Source Term for HLW Glass, Spent Nuclear Fuel, and Compacted Hulls and End Pieces (CSD-C Waste), KIT-SR 7624, Karlsruhe,.

Larue et al. (2012) Analysis of radiological consequences, Report, Draft.

Lührmann, L., Noseck, U., Storck, R. (2000) Spent Fuel Performance Assessment (SPA) for a Hypothetical Repository in Crystalline Formations in Germany. GRS mbH, GRS-154, Braunschweig.

# **APPLICABILITY OF PAST SPENT FUEL RESEARCH IN THE US TO ASALT-BASED HLW REPOSITORY**

Donald T. Reed

Earth and Environmental Sciences Division,  
Los Alamos National Laboratory (LANL), US

A summary of spent fuel interaction studies in the US will be provided and evaluated in the context of the likely safety case for a potential salt-based HLW US repository. Past spent fuel studies were focused on basaltic groundwater interactions performed at Pacific Northwest Laboratory in support of the Basalt Waste Isolation and drip tests that were specific to the proposed Yucca Mountain site. These data, although appropriate for their respective safety cases do not directly address the special considerations possible in a low-probability brine inundation scenario where high ionic strengths, temperatures and irradiated high-chloride brine predominate. An assessment of how the data in hand can be used and the need for future experiments that address the range of options being considered in the US will be presented. The current status of the repository programs in the US will also be given.





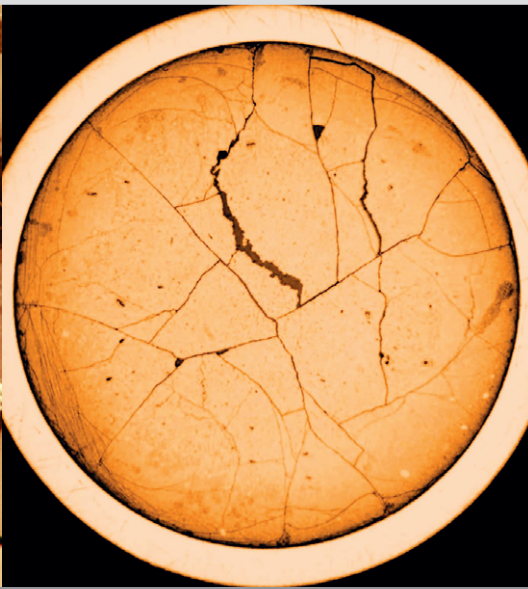
# **OVERVIEW OF USED FUEL DEGRADATION & RADIONUCLIDE MOBILIZATION ACTIVITIES WITHIN THE USED FUEL DISPOSITION CAMPAIGN**

David C. Sassani

Sandia National Laboratories, Department 6225, Advanced Systems Analysis, US

The disposition of used nuclear fuel (UNF) and high level waste (HLW) is fundamental to the nuclear fuel cycle in the USA. There is a need to develop strategies for managing radioactive wastes from any fuel cycle. Following institutions are involved in the Used Fuel Degradation & Radionuclide Mobilization Activities: U.S. Department of Energy (DOE), Office of Nuclear Energy (NE) established the Used Fuel Disposition Campaign (UFDC) as part of its Fuel Cycle Technology (FCT) program. The activities include modeling and experimental work at the collaborating National Laboratories Sandia National Laboratories (SNL), Pacific Northwest National Laboratory (PNNL), Argonne National Laboratory (ANL).

The used fuel degradation and radionuclide mobilization model concepts includes the fast release fraction (or instant release) inventory that includes fission products located in the fuel gap, the plenum regions (fission gases), accessible grain boundaries/pellet fractures. The matrix degradation inventory that covers the matrix itself and fission products located in the inaccessible grain boundaries/pellet fractures, the matrix as solid solution or dissolved within the grain structure, the noble metal particles (which undergo their own degradation rate once exposed) and focuses on the major rate limiting processes (e.g., radiolysis, matrix degradation, noble metal particle degradation). In future, coupling with physical degradation of cladding and mechanical evolution of degrading fuel is foreseen.



ISBN 978-3-86644-980-0

ISBN 978-3-86644-980-0



9 783866 449800 >